Universidade Federal de Minas Gerais
Departamento de Física - Instituto de Ciências Exatas

Quantum Thermodynamics of Quantum Critical Systems

Adalberto D. Varizi

Thesis submitted to the Physics Graduate Program of the Universidade Federal de Minas Gerais in partial fulfillment of the requirements for the degree of Doctor in Sciences.

Supervisor: Prof. Dr. Raphael Campos Drumond
Co-supervisor: Prof. Dr. Gabriel Teixeira Landi

Belo Horizonte
2022

Universidade Federal de Minas Gerais
Departamento de Física - Instituto de Ciências Exatas

Quantum Thermodynamics of Quantum Critical Systems

Adalberto D. Varizi

Tese apresentada ao Programa de Pós-graduação em Física do Instituto de Ciências Exatas da Universidade Federal de Minas Gerais, como requisito parcial para a obtenção do título de Doutor em Ciências.

Orientador: Prof. Dr. Raphael Campos Drumond
Coorientador: Prof. Dr. Gabriel Teixeira Landi

Belo Horizonte
2022

Aos meus pais e irmãos...

Abstract

This thesis is devoted to the study of systems presenting continuous quantum phase transitions subject to a thermodynamic work protocol. Particularly, we investigated how quantum coherences created by a sudden change in the system Hamiltonian can be quantified and their relation to its critical behavior. Therefore, the results here presented lie within the scope of quantum thermodynamics.

The effects of quantum criticality in work protocols have been considerably investigated in recent years. Still, little or nothing was known about the role of quantum coherences. To grasp this, we examined two splittings of entropy production into a classical and quantum parts, the latter related to quantum coherences.

The first splitting have been used in several contexts and maintains an intimate connection with the resource theory of thermodynamics. However, employing it to a quantum Ising model driven out of equilibrium by a sudden quench, we verified some shortcomings: namely, counter-intuitive and immutable behavior at low temperatures and unexpected nonanalyticities unrelated to critical phenomena. This inspired us to introduce a new and complementary separation to the entropy produced following a work protocol.

A surprising and intriguing property of these splittings when applied to critical systems is the fact that they exhibit signatures of the critical point independently of the system initial temperature. In the new splitting we are capable of explaining this as a consequence of their close relation to the derivatives of the energy spectrum.

Keywords: Quantum thermodynamics; Quantum phase transitions; Critical phenomena; Quantum Coherence; Entropy production; Splittings of entropy production; Ising model.

Resumo

Esta tese dedica-se ao estudo de sistemas que apresentam transições de fase quânticas contínuas sujeitos a um protocolo termodinâmico de trabalho. Particularmente, investigamos como as coerências quânticas criadas por uma perturbação repentina na Hamiltoniana do sistema podem ser quantificadas e sua relação com o comportamento crítico. Portanto, os resultados aqui apresentados residem no âmbito da termodinâmica quântica.

Os efeitos da criticalidade quântica em protocolos de trabalho têm sido consideravelmente investigados nos últimos anos. Ainda assim, pouco ou nada se sabia sobre o papel das coerências quânticas. Para entender isso, examinamos duas divisões da produção de entropia em uma parte clássica e outra quântica, a última relacionada às coerências quânticas.

A primeira divisão já foi usada em vários contextos e mantém uma conexão íntima com a teoria de recursos da termodinâmica. No entanto, aplicando-o a um modelo de Ising quântico submetido a uma perturbação repentina, verificamos algumas deficiências: a saber, um comportamento contraintuitivo e imutável em baixas temperaturas e não analiticidades inesperadas não relacionadas a fenômenos críticos. Isso nos motivou a introduzir uma nova e complementar separação para entropia produzida seguindo um protocolo de trabalho.

Uma propriedade surpreendente e intrigante dessas divisões quando aplicadas a sistemas críticos é o fato de exibirem assinaturas do ponto crítico independentemente da temperatura inicial do sistema. Na nova divisão, podemos explicar isso como uma consequência de sua estreita relação com as derivadas do espectro de energia.

Palavras-chave: Termodinâmica quântica; Transições de fase quânticas; Fenômenos críticos; Coerência quântica; Produção de entropia; Divisões da produção de entropia; Modelo de Ising.

Agradecimentos

Gostaria de agradecer inicialmente aos meus orientadores, Raphael Drumond e Gabriel Landi. Ao Raphael por ter aceitado me orientar no meio de uma confusão burocrática, pela disponibilidade, pela flexibilidade e liberdade que me foi dada, e pelas excelentes ideias durante nossas discussões. Ao Gabriel por ter me recebido na USP, por ter me introduzido no mundo da termodinâmica quântica, pelos muitos ensinamentos e por me proporcionar um ambiente excepcional onde eu pudesse entender melhor meu trabalho e amadurecer.

Agradeço à minha família; meus pais, Antônio e Darcy, por tornarem tudo possível, pelo cuidado e esforço. Aos meus irmãos queridos, Debson e Delacy, pela amizade e apoio incondicional. A todos pela confiança e paciência ao longo de toda minha vida acadêmica. Também agradeço ao meu tio Anísio pelo suporte fundamental na minha mudança para São Paulo e, ainda mais, na minha volta pós acidente.

Agradeço ainda aos amigos e colegas que contribuíram no meu desenvolvimento pessoal e desse trabalho. Em particular, um agradecimento especial a Carla, pela companhia, pelo carinho, pela diversão e apoio ao longo desses anos.

Por fim, agradeço o apoio financeiro do Conselho Nacional de Desenvolvimento Científico e Tecnológico (CNPq) e da Coordenação de Aperfeiçoamento de Pessoal de Nível Superior (CAPES).

Contents

List of Figures

Introduction

The superposition principle is at the heart of quantum theory and may be the fundamental aspect of it leading to its departure from classical physics. Formally, this principle is translated into the likely existence of *off-diagonal* elements in the representation of observables and density operators in a particular basis of the system Hilbert space. These off-diagonal elements represent the so-called *quantum coherences*.

The effects of quantum coherences are present in some of the foundational problems of quantum theory — such as in the wave-like behavior of particles — and also in some of its most important and successful technological applications — like the laser. In recent years, the field of quantum information and associated areas have seen and increasing effort in the attempt at characterizing and quantifying coherences. This culminated with the formal development of the resource theories of coherences [1, 2]. Since coherence underlies entanglement, some may regard it as the supreme quantum resource, allowing the realization of tasks impossible in the domain of classical physics. Altogether, this makes the understanding of quantum coherences crucial to practical implementations of quantum sciences.

Coherences are receiving considerable attention in the particular field of quantum thermodynamics, being the subject of several recent studies. This is a consequence of the recognition of its elementary role in the field. For instance, at a fundamental level, energetic coherences are intimately related to the problem of defining work and heat in quantum systems [3–7]; it also imposes constraints on state transformations in thermal processes [8–11]; it alters fluctuation-dissipation relations at linear response [12, 13] and may in fact reverse heat flows [14–17]. Moreover, they can be used to extract work [9, 18–25]; it can enhance the functioning of thermal machines [26–29] and accelerate energy exchanges [30, 31].

One of the most significant applications of classical thermodynamics is in the study of phase transitions. These often drastic changes in a system are indicated by a nonanalytic behavior of some thermodynamic function. In a first-order phase transition the molar entropy and volume as a function of temperature has a discontinuity, while its heat capacity diverges because of latent heat. Second-order phase transitions, instead, are characterized by a diverging susceptibility.

At zero temperature, a system can undergo a quantum phase transition. In this case, the changes in the system are associated with nonanalyticities in its ground state. Indeed, these singular behaviors may also be reflected in some stochastic or quantum thermodynamic quantities. For instance, a discontinuity in the average work done on a quenched system can indicate a first-order quantum phase transition [32]. Alternatively, a singular behavior of the entropy production signals a second-order transition [32–34].

In a quantum system, the entropy production can be typically split into two contributions. One is associated to changes in the populations of the system and can be referred to as a classical contribution; the other comes from the genuinely quantum feature of coherences [12, 35–37]. It becomes relevant then to understand the role of each of these components in these splittings, particularly for quantum critical models.

This thesis explores precisely that. The standard splitting is based on the relative entropy of coherence [1, 35, 36]. We examine it in a transverse field Ising model [38]. Next, inspired by some initial results obtained in [12, 13], we propose a new and more appropriate splitting for unitary work protocols [37]. We further analyse its behavior close to the critical points of a modified quantum Ising model with a transverse field that alternates values for even and odd sites [39]. We show the individual components of entropy production can still pinpoint the existence of a quantum phase transition even when the protocol is realized at arbitrarily high temperatures [40].

The thesis is divided as follows. In Chapter 1 I review the main concepts of phase transitions and critical phenomena. Chapter 2 is dedicated to introduce the Alternating Transverse Field Ising Model (ATFIM) which will be used as an example of quantum critical system. In Chapter 3 I present the thermodynamic Jarzynski-type work protocol, define entropy production at the stochastic and average levels and discuss its physical meaning and mathematical properties. Moreover, the behavior of this quantity in the

vicinity of the critical points of the ATFIM following an instantaneous quench protocol is analysed and discussed. Chapter 4 is dedicated to the first splitting of entropy production, here called the Γ-splitting. I review its physical motivation and significance, study its behavior in a suddenly quenched Ising model and scrutinize its shortcomings. In Chapter 5 our new splitting of entropy production is presented along with its physical meaning. I refer to it as the Λ-splitting. Its specific properties in the case of instantaneous quenches are discussed in detail. Next, the behavior of the Λ-quantities near the critical points of the ATFIM are analysed and an explanation to their singularity at a critical parameter given. This is followed by a concluding chapter.

Additionally, the thesis includes several appendices. Appendix A is devoted to the derivation of some mathematical results concerning the ATFIM. Appendix B presents some quantum mechanics and quantum information definitions, quantities and their properties. These include, for instance, the time-ordering operator, von Neumann entropy, quantum relative entropies and the framework of resource theories. Appendix C provides a rigorous mathematical relation between forward and backward (time-reversed) unitary dynamics. Finally, in Appendix D I compare thermodynamic quantities derived using the full Ising model Hamiltonian against the ubiquitous “positive parity approximation" Hamiltonian. Explicitly, it is revealed the entropy production following a quench protocol does not exhibit significant discrepancies with this approximation.

Chapter 1

Critical Phenomena

A phase transition entails fundamental changes in the macroscopic properties of a system. The quintessential examples are those of solid, liquid, and gaseous transformations. But they are also at the heart of phenomena like superfluidity and superconductivity, with potential technological applications.

In equilibrium thermodynamics, these phase shifts are commonly driven by temperature when it reaches a certain value that places the system on a transition point. In such points, some thermodynamic quantities will present a nonanalytical behavior, characterizing the transition. Returning to one of the aforementioned canonical examples, for water at a pressure of 1 atm, a transition point is attained when the temperature decreases to 0 ºC. The subsequent solidification of water into ice is marked by a discontinuous change in its specific volume and entropy.

This example constitutes a representative case of a transition involving *latent heat*: the water releases a finite amount of energy without altering its temperature as it transforms from one phase to the other. Phase transitions comprising latent heat are classified as discontinuous or first-order phase transitions because of the discontinuity in the first derivatives of the free energy.

Otherwise, transitions which do not involve latent heat are denominated continuous and are often of second-order. In this case, divergences and other singularities appear in the second (or higher-order) derivatives of the free energy. The most elementary example is that of a magnetic material in the absence of an external field at the Curie temperature. Above this temperature the system loses its ferromagnetic property of spontaneous

magnetization and becomes a paramagnet.

The singularities in a continuous transition have frequently a power law form and are associated with diverging length- and time-scales of the system. These peculiar non-analytical behaviors of physical properties are denominated critical phenomena and the transition point in this case is termed the critical point.

Thus far, I have discussed thermally driven, or classical, phase transitions. Contrastingly, quantum phase transitions (QPT) take place at zero temperature and concern distinct changes in the ground state of a many-body system. The phase transformations, in this case, are driven by quantum fluctuations established by a nonthermal parameter g which regulates a competition between separate parts of the system Hamiltonian. It is noteworthy that, although these transitions occur at $T = 0$, they might nonetheless produce consequences at finite temperatures.

My focus here will be on QPTs of second order, but the main ideas are readily extended to higher-order continuous transitions. Similarly to the classical thermal case, these are linked to a critical point and present critical phenomena, which here are further identified with a closing energy gap in the thermodynamic limit. Since many of the concepts in critical phenomena are common to both classical and quantum types, I introduce most of them adopting the more familiar language of the former.

1.1 Thermal phase transitions

Let us consider a system with a Hamiltonian $H(\{C_n\}, \{\theta_n\})$, which is a function of the coupling constants $\{C_n\}$ and of the dynamical degrees of freedom $\{\theta_n\}$. Its free energy is given by

$$F = -T \ln Z, \tag{1.1}$$

$$Z = \mathrm{tr}\{e^{-\beta H}\}, \tag{1.2}$$

where T is the temperature and $\beta = 1/T$. Implicitly I am setting the Boltzmann constant $k_B = 1$ — this is done throughout the thesis. The trace in the definition of the partition function Z is a sum made over all degrees of freedom of the system - all possible values of

the $\{\theta_n\}$ [41]. As previously noted, a phase transition is associated with a nonanalyticity of this free energy.

If H is analytic, the sole way in which Eq. (1.1) can be singular is if the partition function vanishes. But Z represents a sum of positive contributions and, thus, cannot vanish in a finite system. Nonetheless, this might change in the thermodynamic limit of an infinite system (infinite degrees of freedom). The reason for this is that the partition function Z has complex roots that may become real in this limit [42]. Therefore, a phase transition is precisely defined only in the thermodynamic limit.

Having determined one primary requirement for the existence of a phase transition, let us analyze some properties of the free energy. Thermodynamic variables come in two types, extensive and intensive. The former depends on scale or the size of the system, meaning that if the system is rescaled by a factor l, they also rescale by this factor. Some examples are energy, volume, entropy and magnetization: they double when the size of the system is doubled. In contrast, intensive variables do not rescale, and examples include temperature, pressure and magnetic field.

The free energy is a function of both types of variables. For concreteness and simplicity of discussion, I consider a system of spins residing on the vertices (sites) of a d-dimensional hypercubic lattice with linear size L. The volume and number of spins in the system are given by $V = N = L^d$, assuming a lattice spacing $a = 1$. In this case F is a function of the temperature T, an external magnetic field B and N. We should expect the free energy to be extensive. Increasing the size of the system should increase its free energy. In fact this is a direct consequence of the extensivity of energy and entropy (and magnetization), and is captured by the relation

$$F(T, B, N) = l^{-1}F(T, B, lN) = Nf(T, B), \tag{1.3}$$

where in the last equality I made $l = 1/N$. In addition, $f(T, B) = F(T, B, 1)$ is the free energy per spin.

However, Eq. (1.3) is incompatible with critical behavior [43–45]. To see this, let us consider the isothermal susceptibility per spin given by $\chi = -(1/N)(\partial^2 F/\partial B^2)$. This is a significant quantity in the study of critical phenomena in magnetic materials because of

its direct relation to measurable quantities and notable singular behavior. For instance, in many models, the susceptibility per spin diverges at the critical point.

Hence, suppose we have a *finite* system at the critical values of temperature, T_c, and field, B_c. Then the only parameter still not fixed is N. Since we are not at the critical point $(T_c, B_c, N^{-1} \to 0)$ yet, χ is finite. Hence, to get a diverging susceptibility per spin when $N \to \infty$ we must have $\chi(T_c, B_c, N) \propto N^a$, with $a > 0$. But extensivity (1.3) demands that χ must be independent of N in the thermodynamic limit: $\chi = -(\partial^2 f/\partial B^2)$. To emphasize, $f(T, B)$ is independent of N; the previous derivative cannot be finite for $N^{-1} > 0$ and diverge when $N^{-1} \to 0$.

The approach to solving this difficulty is the introduction of a new scaling for the free energy. Actually, the free energy is typically split in an analytic and a nonanalytic parts, with the latter responsible for critical behavior. For simplicity I will neglect the regular part and call the singular part just the free energy.

So, let us assume that, instead of the extensive relation (1.3), the free energy per particle obeys the generalized homogeneous equation

$$f(t, B, L^{-1}) = l^{-d} f(l^{1/\nu} t, l^y B, l L^{-1}), \tag{1.4}$$

where I introduce the reduced temperature $t = (T - T_c)/T_c$ and use L^{-1} instead of N. In the case of magnetic systems, the critical field usually occurs at $B_c = 0$. Hence, the critical point is placed at the origin of the parameter space generated by these variables. In the end, Eq. (1.4) sacrifices one of the properties of the intensive variables t and B, which was the absence of a scaling factor upon rescaling.

Next, let us consider the consequences of the scaling form (1.4). I have already mentioned that some thermodynamic quantities present a nonanalytical power law behavior near a critical point. We should hope this ansatz for the free energy functional gives us that. Only latter I will attempt to justify it.

First, with a little abuse of notation, I denote by $f(t, B) = f(t, B, 0)$ the free energy per particle in the thermodynamic limit. This quantity, the bulk free energy, is always

finite, including in the critical point. By making $l = L$ in (1.4), we get

$$f(t,0) = \lim_{L\to\infty} f(t,0,L^{-1}) = \lim_{L\to\infty} L^{-d} f(L^{1/\nu}t, 0, 1), \tag{1.5}$$

$$f(0,B) = \lim_{L\to\infty} f(0,B,L^{-1}) = \lim_{L\to\infty} L^{-d} f(0, L^{y}B, 1). \tag{1.6}$$

In order for $f(t,B)$ to be finite we must require $f(x,0,1) \sim |x|^q$ and $f(0,x,1) \sim |x|^p$, with $-d + q/\nu = 0$ and $-d + py = 0$, when $x \to \infty$. Here, "$\sim$" means functional dependence on the variable on the right, with coefficients omitted. These lead to $f(t,0) \sim |t|^{d\nu}$ and $f(0,B) \sim |B|^{d/y}$, which, again, finiteness demands $\nu > 0$ and $y > 0$. Moreover, this means the following scaling relation for $f(t,B)$,

$$f(t,B) = l^{-d} f(l^{1/\nu}t, l^{y}B) \tag{1.7a}$$

$$= |t|^{d\nu} \mathcal{F}_{\pm}(B/|t|^{y\nu}), \tag{1.7b}$$

where I made $l^{1/\nu} = 1/|t|$ in the second equality and introduced the scaling function $\mathcal{F}_{\pm}(x) = f(\pm 1, x)$.

Now it is explicit in (1.7b) that the thermodynamic limit bulk free energy will have a power law singularity on the distance from the critical temperature $t = 0$. Further exploring the consequences of Eqs. (1.4) and (1.7a), one notes this power law singular behavior is inherited by the thermodynamic quantities derived from the free energy. The exponents appearing in these derivatives are called *critical exponents* and are functions of the dimension d and the previously introduced ν and y.

For instance, it is observed that the specific heat at the critical field behaves as $c_{B=0} \sim |t|^{-\alpha}$ near the critical point $t = 0$. Finiteness of the energy per particle imposes $\alpha < 1$. Deriving (1.7b) twice with respect to temperature we obtain this general form with the critical exponent $\alpha = 2 - d\nu$, which gives the bound $\nu > 1/d$.

More, deriving (1.7b) with respect to B we obtain the magnetization per spin,

$$m = -\frac{\partial f}{\partial B} = -|t|^{(d-y)\nu} \mathcal{F}'_{\pm}(B/|t|^{y\nu}). \tag{1.8}$$

This shows the magnetization at zero field vanishes in the vicinity of the critical point as

$m_0 = m(B = 0) \sim |t|^\beta$, with $\beta = (d - y)\nu$ and $y < d$. Indeed, in a ferromagnetic to paramagnetic transition, m_0 possesses a nonzero value in the low temperature ordered phase, and vanishes for temperatures $t > 0$. A quantity such as m_0, that vanishes in the high temperature phase and is nonzero in the other, represents a so-called *order parameter*, and β is the order parameter critical exponent. This behavior also implies $\mathcal{F}'_+(0) = 0$ while $\mathcal{F}'_-(0) \neq 0$.

Another exponent related to the order parameter is the one giving the shape of the critical isotherm $t = 0$ near the critical point (B small), and is denoted by δ: $m \sim B^{1/\delta}$. It reads $\delta = y/(d - y)$.

Finally, deriving one more time with respect to B, we obtain the susceptibility

$$\chi(t, B) = -|t|^{(d-2y)\nu}\mathcal{F}''_\pm(B/|t|^{y\nu}) \sim |t|^{-\gamma} \text{ (at zero field)}, \tag{1.9a}$$

$$\chi(t, B, L^{-1}) = L^{2y-d}\mathcal{F}_\chi(L^{1/\nu}t, L^y B), \tag{1.9b}$$

where $\gamma = (2y - d)\nu$. This gives a diverging susceptibility in the critical point when $2y > d$. In (1.9b) I wrote the finite-size scaling of the susceptibility to emphasize that now we get the non extensive behavior we were expecting. If we take the limit $L \to \infty$ in this equation, we can obtain a divergence, which was not compatible with (1.3). Here, $\mathcal{F}_\chi(x, y) = \partial_y^2 f(x, y, 1)$ is another scaling function.

Since all critical exponents are functions of (d, ν, y), several relations may be established between them and these are referred to as *scaling laws*. An example is: $\alpha+2\beta+\gamma = 2$. In addition, the specific heat, magnetization and susceptibility all represent measurable quantities and these exponents can be determined by experiment. In table 1.1 I summarize the most commonly used critical exponents.

Therefore, the scaling hypotheses (1.4) and (1.7a) are capable of expressing a singularity in the free energy and give the power law behavior of thermodynamic quantities characteristic of critical phenomena. The subsequent step is to justify them.

To achieve this, it will be beneficial to consider explicitly the Ising model. This is likely the simplest model exhibiting a continuous phase transition and it will occupy a

leading role in this thesis. Its classical version has a Hamiltonian given by

$$H = -J \sum_{\langle i,j \rangle} \sigma_i \sigma_j - B \sum_i \sigma_i. \tag{1.10}$$

Here, σ_i is the spin variable at site i, which may assume one of two configurations, up or down, or the values ± 1. In the first term, the coupling constant J gives the interaction between spins and $\langle i, j \rangle$ means the sum is between nearest neighbors. The second term represents a coupling between the individual spins and an external (longitudinal) magnetic field B, which we can assume to be measured in units of energy. The magnetization in this model is simply given by $m = (1/N) \sum_i \langle \sigma_i \rangle$, where the brackets mean statistical mechanics average.

For $J > 0$ and $d > 1$ the Ising model is known to present a continuous transition from a ferromagnetic to a paramagnetic phase at vanishing magnetic fields [46–48]. A ferromagnetic interaction ($J > 0$) favors alignment of spins in the same direction. Hence, at $T = 0$ and zero field, the system has all spins pointing up or down and exhibit a spontaneous magnetization $m_0 = \pm 1$, depending on the configuration.

Effectively, the system will choose the up or down state based on the initial conditions, as in if B approached zero from above or bellow. Let us consider the initial configuration is of all spins pointing up. That is, the system is in a ferromagnetic phase with spontaneous magnetization $m_0 = 1$. As T is increased above zero, the spins start to fluctuate, and at all times, a net fraction of them will point down, reducing the spontaneous magnetization. At some temperature T_c, this magnetization eventually drops to zero, and above it, the system will be found in a paramagnetic phase.

Before returning to the problem of justifying the scaling hypothesis (1.7a), let me present another important concept common in many critical phenomena. If we look at the Ising Hamiltonian (1.10), we note $H(\{J, B = 0\}, \{\sigma_i\})$ is invariant under the operation $\{\sigma_i\} \to \{-\sigma_i\}$. This symmetry is reflected on the magnetization in the paramagnetic phase, $m_0 \propto \langle \sigma_i \rangle = 0$. However, this is untrue in the ferromagnetic phase, where $m_0 \propto \langle \sigma_i \rangle \neq 0$. This nonpreservation of a symmetry of the Hamiltonian in the statistical average $\langle \sigma_i \rangle$ below the critical point is denoted an *spontaneous symmetry breaking*.

Next, I introduce the two-point correlation function between spins i and j given by

$$\begin{aligned} G(\mathbf{r}_i, \mathbf{r}_j) &= \langle \sigma_i \sigma_j \rangle - \langle \sigma_i \rangle \langle \sigma_j \rangle \\ &= \langle (\sigma_i - \langle \sigma_i \rangle)(\sigma_j - \langle \sigma_j \rangle) \rangle, \end{aligned} \tag{1.11}$$

where $\mathbf{r}_{i,j}$ gives the position of spin i, j. The second equality shows that G measures the correlation of the fluctuations from the average magnetization of the two spins. This function is manifestly translational invariant for periodic boundary conditions but this also holds for open boundary conditions in the thermodynamic limit. Hence, G is in fact a function of only the distance between spins, $G = G(r = |\mathbf{r}_i - \mathbf{r}_j|)$.

Working with the partition function of (1.10), it is easy to demonstrate that

$$\begin{aligned} \chi &= \frac{1}{T} N^{-1} \sum_{i,j} G(i,j) \\ &= \frac{1}{T} \sum_{\mathbf{r}} G(r), \\ &= \frac{a^{-d}}{T} \int \mathrm{d}^d \mathbf{r}\, G(r), \end{aligned} \tag{1.12}$$

where I utilized the translational invariance of G to get the second equality and the thermodynamic and continuous limits to convert the sum into an integral. In the third line, a is the lattice spacing - the distance between vertices. The susceptibility is an example of a response function; it tells how the system reacts, by changing its magnetization, to a varying magnetic field. Equation (1.12) is an example of the more general fluctuation-dissipation theorem, relating a response function to the fluctuations in the associated extensive variable.

Hence, the behavior of the susceptibility is regulated by the integral on the right, and any divergence of it must come from a long-ranged correlation. Indeed, for sufficiently long distances and $T \neq T_c$, the correlation function behaves as [43, 49]

$$G(r) \sim \frac{e^{-r/\xi}}{r^{(d-1)/2} \xi^{(d-3+2\eta)/2}}, \tag{1.13}$$

where ξ is called the *correlation length*, and provides a measure of the extent over which

the fluctuations in the spins are correlated. Clearly this quantity must depend on the temperature of the system. The fast decaying of correlations at long distances when $T \neq T_c$ gives a nondivergent susceptibility.

In contrast, right at T_c we have [43, 44, 49],

$$G(r) \sim \frac{1}{r^{d-2+\eta}}, \tag{1.14}$$

where η is another critical exponent describing the behavior of the correlation function precisely at T_c. Through the relation between the correlation function and susceptibility we get new scaling laws, like $\gamma = (2y - d)\nu = (2 - \eta)\nu$, which can be used to determine y.

Now, the sole way in which Eqs. (1.13) and (1.14) can be made compatible is through the divergence of the correlation length at the critical point. As a matter of fact, the critical exponent ν introduced on Eq. (1.7a) is precisely the one associated with the divergence of ξ,

$$\xi \sim |T - T_c|^{-\nu} \sim |t|^{-\nu}. \tag{1.15}$$

Having said that, all singularities of critical phenomena can be understood as resulting from this divergent correlation length [43, 50]. To appreciate this, we note the bulk free energy (1.7a) divided by T has dimensions of $[\text{length}]^{-d}$. As a result, we may hope for an expansion in the form [43, 44]

$$\frac{f(t, B)}{T} = \xi^{-d}\left(A_0 + A_1\left(\frac{a_1}{\xi}\right)^{\lambda_1} + A_2\left(\frac{a_2}{\xi}\right)^{\lambda_2} + \ldots\right), \tag{1.16}$$

where a_n are other length scales of the system — such as the lattice spacing a —, A_n are some function coefficients with nonsingular behavior, and λ_n are nonnegative exponents. Thence, sufficiently close to the critical point, ξ becomes the dominant length scale, and all other terms may be ignored, leading to

$$f \sim \xi^{-d} \sim |t|^{d\nu}, \tag{1.17}$$

exactly what we obtained starting with the scaling hypothesis (1.4). Indeed, the divergence of a length scale is the trademark of critical phenomena [43–45, 49].

A qualitative discussion of the results above can be made as follows [44]. At very large temperatures, thermal noise is the completely dominant factor and the spins fluctuate wildly and at total randomness. In this situation there are little correlations between them and the correlation length is small, of the order of one lattice spacing. As T is decreased, the interaction J is able to form small clusters of correlated spins, which can arbitrarily point up or down, and are spread over the system. These clusters will have an average volume given by ξ^d. Further decreasing the temperature, increases the correlation length; the volume of the clusters grows on average.

Now looking at the ordered phase, close to zero temperatures, the spins will be aligned up or down and there is little fluctuations, which occur at random. Once more, the correlation length is small, of the order of the lattice spacing. However, as T is raised, fluctuations increase and allows the interaction between neighbors to produce small clusters of flipped spins. These will have an average volume ξ^d, and will be dispersed over the system. As the temperature is further raised, the average volume of these clusters increase.

Near the critical temperature, the competition between the tendency to order imposed by the interaction and of disordering imposed by the thermal noise is fierce [44]. Just above T_c there is a nearly spontaneous magnetization in the system, and, therefore, there must exists large agglomerations of spins aligned in the same direction. Hence, a large correlation length. A similar picture applies just below T_c. Again, there will be massive clusters of spins pointing up and down, and only a minor fraction makes the difference to give a nonzero magnetization. Additionally, since these large clusters constitute by themselves macroscopic systems, they must contain several other clusters of inverted spins with sizes ranging from 0 to ξ. This means fluctuations occur on all length scales of the system. In the thermodynamic limit, and right at T_c (and B_c), the correlation length diverges.

We are in the position now to discuss the issue with the extensivity of the free energy (1.3) close to the critical point. Extensivity is built on the idea that subsystems may be added together to form a larger system and that the properties of these subparts can be simply extended to the whole. It works as long as interactions are sufficiently short ranged and the pertinent length scales of the subsystems are small, so that boundary effects can

be neglected. Clearly, that is not the case when we have an increasing correlation length as the critical point is approached. In this scenario, the idea of adding subsystems to build a whole can make sense only if applied to the aforementioned clusters, which have an average volume ξ^d. If the total system has N spins, the number of clusters should be close to N/ξ^d, and the total free energy would be given by $F = (N/\xi^d) f_\xi \sim N|t|^{d\nu} f_\xi$, where f_ξ is the free energy of a cluster. This gives a free energy per spin $F/N \sim |t|^{d\nu}$, once again consistent with our previous results. Precisely at the critical point, $\xi \to \infty$, and the entire system must be treated as a single unit.

The divergence of the correlation length also implies a new symmetry to the system [43, 49]. Since the system is highly correlated for distances of order ξ, we may consider the treatment of blocks of spins of linear dimension $la \ll \xi$ as a single spin unity [50]. The block-spin variables can be constructed to possess the same range of values as the originals — $\sigma_{\text{block}} = \pm 1$ in the Ising model — and be placed at the center of the blocks. After this coarse-graining, the system will consist of interacting spins separated by a distance la. In terms of the new length scale unity la, the correlation length would be smaller and the block system would appear as if more distant from criticality. If now we rescale all lengths by a factor l, $x \to x/l$, we essentially recover the original lattice but with an effective Hamiltonian with different coupling constants $\{C'_n\}$.

This two-step procedure forms a renormalization group transformation [43]. And is made in such ways that it preserves the symmetries of the original Hamiltonian, and the partition function and statistical averages, in the sense that [43, 44, 49]

$$Z(\{t', C'_n\}) = Z(\{t, C_n\}) \tag{1.18}$$

$$\langle \bullet \rangle_{\{t', C'_n\}} = \langle \bullet \rangle_{\{t, C_n\}}. \tag{1.19}$$

In (1.19) each side gives averages which are functions of the specified coupling constants.

The fixed points of a renormalization group transformation determine the stable phases as well as the critical point of a system. At the latter, the system becomes scale invariant for distances $r \gg a$, which is reflected on the correlation function (1.14) at T_c, where $G(r/l) = l^{d-2+\eta} G(r)$. That is, the physics of correlations remain the same under this

transformation. More generally, however, we have

$$G(r;t,B) = l^{-(d-2+\eta)}G(r/l;l^{1/\nu}t,l^{y}B), \tag{1.20}$$

where I made explicit the dependence of G on t and B through the correlation length ξ.

The relation (1.20) for the correlation function mirror the scaling hypothesis of the free energy (1.7a). In fact, these generalized homogeneous equations steam from the rescaling of the parameters and physical quantities of the system under a renormalization group transformation. Particularly, for a renormalization parametrized by l, a coupling constant set $\{t, C_n\}$ gets rescaled to $\{t', C_n'\} = \{l^{1/\nu}t, l^{y_n}C_n\}$, with these scaling exponents determined amidst the transformation. Meanwhile the free energy per spin changes as $f(\{t, C_n\}) = l^{-d}f(\{t', C_n'\})$, since N scales with l^d; the form of our starting scaling hypothesis.

Having justified the scaling hypothesis (1.4) and (1.7a), I move to the concepts of universality and crossover phenomena. The exponents ν and y_n associated with the scaling of the coupling constants may be positive, negative or null, and this has great impact on the behavior of the system. To illustrate this, let us revisit Eq. (1.7b), that shows the bulk free energy in a magnetic system may be written as

$$f(t,B) = |t|^{d\nu}\mathcal{F}_{\pm}(B/|t|^{y\nu}). \tag{1.21}$$

If $y > 0$, the limiting behavior we get from $\mathcal{F}_{\pm}$ depends crucially on whether or not B is exactly zero when the critical limit $t \to 0$ is approached. When the field is at its critical value $B = 0$ we get $\mathcal{F}_{\pm}(0)$, otherwise it is the limit $\mathcal{F}_{\pm}(x \to \infty)$ that matters when we take $t \to 0$. Hence, in this example, the presence of a nonzero field takes the system away from criticality. For this reason, coupling constants associated with positive scaling exponents are termed *relevant variables*. To be at a critical point, they must be adjusted to their exactly critical values. The temperature exponent $1/\nu$ is obviously positive, or else it would be impossible for thermally driven phase transitions to exist at all.

Contrarily, if y was negative, it would be inconsequential whether $B \neq 0$, since the combined variable $B/|t|^{y\nu}$ would always vanish as $t \to 0$. Therefore, coupling constants associated with negative exponents constitute *irrelevant variables*.

Ordinary critical points have two relevant variables. For magnetic systems they are temperature and the external magnetic field (or, to be more precise, B/k_BT); for the liquid-gas critical point, they are temperature and pressure. But it is possible to have more than two.

That said, suppose we start with a Hamiltonian containing several parameters describing microscopic details of the system, such that the associated free energy is a function of $f(t, C_2, C_3, C_4, ...)$. Sufficiently close to an ordinary critical point, what matter is almost invariably the limit $f(t, C_2, 0, 0, ...)$ because of the distinction between relevant and irrelevant variables.

It is already clear from this argument that an infinitude of systems differing by distinct microscopic details, expressed in the irrelevant variables, can have similar critical behavior. Concretely, this behavior is characterized by the values of the critical exponents, e.g. ν and η. And it is observed that these exponents depend only on very general features like the dimensionality of the system, the symmetries of the Hamiltonian and range of interactions. This leads to the concept of *universality*: microscopically distinct systems sharing only general features have similar critical behavior. Thence, critical systems characterized by the same exponents form an universality class. For instance, the Ising universality classes also contains various liquid-gas transitions.

The idea of universality also implies the critical behavior of a number of systems can be understood by examining just the simplest model in the same class. This model would focus solely on the relevant variables. The Ising Hamiltonian precisely gives an example of such a model.

Next, from the above discussion on the behavior of parameters under a renormalization group transformation, we note the size of the system constitute a relevant variable. In particular, L^{-1} has an scaling exponent $y_L = 1$, and, consistently, has to be adjusted to the appropriate value $L^{-1} = 0$ for the system to be at the critical point.

Let us consider again our magnetic system at the critical field $B = 0$. For a finite system we have

$$\begin{aligned} f(t, L^{-1}) &= l^{-d} f(l^{1/\nu} t, l L^{-1}) \\ &= |t|^{d\nu} \mathcal{F}_L^{\pm}(L^{-1}|t|^{-\nu}), \end{aligned} \tag{1.22}$$

Table 1.1: Summary of common critical exponents. I use magnetic systems as an example. In the last column I specify their values in the two-dimensional Ising universality class.

Quantity	**exponent**	**relation**	$d = 2$ **Ising**
specific heat	α	$c_{B=0}(t \to 0) \sim \lvert t\rvert^{-\alpha}$	0 (log)
order parameter	β	$m_0(t \to 0^-) \sim (-t)^{\beta}$	1/8
susceptibility	γ	$\chi(t \to 0, B = 0) \sim \lvert t\rvert^{-\gamma}$	7/4
critical isotherm	δ	$m(t = 0, B \to 0) \sim \lvert B\rvert^{1/\delta}$	15
correlation length	ν	$\xi(t \to 0, B = 0) \sim \lvert t\rvert^{-\nu}$	1
critical correlation	η	$G(r; t = 0, B = 0) \sim r^{-(d-2+\eta)}$	1/4
equilibration time	z	$\tau_{\text{eq}}(t \to 0, B = 0) \sim \xi^z$	1

where for simplicity I omitted the dependence on B completely, and $\mathcal{F}_L^{\pm}(x) = f(\pm 1, x)$ is a scaling function.

Under these circumstances, there is a region of large enough L and small enough t such that $L^{-1}|t|^{-\nu} \ll 1$ and the asymptotic behavior of $\mathcal{F}_L^{\pm}$ is the same as if the system was infinite. That is, we get the limit $x \to 0$ of $\mathcal{F}_L^{\pm}(x)$. For an experimentalist working on this regime, the thermodynamic properties of the system look critical.

However, when $|t|$ is further lowered and placed nearer the critical value $t = 0$, one enters the limit $L^{-1}|t|^{-\nu} \gg 1$, and, therefore, gets the limit $x \to \infty$ of $\mathcal{F}_L^{\pm}(x)$. In a finite system sufficiently close to the transition temperature, the asymptotic scaling behavior is deviated from the critical one.

This change in asymptotic behavior is called crossover phenomena. As a consequence of the finiteness of the system, the correlation length cannot surpass the length L as $t \to 0$. The usual divergences of thermodynamic quantities are then replaced by rounded peaks with their maxima displaced from the infinite system transition temperature.

To finish, thus far I made no reference to dynamics, and considered only static properties. The reason for this is the that in classical statistical mechanics, the kinetic and

potential parts of a Hamiltonian usually decouple. If we consider a classical Hamiltonian $H(\mathbf{q}, \mathbf{p}) = H_{\text{kin}}(\mathbf{p}) + H_{\text{pot}}(\mathbf{q})$, where $\mathbf{q}$ and $\mathbf{p}$ are generalized coordinates and momenta, the partition function separates into $Z_{\text{kin}} Z_{\text{pot}}$. The first part usually steams from Gaussian integrals, and, therefore, will present no singularities. This fact greatly simplifies the study of classical critical phenomena, since it allows the use of time-independent models, such as (1.10).

Nonetheless, as we saw, the increase in the correlation length near a critical point means larger regions of fluctuations of the system about its equilibrium condition. Consequently, we could expect the time the system takes reequilibrating to also becomes longer. This phenomenon is known as critical slowing down. A phenomenological dynamical theory [43] of the order parameter shows that, as the system approaches the critical point, the time it takes to reequilibrate diverges as

$$\tau_{\text{eq}} \sim \xi^z \sim |t|^{-z\nu}, \tag{1.23}$$

where z is called the dynamical critical exponent and is independent of the critical exponents presented before.

Moreover, I have been implicitly assuming $d_l < d < d_u$, where d_l and d_u are called the lower and upper critical dimensions [43]. Their meaning is that when $d \leqslant d_l$, the fluctuations on the system are too strong and no ordered phase can exist at $T > 0$. On the other hand, when $d \geqslant d_u$, fluctuations are no longer important for determining the critical exponents; they no longer depend on d and can be obtained using mean-field theory [43, 44, 49].

1.2 Quantum phase transitions

Quantum phase transitions occur at zero temperature and are driven by quantum fluctuations, instead of thermal. At the limit $T = 0$, the free energy is equivalent to the ground state energy, and statistical averages are replaced by ground state averages. A quantum phase of matter, therefore, is characterized by specific properties of the ground state of a quantum many-body system. Accordingly, a quantum phase transition is associated with

singularities of this ground state as a function of some nonthermal parameter g in the system Hamiltonian. To give some examples, g can be a pressure, a magnetic field or a chemical potential.

This nonanalyticity may result, for instance, from a reordering of the ground and an excited energy levels at some point g_1. Where this level crossing occurs, the derivative of the ground state energy has a discontinuity, and the transition is of first-order — see Fig. 1.1(a). First-order transitions can happen even if the system is finite.

Let us consider now the Hamiltonian

$$H(g) = H_0 + gH_1, \tag{1.24}$$

where H_0 and H_1 are independent of g, and $[H_0, H_1] \neq 0$; i.e. they do not commute. This noncommutativity of H_1 with H_0 introduces fluctuations of a quantum nature in the system, controlled by the parameter g. Furthermore, g establishes a clear competition between the two parts of this Hamiltonian. To illustrate, in the limit $g \ll 1$, the system ground state is close to that of H_0, while in the opposite limit, $g \gg 1$, it is close to that of H_1.

In a finite system, the eigenvalues and eigenstates of $H(g)$ are analytic functions of g. Suppose there is a point g_c where an avoided level crossing between ground and first-excited energy levels occurs, a point where the energy gap is minimum — see Fig. 1.1(b). In the thermodynamic limit, this gap might close, and a singularity may develop in the ground state and ground state energy. This constitutes a continuous quantum phase transition, g_c being the quantum critical point.

Indeed, as the system approaches the quantum critical point at g_c, this gap closes as

$$\Delta \sim |g - g_c|^{z\nu}, \tag{1.25}$$

where z and ν are the dynamic and correlation length critical exponents introduced before. Since a diverging time scale is a mark of critical phenomena, by the time-energy uncertainty relation, we should expect quantum criticality to be characterized by a vanishing energy scale.

This can be made formal by a mapping between the partition function of a d-dimensional

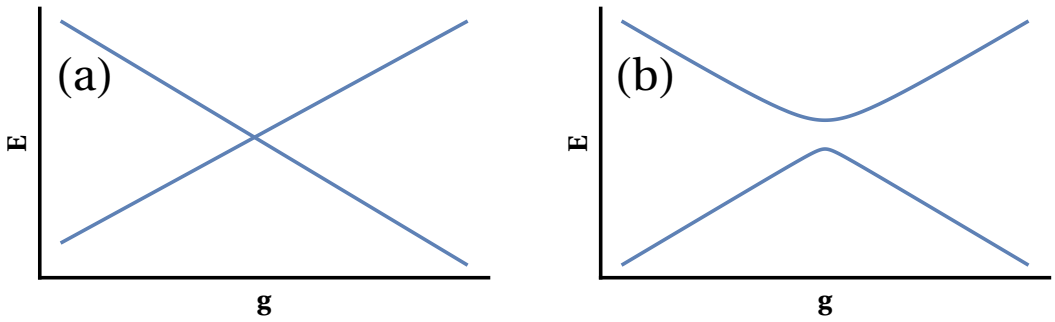

Figure 1.1: Behavior of the two lowest energy levels of $H(g)$ as a function of g. In (a) $[H_0, H_1] = 0$, and there is a level crossing. These are associated with first-order transitions. In (b) $[H_0, H_1] \neq 0$, and there is an avoided level crossing. In the thermodynamic limit the gap might close, in association with the emergence of a singularity. This comprises a continuous transition.

quantum system and a $(d + z)$-dimensional classical model [49, 51–53]. Under this mapping, the inverse of the quantum energy gap maps onto a diverging correlation length in a "time" direction in the classical model. This, in turn, diverges with an exponent $z\nu$.

The general idea is to write the canonical operator $e^{-\beta H}$ as an imaginary-time propagator $e^{-N(\tau/\hbar)H}$, with $\tau \to 0$, $N \to \infty$, such that $N(\tau/\hbar) = \beta$. Then use the path-integral formulation of quantum mechanics to map the quantum partition function onto the partition function of a higher dimensional classical system [53],

$$\begin{aligned} Z = \mathrm{tr}\{e^{-\beta H}\} &= \sum_{n_0} \langle n_0 | e^{-\beta H} | n_0 \rangle \\ &= \sum_{n_0} \sum_{n_1} \dots \sum_{n_N} \langle n_0 | e^{-(\tau/\hbar)H} | n_1 \rangle \langle n_1 | e^{-(\tau/\hbar)H} | n_2 \rangle \dots \langle n_N | e^{-(\tau/\hbar)H} | n_0 \rangle. \end{aligned} \tag{1.26}$$

Above I introduced complete sets of orthonormal bases vectors $\{|n_i\rangle\}$. The numbers n_i play the role of the classical dynamical variables.

Such a map is certainly better understood with an example. The most straightforward case involves the one-dimensional classical Ising model and a single qubit.

The $d = 1$ classical Ising Hamiltonian at zero field is given by

$$H_C = -J \sum_{i=1}^{N} \sigma_i \sigma_{i+1}, \tag{1.27}$$

where N is the number of spins in the chain, and $\sigma_i = \pm 1$. I consider periodic boundary

conditions: $\sigma_{N+1} = \sigma_1$. Then the chain is in fact a ring.

The corresponding partition function for a chain at a temperature T_C reads [43, 49]

$$Z = \sum_{\sigma_1=\pm1} \dots \sum_{\sigma_N=\pm1} e^{-H_C/T_C} = \sum_{\sigma_1=\pm1} \dots \sum_{\sigma_N=\pm1} \prod_{i=1}^{N} T_{\sigma_i,\sigma_{i+1}} = \mathrm{tr}\{T^N\}, \tag{1.28}$$

where T is a so-called transfer matrix and, in this case, is given by

$$T = \begin{pmatrix} T_{1,1} & T_{-1,1} \\ T_{1,-1} & T_{-1,-1} \end{pmatrix} = \begin{pmatrix} e^{J/T_C} & e^{-J/T_C} \\ e^{-J/T_C} & e^{J/T_C} \end{pmatrix} = e^{J/T_C}(1 + e^{-2J/T_C}\sigma^x). \tag{1.29}$$

In the last equality, σ^x is the Pauli matrix

$$\sigma^x = \begin{pmatrix} 0 & 1 \\ 1 & 0 \end{pmatrix}. \tag{1.30}$$

The transfer matrix receives this name because it transfers the trace from one site to the next. In the case of a two-dimensional lattice, the transfer is between one row to the next. If $d = 3$, the transfer is between one plane to another. And so on.

One can also compute the system correlation function, which in the thermodynamic limit $N \to \infty$ is given by [43, 49]

$$\begin{aligned} G(i, i+j) &= \langle \sigma_{i+j}\sigma_i \rangle = e^{-j\tau\xi}, \\ \xi &= \frac{\tau}{\ln \coth(J/T_C)}, \end{aligned} \tag{1.31}$$

where τ is the lattice spacing. As one can see, for $T_C > 0$ these correlations decay exponentially, and in the one-dimensional model an ordered state exists only at zero temperature.

As $T_C \to 0$ the correlation length diverges as $2\xi/\tau \approx e^{2J/T_C}$. Using this on (1.29) we get

$$T \approx e^{J/T_C}\left(1 + \frac{\tau}{2\xi}\sigma^x\right) \approx e^{-(\tau/\hbar)H_Q}, \tag{1.32}$$

$$Z = \mathrm{tr}\{T^N\} \approx \mathrm{tr}\{e^{-H_Q/T_Q}\}, \tag{1.33}$$

where I introduced the single qubit Hamiltonian

$$H_Q = e_0 - \frac{\Delta}{2}\sigma^x, \tag{1.34}$$

with $e_0 = -(\hbar/\tau)J/T_C$, an energy gap Δ, and at a temperature T_Q given by

$$\Delta = \hbar/\xi, \tag{1.35}$$

$$T_Q = \frac{1}{N(\tau/\hbar)}. \tag{1.36}$$

The quantum partition function on the right hand side of (1.33) and the classical one on the left become equivalent precisely in the limit $\xi \to \infty$ (or $\tau \to 0$) [49].

This example illustrates the general features of the quantum-classical mapping. To begin, we see there is an intimate relation between quantum evolution over an imaginary time, represented by $e^{-(\tau/\hbar)H_Q}$, and the transfer matrix of the classical model. This is the reason for calling this direction of "transfering" in the classical system a "time" direction. Note that τ is the lattice spacing in the time direction.

Next, the temperature of the quantum system is completely unrelated with the temperature of the equivalent classical model, and indeed only defines the size of its extra "time" dimension. In the limit $T_Q \to 0$, the classical system is infinite along the "time" axis.

Finally, what is mapped onto the temperature of the classical system, responsible for its phase transitions, is a coupling constant of the quantum Hamiltonian H_Q. This is expressed by the relation between the quantum gap and the correlation length in (1.35). Therefore, T_C on the classical partition function represents a measure of the quantum fluctuations in the equivalent quantum system.

Actually, the relation between an energy gap and a correlation length can me made more general. Let us consider the imaginary time Heisenberg representation of an observable O; this is given by — henceforth making $\hbar = 1$ —

$$O(\tau) = e^{\tau H_Q} O e^{-\tau H_Q}. \tag{1.37}$$

Hence, for a quantum system at zero temperature, we have the following correlation func-

tion for such an observable

$$G(\tau) = \langle 0|O(\tau)O|0\rangle = \sum_n e^{-(\epsilon_n - \epsilon_0)\tau} |\langle 0|O|n\rangle|^2, \tag{1.38}$$

where $H_Q\,|n\rangle = \epsilon_n\,|n\rangle$ are the quantum Hamiltonian eigenvalues and eigenvectors, with $|0\rangle$ the ground state.

According to the quantum-classical mapping, this correlation function is equivalent to the spatial correlators derived from the partition function of the related classical model [49]. The existence of an energy gap, therefore, ensures that for large τ (long distances) the correlation function will decay exponentially with a characteristic length given by $\xi \sim 1/\Delta = 1/(\epsilon_1 - \epsilon_0)$.

However, there are also some particularities in this illustration of such a mapping. First, in this example, $d = 0$ in the quantum system and the classical model has only the "time" dimension. When $d > 0$, the spatial dimensions of the quantum system are mapped onto an equal number of spacial dimensions in the classical model. Additionally, in our example, the correlation length diverges exponentially as a function of T_C, and not in a power law form. As we saw, the latter is the standard fashion in continuous phase transitions and defines the critical exponent ν. Moreover, here the dynamical critical exponent z is equal to unity. Although common, this is not general, and z can have other values, depending on the kinetic part of the quantum Hamiltonian [49, 51–53].

In contrast with classical systems, in quantum mechanics, the kinetic and potential parts of the Hamiltonian generally do not commute. In the quantum regime, dynamics and statics are coupled. This is the reason why the quantum partition function also contains information about the dynamics of the system [49, 51–53]. As explored above, there is an equivalence between the canonical operator $e^{-\beta H}$ and the imaginary time evolution operator $e^{-\tau H}$ over the interval $\tau \in [0, \beta]$. Naturally, one is usually interested in the real-time dynamics of correlators in the quantum system. In principle, this can be obtained from (1.38) by an analytic continuation $\tau \to it$ [49, 53].

It is clear now that the concepts introduced before in the context of classical critical phenomena are readily extended to quantum criticality. Second-order — or, more generally, continuous — quantum phase transitions are also marked by diverging correlation

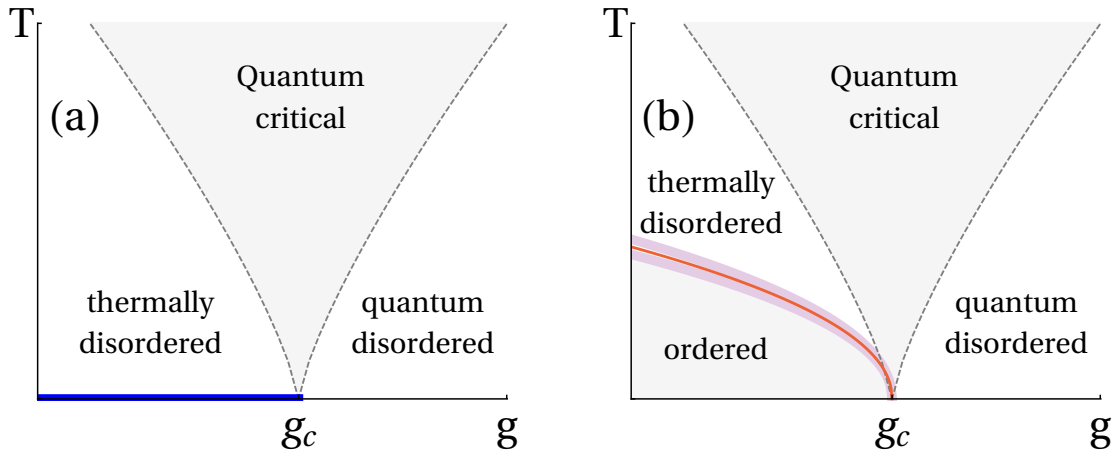

Figure 1.2: Schematic representation of the two possible phase diagrams in the vicinity of a quantum phase transition. In (a), an ordered phase exists solely at $T = 0$ and below a critical value g_c. This is indicated by the blue line. Above the quantum critical point seats a region loosely bounded by $T \sim |g - g_c|^{\nu z}$ where the temperature scaling can be observed. In (b), order is maintained for some temperature range. The line of finite temperature critical points in indicated in red and terminate in the quantum critical point. In the shaded area around it, classical critical phenomena are observed. Based on figures of Refs. [49, 52].

lengths and times in the vicinity of a quantum critical point. And this leads to scaling, universality and power law singularities.

For instance, at zero temperature and in the vicinity of the quantum critical point, the ground state energy per particle satisfies [51, 52]

$$f_0(g - g_c, B) = l^{-(d+z)} f_0(l^{1/\nu}(g - g_c), l^y B). \tag{1.39}$$

This is parallel to Eq. (1.7a) with the nonthermal parameter $g - g_c$ replacing t. The $(d+z)$ exponent in the right-hand side also reemphasizes the relation between quantum phase transitions in d dimensions and classical phase transitions in $(d + z)$ spatial dimensions.

Similar homogeneous equations hold for other quantities. Of particular interest is the susceptibility related to the control parameter g, which is given by the second derivative of the ground state energy density (or the free energy, more generally). This quantity replaces in quantum critical phenomena the role of the classical specific heat. In quantum phase transitions it is this susceptibility which diverges with an exponent α.

Since any experiment is necessarily performed at finite temperatures, quantum phase transitions become really interesting and important if they cause some effect at $T > 0$.

The outcome of a nonzero temperature on the quantum system can be one of two types. For once, it can completely dismantle any ordered state at $T > 0$. In this scenario, a critical point exists only at $T = 0$, and no phase transition can be observed in a real experiment — Fig 1.2(a).

The low temperature phase diagram is then divided in three parts, delimited by the preponderance of thermal or quantum fluctuations. On the left, where $g < g_c$, thermal fluctuations dominate and are responsible for the destruction of long-range order. Conversely, on the right, as in $T = 0$, it is quantum fluctuations that dominates and is responsible for disorder. In both these regions, the excitations on the system are amenable to a classical treatment [49].

In between there exists a region where both classical and quantum fluctuations are relevant. This is termed the quantum critical region and is loosely bounded by $T > |g - g_c|^{\nu z}$. In this part of the phase diagram, quantum effects are always important [49, 51–53]. As a consequence, here the system looks critical and obeys scaling relations, particularly the so-called temperature scaling. Taking the free energy as an illustrative quantity, it satisfies [51–53]

$$\begin{aligned} f((g-g_c), B, T) &= l^{-(d+z)} f(l^{1/\nu}(g-g_c), l^y B, l^z T) \\ &= T^{-(1+d/z)} \mathcal{F}_T(T^{1/\nu z}(g-g_c), T^{y/z} B). \end{aligned} \tag{1.40}$$

Such a behavior can be detected on an experiment at low temperatures and is evidence of an underlying quantum critical point.

On another case, the system may support an ordered phase at low temperatures. Then the phase diagram contains a line of continuous phase transitions that terminates on the quantum critical point at $T = 0$ — Fig. 1.2(b).

Quantum mechanics can be indispensable for the understanding of many finite-temperature ordered phases, like in superfluids and superconductors. Nonetheless, I have insisted that quantum phase transitions, i.e. those that are driven by quantum fluctuations, exists only at zero temperature. The physical argument for this can be presented as follows [51, 52].

Suppose we have a quantum system at $T > 0$, and that a phase transition occurs at a temperature T_c. As discussed in the previous section, near the critical point $t =$

$(T - T_c)/T_c = 0$ the fluctuations on the system take place over diverging distances during diverging times. In accordance, they must have a vanishing typical frequency ω_c. Following (1.23) we have

$$\omega_c \sim |t|^{\nu z}. \tag{1.41}$$

The character of these fluctuations is determined through a comparison between the quantum energy scale $\hbar\omega_c$ and the thermal energy $k_B T$. At this point I write the physical constants for clarity. Quantum effects are significant as long as $\hbar\omega_c \gtrsim k_B T$, while the fluctuations become effectively classical if $\hbar\omega_c \ll k_B T$.

Asymptotically close to $t = 0$, the condition $\hbar\omega_c \ll k_B T_c$ is always satisfied, establishing the dominance of classical behavior on the critical fluctuations. This is why there are no quantum phase transitions at finite T. In transitions at finite temperatures, quantum effects may play a role at microscopic scales, but it is thermal fluctuations that matter on the macroscopic scales relevant for critical phenomena.

If the transition temperature T_c is distinctly low, however, the asymptotic classical limit can be extremely narrow, perhaps even becoming inaccessible in some experiment. Then quantum fluctuations remain relevant very close to the critical point. In this scenario there will be a crossover from quantum critical to classical critical behavior as the transition is approximated.

From the quantum-classical mapping, one can see this is equivalent to a dimensional crossover. As long as the characteristic time τ_{eq} is lower than the "time" direction length $1/T$, the system behaves as if it was $(d + z)$-dimensional. When the transition is so close that τ_{eq} would surpass $1/T$, the system becomes effectively d-dimensional and behaves classically.

In this type of systems, the quantum critical region is again present in the vicinity of the quantum critical point at relative high temperatures [49, 51, 52].

All these effects are expected to occur at very low temperatures compared to some other energy scale set by the system Hamiltonian [49]. In the case of the Ising model, for instance, this scale is set by the exchange interaction J [49].

In the sequence of this thesis, I will consider the nonequilibrium thermodynamic protocol presented in Chapter 3 applied to a system that exhibits continuous quantum phase transitions. One of our chief results is to show there are quantities which display a signa-

ture of the quantum critical point even for systems initially in an arbitrarily high temperature.

But before we get there, I need to introduce our player model in the next chapter. Although our major results are general, it will be interesting and instructive to consider them in this particular example.

Chapter 2

Ising Model in an Alternating Transverse Field

The one-dimensional Ising model in a transverse field is arguably the simplest system displaying a continuous quantum phase transition. The model was introduced in [54–56] and its Hamiltonian may be written as

$$H = -J \sum_{j=1}^{N} \left(\sigma_j^x \sigma_{j+1}^x + g\sigma_j^z \right), \tag{2.1}$$

where N is the total number of spins in the chain and $J > 0$ is the ferromagnetic exchange coupling between nearest neighbors. The intensity of the external transverse magnetic field is controlled by the dimensionless parameter g.

The quantum operators $\sigma_j^{x,y,z}$ acting on a spin-$1/2$ at site j are the well-known Pauli matrices. These are conventionally written as

$$\sigma^z = \begin{pmatrix} 1 & 0 \\ 0 & -1 \end{pmatrix}, \quad \sigma^x = \begin{pmatrix} 0 & 1 \\ 1 & 0 \end{pmatrix}, \quad \sigma^y = i \begin{pmatrix} 0 & -1 \\ 1 & 0 \end{pmatrix}, \tag{2.2}$$

and obey the commutation relations

$$[\sigma_j^a, \sigma_j^b] = 2i\epsilon_{abc}\sigma_j^c, \tag{2.3a}$$

$$[\sigma_j^a, \sigma_l^b] = 0 \text{ for } j \neq l, \tag{2.3b}$$

where $i^2 = -1$, $a, b, c = x, y, z$ and ϵ_{abc} is the Levi-Civita symbol.

The Ising Hamiltonian (2.1) is invariant under the transformation

$$\sigma_j^x \to -\sigma_j^x, \tag{2.4}$$

which is called the Z_2 symmetry, and is generated by the parity operator

$$P = \prod_{j=1}^{N} \sigma_j^z. \tag{2.5}$$

This further means the Ising Hamiltonian and the parity operator commute,

$$[H, P] = 0, \tag{2.6}$$

and, thus, share a common eigenbasis.

In the limit $g \to +\infty$, the Hamiltonian (2.1) is dominated by the second term, and its ground state is the completely polarized vector

$$|0\rangle = \prod_{j=1}^{N} |\uparrow\rangle_j \,, \tag{2.7}$$

where $\sigma_j^z \, |\uparrow\rangle_j = |\uparrow\rangle_j$ and $\sigma_j^z \, |\downarrow\rangle_j = - \, |\downarrow\rangle_j$ are the eigenstates and eigenvalues of σ_j^z. In this state, the longitudinal magnetization per spin is identically zero,

$$m_x = \langle 0 | \sigma_j^x | 0 \rangle = 0, \tag{2.8}$$

consistent with the symmetry property of the Hamiltonian.

Conversely, at zero external field, $g = 0$, this model is equivalent to the classical Ising chain (1.27) and its ground state is one of the two states

$$|0\rangle = \prod_{j=1}^{N} |\rightarrow\rangle_j \quad \text{or} \quad |0\rangle = \prod_{j=1}^{N} |\leftarrow\rangle_j \tag{2.9}$$

where $|\rightarrow\rangle_j$ and $|\leftarrow\rangle_j$ are the eigenstates of σ_j^x with eigenvalues 1 and -1, respectively.

In this case, the order parameter of the model, m_x, evaluates to

$$m_x = \langle 0|\sigma_j^x|0\rangle = \pm 1, \tag{2.10}$$

depending on whether the spins point right or left. The existence of this nonzero magnetization implies an spontaneous breaking of the aforementioned Z_2 symmetry.

In terms of the σ^x eigenstates, the z-component Pauli matrix reads

$$\sigma_j^z = |\rightarrow\rangle_j\langle\leftarrow| + |\leftarrow\rangle_j\langle\rightarrow|.$$

Clearly, the effect of a nonzero field g is to cause the initially ordered spins to flip. In an infinite system, as g increases, these *quantum fluctuations* continuously reduce the spontaneous magnetization m_x until it vanishes when $g_c = J$ [49, 56]. At this point, there is a quantum phase transition from an ordered, symmetry broken, ferromagnetic phase to a quantum paramagnetic phase.

Indeed, under the quantum-classical mapping, the transverse field Ising model is equivalent to the classical $d = 2$ Ising model at zero (longitudinal) field. Therefore, their critical points belong to the same universality class, and their critical exponents are the ones given in Table 1.1.

Because of its simplicity and notable analytical results, the Ising model serves as a playground for testing and unraveling new concepts and techniques. A limited list of examples includes the study of dynamical phase transitions [57]; the development of numerical techniques [58, 59]; the relation between non-Markovianity, decoherence and criticality [60]; and the study of work statistics [61, 62] and work protocols [33, 36–38] in quantum thermodynamics, of course. Moreover, this is a conventional model employed in the testing of quantum information theoretic quantities as tools for detecting critical points. These include fidelity measures [63–66], correlations measures like entanglement [67–69] and discord [70, 71], and coherence measures [40, 72–74]. The model now is also experimentally realizable [75] or simulated [76].

Here I will consider in detail a slightly modified version of the transverse field Ising model. One in which this field assumes distinct values at even or odd lattice positions.

We studied this model in [39], and its Hamiltonian may be written as

$$H = -J \sum_{j=1}^{N} \left[\sigma_j^x \sigma_{j+1}^x + (g - (-1)^j h) \sigma_j^z \right]. \tag{2.11}$$

That is, the system contains a regularly alternating transverse field of period 2. At odd sites, it assumes the value $g + h$, while this changes to $g - h$ at even sites.

The reason for introducing such a feature is twofold. From a theoretical perspective, the enlargement of parameters to be considered can greatly enrich the phase diagram of a model, including the appearance of new critical points [77–80]. Then the analytic treatment possible in one-dimensional transverse field spin systems allows the thorough study of quantum critical points associated with distinct universality classes.

In addition, different magnetic ions couple differently with an external field. That is, have different g-factors. There are several compounds where regularly alternating g-factor values are observed [81–87]. This can be mapped onto an effective Hamiltonian containing a term with an alternating field like the one in (2.11) — see [88].

In the following section, I diagonalize this Hamiltonian and study its gap and critical behavior in detail.

2.1 Hamiltonian diagonalization and gap

The starting point in the diagonalization of the Alternating Transverse Field Ising Model (ATFIM) Hamiltonian (2.11) is its transformation to a model of spinless fermions.

I begin by noting we can associate the eigenstate $|\downarrow\rangle_j$ of σ_j^z with a spinless fermion occupying an orbital j, and the eigenstate $|\uparrow\rangle_j$ with an empty orbital. Accordingly, the action of the operator $\sigma_j^- = (\sigma_j^x - i\sigma_j^y)/2$ of flipping a spin from up to down is equivalent to the creation of a fermion. Conversely, $\sigma_j^+ = (\sigma_j^-)^\dagger = (\sigma_j^x + i\sigma_j^y)/2$ corresponds to annihilation.

The problem with this analogy, though, is that spin operators acting on different sites always commute, while fermionic operators anticommute. This issue was overcomed by Jordan and Wigner [89, 90] who introduced a counting factor that produces the correct commutation relations.

Letting a_j be the annihilation fermionic operator at site j, the Jordan-Wigner transformation reads

$$\sigma_j^+ = \exp\left(i\pi \sum_{l=1}^{j-1} a_l^\dagger a_l\right) a_j.$$

The string $e^{i\pi \sum_{l=1}^{j-1} a_l^\dagger a_l}$ is, actually, a partial parity operator. It counts the number of fermions to the left of j and returns the value 1 or -1 if this number is even or odd.

The transformation can also be inverted to give

$$a_j = \prod_{l=1}^{j-1} (\sigma_l^z) \sigma_j^+.$$

Using this and the commutation relations (2.3) it is straightforward to show the operators $\{a_j\}$ indeed satisfy the canonical fermionic anticommutation relations,

$$\{a_j, a_l^\dagger\} = \delta_{jl}, \quad \{a_j, a_l\} = \{a_j^\dagger, a_l^\dagger\} = 0,$$

where $\{x, y\} = xy + yx$.

In our case, because of the alternating field, it is convenient to consider two fermion species and define

$$\sigma_{2j+1}^+ = \exp\left(i\pi \sum_{l=0}^{j-1} a_{2l+1}^\dagger a_{2l+1} + i\pi \sum_{l=1}^{j} b_{2l}^\dagger b_{2l}\right) a_{2j+1}, \tag{2.12}$$

$$\sigma_{2j}^+ = \exp\left(i\pi \sum_{l=1}^{j} a_{2l-1}^\dagger a_{2l-1} + i\pi \sum_{l=1}^{j-1} b_{2l}^\dagger b_{2l}\right) b_{2j}, \tag{2.13}$$

with

$$\{a_j, a_l^\dagger\} = \{b_j, b_l^\dagger\} = \delta_{jl}, \tag{2.14}$$

and all other anticommutators vanishing.

Next, some assumptions are necessary. I will consider periodic boundary conditions: $\sigma_{N+1}^a = \sigma_1^a$. For convenience I further take $N/2$ even. This makes the problem more symmetric, with an equal number of degrees of freedom for the two fermionic species. The reader interested in the case $N/2$ odd can have a look at it in [39]. Without loss of generality I also set $J = 1$.

With this, the Hamiltonian (2.11) becomes

$$\begin{aligned} H = &- \sum_{j=1}^{N/2-1} \left[r(a_{2j-1}, b_{2j}) + r(b_{2j}, a_{2j+1}) \right] - r(a_{N-1}, b_N) - r(b_N, a_1) P \\ &- \sum_{j=1}^{N/2} \left[(g+h)\, t(a_{2j-1}) + (g-h)\, t(b_{2j}) \right] \end{aligned} \tag{2.15}$$

where

$$r(a_j, b_l) = (a_j^\dagger - a_j)(b_l^\dagger + b_l), \tag{2.16}$$

$$t(a_j) = (1 - 2a_j^\dagger a_j), \tag{2.17}$$

and P is again the parity operator,

$$\begin{aligned} P = \prod_{j=1}^{N} \sigma_j^z &= \exp\left(i\pi \sum_{l=1}^{N/2} a_{2l-1}^\dagger a_{2l-1} + i\pi \sum_{l=1}^{N/2} b_{2l}^\dagger b_{2l} \right) \\ &= \prod_{j=1}^{N/2} (1 - 2a_{2j-1}^\dagger a_{2j-1})(1 - 2b_{2j}^\dagger b_{2j}). \end{aligned} \tag{2.18}$$

As indicated above, this operator has eigenvalue $+1$, or -1, when the state of the system has an even, or odd, number of spins pointing down. Equivalently, we could think in terms of an even or odd number of fermions. The projectors onto these positive and negative parity subspaces are defined by

$$P^\pm = \frac{1}{2}(\mathbb{1} \pm P). \tag{2.19}$$

Utilizing these we obtain

$$H = P^+ H^+ P^+ + P^- H^- P^-, \tag{2.20}$$

$$H^\pm = -\sum_{j=1}^{N/2} \left[r(a_{2j-1}, b_{2j}) + r(b_{2j}, a_{2j+1}) + (g+h) t(a_{2j-1}) + (g-h) t(b_{2j}) \right], \tag{2.21}$$

with the boundary conditions

$$a_{N+1} = -a_1 \qquad \text{for } H^+, \tag{2.22}$$

$$a_{N+1} = a_1 \qquad \text{for } H^-. \tag{2.23}$$

Because H and P commute and share a common set of eigenstates, we can diagonalize the former independently in each parity subspace.

Let us consider first the positive parity subspace. To explore the translational invariance in our system we can introduce the Fourier transform

$$a_{2j-1} = \frac{e^{-i\pi/4}}{\sqrt{N}} \sum_{k\in K^+} (a_k + b_k) e^{ik(2j-1)}, \quad b_{2j} = \frac{e^{-i\pi/4}}{\sqrt{N}} \sum_{k\in K^+} (a_k - b_k) e^{ik(2j)}, \tag{2.24}$$

$$K^+ = \Big\{ k = \pm(2n+1)\frac{\pi}{N};\ n = 0, 1, ..., N/4 - 1 \Big\}, \tag{2.25}$$

where a_k and b_k are fermionic operators, and the pseudo-momenta $k \in K^+$ satisfy the condition (2.22). The above equations implicitly set the lattice spacing to $a = 1$. It is easy to show this transformation preserves both parity and particle number,

$$\sum_{j=1}^{N/2} \left(a^\dagger_{2j-1} a_{2j-1} + b^\dagger_{2j} b_{2j} \right) = \sum_{k\in K^+} \left(a^\dagger_k a_k + b^\dagger_k b_k \right). \tag{2.26}$$

In terms of these new operators the positive parity Hamiltonian is given by

$$H^+ = 2 \sum_{k\in K^+_>} A^\dagger_k H_k A_k, \tag{2.27}$$

where $K^+_>$ is the set with only the positive elements of K^+, and

$$A_k = \begin{pmatrix} a_k \\ a^\dagger_{-k} \\ b_k \\ b^\dagger_{-k} \end{pmatrix}, \quad H_k = \begin{pmatrix} g - \cos k & \sin k & h & 0 \\ \sin k & -g + \cos k & 0 & -h \\ h & 0 & g + \cos k & -\sin k \\ 0 & -h & -\sin k & -g - \cos k \end{pmatrix}. \tag{2.28}$$

The matrix H_k is real and symmetric. This means there exists a real and orthogonal

matrix O_k that diagonalizes it,

$$H_k = O_k D_k O_k^\dagger, \quad O_k O_k^\dagger = O_k^\dagger O_k = \mathbb{1}. \tag{2.29}$$

The matrix $D_k = \text{diag}(-\epsilon_k^-, \epsilon_k^-, -\epsilon_k^+, \epsilon_k^+)$ is the diagonal matrix whose entries are the eigenvalues of H_k. These are given by

$$\epsilon_k^\pm = \sqrt{1 + g^2 + h^2 \pm 2\sqrt{g^2h^2 + g^2\cos^2 k + h^2 \sin^2 k}}. \tag{2.30}$$

The general expression for O_k, on the other hand, is immensely complicated, and not at all informative. Latter I will consider a particular case and will write it explicitly.

In addition, the transformation $O_k^\dagger A_k$ also defines a new set of fermionic operators $\{\eta_{k,\pm}\}$ satisfying the (anti)commutation relations [90]

$$\{\eta_{k,s}, \eta_{k',s'}^\dagger\} = \delta_{k,k'}\delta_{s,s'}, \quad \{\eta_{k,s}, \eta_{k',s'}\} = \{\eta_{k,s}^\dagger, \eta_{k',s'}^\dagger\} = 0, \tag{2.31}$$

where $s = +$ or $s = -$. This transformation is such that it does not preserve the number of particles, but, of course, it preserves parity.

In terms of the η-fermions we can write [90]

$$H^+ = \sum_{k \in K^+} \sum_{s=+,-} \epsilon_k^s (2\eta_{k,s}^\dagger \eta_{k,s} - 1). \tag{2.32}$$

In fact, the eigenstates of H^+ are classified by the number of η-fermions they contain. In particular, since $\epsilon_k^\pm \geqslant 0$, the ground state is the state annihilated by all $\eta_{k,\pm}$. One can show that in terms of the original a and b fermions the ground state is given by [91]

$$\eta_{k,+} \left|0^+\right\rangle = \eta_{k,-} \left|0^+\right\rangle = 0, \quad \forall\, k \in K^+,$$

$$\left|0^+\right\rangle = \prod_{k \in K_>^+} \left|0\right\rangle_k,$$

$$\left|0\right\rangle_k = \left(\alpha_1^k + \alpha_2^k a_k^\dagger a_{-k}^\dagger + \alpha_3^k b_k^\dagger b_{-k}^\dagger + \alpha_4^k a_k^\dagger b_{-k}^\dagger + \alpha_5^k a_{-k}^\dagger b_k^\dagger + \alpha_6^k a_k^\dagger a_{-k}^\dagger b_k^\dagger b_{-k}^\dagger\right) \left|0_{ab}^+\right\rangle,$$

where $\left|0_{ab}^+\right\rangle$ is the state annihilated by all a_k and b_k, and the coefficients α_j^k satisfy

$\sum_j |\alpha_j^k|^2 = 1$. Indeed the ground state has an even number of the a and b fermions in it, and, therefore, has a parity $+1$.

From (2.32) we obtain that the ground state energy in the positive parity subspace is given by

$$\epsilon^+ = -\sum_{k\in K^+} (\epsilon_k^- + \epsilon_k^+). \tag{2.33}$$

Next we can move to the negative parity subspace. The first step is again the Fourier transform (2.24), but with the different momenta

$$K^- = \left\{k = 0, k = \pm 2n\frac{\pi}{N}, k = \frac{\pi}{2};\ n = 1, ..., N/4 - 1\right\}, \tag{2.34}$$

such that the periodic condition (2.23) is satisfied.

Proceeding in the same manner as before, one arrives at

$$H^- = 2\sum_{k\in K_>^-} A_k^\dagger H_k A_k + A_0^\dagger H_0 A_0 + A_{\frac{\pi}{2}}^\dagger H_{\frac{\pi}{2}} A_{\frac{\pi}{2}}, \tag{2.35}$$

where $K_>^- = \{k = 2n\pi/N;\ n = 1, 2, ..., N/4 - 1\}$, A_k and H_k are the ones in (2.28), and

$$\begin{aligned} A_0 &= \begin{pmatrix} a_0 \\ a_0^\dagger \\ b_0 \\ b_0^\dagger \end{pmatrix}, \quad H_0 = \begin{pmatrix} g-1 & 0 & h & 0 \\ 0 & -g+1 & 0 & -h \\ h & 0 & g+1 & 0 \\ 0 & -h & 0 & -g-1 \end{pmatrix}, \\ A_{\frac{\pi}{2}} &= \begin{pmatrix} a_{\frac{\pi}{2}} \\ a_{\frac{\pi}{2}}^\dagger \\ b_{\frac{\pi}{2}} \\ b_{\frac{\pi}{2}}^\dagger \end{pmatrix}, \quad H_{\frac{\pi}{2}} = \begin{pmatrix} g & 0 & h & -1 \\ 0 & -g & 1 & -h \\ h & 1 & g & 0 \\ -1 & -h & 0 & -g \end{pmatrix}. \end{aligned} \tag{2.36}$$

These matrices are all real and symmetric, and, therefore, diagonalizable. We already saw the eigenvalues of H_k are $\pm\epsilon_k^\pm$, given in (2.30). In the case of H_0 and $H_{\frac{\pi}{2}}$, they are $\pm(g \pm \sqrt{1+h^2})$ and $\pm(\sqrt{1+g^2} \pm h)$, respectively.

Moreover, the diagonalizing orthogonal matrices O_0 and $O_{\frac{\pi}{2}}$ have a simple expression,

and the fermionic operators they define are given by

$$\eta_{0,-} = \sin(\theta_0/2)a_0 - \cos(\theta_0/2)b_0, \tag{2.37}$$

$$\eta_{0,+} = \cos(\theta_0/2)a_0 + \sin(\theta_0/2)b_0, \tag{2.38}$$

where $\cos\theta_0 = 1/\sqrt{1+h^2}$, and

$$\eta_{\frac{\pi}{2},-} = \frac{1}{\sqrt{2}}\big[\sin\big(\theta_{\frac{\pi}{2}}/2\big)(a_{\frac{\pi}{2}} + b_{\frac{\pi}{2}}) - \cos\big(\theta_{\frac{\pi}{2}}/2\big)(a^\dagger_{\frac{\pi}{2}} - b^\dagger_{\frac{\pi}{2}})\big], \tag{2.39}$$

$$\eta_{\frac{\pi}{2},+} = \frac{1}{\sqrt{2}}\big[\sin\big(\theta_{\frac{\pi}{2}}/2\big)(a_{\frac{\pi}{2}} - b_{\frac{\pi}{2}}) + \cos\big(\theta_{\frac{\pi}{2}}/2\big)(a^\dagger_{\frac{\pi}{2}} + b^\dagger_{\frac{\pi}{2}})\big], \tag{2.40}$$

where $\cos\theta_{\frac{\pi}{2}} = g/\sqrt{1+g^2}$. It is straightforward to check they satisfy the proper (anti)commutation relations.

Therefore, the negative parity Hamiltonian is given in diagonal form by

$$H^- = \sum_{k\in K^-}\sum_{s=+,-} \epsilon^s_k(2\eta^\dagger_{k,s}\eta_{k,s} - 1), \tag{2.41}$$

where I define

$$\epsilon^\pm_0 = g \pm \sqrt{1+h^2}, \tag{2.42}$$

$$\epsilon^\pm_{\frac{\pi}{2}} = \sqrt{1+g^2} \pm h. \tag{2.43}$$

Note that $\epsilon^\pm_0$ and $\epsilon^\pm_{\frac{\pi}{2}}$ are not the same as doing $k=0$ or $k=\pi/2$ on $\epsilon^\pm_k$. For instance, $\epsilon^\pm_{0,\frac{\pi}{2}}$ can be negative, while $\epsilon^\pm_k$ never are.

By definition, the negative parity ground state have an odd number of particles in it. This means an odd number of the fermionic modes (k,s) must be occupied. We showed in [39] that the lowest energy is always obtained when the mode $(0,-)$ is excited. Hence, the ground state energy in the negative parity subspace is given by

$$\epsilon^- = -\sum_{k\in K^-\setminus\{0,\pi\}}(\epsilon^-_k + \epsilon^+_k) - 2\sqrt{1+g^2} - 2\sqrt{1+h^2}. \tag{2.44}$$

We are in the position now to analyse the ground state energy gap in this model. We

may start with the identification of the candidates for the quantum critical points, i.e., the points where the gap closes.

A zero gap means an excitation can be created in the system without any energy expenditure. Scrutinizing the dispersion relations (2.30) we find this is possible when

$$|g^2 - h^2| = 1, \tag{2.45}$$

in the limit $N \to \infty$. Indeed in [92, 93] the authors showed that for an Ising model with random exchange couplings $(J_1, J_2, ..., J_N)$ and transverse fields $(g_1, g_2, ..., g_N)$, the critical points must satisfy

$$\prod_{j=1}^{N} g_i = \prod_{j=1}^{N} J_i,$$

which is in agreement with Eq. (2.45).

Hence, the zero temperature phase diagram of the ATFIM is marked by hyperbolic critical curves separating the ordered and disordered phases. This is represented by the red lines in Fig. 2.1.

Next, we want to compute

$$\Delta = \epsilon^- - \epsilon^+. \tag{2.46}$$

To do this I introduce the Fourier series

$$\epsilon_k^+ = \sum_{l=0}^{\infty} u_l \cos(2kl), \tag{2.47}$$

$$\epsilon_k^- = \sum_{l=0}^{\infty} v_l \cos(2kl), \tag{2.48}$$

where the coefficients u_l and v_l are given by

$$u_l = \frac{2}{\pi} \int_{-\frac{\pi}{2}}^{\frac{\pi}{2}} \mathrm{d}k \cos(2kl)\epsilon_k^+, \quad v_l = \frac{2}{\pi} \int_{-\frac{\pi}{2}}^{\frac{\pi}{2}} \mathrm{d}k \cos(2kl)\epsilon_k^-. \tag{2.49}$$

After some lengthy calculations I leave to Appendix A, we observe the behavior of the gap Δ is indeed divided into three regimes, delimited by: $|g^2 - h^2| < 1$, $|g^2 - h^2| = 1$ and $|g^2 - h^2| > 1$. These are expected to be in correspondence with the ordered, critical and quantum paramagnetic phases. In the sequence I consider them separately. The results

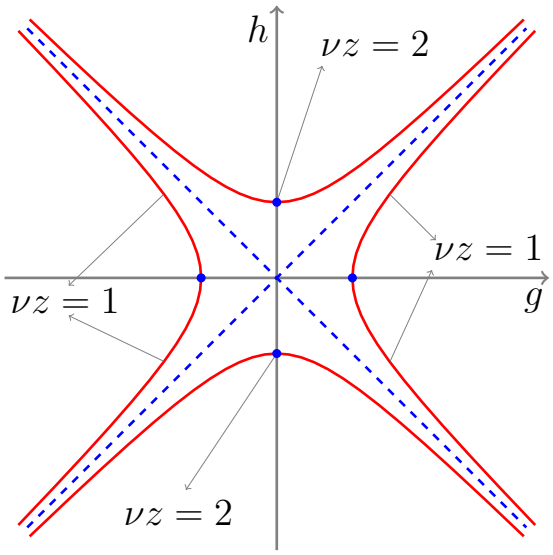

Figure 2.1: Zero temperature phase diagram of the ATFIM. The red hyperbolic critical lines marks the transition from an ordered phase, interior to these curves, to a quantum paramagnetic phase, exterior to these curves. Most of these critical points belong to the $d = 2$ classical Ising universality class. The blue dots at $(g = \pm 1, h = 0)$ and $(g = 0, h = \pm 1)$ are possible exceptions. This is explained in the text. External to the red curves, the ground state energy gap Δ never vanishes. Along the critical lines, the gap closes as $\Delta = \mathcal{O}(1/N)$ as a function of the system size N. Inside it, Δ is exponentially small in the thermodynamic limit. The dashed diagonal lines, marks an exact degeneracy in the system ground state for any system size.

are summarized in Fig. 2.1.

Region $|g^2 - h^2| < 1$:

The gap in this region is given by

$$\Delta = |g^2 - h^2|^{\frac{N}{2}} \frac{4N}{\pi} \int_0^1 \frac{\mathrm{d}t\, t^{N-1}}{1 - (|g^2 - h^2|^{\frac{1}{2}} t)^{2N}} \left[\sqrt{\frac{(1-t^2)[1 - |g^2 - h^2|^2 t^2]}{t^2} + R^2} - R \right]^{\frac{1}{2}}, \tag{2.50}$$

where I define

$$R = 1 + g^2 + h^2. \tag{2.51}$$

The first conclusion we can establish about (2.50) is that for $N/2$ even, the ground state of the system has a positive parity. Therefore, Eq. (2.33) corresponds to the ground state energy. In [39] we showed that a negative parity ground state is only possible when $N/2$ is odd and $g^2 - h^2 < 0$.

Second, the system has an exact degeneracy on the diagonals $g^2 = h^2$ for any system size. These diagonals are indicated by the dashed lines in Fig. 2.1 and may be viewed as an extension of the point $g = 0$ in the homogeneous field model. The exact degeneracy can be understood in terms of a symmetry acquired by the Hamiltonian (2.11) on these lines.

When $g = h$, the transverse field vanishes on the even sites. As a consequence, the spin operators σ^x_{2j} commute with the Hamiltonian, $[H, \sigma^x_{2j}] = 0$. In contrast, they anticommute with the parity operator, $P\sigma^x_{2j} = -\sigma^x_{2j}P$. Let $|p, \epsilon\rangle$ be an eigenstate of P with parity p and of H with energy ϵ, we have that

$$\begin{aligned} P(\sigma^x_{2j}\,|p,\epsilon\rangle) &= -p(\sigma^x_{2j}\,|p,\epsilon\rangle), \\ H(\sigma^x_{2j}\,|p,\epsilon\rangle) &= \epsilon(\sigma^x_{2j}\,|p,\epsilon\rangle). \end{aligned} \tag{2.52}$$

Hence, if $|p, \epsilon\rangle$ belongs to the subspace of lowest energy of H, so does the opposite parity state $\sigma^x_{2j}\,|p, \epsilon\rangle$. When $g = -h$, the same reasoning can be applied with σ^x_{2j+1} replacing σ^x_{2j}.

Moreover, in [39] (see also Appendix A) we show the gap (2.50) is bounded by

$$\begin{aligned} &\frac{|g^2-h^2|^{\frac{N}{2}}}{\sqrt{2R}} \max\left\{\frac{2}{\sqrt{\pi}}\frac{\sqrt{1-|g^2-h^2|}}{\sqrt{N}}, \frac{4|g^2-h^2|^{\frac{1}{2}}}{\pi N}\right\} \leqslant \Delta \leqslant \\ &|g^2-h^2|^{\frac{N}{2}}\sqrt{2(1+|g^2-h^2|)}\left(\frac{\pi|g^2-h^2|^{\frac{1}{2}}}{2N-1} + 2\frac{\sqrt{1-|g^2-h^2|}}{\sqrt{N-1}}\right) \end{aligned} \tag{2.53}$$

with equality again when $g^2 = h^2$.

This exponentially vanishing gap in the thermodynamic limit $N \to \infty$ is completely similar to the behavior found in the homogeneous field case [94]. Moreover, this is consistent with a symmetry broken phase where the spins are found to be highly correlated over a length [39]

$$\xi \sim \frac{1}{\left|\ln|g^2-h^2|\right|}. \tag{2.54}$$

That is, for $|g^2 - h^2| < 1$ the system exhibits a (longitudinal) spontaneous magnetization, a fact that was already noted in [93] and further numerically verified in [95].

Assuming (2.54) to be the correlation length in the infinite system, we see in most

cases this diverges as

$$\xi \sim |g - g^*|^{-1}, \tag{2.55}$$

rendering the critical exponent $\nu = 1$. Here I considered h fixed and a varying g, thus $g^* = \pm\sqrt{1+h^2}$. We may equivalently consider interchanged roles $g \leftrightarrow h$ and obtain similar results.

An exception to this behavior occurs when $h = \pm 1$ and $g \to 0$. In this case, the correlation length diverges with a critical exponent $\nu = 2$,

$$\xi \sim |g|^{-2}. \tag{2.56}$$

Note that it is important here that h is fixed and we approach this critical point by varying g. Conversely, if we fix $g = 0$ and vary h, instead, we obtain $\nu = 1$. Replacing the roles of g and h, the point $(g = 1, h = 0)$ approached along the line $h = 0$ corresponds to the usual critical point of the homogeneous Ising model; therefore, it must have $\nu = 1$.

The previous analysis is consistent with the numerical results of [95]. Therefore, our analytical evaluation of the ground state gap allowed us to derive the asymptotic behavior of the correlation length of this model without ever calculating any correlation function. The latter has a nonlocal character in the fermionic representation, and this makes it really difficult to compute in general [56, 90, 96, 97].

Furthermore, the authors in [95] found that for most critical points, where $\nu = 1$, the other critical exponents are $\alpha = 0$, $\beta = 1/8$, $\eta = 1/4$ and $z = 1$. Therefore, these points belong to the same universality class of the homogeneous transverse field Ising model and the $d = 2$ square lattice classical model.

In comparison, for the points where $\nu = 2$, the other critical exponents are $\alpha = -2$, $\beta = 1/4$, $\eta = 1/4$ and $z = 1$ [95]. Hence, these points belong to a different universality class. They are represented by blue dots in Fig. 2.1.

Lines $|g^2 - h^2| = 1$:

Next, we may move to the critical lines. Along them, the expression for the gap reads,

$$\Delta = \frac{4N}{\pi}\int_0^1 \mathrm{d}t\, \frac{t^{N-3/2}}{1-t^{2N}}\sqrt{\sqrt{(1-t^2)^2+(2G^2t)^2}-2G^2t}, \tag{2.57}$$

where $G^2 = g^2$ for $g^2 - h^2 = 1$ and $G^2 = h^2$ for $g^2 - h^2 = -1$.

Here the gap is bounded by [39] (Appendix A)

$$\frac{1}{2\sqrt{G^2}}\left[2\tanh\left(\frac{\pi}{4N}\right)+\frac{\pi}{6N}\right] \leqslant \Delta \leqslant 4\tanh\left(\frac{\pi}{4N}\right). \tag{2.58}$$

Indeed, in the thermodynamic limit the gap closes as

$$\Delta \sim 1/N. \tag{2.59}$$

Again this is analogous to the behavior in the homogeneous field case. At these points the spontaneous magnetization vanishes [93].

Regions $|g^2 - h^2| > 1$:

Over this region the gap is given by

$$\begin{aligned}\Delta =& 2\left(|g|-\sqrt{1+h^2}\right)\Theta\left(|g|-\sqrt{1+h^2}\right)+2\left(|h|-\sqrt{1+g^2}\right)\Theta\left(|h|-\sqrt{1+g^2}\right)\\ &+\frac{4N}{\pi|g^2-h^2|^{\frac{N}{2}}}\int_0^1 \frac{\mathrm{d}t\, t^{N-1}}{1-(t/|g^2-h^2|^{\frac{1}{2}})^{2N}}\left[\sqrt{\frac{(1-t^2)[|g^2-h^2|^2-t^2]}{t^2}+R^2}-R\right]^{\frac{1}{2}},\end{aligned} \tag{2.60}$$

where I remember $R = 1 + g^2 + h^2$.

Therefore, for $|g^2 - h^2| > 1$, the gap is manifestly nonzero even in the in thermodynamic limit. This ensures the Z_2 symmetry is not broken. There is no spontaneous magnetization in this case. Here the system is found in a quantum paramagnetic phase.

From (2.60) we may also confirm that, for fixed h and $g \to g^* = \pm\sqrt{1+h^2}$, the gap closes as

$$\Delta \sim |g - g^*|^1, \tag{2.61}$$

meaning $\nu z = 1$. Combined with (2.55) this corroborates that $z = 1$.

On the other hand, when $h \to 1^+$ and $g \to 0$, we obtain

$$\Delta \sim g^2, \tag{2.62}$$

rendering $\nu z = 2$ and $z = 1$.

This ends the analysis about the gap behavior in the alternating transverse field Ising model. Before concluding this chapter, let us analyse the ground state energy in some detail.

As noted above, the ground state energy is given by (2.33). Taking the thermodynamic limit $N \to \infty$ we may convert this sum into an integral,

$$\frac{1}{N}\epsilon_0 = -\frac{1}{2\pi}\int_{-\frac{\pi}{2}}^{\frac{\pi}{2}} \mathrm{d}k(\epsilon_k^+ + \epsilon_k^-), \tag{2.63}$$

where ϵ_0/N is the ground state energy per spin.

Let us consider $h = 0$, and so we are dealing now with the homogeneous transverse field Ising model. This integral evaluates to

$$\begin{aligned}\frac{1}{N}\epsilon_0 &= -\frac{1}{2\pi}\int_{-\frac{\pi}{2}}^{\frac{\pi}{2}} \mathrm{d}k(\sqrt{1+g^2+2|g|\cos k} + \sqrt{1+g^2-2|g|\cos k}) \\ &= -\frac{1}{2\pi}\int_{-\pi}^{\pi} \mathrm{d}k\sqrt{1+g^2-2g\cos k} \\ &= -\frac{2}{\pi}|g+1|\,E\left(\frac{4g}{(1+g)^2}\right),\end{aligned} \tag{2.64}$$

where $E(x)$ is the complete elliptic integral

$$E(x) = \int_0^{\frac{\pi}{2}} \mathrm{d}k\sqrt{1-x\sin^2 k}.$$

If we Taylor expand (2.64) around the critical point $g^* = 1$ we find there is a singular contribution to the ground state energy per particle given by

$$\frac{1}{N}\epsilon_0 \sim (g-1)^2 \ln|g-1|. \tag{2.65}$$

This leads to a logarithmically diverging transverse susceptibility per spin

$$\chi = -\frac{1}{N}\partial_g^2 \epsilon_0 \sim \ln|g-1|. \tag{2.66}$$

The divergence of this second derivative of the ground state energy shows this critical point is indeed associated with a second-order continuous quantum phase transition. Moreover, the transverse susceptibility plays in the quantum Ising model the equivalent role of the specific heat in a thermal phase transition. Its critical exponent α, in this case, vanishes, $\alpha = 0$.

Finally, I emphasize this quantum critical point is representative of all critical points in its universality class. This means, all points in the red critical lines of Fig. 2.1 will exhibit analogous behavior.

Conversely, let us take $h = 1$. It was shown in [93] that, in this case, the singularity in the ground state energy is of the form

$$\frac{1}{N}\epsilon_0 \sim g^4 \ln|g|. \tag{2.67}$$

As a consequence, the transverse susceptibility here is finite, and only its second derivative exhibits a logarithmic divergence,

$$\chi \sim g^2 \ln|g|, \tag{2.68}$$

$$\partial_g^2 \chi \sim \ln|g|. \tag{2.69}$$

Therefore, the distinct critical points in the ATFIM (2.11), represented by blue dots in Fig. 2.1, are not associated with second-order but, in fact, with fourth-order quantum phase transitions [93]. The main concepts of continuous second-order phase transitions discussed in the previous chapter are readily extended to high-order transitions. The difference being the divergences occurring on the higher-order derivatives of the ground state energy.

In the next chapter I introduce a nonequilibrium quantum thermodynamic protocol which will be applied to this model. In particular I will be interested in the entropy production in the vicinity of these quantum critical points.

Chapter 3

Thermodynamics of a Driven Isolated Quantum System

Thermodynamics was initially developed to deal with macroscopic systems in equilibrium. The colossal number of particles in these situations makes the probability of obtaining the value of some thermodynamic quantity different from the average and most likely one negligible [41]. However, as classical systems with smaller degrees of freedom are considered, fluctuations become increasingly relevant and the second law of thermodynamics holds only on average [98, 99].

For quantum systems, we additionally have the effects of coherence and the backaction of quantum measurements. These features greatly enrich (or complicate) the possibilities for defining work and heat [28, 100–112], and even entropy (production) [113–118] in quantum thermodynamics. In fact, different definitions may acquire operational value in specific scenarios and, in light of this, here I present these concepts as suitable for this thesis and its results in subsequent chapters.

Therefore, I regard the von Neumann entropy as the appropriate thermodynamic entropy. Heat is defined as the energy change in the bath or environment coupled to the system of interest. Finally, irreversibility, quantified by entropy production, will emerge as a consequence of disregarding any correlations between the system and the bath as well as the bath itself [113, 117]. Furthermore, the stochastic approach will be based on the Two Point Measurement (TPM) scheme, formalized in [107]. Since I will always consider the system to be initially incoherent in the energy basis, i.e. to commute with the

initial Hamiltonian, we will not need to be concerned with the limitations of this approach [3].

As a final comment on nomenclature, I shall consider any system that evolves according to a unitary dynamics as an isolated system. A driven isolated system thus comprises an isolated system with a time-dependent Hamiltonian.

3.1 Work and entropy production in unitary drives

Suppose a finite isolated quantum system with Hamiltonian $H(g(t))$ that is driven according to some work protocol $g_t = g(t)$. Here, the work parameter g is controlled by some external agent or experimenter. It may represent the action of a piston that controls the volume of the system or an applied magnetic field, for instance. A work protocol is performed when this agent changes g in a prescribed way — see Fig. 3.1.

Let $\rho(t)$ be the state of the system at time t, then its internal energy is identified as

$$E(t) = \mathrm{tr}\{\rho(t)H(t)\}. \tag{3.1}$$

Assume that for $t < 0$ the work parameter is kept fixed at $g_0 = g(t = 0)$ and the system is not isolated but in contact with a heat bath at temperature T. This will force the system to thermal equilibrium — Fig. 3.1a). Thus, we consider that at $t = 0$ the state of the system is the thermal (or Gibbs) state

$$\rho_0^{\mathrm{th}} = \frac{e^{-\beta H(g_0)}}{Z_0}, \tag{3.2}$$

where $\beta = 1/T$ is the inverse temperature and $Z_0 = \mathrm{tr}\{e^{-\beta H(g_0)}\}$ is the partition function. Here and throughout this thesis we set the Boltzmann constant to $k_B \equiv 1$. The Gibbs state can be regarded as the quantum equivalent of the canonical ensemble of classical statistical mechanics. It is the state that maximizes the von Neumman entropy for a fixed internal energy - or, conversely, the state that minimizes the internal energy for a fixed von Neumman entropy. Then β is recognized as the Lagrange multiplier associated with the constraint.

Next, at $t = 0$ the system is decoupled from the bath, becoming *isolated*. The work

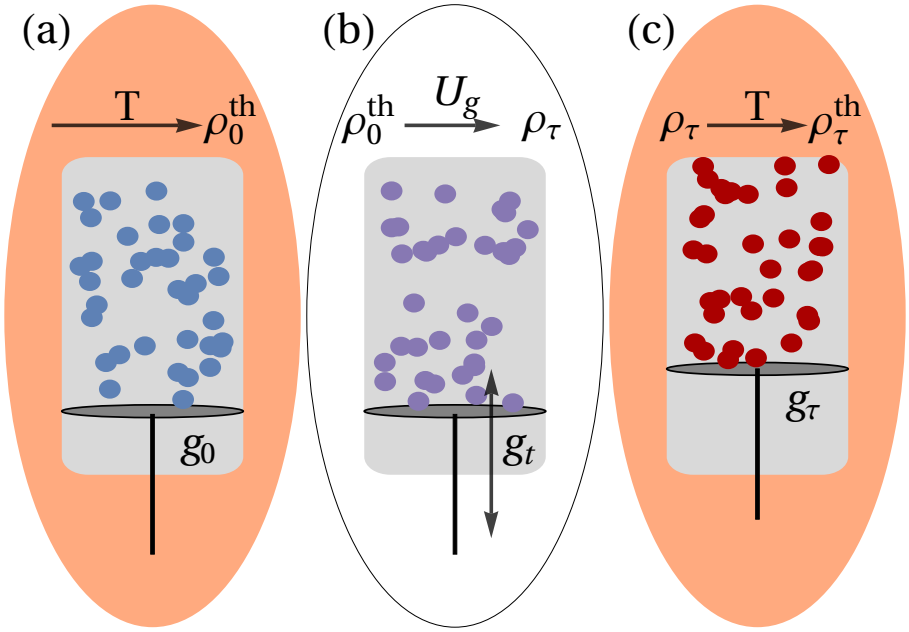

Figure 3.1: Example of the work protocol for a system consisting of a gas inside a container whose volume is altered by a moving piston. a) For $t < 0$, with the work parameter fixed at g_0, the system is in contact with a bath at temperature T which forces it to equilibrium. b) During $0 \leqslant t \leqslant \tau$ the work protocol g_t is applied (the piston is shaken in a prescribed way), and the state of the system evolves from the initial thermal state ρ_0^{th} to a final state ρ_τ according to the unitary U_g. c) For $t > \tau$ with fixed g_τ, the system is put again in contact with a bath at the same initial temperature T and eventually reaches the equilibrium state ρ_τ^{th}.

parameter g is then changed according to the driving protocol g_t that lasts for a total time τ. We emphasize that no further restriction is placed on this driving: it can mean a violent perturbation on the system; a wiggling movement of the piston, for instance — Fig. 3.1b). Let $U_g(\tau, 0)$ be the unitary time-evolution operator associated with the protocol g_t. This is given by

$$U_g(\tau, 0) = \mathcal{T}\text{exp}\left(-i \int_0^\tau \mathrm{d}t H(g_t) \right), \tag{3.3}$$

where $\mathcal{T}$ is the time-ordering operator — see Appendix B. We also set the reduced Planck's constant to $\hbar \equiv 1$ throughout this thesis. Accordingly, at the end of the drive, the final *nonequilibrium* state of the system will be given by

$$\rho_\tau = U_g(\tau, 0)\rho_0^{\text{th}}U_g^\dagger(\tau, 0). \tag{3.4}$$

Since during the work protocol the system is isolated, all changes in its internal energy results from the work done by the external agent. Hence, the first law of thermodynamics dictates that the *average* work associated with this drive is given by

$$W = \mathrm{tr}\{\rho_\tau H(g_\tau)\} - \mathrm{tr}\{\rho_0^{\mathrm{th}} H(g_0)\}, \tag{3.5}$$

where $g_\tau = g(t = \tau)$. We consider here the convention that $W > 0$ means work was done on the system, while $W < 0$ means work was extracted from it.

Subsequently, at $t = \tau$ and with the work parameter kept fixed at g_τ, the system is again put in contact with a reservoir at the same initial temperature T. Ultimately, the system will reach the thermal equilibrium state

$$\rho_\tau^{\mathrm{th}} = \frac{e^{-\beta H(g_\tau)}}{Z_\tau}, \tag{3.6}$$

where $Z_\tau = \mathrm{tr}\{e^{-\beta H(g_\tau)}\}$ — Fig. 3.1c). Note that since g remains constant, no work is performed during this step.

At the end of this thermalization process, the system will have evolved from an initial equilibrium state to a final one, generally being far from equilibrium in the intermediate. Between these two endpoint states, there is a difference in equilibrium free energy given by $\Delta F = -T \ln Z_\tau / Z_0$.

From the second law, we expect the work performed on the system in a generic situation to be larger, or at least equal, than this free energy change,

$$W \geqslant \Delta F, \tag{3.7}$$

with equality only in the case of an isothermal quasistatic evolution, such that the system remains in equilibrium at all times.

This is predominantly not the case for an arbitrary work protocol, and it already suggests the definition of an entropy production given by

$$\Sigma = \beta(W - \Delta F). \tag{3.8}$$

Indeed, using Eqs. (3.2), (3.5), (3.6) and the definition of equilibrium free energy, this thermodynamic formula can be neatly rewritten as a *nonnegative* information-theoretic expression [119]:

$$\begin{aligned}\Sigma &= \operatorname{tr}\{-\rho_\tau \ln \rho_\tau^{\text{th}} - \rho_0^{\text{th}} \ln \rho_0^{\text{th}}\} \\ &= -\operatorname{tr}\{\rho_\tau \ln \rho_\tau^{\text{th}}\} + S(\rho_0^{\text{th}}) \\ &= S(\rho_\tau||\rho_\tau^{\text{th}}) \geqslant 0,\end{aligned} \tag{3.9}$$

where I introduced the von Neumann entropy $S(\rho) = -\operatorname{tr}\{\rho \ln \rho\}$ and used its invariance under unitary transformations, $S(U\rho U^\dagger) = S(\rho)$. The von Neumann entropy can be viewed as a thermodynamic entropy. The latter property is thus regarded as equivalent to the classical invariance of entropy under reversible processes. In the last equality, $S(\rho||\sigma) = \operatorname{tr}\{\rho(\ln \rho - \ln \sigma)\} \geqslant 0$ is the quantum relative entropy, which is a measure of distinguishability between states. More details about these two quantities are provided in Appendix B.

However, since the work protocol is described by a unitary, and unitaries do not change the von Neumann entropy, where does this entropy production comes from? To show that Eq. (3.9) truly quantifies an entropy production, let us consider the relaxation of the nonequilibrium state ρ_τ generated by the drive (3.3) to the equilibrium state ρ_τ^{th}.

Suppose H_E is the Hamiltonian of the bath coupled to the system at the end of the work protocol, which is initially in the thermal state $\rho_E^{\text{th}} = e^{-\beta H_E} / \operatorname{tr}\{e^{-\beta H_E}\}$. Assume also the composite system and bath to be completely isolated, and the thermalization process to be described by a joint unitary U_{SE}, where S labels the system. Let us require U_{SE} to satisfy strict energy conservation,

$$[U_{SE},\, H(g_\tau) + H_E] = 0. \tag{3.10}$$

This is a standard assumption in the resource-theoretic approach to quantum thermodynamics and defines a thermal operation [9, 120–122] — see Appendix B. Moreover, such a description can be seen as closely related to the weak coupling approximation [117].

Two notable consequences follow from (3.10). First, the thermal state ρ_τ^{th} is a global

fixed point of the dynamics, meaning

$$U_{SE}(\rho_\tau^{\text{th}} \otimes \rho_E^{\text{th}})U_{SE}^\dagger = \rho_\tau^{\text{th}} \otimes \rho_E^{\text{th}}. \tag{3.11}$$

And second, it implies that any energy change in the system must equal an opposite energy change in the bath:

$$\Delta E_S = -\Delta E_E. \tag{3.12}$$

Initially, system and bath are uncorrelated, and their global state is given by $\rho_\tau \otimes \rho_E^{\text{th}}$. For $t > \tau$, this global state will evolve to something which predominantly contains *correlations*. At the end of the thermalization process, the reduced state of the system will be precisely $\rho_\tau^{\text{th}} = \text{tr}_E\{\rho'_{SE}\}$, where $\rho'_{SE} = U_{SE}(\rho_\tau \otimes \rho_E^{\text{th}})U_{SE}^\dagger$. Let $\rho'_E = \text{tr}_S\{\rho'_{SE}\}$ be the reduced state of the environment. The (von Neumann) entropy change in the system is given by

$$\begin{aligned}\Delta S_S = S(\rho_\tau^{\text{th}}) - S(\rho_\tau) &= -\,\text{tr}_S\{\rho_\tau^{\text{th}} \ln \rho_\tau^{\text{th}}\} - S(\rho_\tau) = -\,\text{tr}\big\{\rho'_{SE} \ln \rho_\tau^{\text{th}}\big\} - S(\rho_\tau) \\ &= -\,\text{tr}\big\{\rho'_{SE} \ln\big(\rho_\tau^{\text{th}} \otimes \rho_E^{\text{th}}\big)\big\} - S(\rho_\tau) + \text{tr}_E\{\rho'_E \ln \rho_E^{\text{th}}\}.\end{aligned}$$

Using Eq. (3.11) we may rewrite $\text{tr}\big\{\rho'_{SE} \ln\big(\rho_\tau^{\text{th}} \otimes \rho_E^{\text{th}}\big)\big\} = \text{tr}\big\{(\rho_\tau \otimes \rho_E^{\text{th}}) \ln\big(\rho_\tau^{\text{th}} \otimes \rho_E^{\text{th}}\big)\big\}$ and so

$$\Delta S_S = \Sigma - \Phi_E, \tag{3.13}$$

where Σ is given in (3.9) and $\Phi_E = \text{tr}_E\{(\rho_E^{\text{th}} - \rho'_E) \ln \rho_E^{\text{th}}\}$. Equation (3.13) possesses the form of the usual slicing of entropy change in an entropy production, $\Sigma \geqslant 0$, and an entropy flux Φ_E, which can be positive or negative [123]. If we now use that the initial state of the bath is thermal at inverse temperature β, we obtain

$$\Phi_E \equiv \beta Q = \beta\,\text{tr}_E\{(\rho'_E - \rho_E^{\text{th}})H_E\} = -\beta\,\text{tr}_S\{(\rho_\tau^{\text{th}} - \rho_\tau)H(g_\tau)\}, \tag{3.14}$$

where we used (3.12) to arrive at the last equality. Here, we define the *heat* Q as the energy change in the bath, which is also equal to the opposite energy change in the system. This

allows us to recover the Clausius-like expression

$$\Sigma = \Delta S_S + \beta Q, \tag{3.15}$$

which is a conventional definition of entropy production [117, 123].

Some essential remarks are in order now. To begin with, we note that β entering (3.15) is the inverse temperature of the initial equilibrium state of the bath. After system and bath interact, the bath is typically out of equilibrium and is not even possible, in general, to define its temperature. Because of this, Eq. (3.15) might seem odd at first sight. Its significance and utility, however, are in no sense more limited than what one obtains in a classical setting. In classical thermodynamics and statistical mechanics a weak coupling between system and bath is almost invariably assumed, which leads to (3.12) holding approximately. Equivalently then, we could have started with the right-hand side of (3.15), defined Q as the energy exchanged between the system and the bath and arrived at (3.9). Therefore, Eq. (3.9) precisely quantifies the entropy produced in the relaxation of the driven system from the final state ρ_τ to the equilibrium state ρ_τ^{th}.

Next, the previous paragraphs reveal us that entropy is produced truly during the thermalization of the system. But once more, since the global evolution of system and bath is unitary, and therefore preserves the global von Neumann entropy, where does this entropy production comes from? To answer this, we notice the entropy production is equivalently given by [113, 117]

$$\begin{aligned}\Sigma = \Delta S_S + \Phi_E &= S(\rho_\tau^{\text{th}}) - S(\rho_\tau) + \text{tr}\big\{(\rho_E^{\text{th}} - \rho'_E)\ln \rho_E^{\text{th}}\big\} \\ &= -S(\rho'_E) - \text{tr}\big\{\rho'_E \ln \rho_E^{\text{th}}\big\} + S(\rho_\tau^{\text{th}}) + S(\rho'_E) - S(\rho_\tau) - S(\rho_E^{\text{th}}) \\ &= S(\rho'_E||\rho_E^{\text{th}}) + I(\rho'_{SE}),\end{aligned} \tag{3.16}$$

where the last term is the mutual information — see Appendix B,

$$\begin{aligned}I(\rho'_{SE}) &= S(\rho'_{SE}||\rho_\tau^{\text{th}} \otimes \rho'_E) \\ &= S(\rho_\tau^{\text{th}}) + S(\rho'_E) - S(\rho'_{SE})\end{aligned} \tag{3.17}$$

and once again we use the invariance of the von Neumman entropy under unitarity transformations

$$S(\rho'_{SE}) = S(U_{SE}(\rho_\tau \otimes \rho_E^{\text{th}})U_{SE}^\dagger) = S(\rho_\tau) + S(\rho_E^{\text{th}}).$$

Therefore, the entropy production essentially comes from the fact that we are merely interested in, or have control only over, the system and ignore/discard the bath in the end of the process. When we do this, we irreversibly lose information about the correlations shared by the system and the bath — quantified by $I(\rho'_{SE})$, and information about the bath itself — quantified by $S(\rho'_E||\rho_E^{\text{th}})$. It is this irreversible loss of information that amounts to the entropy production given by Eq. (3.9) [113, 117]. One satisfying aspect of this notion and perspective of irreversibility and entropy production is its straightforward generalization to nonthermal situations [124, 125].

Lastly, although Eq. (3.9) quantifies the entropy produced in the thermalization step described above, we still associate it with the unitary drive (3.3). This is because it is this drive that forces the system out of equilibrium in the first place. Indeed, it is customary to make no reference at all to the thermalization process and to define Eq. (3.9) in sole connection with the protocol given by (3.3). When that is the case, Eq. (3.9) is often referred to as the *nonequilibrium lag*. I shall consider this synonym to entropy production in this thesis.

3.2 Stochastic approach and fluctuation theorems

Until now I have considered only average quantities, which result from multiple realizations of the same protocol g_t. This section defines the stochastic quantities associated with these averages, obtained from a unique quantum trajectory. I also introduce a *backward* process in relation to a time-reversed protocol $\tilde{g}_t$ to arrive at the so-called fluctuation theorems. For irreversible scenarios, the second law is usually stated as an inequality. These theorems allow its reformulation as an equality instead [98, 99, 126–129].

It is clear from thermodynamics that work results from a process and therefore cannot be identified with a quantum observable (Hermitian operator) in general. In this spirit, the two point measurement scheme [107] provides a way of defining the stochastic work done on a system in terms of two projective energy measurements. These two measurements

are made at times $t = 0$ and $t = \tau$, and the work performed in a unique realization of g_t is defined as the difference between the two energies.

Suppose the initial Hamiltonian of the system has the eigendecomposition

$$H(g_0) = \sum_i \epsilon_i^0 \Pi_i^0, \tag{3.18}$$

where ϵ_i^0 are the energy eigenvalues and Π_i^0 the corresponding eigenprojectors. The initial state of the system thus reads

$$\rho_0^{\text{th}} = \sum_i p_i^0 \Pi_i^0; \quad p_i^0 = \frac{e^{-\beta\epsilon_i^0}}{Z_0}. \tag{3.19}$$

Similarly, the final Hamiltonian $H(g_\tau)$ may be written as

$$H(g_\tau) = \sum_j \epsilon_j^\tau \Pi_j^\tau. \tag{3.20}$$

At $t = 0$, the first energy measurement is performed and the eigenvalue ϵ_i^0 is obtained with probability

$$\operatorname{tr}\{\Pi_i^0 \rho_0^{\text{th}}\} = r_i^0 p_i^0, \tag{3.21}$$

where $r_i^0 = \operatorname{tr}\{\Pi_i^0\}$ gives the degeneracy of the eigenvalue ϵ_i^0. As a result of the backaction of the measurement, the state of the system is updated to

$$\rho_i^0 = \frac{1}{r_i^0 p_i^0} \Pi_i^0 \rho_0^{\text{th}} \Pi_i^0 = \frac{1}{r_i^0} \Pi_i^0. \tag{3.22}$$

The work protocol g_t is then applied to the system, and its state evolves, dictated by the unitary U_g in (3.3), to

$$\rho_i^\tau = U_g(\tau, 0) \rho_i^0 U_g^\dagger(\tau, 0). \tag{3.23}$$

At $t = \tau$ the second energy measurement is realized and the eigenvalue ϵ_j^τ is obtained with probability

$$p_g(i \to j) = \operatorname{tr}\{\Pi_j^\tau \rho_i^\tau\} = \frac{1}{r_i^0} \operatorname{tr}\{\Pi_j^\tau U_g(\tau, 0) \Pi_i^0 U_g^\dagger(\tau, 0)\}. \tag{3.24}$$

In connection with the measurement outcomes, we may define the quantum trajectory $i \to j$ with *forward* path probability

$$P_F[i,j] = r_i^0 p_i^0\, p_g(i \to j) = p_i^0\, \mathrm{tr}\big\{\Pi_j^\tau U_g(\tau,0)\Pi_i^0 U_g^\dagger(\tau,0)\big\}. \tag{3.25}$$

The work performed on the system in a particular realization of the protocol is thus defined as

$$w[i,j] = \epsilon_j^\tau - \epsilon_i^0. \tag{3.26}$$

And the corresponding work probability distribution is given by

$$p_F(w) = \sum_{i,j} \delta(w - w[i,j]) P_F[i,j], \tag{3.27}$$

where δ is the Dirac delta function. Utilizing this, it is straightforward to verify that the average $\langle w \rangle$ with respect to $p_F(w)$ produces the correct result

$$W = \langle w \rangle = \int_{-\infty}^{+\infty} \mathrm{d}w\, p_F(w)\, w = \mathrm{tr}\{\rho_\tau H(g_\tau)\} - \mathrm{tr}\big\{\rho_0^{\mathrm{th}} H(g_0)\big\}. \tag{3.28}$$

Before defining the stochastic entropy production, let us consider the backward or time-reversed version of this process. In this backward process, one performs on the system the work protocol

$$\tilde{g}_t = g_{\tau - t} \tag{3.29}$$

during the time $0 \leqslant t \leqslant \tau$. Hence, $\tilde{g}_t$ reverses the temporal sequence of values of the work parameter g — see Fig. 3.2a). Associated to this time-reversed protocol there will be a unitary $U_{\tilde{g}}(t,0)$ that drives the system.

Let Θ be the quantum time-reversal operator. This is an antilinear operator, $\Theta c = c^* \Theta$ for $c \in \mathbb{C}$, that reverses magnetic fields and linear and angular momenta but keeps position unchanged [130]. Let us assume the Hamiltonian of the system $H(g)$ is invariant under time reversal: $\Theta H \Theta^{-1} = H$; or in case H depends on a magnetic field B, that $\Theta H(B)\Theta^{-1} = H(-B)$. As a consequence, the thermal states $\rho_0^{\mathrm{th}} = e^{-\beta H(g_0)}/Z_0$ and $\rho_\tau^{\mathrm{th}} = e^{-\beta H(g_\tau)}/Z_\tau$ are also time-reversal invariant[1]. Furthermore, as shown in Ap-

[1] In case H depends on a magnetic field, the field must be reversed also in these states. Their eigenvalues

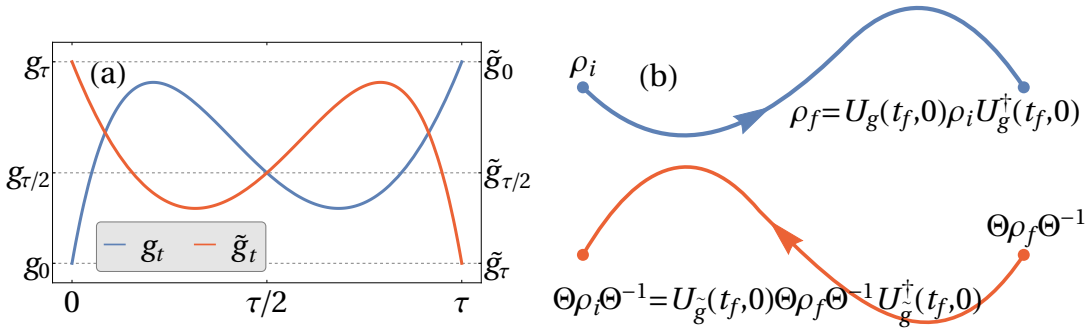

Figure 3.2: Forward and backward evolutions. a) In the time-reversed protocol, the temporal sequence of values of the work parameter g is reversed: $\tilde{g}_t = g_{\tau-t}$. b) In a time-reversal symmetric system, if a initial state ρ_i evolves up to time t_f to a final state ρ_f according to the unitary U_g, then the time-reversed state $\Theta\rho_f\Theta^{-1}$ evolves up to time t_f to $\Theta\rho_i\Theta^{-1}$ under the action of the unitary $U_{\tilde{g}}$. This suggests that $U_{\tilde{g}}(t,0) = \Theta U_g^\dagger(t,0)\Theta^{-1}$, which is made mathematically precise in Appendix C.

pendix C, the unitary $U_{\tilde{g}}$ of the time-reversed drive is then related to the unitary of the forward process U_g by

$$U_{\tilde{g}}(t,0) = \Theta U_g^\dagger(t,0)\Theta^{-1}. \tag{3.30}$$

Finally, assume the thermal state ρ_τ^{th} to be the initial state in the backward process. Then, the first energy measurement at time $t = 0$ in the time-reversed protocol gives the eigenvalue ϵ_j^τ with probability

$$\text{tr}\{\Pi_j^\tau \rho_\tau^{\text{th}}\} = r_j^\tau p_j^\tau, \tag{3.31}$$

where $p_j^\tau = e^{-\beta\epsilon_j^\tau}/Z_\tau$ and $r_j^\tau = \text{tr}\{\Pi_j^\tau\}$ gives the degeneracy of ϵ_j^τ. After the measurement, the state of the system is updated to $\tilde{\rho}_j^\tau = (1/r_j^\tau)\Pi_j^\tau$ and then evolves according to the unitary $U_{\tilde{g}}$ up to time $t = \tau$. The Hamiltonian of the system at the end of the time-reversed process, when the second energy measurement is performed, is $H(g_0)$.

Hence, in this second measurement, the eigenvalue ϵ_i^0 is obtained with probability

$$p_{\tilde{g}}(j \to i) = \frac{1}{r_j^\tau}\,\text{tr}\Big\{\Pi_i^0 U_{\tilde{g}}(\tau,0)\Pi_j^\tau U_{\tilde{g}}^\dagger(\tau,0)\Big\}. \tag{3.32}$$

will remain the same as those of the "forward" state, but their eigenprojectors will be related with "forward" ones by $\Pi_i^{\tau\,\Theta} = \Theta\Pi_i^\tau\Theta^{-1}$.

Analogously to (3.25), we compute the time-reversed path probability as

$$P_B[j,i] = r_j^\tau p_j^\tau p_{\tilde{g}}(j \to i) = p_j^\tau \,\mathrm{tr}\Big\{\Pi_i^0 U_{\tilde{g}}(\tau,0)\Pi_j^\tau U_{\tilde{g}}^\dagger(\tau,0)\Big\}. \tag{3.33}$$

The stochastic entropy production σ is then simply defined as the log-ratio between the forward and backward quantum trajectory probabilities [131]

$$\sigma[i,j] = \ln \frac{P_F[i,j]}{P_B[j,i]} = \ln \frac{p_i^0}{p_j^\tau}, \tag{3.34}$$

where I used Eq. (3.30) to obtain the last equality.

Manipulating the right-hand side of this equation, it is straightforward to show the stochastic entropy production is connected to the stochastic work by $\sigma[i,j] = \beta(w[i,j] - \Delta F)$. Since ΔF is a constant, this means the statistics of the random variables σ and w are directly linked. Moreover, given the probability distribution of σ,

$$p_F(\sigma) = \sum_{i,j} \delta(\sigma - \sigma[i,j]) P_F[i,j], \tag{3.35}$$

we have

$$\Sigma = \langle\sigma\rangle = \int_{-\infty}^{+\infty} \mathrm{d}\sigma p_F(\sigma)\sigma = S(\rho_\tau || \rho_\tau^{\mathrm{th}}). \tag{3.36}$$

Thus far we have verified that the stochastic definitions of work (3.26) and entropy production (3.34) are consistent with the averages discussed in the previous section. Furthermore, it worth noticing their relation is parallel to (3.8). More interesting than that, though, they allow us to arrive at some impressive results.

First, from Eq. (3.34) and the fact that $P_B[j,i]$ is a probability distribution, it directly follows the *Integral Fluctuation Theorem* (IFT)

$$\langle e^{-\sigma}\rangle = \sum_{i,j} e^{-\sigma[i,j]} P_F[i,j] = \sum_{i,j} P_B[j,i] = 1. \tag{3.37}$$

Or in terms of the work, we obtain the *Jarzysnki relation* [98]

$$\langle e^{-\beta w}\rangle = \sum_{i,j} e^{-\beta w[i,j]} P_F[i,j] = \sum_{i,j} e^{-\beta w[i,j]} e^{\sigma[i,j]} P_B[j,i] = e^{-\beta\Delta F}. \tag{3.38}$$

Exploiting (3.34) in (3.35) we get the *Detailed Fluctuation Theorem* (DFT), from which the IFT (3.37) is a direct consequence:

$$\begin{aligned} p_F(\sigma) &= \sum_{i,j} \delta(\sigma - \sigma[i,j]) P_F[i,j] = \sum_{i,j} \delta(\sigma - \sigma[i,j]) e^{\sigma[i,j]} P_B[j,i] \\ &= e^{\sigma} \sum_{i,j} \delta(\sigma - \sigma[i,j]) P_B[j,i] = e^{\sigma} \sum_{i,j} \delta(\sigma + \sigma[j,i]) P_B[j,i] \\ &= e^{\sigma} p_B(-\sigma), \end{aligned} \tag{3.39}$$

where $p_B(\sigma)$ is the probability distribution of the entropy production in the backward protocol. This may be rewritten in the more familiar form

$$\frac{p_F(\sigma)}{p_B(-\sigma)} = e^{\sigma}. \tag{3.40}$$

A similar result, known as the Tasaki-Crooks fluctuation theorem, holds for the distribution of work,

$$\frac{p_F(w)}{p_B(-w)} = e^{\beta(w-\Delta F)}. \tag{3.41}$$

The fluctuation theorems (3.37) - (3.41) may be regarded as a deeper manifestation of the second law [126, 127, 129]. They impose not only a constrain in the first moment Σ (or W) but reveal a symmetry property of the distribution $p_F(\sigma)$ ($p_F(w)$). Using Jensen's inequality, $\langle e^x \rangle \geqslant e^{\langle x \rangle}$, they imply the traditional form of the second law,

$$\Sigma = \beta(W - \Delta F) \geqslant 0, \tag{3.42}$$

as well as linear response theory [129].

Along the work protocol g_t, the system will generally pass through nonequilibrium states. Nonetheless, Eq. (3.38) means, on one hand, that the average $\langle e^{-\beta w} \rangle$ depends only on the initial and final equilibrium states via $e^{-\beta \Delta F}$. And on the other hand, that the equilibrium free energy difference ΔF can be determined from this nonequilibrium process by making many realizations of it. That is, the fluctuations of the stochastic work w generated by the driving encompass information about equilibrium quantities. This is equally true for Eq. (3.41). Moreover, the IFT (3.37) entails not only that stochastic

violations of the second law, meaning $\sigma < 0$, do occur, but in fact that they *must* occur for it to hold.

All of this make fluctuation theorems a highly desirable and valuable property for stochastic thermodynamic quantities.

Customarily, instead of working with the distribution $p_F(\sigma)$, it is easier to consider its Cumulant Generating Function (CGF)

$$K_\sigma(u) \equiv \ln\langle e^{-u\sigma}\rangle = \ln \int \mathrm{d}\sigma p_F(\sigma) e^{-u\sigma} = \sum_{n=1}^{+\infty} \kappa_n(\sigma) \frac{(-1)^n u^n}{n!}, \tag{3.43}$$

where κ_n is the n-th cumulant, and is given by

$$\kappa_n(\sigma) = (-1)^n \frac{\mathrm{d}}{\mathrm{d}u} K_\sigma(u)|_{u=0}. \tag{3.44}$$

The cumulants of a probability distribution are an alternative to the moments. In particular, the first cumulant gives the average $\kappa_1(\sigma) = \Sigma$, and the second one gives the variance $\kappa_2(\sigma) = \langle(\sigma - \Sigma)^2\rangle$. Moreover, the CGF is a polynomial of order two only if the distribution is Gaussian, and has the advantage of being additive for statistically independent variables.

In terms of the CGF, the fluctuation theorems may be stated as

$$K_\sigma(1) = 0 \Leftrightarrow \langle e^{-\sigma}\rangle = 1 \tag{3.45}$$

$$K_\sigma(u) = K^B_\sigma(1-u) \Leftrightarrow \frac{p_F(\sigma)}{p_B(-\sigma)} = e^\sigma, \tag{3.46}$$

where $K^B_\sigma(u)$ is the CGF associated with the backward distribution $p_B(\sigma)$.

Finally, employing Eq. (3.34), the CGF of entropy production can be explicitly written as

$$K_\sigma(u) = \ln \mathrm{tr}\left\{(\rho^{\mathrm{th}}_\tau)^u (\rho_\tau)^{1-u}\right\} = (u-1) S_u(\rho^{\mathrm{th}}_\tau || \rho_\tau), \tag{3.47}$$

where $S_u(\rho||\sigma) = (u-1)^{-1} \ln \mathrm{tr}\{\rho^u \sigma^{1-u}\}$ are the Rényi divergences — see Appendix B.

Before concluding this Chapter, it is necessary to mention that fluctuation theorems were first derived for classical systems evolving under a Hamiltonian dynamics [98, 132]. They are further encountered in several contexts: For classical and quantum systems,

open or closed/isolated, and evolving under several types of dynamics. They may apply to entropy production, work or heat exchange. Additional comments on this may be encountered, for instance, in the reviews [99, 126–129]. In quantum systems, the usual recipe for their derivation involves an initial equilibrium state, time-reversal symmetry of the dynamics and the TPM scheme [128, 129]. A notable exception is given by [4] where neither the initial state is thermal nor the TPM scheme is used.

Concerning their experimental validation in the specific scenario considered in this Chapter, in Refs. [133, 134] the authors proposed an interferometric scheme which allows the determination of the characteristic function of work $\chi_w^F(u) = e^{K_w(iu)}$ — i.e., the Fourier transform of the distribution $p_F(w)$ — by means of measurements on a single qubit probe. This method also enables the circumvention of having to perform the two projective energy measurements at the beginning and the end of the work protocol.

Adopting this strategy, in Ref. [135] the authors were able to determine $\chi_w^{F,B}$ for an isolated driven qubit system. Applying an inverse Fourier transform they obtained $p_{F,B}(w)$ and verified both the Jarzynski relation (3.38) and the Tasaki-Crooks theorem (3.41). In addition, since the entropy production is connected with the work by $\sigma = \beta(w - \Delta F)$, the experiment permits the establishment of $p_F(\sigma)$ and Σ. This was further exploited in [136] to compare the thermodynamic expression (3.8) with the information-theoretic Eq. (3.9). The quantum relative entropy was determined by performing quantum state tomography on the qubit system.

The work distribution $p_F(w)$ may also be directly accessed through a generalized quantum measurement (POVM) [137]. One way to achieve this is to couple the system to an ancilla described by a continuous degree of freedom, like position. Then let the two evolve via a particular entangling interaction (see [137]) applied before and after the work protocol described by U_g. Ultimately, a measurement of the translated state of the ancilla will reveal the work w with probability $p_F(w)$. This procedure was implemented in [138] using cold atoms representing an effective two-level system. The experiment also allowed the verification of the Jarzynski relation (3.38).

Employing some actual projective measurements, in Ref. [139] the authors were able to determine the path probabilities $P_F[i, j]$ in a trapped-ion system behaving as an effective qubit. They further computed the free-energy difference ΔF, average entropy pro-

duction Σ and tested Eq. (3.37) (in fact $\ln\langle e^{-\sigma}\rangle = 0$). They also analysed the fluctuation-dissipation relation $\Sigma = (1/2)\beta^2\langle(\sigma - \Sigma)^2\rangle$, valid in the linear response regime.

To conclude, Ref. [140] proposed a general method for obtaining the transition probabilities $r_i^0 p_g(i \to j) = r_j^\tau p_{\tilde{g}}(j \to i) = \mathrm{tr}\{\Pi_j^\tau U_g(\tau,0)\Pi_i^0 U_g^\dagger(\tau,0)\}$ in a many-body system. The essential idea goes as follows. Suppose an easily measurable observable O that commutes with the final Hamiltonian $H(g_\tau)$. Its expected value at the end of the protocol is given by

$$\langle O\rangle = \mathrm{tr}\{O\rho_\tau\} = \sum_{i,j,\alpha} o_{j,\alpha} p_i^0 p_\alpha,$$

$$p_\alpha = \langle\psi_{j,\alpha}^\tau|U_g(\tau,0)\Pi_i^0 U_g^\dagger(\tau,0)|\psi_{j,\alpha}^\tau\rangle,$$

where $\Pi_i^\tau = \sum_\alpha |\psi_{j,\alpha}^\tau\rangle\langle\psi_{j,\alpha}^\tau|$, $o_{j,\alpha} = \langle\psi_{j,\alpha}^\tau|O|\psi_{j,\alpha}^\tau\rangle$ and, crucially, $\sum_\alpha p_\alpha = r_i^0 p_g(i \to j)$. Note that the probabilities p_α are independent of O, and of the initial temperature. Therefore, by measuring many such observables O and/or using different temperatures, one can determine the p_α's, and from them, the desired transition probabilities. Implementing this method, the authors were capable of verifying the detailed fluctuation theorem (3.41) in an interacting system of two qubits [140].

3.3 Entropy production in the quantum Ising model

We are in the position now to apply the work protocol described in the previous sections to a quantum critical system. We are particularly interested in one specific example of it: the instantaneous and infinitesimal quench.

The instantaneous quench is likely the simplest possible work protocol. It consists of performing a single change in the working parameter g with a vanishing duration, $\tau \to 0$. This considerably simplifies the problem because in this case we do not have to be concerned with some complicated and specific details of the dynamics generated by a more general protocol g_t.

In mathematical terms, since the duration of the protocol goes to zero, the unitary associated with the drive is simplified to the identity $U_{\text{quench}} = \mathbb{1}$. Therefore, the final state,

$$\rho_\tau = U_{\text{quench}}\rho_0^{\text{th}}U_{\text{quench}}^\dagger, \tag{3.48}$$

is equal to the initial thermal state ρ_0^{th}. The system is, nonetheless, driven out of equilibrium because its Hamiltonian is transformed from $H_0 = H(g_0)$ to $H_\tau = H(g_\tau)$.

Although simple, this protocol still exhibits attractive features. For instance, it allows analytical insight even when applied to many-body systems. And, as we will see, its fundamental quantities, work and entropy production, display peculiar behaviors linked to phase transitions [32, 33]. The latter, in particular, presents critical behavior. For this reason, the instantaneous quench protocol has been employed in a number of studies involving phase transitions and critical phenomena [32, 33, 37, 38, 40, 141–146].

Let us consider as our system here the alternating transverse field Ising model (ATFIM) presented in Chapter 2. To recap, this model is described by the Hamiltonian

$$H = -\sum_{j=1}^{N} \left[\sigma_j^x \sigma_{j+1}^x + (g - (-1)^j h)\sigma_j^z\right], \tag{3.49}$$

and have critical curves in the thermodynamic limit defined by

$$|g^2 - h^2| = 1. \tag{3.50}$$

As saw in Chapter 2, most of this model critical points belong to the same universality class of the homogeneous transverse field Ising model, to which it reduces when $h = 0$. However, the critical points $(g = 0, h = \pm 1)$ and $(g = \pm 1, 0)$, when approached by some specific paths, fall into a different universality class. Moreover, they are associated not with second-order phase transitions but with fourth-order transitions.

Both external fields g and h may be viewed as the working parameter that is varied and drives the system out of equilibrium. For simplicity, I will assume that *during the quench* h is fixed and only g is changed. This still allows us to reach the two types of critical points in the model.

As previously shown, after a series of transformations, the Hamiltonian (3.49) can be written as

$$H(g) = P^+ H^+(g) P^+ + P^- H^-(g) P^-, \tag{3.51}$$

where I write $H = H(g)$ to emphasize that g is the varying parameter, and

$$P^{\pm} = \frac{1}{2}(1 \pm P), \quad P = \prod_{j=1}^{N} \sigma_j^z,$$

are the projectors onto the positive and negative parity subspaces. That is, the subspaces of states with even and odd number of down spins, or fermions (see below), respectively.

The Hamiltonians $H^{\pm}$ assume the diagonal form

$$H^{\pm}(g) = \sum_{k \in K^{\pm}} \sum_{s=-,+} \epsilon_k^s(g)(2\eta_{k,s}^{\dagger}(g)\eta_{k,s}(g) - 1), \tag{3.52}$$

where the sets $K^{\pm}$ are given by

$$K^{+} = \Big\{k = \pm(2n+1)\frac{\pi}{N};\ n = 0, 1, ..., N/4 - 1\Big\}, \tag{3.53}$$

$$K^{-} = \Big\{k = 0,\ k = \pm 2n\frac{\pi}{N},\ k = \frac{\pi}{2};\ n = 1, ..., N/4 - 1\Big\}, \tag{3.54}$$

and $\{\eta_{k,s}\}$ are fermionic operators,

$$\{\eta_{k,s}, \eta_{k',s'}^{\dagger}\} = \delta_{k,k'}\delta_{s,s'}, \quad \{\eta_{k,s}, \eta_{k',s'}\} = 0. \tag{3.55}$$

Finally, the single-particle energies read

$$\epsilon_k^{\pm}(g) = \sqrt{1 + g^2 + h^2 \pm 2\sqrt{g^2h^2 + h^2\cos^2 k + g^2 \sin^2 k}}, \tag{3.56}$$

$$\epsilon_0^{\pm}(g) = g \pm \sqrt{1 + h^2}, \tag{3.57}$$

$$\epsilon_{\frac{\pi}{2}}^{\pm}(g) = \sqrt{1 + g^2} \pm h. \tag{3.58}$$

In what follows, it is convenient to make an approximation and consider

$$H(g) = H^{+}(g). \tag{3.59}$$

This amounts to ignoring the change in the Hamiltonian when the system changes to the negative parity subspace. And, again, greatly simplifies all expressions for the thermo-

dynamic quantities we are interested in. Moreover, this is an almost ubiquitous approximation in one-dimensional spin chains, and is expected to produce exact results in the thermodynamic limit.

Actually, for a *finite* homogeneous transverse field Ising model, this approximation gives a 50% error on the partition function at low temperatures in the region corresponding to the ferromagnetic phase [147]. This is typically the region of greater interest, and the discrepancy occurs because the approximation ignores the degeneracy of the ground state in the thermodynamic limit [147]. As shown in Eq. (2.53), the energy gap between the positive and negative parity ground states of H vanishes exponentially with the system size.

We are more interest here in ratios of partition functions, and, therefore, our quantities are not subjected to such errors. Although our main focus is on the thermodynamic limit, for completeness, we compare the thermodynamics of the full and positive parity only Hamiltonians in Appendix D.

Moving forward, our protocol begins with the system prepared in a thermal state at temperature $T = 1/\beta$, with initial field g_0. Thus, we write

$$\rho_0^{\text{th}} = \frac{e^{-\beta H_0}}{Z_0} = \prod_{k\in K^+}\prod_{s=-,+} \frac{e^{\beta\epsilon^s_{k|0}}|0_{k,s}\rangle\langle 0_{k,s}| + e^{-\beta\epsilon^s_{k|0}}|1_{k,s}\rangle\langle 1_{k,s}|}{2\cosh\left(\beta\epsilon^s_{k|0}\right)}, \tag{3.60}$$

where $\eta_{k,s}\,|0_{k,s}\rangle = 0$ and $|1_{k,s}\rangle = \eta^\dagger_{k,s}\,|0_{k,s}\rangle$ are fermionic states, and $\epsilon^\pm_{k|0} = \epsilon^\pm_k(g_0)$.

Next we apply the instantaneous quench protocol, where the external field is suddenly changed from g_0 to g_τ. Since, the state of the system remains the same, the work associated with this drive is given by

$$W = \text{tr}\big\{(H_\tau - H_0)\rho_0^{\text{th}}\big\} = \text{tr}\big\{\Delta H \rho_0^{\text{th}}\big\}. \tag{3.61}$$

To compute this trace I will use a trick of crucial importance in one of our chief results in Chapter 5. First, let $\{\Pi_i^0\}$ be the eigenprojectors of H_0 and ρ_0^{th}. That is, assume

$$H_0 = \sum_i \epsilon_i^0 \Pi_i^0. \tag{3.62}$$

The eigenvalues ϵ_i^0 are made of linear combinations of $\epsilon_{k|0}^{\pm}$ and the eigenprojetors Π_i^0 of $|0_{k,s}\rangle\langle 0_{k,s}|$ and $|1_{k,s}\rangle\langle 1_{k,s}|$.

Next, I note that

$$\mathrm{tr}\{\Delta H \rho_0^{\mathrm{th}}\} = \mathrm{tr}\{\Delta H^{\mathrm{d}} \rho_0^{\mathrm{th}}\}, \tag{3.63}$$

where

$$\Delta H^{\mathrm{d}} = \sum_i \Pi_i^0 \Delta H \Pi_i^0, \tag{3.64}$$

is the part of the perturbation ΔH that is diagonal in the initial energy basis. I refer to it as the *dephased*, or incoherent, part of the perturbation. Its complement, $\Delta H^{\mathrm{c}} = \Delta H - \Delta H^{\mathrm{d}}$ is the *coherent* part. This separation of the perturbation ΔH plays a key role in Chapter 5 where I introduce a new quantum/classical split for the entropy production.

Now, since $H(g)$ is continuous and linear on g we must have

$$\begin{aligned} \Delta H = H_\tau - H_0 &= \delta g \left(\partial_g H(g)\right)|_{g_0}, \\ &= \delta g \sum_i (\partial_{g_0} \epsilon_i^0) \Pi_i^0 + \delta g \sum_i \epsilon_i^0 (\partial_{g_0} \Pi_i^0), \end{aligned} \tag{3.65}$$

where $\delta g = g_\tau - g_0$, and, with some abuse of notation, $\partial_{g_0} \epsilon_i^0 = \partial_g \epsilon_i(g)|_{g_0}$ and similarly for $\partial_{g_0} \Pi_i^0$. Note that for systems presenting continuous, second- or higher-order, transitions, these derivatives are *continuous* functions of g. In particular, for second-order systems, they will have a kink or cusp at a critical point but are still well-defined.

From (3.65) we readily obtain that

$$\Delta H^{\mathrm{d}} = \delta g \sum_i (\partial_{g_0} \epsilon_i^0) \Pi_i^0, \tag{3.66}$$

$$\Delta H^{\mathrm{c}} = \delta g \sum_i \epsilon_i^0 (\partial_{g_0} \Pi_i^0). \tag{3.67}$$

That is, the dephased and coherent parts of the perturbation are directly linked to the derivatives of the system eigenenergies and eigenbasis, respectively.

Equivalently, we may write

$$\Delta H^{\mathrm{d}} = \delta g \sum_{k \in K^+} \sum_{s=-,+} (\partial_{g_0} \epsilon_{k|0}^s)(2\eta_{k,s}^\dagger \eta_{k,s} - 1). \tag{3.68}$$

The work (3.61) associated with the instantaneous quench protocol is now easily computed,

$$W = -\delta g \sum_{k\in K^+} \sum_{s=-,+} (\partial_{g_0} \epsilon^s_{k|0}) \tanh\left(\beta \epsilon^s_{k|0}\right). \tag{3.69}$$

After the sudden quench, if the system is in contact with a bath at temperature T, it will relax to the final equilibrium state

$$\rho^{\text{th}}_\tau = \frac{e^{-\beta H_\tau}}{Z_\tau} = \prod_{k\in K^+} \prod_{s=-,+} \frac{e^{\beta\epsilon^s_{k|\tau}} |0^\tau_{k,s}\rangle\langle 0^\tau_{k,s}| + e^{-\beta\epsilon^s_{k|0}} |1^\tau_{k,s}\rangle\langle 1^\tau_{k,s}|}{2\cosh\left(\beta\epsilon^s_{k|\tau}\right)}, \tag{3.70}$$

where, similarly to (3.60), $\eta_{k,s}(g_\tau)\left|0^\tau_{k,s}\right\rangle = 0$, $\eta^\dagger_{k,s}(g_\tau)\left|0^\tau_{k,s}\right\rangle = \left|1^\tau_{k,s}\right\rangle$, and $\epsilon^\pm_{k|\tau} = \epsilon^\pm_k(g_\tau)$.

Hence, the entropy production in a sudden quench reads

$$\begin{aligned}\Sigma &= S(\rho^{\text{th}}_0 || \rho^{\text{th}}_\tau) = \beta(W - \Delta F) \\ &= \frac{N}{2\pi} \sum_{s=-,+} \int_{-\frac{\pi}{2}}^{\frac{\pi}{2}} \mathrm{d}k \left\{ \ln\left[\frac{\cosh\left(\beta\epsilon^s_{k|\tau}\right)}{\cosh\left(\beta\epsilon^s_{k|0}\right)}\right] - \beta\delta g (\partial_{g_0}\epsilon^s_{k|0}) \tanh\left(\beta\epsilon^s_{k|0}\right)\right\},\end{aligned} \tag{3.71}$$

where I took the thermodynamic limit $N \to \infty$ to convert the sum over k into an integral. I remark the first equality highlights that, in this protocol, the entropy production is a measure of the distinguishability between the equilibrium states associated with the pre- and postquench Hamiltonians. This general formula is valid for any fixed field h and any quench size δg.

Let us consider now some particular cases. We start with $h = 0$. This reduces our system to the usual homogeneous transverse field Ising model, which was studied in [33]. As noted earlier, the critical point of this model located at $g = 1$ is representative of all critical points in the same universality class — all points in the red lines of Fig. 3.4 (see also Fig. 2.1). From now on I refer to it as the Ising critical point.

In Fig. 3.3 it is shown the behavior of the entropy production as a function of the initial field g_0 at several inverse temperatures β. Each point in these curves corresponds to the value of Σ in a realization of the protocol which starts at g_0 and has a quench amplitude $\delta g = 0.01$.

The results may be interpreted as follows [33, 38]. Let us consider first the low tem-

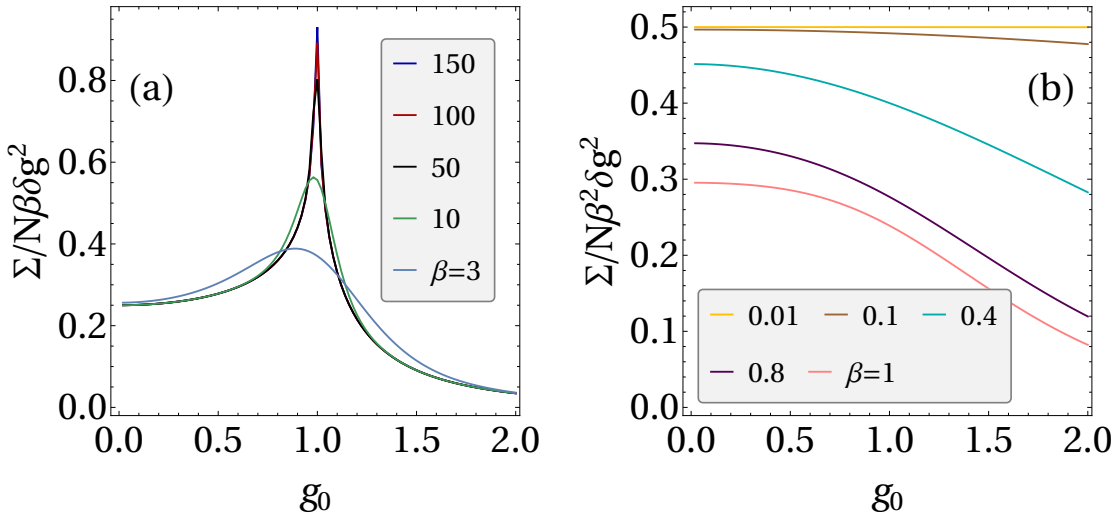

Figure 3.3: Entropy production per spin in the vicinity of the Ising critical point. (a) The behavior at low temperatures (large β). In this case Σ generally scales linearly with β. The increase in the height of the peak at $g_0 = 1$ indicates a logarithmic divergence at this point in the limit $T \to 0$ ($\beta \to \infty$). (b) Behavior at high temperatures. Here Σ scales with β^2 when $\beta \to 0$. In this limit there is no indication of the quantum critical point from Σ. In all points, $\delta g = 0.01$.

perature regime — Fig.3.3(a). Near the critical point the gap is close to zero, and hence, even a small quench is able to create excitations on the system [33]. As a consequence, there is an increase in the production of entropy in the vicinity of the critical point.

The entropy production can, otherwise, be seen as a measure of distinguishability between the equilibrium states associated with the initial and final Hamiltonians. Then, its sharp increase near $g_0 = 1$ at low temperatures, demonstrate that in the critical region a subtle change in the transverse field leads to a substantial change in the equilibrium state [33].

Contrastingly, at high temperatures — Fig. 3.3(b), the large presence of thermal fluctuations obliterates any sign of the quantum criticality [33]. There is no distinct feature, such a pronounced peak or singularity, on the behavior of Σ as a function of the initial field g_0. Particularly, in the limit $T \to \infty$ ($\beta \to 0$) the curve for $\Sigma/N\beta^2$ as a function of g_0 becomes flat.

Moving forward, the increasing height of the peak at $g_0 = 1$ with decreasing temperatures in Fig. 3.3(a) indicates the possibility of a divergence of the entropy production at $T \to 0$. In fact, it is straightforward to show that, for an infinitesimal quench, Σ is

proportional to the transverse magnetic susceptibility. One merely has to note that

$$W = \mathrm{tr}\{\Delta H \rho_0^{\mathrm{th}}\} = \delta g \,\mathrm{tr}\{(\partial_{g_0} H_0)\rho_0^{\mathrm{th}}\} = \delta g \,\partial_{g_0} F(g_0),$$
$$\Delta F = F(g_\tau) - F(g_0) = \delta g \partial_{g_0} F(g_0) + \frac{1}{2}\delta g^2 \partial_{g_0}^2 F(g_0) + \mathcal{O}(\delta g^3).$$

Hence, to leading order on the perturbation [34, 61, 117, 148],

$$\Sigma = \frac{\beta \delta g^2}{2}\chi, \tag{3.72}$$

where $\chi = -\partial_{g_0}^2 F(g_0)$ is the (total) transverse magnetic susceptibility. As we saw in (2.66), this quantity diverges logarithmically at the Ising critical point. Accordingly, $\Sigma/N\beta$ diverges at $g_0 = 1$ when $T \to 0$ ($\beta \to \infty$).

To conclude our analysis on the behavior of the entropy production in the vicinity of a second-order quantum critical point, we note the above result is obviously more general. Equation (3.72) holds for any system subjected to the small and sudden quench work protocol. Hence, in any system exhibiting a second-order continuous quantum phase transition, the entropy production will exhibit critical behavior in a similar way to the susceptibility of the control parameter.

Next we may wish to probe the other type of critical point in the alternating transverse field Ising model. One such a point is located at $(g = 0, h = 1)$ - blue dot in Fig. 3.4 - and is associated with a fourth-order transition. We should note this point is surrounded by Ising-type (second-order) critical points — red lines in Fig. 3.4. The transverse magnetic susceptibility of this model diverges on these Ising-type critical points at $T = 0$, while it is only its second derivative with respect to g which diverges at the fourth-order point. This means the entropy production grows faster near the red lines than near the blue dot in Fig. 3.4. Hence, we should be extra careful on how we approach the latter and use a path that keeps us sufficiently far from the other points in the critical hyperbolas. In this way, the behavior of the entropy production in the vicinity of the blue dot will not be spoiled by the adjacent second-order critical points.

In Fig. 3.5 it is shown the behavior of the entropy production and its second derivative as a function of the initial field g_0 at several inverse temperatures. The path chosen to approach the critical point in these plots was through the curve $h = 1 + 10g^2$. That

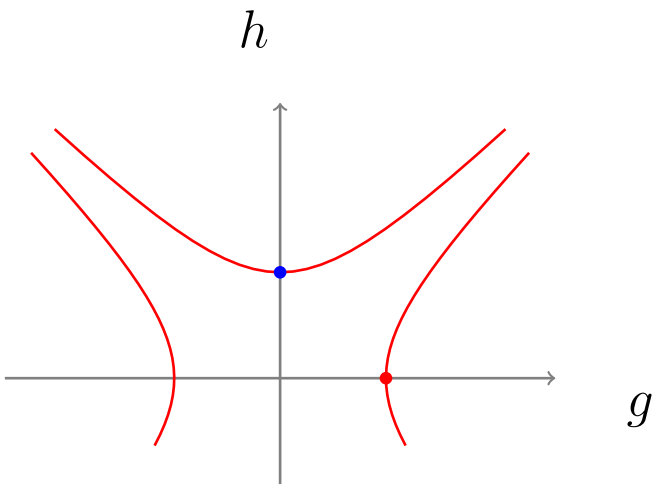

Figure 3.4: Piece of the zero temperature phase diagram of the ATFIM. The hyperbolic red lines are composed of Ising critical points for which the big red point at $(g = 1, h = 0)$ is a representative. The model also has some fourth-order critical points, of which the blue dot at $(g = 0, h = 1)$ is an example.

is, in each realization of the quench protocol, h is kept fixed at the same initial value $h_0 = 1 + 10g_0^2$ and only the field g is changed by an amount $\delta g = 0.01$. This ensures the general expression (3.71) holds.

As expect, in this case the entropy production is always finite at the critical point and only its second derivative diverges. The peak in Fig. 3.5(a) is again explained by an increase in the amount of excitations created by the quench as the gap closes in the vicinity of the critical point. I note the entropy production scales linearly with β at sufficiently low temperatures. A transient regime is what makes the curves for $\beta = 3$ and $\beta = 10$ lie above the others in Fig. 3.5(a).

With rising temperatures, thermal fluctuations cause a broadening of this peak until its eventual disappearance in the limit $T \to \infty$ ($\beta \to 0$) — Fig. 3.5(b).

In Fig. 3.5(c) it is further shown the behavior of the second derivative of the entropy production with respect to the initial field g_0. This quantity is proportional to the second derivative of the transverse magnetic susceptibility, which diverges logarithmically at $g_0 = 0$ when $T = 0$. This divergence is indicated by the increasing depth of the minimum at the critical field.

Significantly, I must highlight that if the fourth-order critical point at $(g = 0, h = 1)$ is approached by a different path, one can obtain qualitatively different behaviors for the

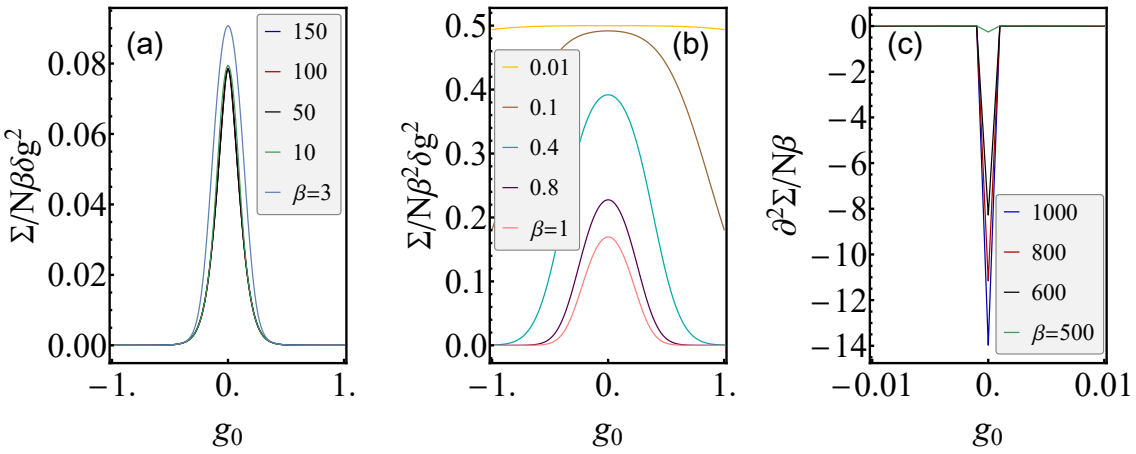

Figure 3.5: Entropy production per spin in the vicinity of the fourth-order critical point in the ATFIM. (a) The behavior at low temperatures, where Σ generally scales linearly with β. The curves for $\beta = 3$ and $\beta = 10$ are above the others because in these cases Σ is still growing faster than linearly with β. (b) Behavior at high temperatures. (c) The second derivative of the entropy production $\partial^2_{g_0}\Sigma/N\beta$ diverges in the limit $\beta \to \infty$. Note that we must go to extremelly low temperatures to capture this. In all points, $\delta g = 0.01$.

entropy production. For instance, if we approach it along the line $h = 1$, the entropy production will display a minimum at this point and not a maximum as shown in Fig. 3.5(a) and (b). As explained above, this happens because of the proximity to the Ising critical points to the left and right of $g = 0$ along this path. This makes the entropy production grows faster on these regions than it does on the vicinity of the fourth-order critical point, and this is why one obtains a minimum.

This brings to an end the examination of the entropy production behavior on the vicinity of the critical points of the ATFIM. The take-home message is that in an infinitesimally and instantaneously quenched quantum critical system, the entropy production is related to the susceptibility of the control (working) parameter. Therefore, the entropy production will exhibit a maximum at the critical parameter that becomes a divergence in the limit $T = 0$ if the system presents a second-order quantum phase transition. For higher order transitions, it is one of its derivatives which diverges, instead.

This behavior makes the entropy production an effective tool, at least theoretically, to detect quantum critical points at low but finite temperatures [32–34]. In the following two chapters I will present two ways in which the entropy production may be split into a classical and quantum contributions. As previously mentioned, one of the essential goals in this thesis is to show these separate contributions can provide an even superior

performance as instruments for detecting quantum critical points.

For completeness, I also mention that in [32] the authors showed a relation between the work performed in a quench and a first-order phase transition. In this case, there is a discontinuity in the work as a function of the control parameter at the transition point in the limit $T \to 0$.

Chapter 4

Populations and Coherences: Relative Entropy of Coherence

Quantum coherences are associated with off-diagonal elements of observables and density operators in a particular basis of the system Hilbert space. Hence, it is evident from its definition that quantum coherences depend on the particular basis being used.

In principle, all conceivable orthonormal bases for a system Hilbert space are completely equivalent, meaning they are equally appropriate to describe the quantum system.

Nonetheless, the interaction with an environment and/or the existence of some conservation law, perhaps, may impose a *preferred basis* [149, 150].

For instance, in Chapter 3, I considered the relaxation of a system from a state ρ_τ to an equilibrium state $\rho_\tau^{\text{th}} = e^{-\beta H_\tau}/Z_\tau$, at temperature $T = 1/\beta$, through a thermal operation. Such an operation is described by a globally energy conserving unitary acting jointly on the system and an environment E initially in the thermal state $\rho_E^{\text{th}} = e^{-\beta H_E}/Z_E$.

This energy conserving condition enforces severe restrictions on the evolved state of the system of interest. Concretely, let us take the spectrum of the system Hamiltonian H_τ to be nondegenerate. Then, if ρ_τ is *incoherent* — in other words *diagonal* — in the eigenbasis of H_τ, so is any subsequent state of the system evolving under a thermal operation [1, 9, 35, 121, 122]. To put it another way, thermal operations cannot create coherences in the energy basis. Moreover, these coherences can be separated in modes defined by energy differences $\omega_{ij} = |\epsilon_j - \epsilon_i|$, where $\{\epsilon_i\}$ are eigenvalues of H_τ. Then if ρ_τ contains coherences in the energy basis, each coherence mode evolve independently from

the others and the state *populations* — i.e. the *diagonal* elements — evolve independently of all coherences [9–11, 35].

In no other basis, such a decoupled evolution of populations and coherences in this process is possible. In this sense, the eigenbasis of H_τ emerges as a preferred basis in the described scenario.

Inspired by these observations, reference [35] proposed the following splitting for the entropy production (3.9),

$$\Sigma = \Gamma_{\text{cl}} + \Gamma_{\text{qu}}, \tag{4.1}$$

$$\Gamma_{\text{cl}} = S(\mathbb{D}_{H_\tau}(\rho_\tau)||\rho_\tau^{\text{th}}), \tag{4.2}$$

$$\Gamma_{\text{qu}} = S(\rho_\tau||\mathbb{D}_{H_\tau}(\rho_\tau)), \tag{4.3}$$

where

$$\mathbb{D}_{H_\tau}(\rho) = \sum_j |j_\tau\rangle\langle j_\tau|\rho|j_\tau\rangle\langle j_\tau|, \tag{4.4}$$

is the dephasing operator in the eigenbasis $\{|j_\tau\rangle\}$ of H_τ. Its effect is to remove all coherences in the state ρ in this basis. I will often refer to Eqs. (4.1)-(4.3) as the Γ-splitting of entropy production.

Both terms in (4.1) are given by relative entropies and, therefore, are nonnegative by construction. In particular, Eq. (4.3) vanishes if and only if ρ_τ is incoherent [1].

Therefore, Eq. (4.2) quantifies the contribution to the entropy production coming from the mismatch in populations between $\mathbb{D}_{H_\tau}(\rho_\tau)$ and the equilibrium state ρ_τ^{th}. Since both these states are diagonal in the same basis, Γ_{cl} is equivalent to a relative entropy between classical probability distributions.

Precisely, if $\{q_j^\tau\}$, with

$$q_j^\tau = \langle j_\tau|\rho_\tau|j_\tau\rangle, \tag{4.5}$$

are the populations of ρ_τ in the basis $\{|j_\tau\rangle\}$, and $\{p_j^\tau\}$ are those of the equilibrium state ρ_τ^{th},

$$\Gamma_{\text{cl}} = \sum_j q_j^\tau \ln \frac{q_j^\tau}{p_j^\tau}, \tag{4.6}$$

where in the right-hand-side we have the Kullback-Leibler divergence. Hence, (4.2) may

be regarded as a classical part of the total entropy production.

In contrast, the second term (4.3) is the *relative entropy of coherence* [1]. This quantifies the contribution to the entropy production steaming from the coherences in ρ_τ in the final energy basis $\{|j_\tau\rangle\}$. Therefore, Γ_{qu} accounts for an authentic quantum contribution to the production of entropy. One that, being nonnegative, demonstrates the presence of coherences increases the entropy production total amount.

In general, the Hamiltonian H_τ will be degenerate. In this case, the previous arguments are equivalently valid if we consider as incoherent states those which commute with H_τ. Moreover, the dephasing operator becomes

$$\mathbb{D}_{H_\tau}(\rho) = \sum_j \Pi_j^\tau \rho \Pi_j^\tau, \tag{4.7}$$

where Π_j^τ are the eigenprojectors of H_τ. The difference between (4.4) and (4.7) is that the latter eliminates only coherences between different energy subspaces of H_τ, maintaining those in the same subspace intact. Conversely, the former removes all coherences in a given basis.

The two quantities (4.2) and (4.3) fulfil an important role in the thermodynamic resource theory defined by thermal operations [9, 117, 120–122]. This is because both of them are monotones of the theory. Explicitly, let us consider a system with Hamiltonian H_S in the initial state ρ_S, and a thermal bath with Hamiltonian H_E in the equilibrium state $\rho_E^{\text{th}} = e^{-\beta H_E}/Z_E$. If

$$\rho_S' = \text{tr}_E\{U(\rho_S \otimes \rho_E^{\text{th}})U^\dagger\}, \quad [U, H_S + H_E] = 0, \tag{4.8}$$

is the state of the system after the thermal operation (4.8), then

$$\Gamma_{\text{cl}}(\rho_S') \leqslant \Gamma_{\text{cl}}(\rho_S), \tag{4.9}$$

$$\Gamma_{\text{qu}}(\rho_S') \leqslant \Gamma_{\text{qu}}(\rho_S). \tag{4.10}$$

In this resource theory, the thermal state $\rho_S^{\text{th}} = e^{-\beta H_S}/Z_S$ is the free state and fixed point of the dynamics. It is the state from which no work can be extracted. Therefore,

any other incoherent state is endowed with the resource of *athermality* [117, 121, 122]. This is the resource consumed in work extraction through a thermal operation. Moreover, if a state contains energetic coherences, this state is further endowed with the resource of *coherence of asymmetry* [9–11, 117]. In the presence of another source of coherence, this resource can also be converted into work [9, 18].

The meaning of Eqs. (4.9) and (4.10) is, thus, that these resources are never created and can only be consumed under a thermal operation. In fact, the relative entropy of coherence is a monotone in several other resource theories [2], including the closely related resource theory of asymmetry [151] and the resource theory of coherences [1] — see also Appendix B. Moreover, Γ_{qu} is also related to the failure of a system to follow an adiabatic evolution [36] and to coherent ergotropy [25]. The quantities Γ_{cl} and Γ_{qu} were further employed to characterize the thermal equilibrium versus nonequilibrium steady state regimes in a quantum optical system [152].

The splitting in the entropy production given in (4.1)-(4.3) was also independently proposed by [36] in connection with the work protocols presented in Chapter 3.

The interpretation of Γ_{cl} and Γ_{qu} given by [36] in this case goes as follows. The work protocol g_t lasting a total time τ drives the system out of the initial equilibrium state

$$\rho_0^{\text{th}} = \frac{e^{-\beta H_0}}{Z_0}, \tag{4.11}$$

to the final state

$$\rho_\tau = U_g(\tau, 0)\rho_0^{\text{th}} U_g^\dagger(\tau, 0), \tag{4.12}$$

where U_g is the unitary associated with the drive g_t. Besides a change in the energy eigenvalues, the Hamiltonian of the system at two different times will generally not commute, $[H_{t_1}, H_{t_2}] \neq 0$ for $t_1 \neq t_2$. Therefore, the drive will generally imbue the system with nonthermal populations and quantum coherences in the final energy basis. Then, Γ_{qu} quantifies the contribution to the entropy production coming from the energetic coherences contained in the state of the system, ρ_τ, at the end of the drive. Complementarily, Γ_{cl} computes the part of the entropy production steaming from the population imbalances

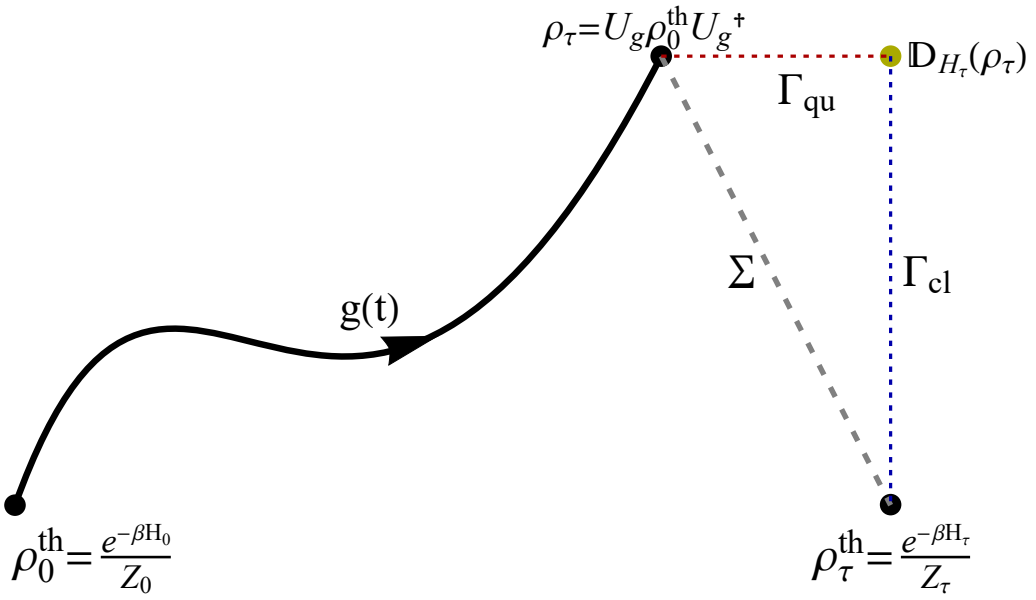

Figure 4.1: Γ-splitting of the entropy production in the work protocol described in Chapter 3. The entropy production Σ - represented by the gray dashed line - may be split into two contributions Γ_{cl} and Γ_{qu}. This is achieved by introducing the dephased state $\mathbb{D}_{H_\tau}(\rho_\tau)$ - yellow dot. Γ_{qu} steam from energy coherences in the system state at the end of the drive, ρ_τ, while Γ_{cl} is related to a mismatch in populations between ρ_τ and ρ_τ^{th}.

between ρ_τ and the updated equilibrium state

$$\rho_\tau^{\text{th}} = \frac{e^{-\beta H_\tau}}{Z_\tau}. \tag{4.13}$$

This is schematically represented in Fig. 4.1.

Furthermore, [36] also provided a stochastic formulation for these quantities in the framework of work protocols and the two-point measurement scheme.

To recapitulate — see Sec. 3.2 —, by performing energy measurements in the beginning and the end of the work protocol, one may define the stochastic entropy production

$$\sigma[i,j] = \ln \frac{p_i^0}{p_j^\tau} = \beta(w[i,j] - \Delta F). \tag{4.14}$$

In the last equality, $w[i,j] = \epsilon_j^\tau - \epsilon_i^0$ is the stochastic work done on the system, while $\beta \Delta F = -\ln Z_\tau / Z_0$ is the change in free energy between ρ_0^{th} and ρ_τ^{th}. Moreover, ϵ_i^0 and ϵ_j^τ are the respective energy eigenvalues obtained in the measurements, and $p_i^0 = e^{-\beta \epsilon_i^0}/Z_0$ and $p_j^\tau = e^{-\beta \epsilon_j^\tau}/Z_\tau$ are the corresponding thermal populations of the initial and final

equilibrium states.

The entropy production has a probability distribution given by

$$p_F(\sigma) = \sum_{i,j} \delta(\sigma - \sigma[i,j]) P_F[i,j], \tag{4.15}$$

where

$$P_F[i,j] = p_i^0 \operatorname{tr}\{\Pi_j^\tau U_g(\tau,0)\Pi_i^0 U_g^\dagger(\tau,0)\} \tag{4.16}$$

is the forward path probability of the quantum trajectory $[i,j]$; Π_i^0 and Π_j^τ being the respective eigenprojectors of H_0 and H_τ associated with the eigenvalues ϵ_i^0 and ϵ_j^τ.

With this at hand, it is straightforward to show that

$$\Sigma = \langle \sigma \rangle = \int_{-\infty}^{+\infty} \mathrm{d}\sigma p_F(\sigma)\sigma = S(\rho_\tau || \rho_\tau^{\text{th}}), \tag{4.17}$$

and that σ satisfy the integral fluctuation theorem

$$\langle e^{-\sigma} \rangle = 1. \tag{4.18}$$

Now, the final state of the system at the end of the work protocol dephased in the final energy basis may be written as

$$\mathbb{D}_{H_\tau}(\rho_\tau) = \sum_j \Pi_j^\tau \rho_\tau \Pi_j^\tau = \sum_j q_j^\tau \Pi_j^\tau. \tag{4.19}$$

Here,

$$q_j^\tau = \operatorname{tr}\{\rho_\tau \Pi_j^\tau\} = \sum_i P_F[i,j], \tag{4.20}$$

are the populations of the final state in this basis and is equal to the marginal distribution of the final energy measurements.

Similarly to (4.14), we can define the stochastic versions of Γ_{cl} and Γ_{qu} [36, 37]

$$\gamma_{\text{cl}}[i,j] = \ln q_j^\tau / p_j^\tau, \tag{4.21}$$

$$\gamma_{\text{qu}}[i,j] = \ln p_i^0 / q_j^\tau. \tag{4.22}$$

Clearly, $\sigma[i,j] = \gamma_{\rm cl}[i,j] + \gamma_{\rm qu}[i,j]$.

Assuming these stochastic variables follow the probability distributions

$$p_F(\gamma_{\rm cl}) = \sum_{i,j} \delta(\gamma_{\rm cl} - \gamma_{\rm cl}[i,j]) P_F[i,j], \tag{4.23}$$

$$p_F(\gamma_{\rm qu}) = \sum_{i,j} \delta(\gamma_{\rm qu} - \gamma_{\rm qu}[i,j]) P_F[i,j], \tag{4.24}$$

it is simple to show that we obtain the expected averages,

$$\Gamma_{\rm cl} = \langle \gamma_{\rm cl} \rangle, \tag{4.25}$$

$$\Gamma_{\rm qu} = \langle \gamma_{\rm qu} \rangle. \tag{4.26}$$

Remarkably, these variables, moreover, satisfy individual integral fluctuation theorems

$$\langle e^{-\gamma_{\rm cl}} \rangle = \langle e^{-\gamma_{\rm qu}} \rangle = 1. \tag{4.27}$$

As I did for work and entropy production in Sec. 3.2, it is often more convenient to consider the cumulant generating functions (CGF) of these random variables. The full statistics of a random variable is equally well characterized by its cumulants.

It is fruitful in this case to take into account the joint probability distributions of $\gamma_{\rm cl}$ and $\gamma_{\rm qu}$,

$$p_F(\gamma_{\rm cl}, \gamma_{\rm qu}) = \sum_{i,j} \delta(\gamma_{\rm cl} - \gamma_{\rm cl}[i,j]) \delta(\gamma_{\rm qu} - \gamma_{\rm qu}[i,j]) P_F[i,j].$$

Then, the joint CGF of these variables reads

$$\begin{aligned} K_{\gamma_{\rm cl},\gamma_{\rm qu}}(v,u) &= \ln \langle e^{-v\gamma_{\rm cl} - u\gamma_{\rm qu}} \rangle \\ &= \ln \mathrm{tr}\big\{ (\rho_\tau^{\rm th})^v (\mathbb{D}_{H_\tau}(\rho_\tau))^{u-v} (\rho_\tau)^{1-u} \big\}. \end{aligned} \tag{4.28}$$

Several remarks can be made now. To begin, the fact that (4.28) cannot, in general, be written as a sum of individual CGFs of these two variables, means $\gamma_{\rm cl}$ and $\gamma_{\rm qu}$ are typically *statistically dependent*. Second, the reduced CGFs of $\gamma_{\rm cl}$ and $\gamma_{\rm qu}$ are obtained from the

joint CGF (4.28) by setting $u = 0$ and $v = 0$, respectively. They read

$$K_{\gamma_{\rm cl}}(v) = \ln \mathrm{tr}\big\{(\rho_\tau^{\rm th})^v(\mathbb{D}_{H_\tau}(\rho_\tau))^{1-v}\big\} = (v-1)S_v(\rho_\tau^{\rm th}||\mathbb{D}_{H_\tau}(\rho_\tau)), \tag{4.29}$$

$$K_{\gamma_{\rm qu}}(u) = \ln \mathrm{tr}\big\{(\mathbb{D}_{H_\tau}(\rho_\tau))^u(\rho_\tau)^{1-u}\big\} = (u-1)S_u(\mathbb{D}_{H_\tau}(\rho_\tau)||\rho_\tau), \tag{4.30}$$

where in the first equation I used that $\mathbb{D}_{H_\tau}(\rho_\tau)$ and ρ_τ have the same populations in the basis of $\rho_\tau^{\rm th}$. In addition, $S_\alpha(\rho||\sigma)$ is the α-Rényi divergence — see Appendix B. It is straightforward to derive from the previous relations that their respective first cumulants are given by Eqs. (4.2) and (4.3).

Furthermore, it is interesting to note the CGF of the entropy production σ is obtained from (4.28) by making $u = v$ — see Eq. (3.47).

The discussion thus far makes evident the significance of the splitting (4.1) of the entropy production in characterizing the nonequilibrium thermodynamics of quantum systems. Namely, the two components in this division bear a notable interpretation in thermodynamic resource theory and satisfy individual fluctuation theorems when analysed from the perspective of work protocols. In the subsequent section I apply it to the problem of an infinitesimally and instantaneously quenched critical system. The results will show that despite all its merits and qualities, this splitting has also some shortcomings.

4.1 Γ-splitting in the quantum Ising model

In [38], we studied the behaviors of $\Gamma_{\rm cl}$ and $\Gamma_{\rm qu}$ in the vicinity of a quantum critical point. I repeat the analysis here. For this, let us start with our model Hamiltonian

$$H = -\sum_{j=1}^{N}\big[\sigma_j^x\sigma_{j+1}^x + (g-(-1)^j h)\sigma_j^z\big]. \tag{4.31}$$

As in Sec. 3.3, I will consider an instantaneous quench protocol, for which $U_{\rm quench} = \mathbb{1}$ and $\rho_\tau = \rho_0^{\rm th}$. Moreover, I will again ignore the change in the Hamiltonian of our spin chain caused by the parity and make the approximation $H(g) = H(g)^+$.

Furthermore, to compute the dephased state $\mathbb{D}_{H_\tau}(\rho_\tau)$, we need to know the relation between the eigenbasis of the initial Hamiltonian $H_0 = H(g_0)$ and the final Hamiltonian

$H_\tau = H(g_\tau)$. Ultimately, this amounts to obtaining the exact form of the matrices O_k diagonalizing the matrices (2.28),

$$A_k = \begin{pmatrix} a_k \\ a^\dagger_{-k} \\ b_k \\ b^\dagger_{-k} \end{pmatrix}, \quad H_k = \begin{pmatrix} g - \cos k & \sin k & h & 0 \\ \sin k & -g + \cos k & 0 & -h \\ h & 0 & g + \cos k & -\sin k \\ 0 & -h & -\sin k & -g - \cos k \end{pmatrix},$$

giving the single-particles eigenenergies of $H(g)$,

$$\epsilon^\pm_k = \sqrt{1 + g^2 + h^2 \pm \sqrt{g^2h^2 + g^2\cos^2 k + h^2 \cos^2 k}}.$$

As discussed in Chapter 2, these matrices are immensely complicated for general values of g and h. On that account, I will consider only the case $h = 0$ in this section. Accordingly, O_k assumes the simple form

$$O_k = \begin{pmatrix} \cos\left(\theta^-_k/2\right) & \sin\left(\theta^-_k/2\right) & 0 & 0 \\ -\sin\left(\theta^-_k/2\right) & \cos\left(\theta^-_k/2\right) & 0 & 0 \\ 0 & 0 & \cos\left(\theta^+_k/2\right) & -\sin\left(\theta^+_k/2\right) \\ 0 & 0 & \sin\left(\theta^+_k/2\right) & \cos\left(\theta^+_k/2\right) \end{pmatrix},$$

where

$$(\cos\theta^\pm_k,\, \sin\theta^\pm_k) = \left(\frac{g \pm \cos k}{\epsilon^\pm_k},\, \frac{\sin k}{\epsilon^\pm_k}\right),$$

$$\epsilon^\pm_k(g) = \sqrt{1 + g^2 \pm 2g\cos k},$$

such that

$$O_k H_k O^\dagger_k = \text{diag}(\epsilon^-_k, -\epsilon^-_k, \epsilon^+_k, -\epsilon^+_k).$$

Hence, the Hamiltonian (4.31) with $h = 0$ and the parity approximation can be written in diagonal form as

$$H(g) = \sum_{k \in K^+} \sum_{s=-,+} \epsilon^s_k (2\eta^\dagger_{k,s}\eta_{k,s} - 1),$$

where

$$K^{+}=\Big\{k=\pm(2n+1)\frac{\pi}{N};\, n=0,1,...,N/4-1\Big\},$$

and

$$\eta_{k,-}=\cos\big(\theta_k^{-}/2\big)a_k+\sin\big(\theta_k^{-}/2\big)a_{-k}^{\dagger},\quad \eta_{k,+}=\cos\big(\theta_k^{+}/2\big)b_k-\sin\big(\theta_k^{+}/2\big)b_{-k}^{\dagger}.$$

The fermionic operators a_k and b_k were introduced in Chapter 2.

Everything may be further simplified by noticing we can make [90, 94]

$$b_k=\begin{cases}a_{k-\pi}, & \text{if}\quad 0<k<\pi/2,\\ \\ a_{k+\pi}, & \text{if}\quad -\pi/2<k<0,\end{cases}$$

and that

$$\epsilon_k^{+}=\epsilon_{k\pm\pi}^{-},\qquad (\cos\theta_k^{+},\,\sin\theta_k^{+})=(\cos\theta_{k\pm\pi}^{-},\,-\sin\theta_{k\pm\pi}^{-}).$$

This allows us to write

$$H(g)=\sum_{k\in K_I^{+}}\epsilon_k(g)(2\eta_k^{\dagger}\eta_k-1), \tag{4.32}$$

where

$$K_I^{+}=\Big\{k=\pm(2n+1)\frac{\pi}{N};\, n=0,1,...,N/2-1\Big\} \tag{4.33}$$

$$\epsilon_k(g)=\sqrt{(g-\cos k)^2+\sin^2 k}=\sqrt{1+g^2-2g\cos k}, \tag{4.34}$$

$$(\cos\theta_k,\,\sin\theta_k)=\left(\frac{g-\cos k}{\epsilon_k},\,\frac{\sin k}{\epsilon_k}\right), \tag{4.35}$$

$$\eta_k=\cos(\theta_k/2)a_k+\sin(\theta_k/2)a_{-k}^{\dagger}, \tag{4.36}$$

with $\{\eta_k\}$ satisfying the fermionic anticommutation relations

$$\{\eta_k,\eta_{k'}\}=0,\quad \{\eta_k,\eta_{k'}^{\dagger}\}=\delta_{k,k'}. \tag{4.37}$$

It is worth emphasizing $\{\eta_k\}$ are functions of the transverse field g.

In this section I work with the specialized Eqs. (4.32)-(4.37). We can finally move forward.

At the beginning of the work protocol, the system is prepared in the thermal state

$$\rho_0^{\text{th}} = \prod_{k\in K_{I>}^+} \sum_{n_{-k}^0,\, n_k^0=0}^{1} \frac{e^{2\beta\epsilon_k^0(1-n_k^0-n_{-k}^0)}}{4\cosh^2(\beta\epsilon_k^0)} |n_{-k}^0 n_k^0\rangle\langle n_{-k}^0 n_k^0|, \tag{4.38}$$

where $\epsilon_k^0 = \epsilon_k(g_0)$, $K_{I>}^+$ is the set composed of only the positive elements of (4.33), and $\left|n_{-k}^0 n_k^0\right\rangle$ are the joint eigenstates of $\eta_{-k}^{0\,\dagger}\eta_{-k}^0$ and $\eta_k^{0\,\dagger}\eta_k^0$.

Subsequently an instantaneous quench is applied changing the transverse field to a final value g_τ. This transforms the Hamiltonian of the system to H_τ, leaving its state unaffected. The varying Hamiltonian establishes a new equilibrium state at temperature $T = 1/\beta$. It reads

$$\rho_\tau^{\text{th}} = \prod_{k\in K_{I>}^+} \sum_{n_{-k}^\tau,\, n_k^\tau=0}^{1} \frac{e^{2\beta\epsilon_k^\tau(1-n_k^\tau-n_{-k}^\tau)}}{4\cosh^2(\beta\epsilon_k^\tau)} |n_{-k}^\tau n_k^\tau\rangle\langle n_{-k}^\tau n_k^\tau|, \tag{4.39}$$

where $\epsilon_k^\tau = \epsilon_k(g_\tau)$ and $\left|n_{-k}^\tau n_k^\tau\right\rangle$ are the eigenstates of $\eta_{-k}^{\tau\,\dagger}\eta_{-k}^\tau$ and $\eta_k^{\tau\,\dagger}\eta_k^\tau$.

In general, H_0 and H_τ do not commute, which means the state of the system at the end of drive $\rho_\tau = \rho_0^{\text{th}}$ will contain coherences in the final energy basis. From Eqs. (4.35) and (4.36) we obtain that the postquench operators $\{\eta_k^\tau\}$ are related to the prequench $\{\eta_k^0\}$ by [33]

$$\eta_k^\tau = \cos(\Delta_k/2)\eta_k^0 + \sin(\Delta_k/2)\eta_{-k}^{0\,\dagger}. \tag{4.40}$$

Here, $\Delta_k = \theta_k^\tau - \theta_k$ is the difference between the post- and prequench Bogoliubov angles (4.35) and satisfy

$$\sin\Delta_k = -\delta g \frac{\sin k}{\epsilon_k^\tau \epsilon_k^0}, \tag{4.41}$$

where, again, $\delta g = g_\tau - g_0$.

From (4.40) we have the following relations between the energy states of the initial

and final basis

$$\left|0^0_{-k}0^0_k\right\rangle = \cos(\Delta_k/2)\left|0^\tau_{-k}0^\tau_k\right\rangle - \sin(\Delta_k/2)\left|1^\tau_{-k}1^\tau_k\right\rangle, \tag{4.42}$$

$$\left|1^0_{-k}1^0_k\right\rangle = \sin(\Delta_k/2)\left|0^\tau_{-k}0^\tau_k\right\rangle + \cos(\Delta_k/2)\left|1^\tau_{-k}1^\tau_k\right\rangle, \tag{4.43}$$

while the states with a single particle occupying the mode k or $-k$ remain equal.

Working with the above relations, we may express the initial state ρ_0^{th} in the final energy basis and then dephase it to obtain

$$\begin{aligned}\mathbb{D}_{H_\tau}(\rho_0^{\text{th}}) = \prod_{k\in K^+_{I>}} \Big\{ &\frac{1}{4}\big(1+\tanh^2(\beta\epsilon^0_k) + 2\tanh\big(\beta\epsilon^0_k\big)\cos\Delta_k\big)|0^\tau_{-k}0^\tau_k\rangle\langle 0^\tau_{-k}0^\tau_k| \\ &+\frac{1}{4}\big(1+\tanh^2(\beta\epsilon^0_k) - 2\tanh\big(\beta\epsilon^0_k\big)\cos\Delta_k\big)|1^\tau_{-k}1^\tau_k\rangle\langle 1^\tau_{-k}1^\tau_k| \\ &+|1^\tau_{-k}0^\tau_k\rangle\langle 1^\tau_{-k}0^\tau_k| + |0^\tau_{-k}1^\tau_k\rangle\langle 0^\tau_{-k}1^\tau_k|\Big\}.\end{aligned} \tag{4.44}$$

We are ready now to compute the two components of the entropy production (4.2) and (4.3) in a quenched Ising model. For the latter, I further notice Γ_{qu} is a very special relative entropy since it can be written as the difference between two von Neumann entropies [1],

$$\Gamma_{\text{qu}} = S(\rho_\tau||\mathbb{D}_{H_\tau}(\rho_\tau)) = S(\mathbb{D}_{H_\tau}(\rho_\tau)) - S(\rho_\tau).$$

Hence, the results are [38]

$$\begin{aligned}\Gamma_{\text{qu}} =& N\int_0^\pi \frac{\mathrm{d}k}{2\pi}\Bigg\{ -\frac{1}{4}\big(1+\tanh^2(\beta\epsilon^0_k)\big)\ln\left(1+\sinh^2(2\beta\epsilon^0_k)\sin^2\Delta_k\right) \\ &+\frac{1}{2}\tanh\big(\beta\epsilon^0_k\big)\left[\ln\left(\frac{1+\tanh(2\beta\epsilon^0_k)}{1-\tanh(2\beta\epsilon^0_k)}\right) - \cos\Delta_k\ln\left(\frac{1+\tanh(2\beta\epsilon^0_k)\cos\Delta_k}{1-\tanh(2\beta\epsilon^0_k)\cos\Delta_k}\right)\right]\Bigg\},\end{aligned} \tag{4.45}$$

and

$$\Gamma_{\text{cl}} = N\int_0^\pi \frac{\mathrm{d}k}{2\pi}\left\{2\ln\left(\frac{\cosh(\beta\epsilon_k^\tau)}{\cosh(\beta\epsilon_k^0)}\right) + \frac{1}{4}\big(1+\tanh^2(\beta\epsilon_k^0)\big)\ln\big(1+\sinh^2(2\beta\epsilon_k^0)\sin^2\Delta_k\big)\right.$$
$$\left. -\frac{1}{2}\tanh\big(\beta\epsilon_k^0\big)\cos\Delta_k\left[\ln\left(\frac{1+\tanh(2\beta\epsilon_k^0)}{1-\tanh(2\beta\epsilon_k^0)}\right) - \ln\left(\frac{1+\tanh(2\beta\epsilon_k^0)\cos\Delta_k}{1-\tanh(2\beta\epsilon_k^0)\cos\Delta_k}\right)\right]\right\}, \tag{4.46}$$

where I used the thermodynamic limit $N\to\infty$ to convert the sums over k into integrals.

For completeness and comparison, I also write down the full entropy production [33, 62]

$$\Sigma = N\int_0^\pi \frac{\mathrm{d}k}{2\pi}2\left\{\ln\left(\frac{\cosh(\beta\epsilon_k^\tau)}{\cosh(\beta\epsilon_k^0)}\right) - \beta(\epsilon_k^\tau\cos\Delta_k - \epsilon_k^0)\tanh\big(\beta\epsilon_k^0\big)\right\}. \tag{4.47}$$

Note that $\epsilon_k^\tau\cos\Delta_k - \epsilon_k^0 = \delta g\cos\theta_k = \delta g(\partial_g\epsilon_k)|_{g_0}$. This can be compared with Eq. (3.71).

Figure 4.2 displays the behaviors of these contributions to the entropy production as functions of the initial field g_0 at several inverse temperatures β. In all points, the size of the quench is given by $\delta g = 0.01$.

The general expressions for Γ_{cl} and Γ_{qu} are not at all instructive. To explain these results, we can consider first the low-temperature limit and note that to leading order on β, Eqs. (4.45)-(4.47) become [38]

$$\Gamma_{\text{qu}}/N = \int_0^\pi \frac{\mathrm{d}k}{2\pi}\big[-p_k\ln p_k - (1-p_k)\ln(1-p_k)\big] \tag{4.48}$$

$$\Gamma_{\text{cl}}/N = 4\beta\int_0^\pi \frac{\mathrm{d}k}{2\pi}\epsilon_k^\tau p_k - \Gamma_{\text{qu}}/N, \tag{4.49}$$

$$\Sigma/N = 4\beta\int_0^\pi \frac{\mathrm{d}k}{2\pi}\epsilon_k^\tau p_k, \tag{4.50}$$

where $p_k = \sin^2(\Delta_k/2)$.

From Eqs. (4.42)-(4.43), we see p_k gives the probability of the $\pm k$ modes to transition from a prequench fully unoccupied/occupied state to fully occupied/unoccupied state after the quench. Together with (4.50), this confirms the interpretation of the increase in en-

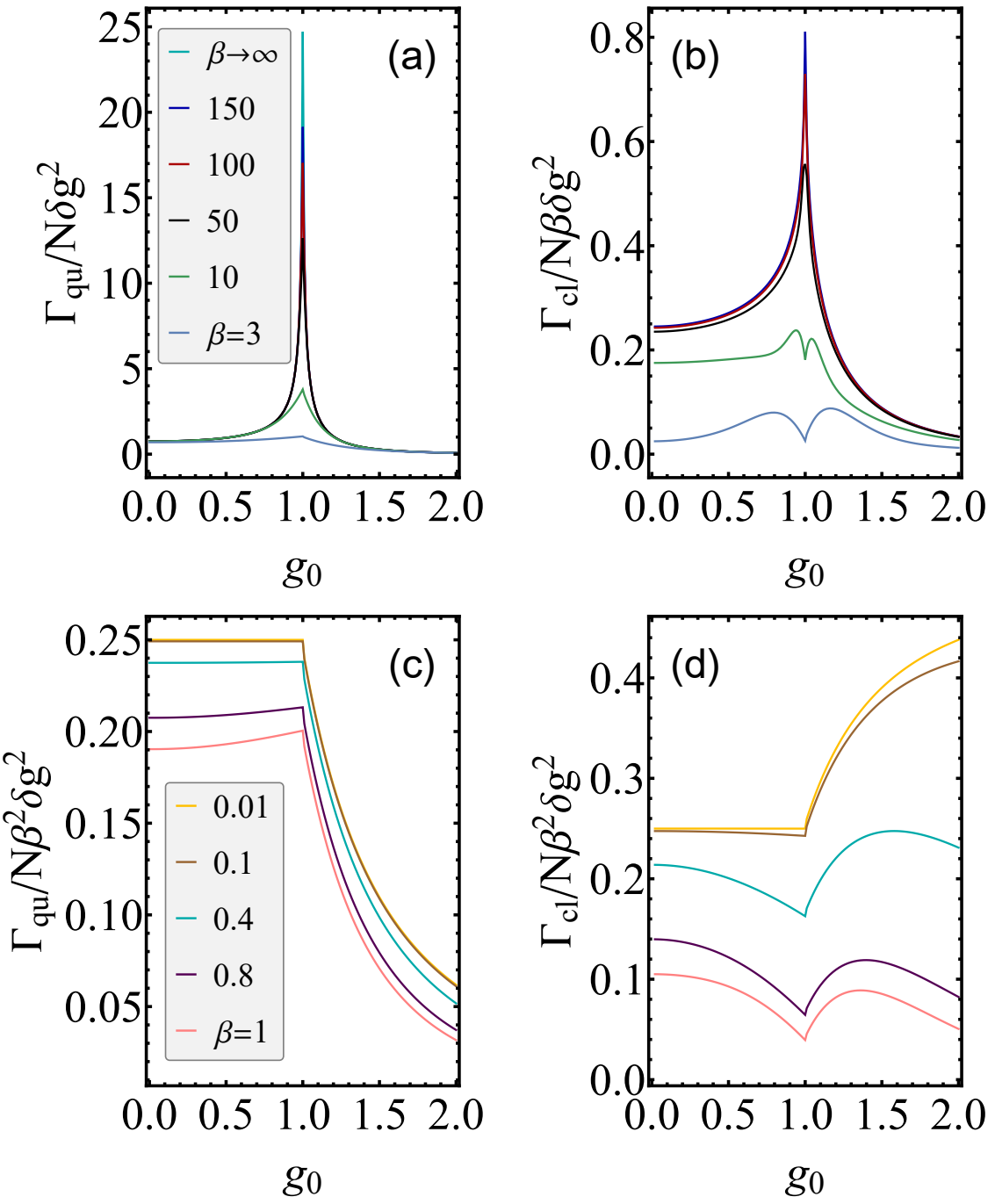

Figure 4.2: Γ_{qu} and Γ_{cl} per spin in the vicinity of the Ising critical point. Above, the behaviors at low temperatures (large β) of (a) Γ_{qu} and (b) Γ_{cl}. In this limit, Γ_{cl} scales linearly with β at sufficiently low temperatures, while Γ_{qu} is bounded. The divergence in the entropy production at $g_0 = 1$ in the limit $T \to 0$ ($\beta \to \infty$) comes from the classical part Γ_{cl}. Below, the behaviors at high temperatures of (c) Γ_{qu} and Γ_{cl}. Here both contributions scale with β^2 at sufficiently high temperatures. Contrarily to the full entropy production, even in this limit the quantum critical point is indicated by a kink in Γ_{qu} and Γ_{cl}. In all points, $\delta g = 0.01$.

tropy production near a quantum critical point as resulting from the creation of excitations by the quench.

Moreover, the contribution from coherences in this limit steam from the integrated binary entropy associated with the probability p_k. Since the maximum of a binary entropy is $\ln 2$, Γ_{qu} per spin cannot diverge and, in fact, is bounded by $\frac{1}{2}\ln 2$. Such a maximum would be obtained only if $p_k = 1/2$ for all k's. This finiteness of the coherence contribution to the entropy production per spin is illustrated by the curve $\beta \to \infty$ on Fig. 4.2(a). This was plotted using (4.48).

Considering that Σ/N begins to diverge as $T \to 0$, the finitude of Γ_{qu}/N further means the relative contribution from coherences to the entropy production decreases with lowering temperature. Intuitively, one would expect precisely the opposite of this, with quantum coherences fulfilling a more prominent role at low temperatures. We will see more on this in the next section.

Curiously, the height of the cusp at the critical field $g_0 = 1$ of Γ_{qu}/N scales linearly with δg when $T = 0$. In contrast, I will show later Σ/N always scales with δg^2 in an infinitesimal instantaneous quench.

This result on the behavior of the coherent contribution Γ_{qu} may be proven as follows [38]. The integral in (4.48) is dominated by the contributions at low pseudomomenta $k \to 0$. The idea is then to replace the complicated integrand $C_k = -p_k \ln p_k - (1-p_k)\ln(1-p_k)$ by a more tractable function that is close to it in the appropriate limit. This is achieved by the following function,

$$\begin{aligned} F_k &= -\frac{1+f_k}{2}\ln\frac{1+f_k}{2} - \frac{1-f_k}{2}\ln\frac{1-f_k}{2}, \\ f_k &= \frac{k(1+\delta g/2)}{\sqrt{\delta g^2 + (1+\delta g)k^2}} \end{aligned} \tag{4.51}$$

where f_k is equal to $\cos\Delta_k = 1 - 2p_k$ at $g_0 = 1$ when k is small. Note in the interval $2 < k < \pi$, C_k is of order $\delta g^2 \ln \delta g^2$, when δg^2 is small. Moreover, when $0 < k < 2$, one can check $C_k - F_k$ is a monotonically increasing function of k, and $F_{k=2} \to 0$. That is, this difference is also of order $\delta g^2 \ln \delta g^2$. Thus, at $T = 0$ and $g_0 = 1$,

$$\Gamma_{\text{qu}}/N = \int_0^2 \frac{\mathrm{d}k}{2\pi} F_k + \mathcal{O}(\delta g^2 \ln \delta g^2). \tag{4.52}$$

Lastly,

$$\int_0^2 \frac{\mathrm{d}k}{2\pi} F_k = \frac{1}{4}\delta g + \mathcal{O}(\delta g^2 \ln \delta g^2), \tag{4.53}$$

which completes the proof.

Continuing, the creation of excitations near a quantum critical point at low temperatures is captured by the populations part of the entropy production in the Γ-splitting. Hence, Γ_{cl}/N is the contribution responsible for the divergence of Σ/N in the limit $T = 0$. Precisely, at zero temperature $\Gamma_{\text{cl}}/N\beta \sim \ln ||g_0| - 1|$. This asymptotically singular behavior is indicated by the increasing height of the peaks in Fig. 4.2(b) — this should be compared with Fig. 3.3(a).

Next, let us move to the high-temperature limit. In this case, Eqs. (4.45)-(4.47) may be written, at sufficiently high temperatures, as [38]

$$\Gamma_{\text{qu}}/N = \beta^2 \int_0^\pi \frac{\mathrm{d}k}{2\pi} (\epsilon_k^0)^2 \sin^2 \Delta_k, \tag{4.54}$$

$$\Gamma_{\text{cl}}/N = \beta^2 \int_0^\pi \frac{\mathrm{d}k}{2\pi} (\epsilon_k^\tau - \epsilon_k^0 \cos \Delta_k)^2, \tag{4.55}$$

$$\Sigma/N = \beta^2 \int_0^\pi \frac{\mathrm{d}k}{2\pi} \left[(\epsilon_k^\tau)^2 - 2\epsilon_k^\tau \epsilon_k^0 \cos \Delta_k + (\epsilon_k^0)^2\right]. \tag{4.56}$$

These equations show that, to leading order, all three quantities scale in the same manner as a function of β in the high-temperature limit. Moreover, these are valid for any quench size. If we further consider a small quench, we obtain [38]

$$\Gamma_{\text{qu}}/N = \beta^2 \delta g^2 \int_0^\pi \frac{\mathrm{d}k}{2\pi} \sin^2 \theta_k, \tag{4.57}$$

$$\Gamma_{\text{cl}}/N = \beta^2 \delta g^2 \int_0^\pi \frac{\mathrm{d}k}{2\pi} \cos^2 \theta_k, \tag{4.58}$$

$$\Sigma/N = \frac{1}{2}\beta^2 \delta g^2, \tag{4.59}$$

also to leading order on the perturbation δg. In addition, I remember

$$(\cos \theta_k,\ \sin \theta_k) = \left(\frac{g_0 - \cos k}{\epsilon_k^0},\ \frac{\sin k}{\epsilon_k^0}\right). \tag{4.60}$$

Equation (4.59) shows indeed, as discussed in Sec. 3.3, the entropy production becomes a flat function of the initial field g_0 at high temperatures and small quench sizes.

Contrarily to the full entropy production, the individual contributions Γ_{cl} and Γ_{qu} still exhibit a signature of the quantum critical field, manifested as a kink, even this high-temperature limit — Fig. 4.2(c) and (d). In fact, looking at Fig. 4.2, no matter the temperature, the classical and quantum parts of the entropy production consistently present a kink or cusp singularity at the critical field $g_0 = 1$. As previously discussed, particularly at $T = 0$, the cusp on Γ_{cl} becomes a divergence.

Analysing Eqs. (4.45) and (4.46), one can hardly give any intuitive reason for such eccentric (singular) behaviors. I will approach this problem again when a new splitting for the entropy production is proposed. For now, let us return to the analysis of the behaviors of Γ_{qu} and Γ_{cl} at high temperatures.

Figure 4.2(c) shows the relative entropy of coherence behaves differently in the regions of g_0 corresponding to different phases in the model. Precisely, in the limit $T \to \infty$ ($\beta \to 0$), Γ_{qu} exhibits a plateau for field values associated with the ferromagnetic phase, while it monotonically decreases in the region corresponding to the quantum paramagnet. Complementarily, Γ_{cl} presents a flat depression for $g_0 < 1$ and increases monotonically when $g_0 > 1$ — Fig. 4.2(d).

Indeed, Eq. (4.57) can be analytically evaluated to give [38]

$$\Gamma_{\text{qu}}/N = \frac{1}{4}\beta^2\delta g^2 \begin{cases} 1, & \text{for } |g_0| \leqslant 1, \\ 1/|g_0|^2, & \text{for } |g_0| > 1, \end{cases} \tag{4.61}$$

consistent with the aforementioned behavior. Comparing this to Eq. (4.59), we see the contribution from coherences amounts to half the total entropy production in the high-temperature limit and $g_0 \leqslant 1$. Therefore, in the Γ-splitting, the relative contribution to the entropy production coming from quantum coherences is considerably high at high temperatures, but, afterwards, decreases as the temperature is lowered. This is again counter-intuitive.

In Fig. 4.3 I further show the behavior of the ratio $\Gamma_{\text{qu}}/\Sigma$ both as a function of β and as a function of the initial field g_0. The purple curve in the center of Fig. 4.3(a) confirms

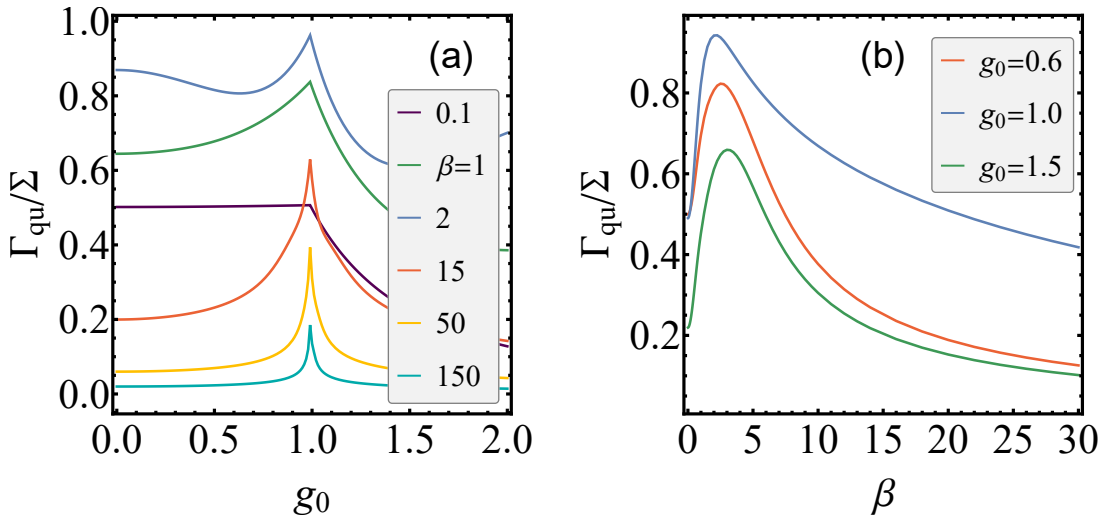

Figure 4.3: Ratio $\Gamma_{\rm qu}/\Sigma$ (a) as a function of the initial field g_0 for several β; and (b) as a function of β for different values of the initial field g_0 associated with the ferromagnetic, critical point and paramagnetic phases. It is lucid from these figures that there is an optimal temperature near $\beta = 2$ where the contribution from coherences reaches its maximum value. In all points, $\delta g = 0.01$.

the results in Eq. (4.61). At very high temperatures and $g_0 \leqslant 1$, $\Gamma_{\rm qu}$ amounts to 50% of the total entropy production. As the temperature decreases (β increases), there is an initial increase in the ratio $\Gamma_{\rm qu}/\Sigma$ up to an optimal temperature close to $\beta = 2$. But then, further lowering the temperature decreases this ratio. As we will see in the subsequent section, this is related to a fundamental change in the behaviors of $\Gamma_{\rm qu}$ and $\Gamma_{\rm cl}$ near this point. Namely, these two functions cease to be analytic in terms of the perturbation δg. That is, we can no longer make a Taylor expansion on them in terms of the quench amplitude. This is already obvious from (4.48).

At very low temperatures, the ratio $\Gamma_{\rm qu}/\Sigma$ becomes increasingly small, approaching zero. This is expected following the previous discussion on the low-temperature behavior of this splitting of the entropy production. Notwithstanding, there is still a considerable increase on $\Gamma_{\rm qu}/\Sigma$ in the vicinity of the critical field value $g_0 = 1$. This is related to the sharp cusp on $\Gamma_{\rm qu}$ shown in Fig. 4.2(a) in the vicinity of this point.

This concludes the analysis of the Γ-splitting in a suddenly quenched Ising model. The somewhat strange and counter-intuitive behaviors of this splitting of the entropy production illustrated here, actually, reflects general features of these quantities when applied to work protocols. In the next section I discuss in detail the roots of such shortcomings.

4.2 Shortcomings of the Γ-splitting

Now I address the flaws in the Γ-splitting. There are mainly two, and we pointed them out firstly on [37].

As a start, thus far I have largely considered instantaneous quenches with an amplitude $\delta g \ll 1$. The consideration of such small perturbations naturally leads to the question of whether the quantities of interest can be analyzed perturbatively.

Indeed, as shown bellow, given an quench amplitude δg, the entropy production is an analytical function of this perturbation over a large range of temperatures. However, that is not the case with Γ_{cl} and Γ_{qu} [37]. When we try a Taylor expansion of these quantities on δg, we obtain a radius of convergence that goes exponentially fast to zero as β increases (T decreases). The reason is that δg on the expressions for Γ_{cl} and Γ_{qu} usually appears multiplied by an exponentially increasing function of β [37].

This feature is obvious, for instance, in Eqs. (4.45) and (4.46). I recall $\sin\Delta_k = -\delta g \sin\theta_k/\epsilon_k^\tau$, thus, the term containing

$$\ln\big(1+\sinh^2(2\beta\epsilon_k^0)\sin^2\Delta_k\big)$$

on them does not have a converging Taylor expansion on δg unless $\sinh^2(2\beta\epsilon_k^0)\sin^2\Delta_k < 1$. But the first part, $\sinh^2(2\beta\epsilon_k^0)$, means this function scales exponentially with β, while the second part, $\sin^2\Delta_k$, makes it scale only polynomially with the perturbation. The condition on δg for convergence, therefore, becomes scandalously unreasonable at low temperatures. To illustrate this, at $g_0 = 0$, $\epsilon_k^0 = 1$ for all k's and $\sin\Delta_k$ is maximum for $k \to \pi/2$; if we consider $\delta g = 0.01$, we have $\sinh^2(2\beta\epsilon^0_{k=\frac{\pi}{2}})\sin^2\Delta_{k=\frac{\pi}{2}} < 1$ only if $\beta < 2.6492$.

There is no such an issue with the full entropy production Σ, which is also obvious from (4.50). Concretely, using matrix analysis, one can show the final thermal state after the quench can be written as [12, 153, 154]

$$\rho_\tau^{\text{th}} = \frac{e^{-\beta(H_0+\Delta H)}}{Z_\tau} = \rho_0^{\text{th}} - \beta\big(\mathbb{J}_{\rho_0^{\text{th}}}[\Delta H] - \rho_0^{\text{th}}\langle\Delta H\rangle_0\big) + \mathcal{O}(\beta^2\Delta H^2), \tag{4.62}$$

where, from now on, $\langle\bullet\rangle_0 = \text{tr}\{\bullet\,\rho_0^{\text{th}}\}$, $\Delta H = H_\tau - H_0$ is the perturbation on the

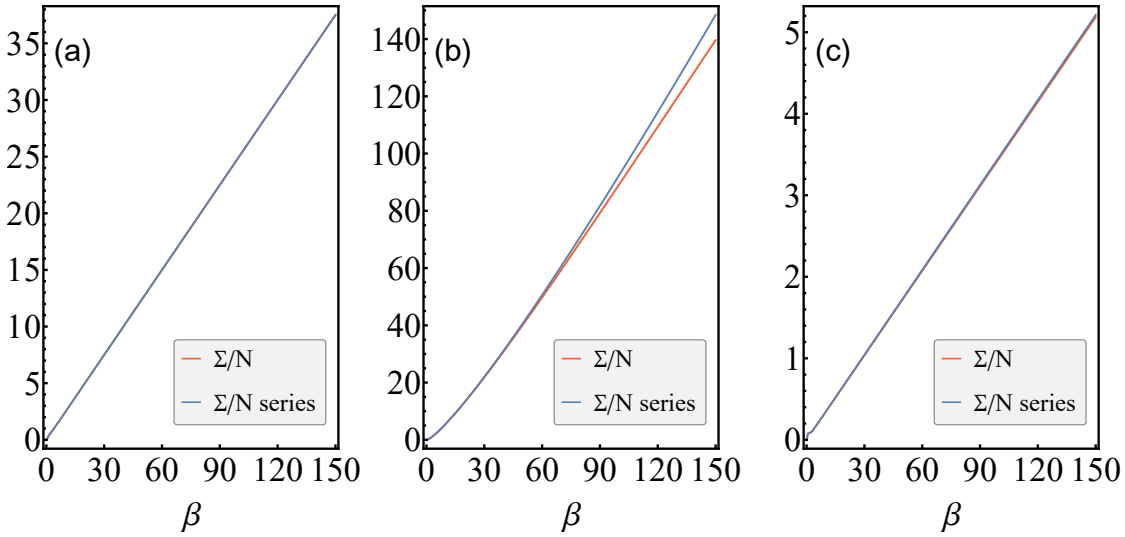

Figure 4.4: Comparison between Eqs. (4.47) and (4.65) as functions of β for initial fields (a) $g_0 = 0$, (b) $g_0 = 1$ and (c) $g_0 = 2$. Only at the critical field the discrepancy becomes important. In all points, $\delta g = 0.01$, and the curves are rescaled by $1/\delta g^2$.

Hamiltonian of the system and $\mathbb{J}_\rho$ is the superoperator

$$\mathbb{J}_\rho[X] = \int_0^1 \mathrm{d}x\, \rho^x X \rho^{1-x}. \tag{4.63}$$

This leads to an entropy production following an instantaneous quench given by [12]

$$\Sigma = S(\rho_0^{\mathrm{th}} || \rho_\tau^{\mathrm{th}}) = \frac{1}{2}\beta^2 \left(\mathrm{tr}\left\{ \Delta H \mathbb{J}_{\rho_0^{\mathrm{th}}}[\Delta H] \right\} - \langle \Delta H \rangle_0^2 \right), \tag{4.64}$$

to leading order on ΔH. In the cases we are interested in, the Hamiltonian is linear on the working parameter g. Hence, it is clear from the above equation that Σ scales with δg^2.

In the case of the homogeneous transverse field Ising model, Eq. (4.64) becomes [37]

$$\Sigma/N = \beta^2 \delta g^2 \int_0^\pi \frac{\mathrm{d}k}{2\pi} \left(\mathrm{sech}^2(\beta\epsilon_k^0) \cos^2\theta_k + \frac{\tanh(\beta\epsilon_k^0)}{\beta\epsilon_k^0} \sin^2\theta_k \right). \tag{4.65}$$

In Fig. 4.4 I compare Eqs. (4.47) and (4.65) as a function of β for quenches of amplitude $\delta g = 0.01$ and several initial fields. It is evident from this figure that the latter equation effectively provides an excellent approximation to the former and is applicable for a considerably broader range of temperatures than $\beta \lesssim 3$. As one could expect, the discrepancy may be important near the critical field.

Peculiarly, the second term on (4.65) goes onto Γ_{qu} at high temperatures — we just need to make $\tanh(\beta\epsilon_k^0) \approx \beta\epsilon_k^0$ to obtain (4.57) — while it goes to Γ_{cl} at low temperatures — this can be checked by Taylor expanding $\epsilon_k^\tau p_k$ on δg in (4.49) and remembering $\tanh(x) \to 1$ when $x \to \infty$.

The expansion in (4.62) and subsequently (4.64), work because thermal states form an smooth family of full rank density operators in terms of the parameter β [154]. However, the same is not true for the dephased state $\mathbb{D}_{H_\tau}(\rho_0^{\text{th}})$ that enters the components Γ_{cl} and Γ_{qu} of the entropy production.

We can try an expansion similar to (4.62) for the dephased state. In this case, it is beneficial to note the dephasing map (4.7) may be written as

$$\mathbb{D}_H(\rho) = \lim_{s\to\infty} \frac{1}{s} \int_0^s \mathrm{d}t\, e^{-iHt}\rho e^{iHt}.$$

This allows us to obtain [37]

$$\mathbb{D}_{H_\tau}(\rho_0^{\text{th}}) = \rho_0^{\text{th}} + \lim_{s\to\infty} \frac{i}{s} \int_0^s \mathrm{d}t \int_0^1 \mathrm{d}x\, te^{-ixH_0t}[\rho_0^{\text{th}}, \Delta H]e^{ixH_0t}, \tag{4.66}$$

to leading order on ΔH. Contrarily to (4.62) this expansion is not on a power series of $\beta\Delta H$, and the dependence on β can be particularly intricate. This is behind the problem of analyticity of Γ_{cl} and Γ_{qu} and becomes, perhaps, more clear when we consider below the stochastic version of the Γ-splitting.

Next let us move to the second and, possibly, most important shortcoming of Γ_{cl} and Γ_{qu}. For a protocol starting with a system in a thermal state at low temperatures, Γ_{cl} will consistently dominate and be much larger than Γ_{qu}. As a consequence, it is virtually impossible to have a low-temperature protocol where the coherence term prevails [37]. This can be explained as follows [37].

As noted before, the contribution from the coherences in the Γ-splitting after the driving protocol is given by a difference between two von Neumann entropies,

$$\Gamma_{\text{qu}} = S(\mathbb{D}_{H_\tau}(\rho_\tau)) - S(\rho_\tau), \tag{4.67}$$

where $\rho_\tau = U_g\rho_0^{\text{th}}U_g^\dagger$. Hence, when the temperature of the initial state is low ($\beta \to \infty$),

ρ_0^{th} tends to a pure state and so does ρ_τ. Accordingly, this leads to a vanishing entropy $S(\rho_\tau) \to 0$. On the other hand, $S(\mathbb{D}_{H_\tau}(\rho_\tau))$ is bounded from above by $\ln d$, where d is the dimension of the system Hilbert space. This makes Γ_{qu} finite.

Conversely, Γ_{cl} can grow unboundedly when $\beta \to \infty$. The reason is that ρ_τ^{th} also tends to a pure state in this case, while that is typically not the case with the dephased state $\mathbb{D}_{H_\tau}(\rho_\tau)$. Then the support of the latter may intersect the kernel of the former leading to a divergence in their relative entropy [155] — see Appendix B.

The contribution Γ_{qu} is supposed to measure how much of the entropy production steam from quantum features. From the last two paragraphs, it would appear that there is nothing quantum in the entropy production at low temperatures following a work protocol.

Notwithstanding, precisely at $T = 0$, a thermal state is insensitive to any changes in the spectrum of the system Hamiltonian and is affected merely by variations in the energy eigenbasis. Therefore, the entropy production in such a scenario possesses indeed an intrinsically quantum nature - there is nothing classical on rotating noncommuting eigenbases. However, this is not captured by the Γ-splitting. Even in this situation, the "classical" part Γ_{cl} gives the dominant contribution. This happens because this splitting does not quantify how coherent the driving protocol is, but, instead, how populations and off-diagonal elements on ρ_τ contribute to the entropy production.

These shortcomings of the Γ-splitting can complementarily be analysed from the perspective of its stochastic version [37].

For simplicity, let us assume the Hamiltonian of the system is nondegenerate. In an instantaneous quench, the path probability (4.16) associated with a quantum trajectory $|i_0\rangle \to |j_\tau\rangle$ becomes

$$P_F[i,j] = p_i^0 |\langle j_\tau | i_0 \rangle|^2,$$

where $\{|i_0\rangle\}$ and $\{|j_\tau\rangle\}$ are eigenstates of the initial and final Hamiltonians, respectively; and p_i^0, the populations of the initial thermal state ρ_0^{th}.

Assuming the quench is further small, standard perturbation theory, up to second order

on ΔH, leads to

$$|\langle j_\tau|i_0\rangle|^2 = \begin{cases} \frac{|\Delta H_{ij}|^2}{(\epsilon_j^0-\epsilon_i^0)^2}, & \text{if } j \neq i \\ 1-\sum_{\ell\neq j}|\langle j_\tau|\ell_0\rangle|^2, & \text{if } j=i, \end{cases} \tag{4.68}$$

where ϵ_i^0 are the eigenvalues of H_0 and $\Delta H_{ij} = \langle i_0|\Delta H|j_0\rangle$. Moreover, the final energy eigenvalues are given by

$$\epsilon_j^\tau = \epsilon_j^0 + \Delta H_{jj} + E_j^{(2)}, \tag{4.69}$$

with

$$E_j^{(2)} = \sum_{\ell\neq j}\frac{|\Delta H_{j\ell}|^2}{\epsilon_j^0-\epsilon_\ell^0}.$$

With this at hand, we can Taylor expand the populations $\{q_j^\tau\}$ and $\{p_j^\tau\}$ of the dephased and final thermal states. They read

$$q_j^\tau = p_j^0(1-s_j), \tag{4.70}$$

$$p_j^\tau = p_j^0(1-f_j), \tag{4.71}$$

where

$$f_j = \beta(1-\beta\langle\Delta H^{\rm d}\rangle_0)(\Delta H_{jj}-\langle\Delta H^{\rm d}\rangle_0) + \frac{1}{2}\beta^2(\Delta H_{jj}^2 - \langle(\Delta H^{\rm d})^2\rangle_0 + \beta\big(E_j^{(2)}-\langle E^{(2)}\rangle_0\big), \tag{4.72}$$

$$s_j = \sum_{\ell\neq j}\frac{1-\epsilon^{-\beta(\epsilon_\ell^0-\epsilon_j^0)}}{(\epsilon_j^0-\epsilon_\ell^0)^2}|\Delta H_{j\ell}|^2, \tag{4.73}$$

with $\langle E^{(2)}\rangle_0 = \sum_i p_i^0 E_i^{(2)}$, and $\Delta H^{\rm d}$ is the diagonal part of the perturbation in the initial energy basis,

$$\Delta H^{\rm d} = \sum_i \Delta H_{ii}|i_0\rangle\langle i_0|. \tag{4.74}$$

Inserting Eqs. (4.70) and (4.71) onto the definitions of the stochastic version of the

Γ-splitting (4.21)-(4.22) we arrive at

$$\sigma[i,j] = \ln p_i^0/p_j^0 - \ln(1-f_j), \tag{4.75}$$

$$\gamma_{\text{cl}}[i,j] = \ln(1-s_j) - \ln(1-f_j) \tag{4.76}$$

$$\gamma_{\text{qu}}[i,j] = \ln p_i^0/p_j^0 - \ln(1-s_j). \tag{4.77}$$

We may now investigate the analyticity of the stochastic entropy production and the Γ-splitting quantities. First, $p_i^0/p_j^0 = e^{-\beta(\epsilon_i^0-\epsilon_j^0)}$ is a well-behaved function. Moreover, a series expansion of $\ln(1-x)$ is convergent only if $|x|<1$. Therefore, the analyticity of σ is conditioned on having $|f_j|<1$. Looking at (4.72), this is roughly satisfied if $\beta|\Delta H_{ij}| \lesssim 1$, showing σ is indeed expanded in a power series of $\beta\Delta H$.

Conversely, the analyticity of γ_{cl} and γ_{qu} depend on $|s_j|<1$. Looking at (4.73), we note s_j is a sum over all elements $\Delta H_{\ell j}$, with $\ell \neq j$, weighted by a function of β and the energies ϵ_ℓ^0. At low temperatures (large β), the energies for which $\epsilon_\ell^0 > \epsilon_j^0$ contribute negligibly to the sum. However, those for which $\epsilon_\ell^0 < \epsilon_j^0$ add an exponentially large contribution. This shows, contrarily to σ, the expansion of γ_{cl} and γ_{qu} is in powers of ΔH with coefficients that are exponential functions of β. In conclusion, violating the condition $|s_j|<1$ is exponentially easier at low temperatures than violating $|f_j|<1$.

Moreover, except for the ground-state populations, p_i^0 and p_j^τ are exponentially small at low temperatures. In contrast, the populations q_j^τ are only polynomially small on the perturbation ΔH,

$$q_{j\neq 0}^\tau = p_{j\neq 0}^\tau(1-s_{j\neq 0}) \xrightarrow{\beta\to\infty} \frac{|\Delta H_{0j}|^2}{(\epsilon_j^0-\epsilon_0^0)^2}, \tag{4.78}$$

where ϵ_0^0 is the ground-state energy. Hence, when we compute Γ_{qu}, we compare a state with a support exponentially close to zero with another that is effectively full rank - its support is only polynomially close to zero. However, the converse occurs when we compute Γ_{cl}. As a consequence, the latter becomes considerably larger than the former on this regime of temperatures.

The discussion on this section can be neatly illustrate with a single qubit model [37]. Consider a qubit with an initial Hamiltonian $H_0 = \omega\sigma^z$, where $\sigma^{x,y,z}$ are the Pauli operators, prepared in the thermal state $\rho_0^{\text{th}} = e^{-\beta H_0}/Z_0$. This system is then suddenly quenched

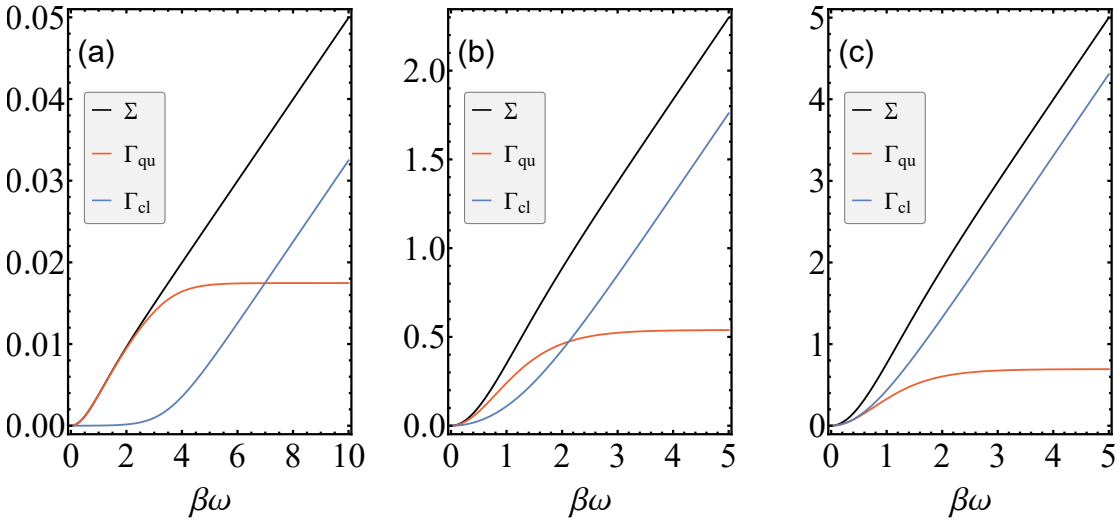

Figure 4.5: Σ, $\Gamma_{\rm cl}$ and $\Gamma_{\rm qu}$ as functions of $\beta\omega$ for quench rotations (a) $\theta = 0.1$, (b) $\theta = 1$ and (c) $\theta = \pi/2$. As the temperature is lowered, $\Gamma_{\rm cl}$ always surpasses and dominates over $\Gamma_{\rm qu}$.

to $H_\tau = \omega(\cos\theta\sigma^z + \sin\theta\sigma^x)$. The work parameter here is the angle θ.

The effect of this process is to solely rotate the energy eigenbasis by an amount θ, while the energy eigenvalues remain the same. Accordingly, this constitutes a truly quantum mechanical process. It is straightforward to verify the associated entropy production is given by

$$\Sigma = 2t\tanh^{-1}(t)\sin^2(\theta/2), \tag{4.79}$$

where $t = \tanh(\beta\omega)$. Besides, the Γ-contributions read,

$$\Gamma_{\rm qu} = t\tanh^{-1}(t) - t\cos\theta\tanh^{-1}(t\cos\theta) - \frac{1}{2}\ln\left(1+\sinh^2(\beta\omega)\sin^2\theta\right), \tag{4.80}$$

$$\Gamma_{\rm cl} = -t\cos\theta\left(\tanh^{-1}(t) - \tanh^{-1}(t\cos\theta)\right) + \frac{1}{2}\ln\left(1+\sinh^2(\beta\omega)\sin^2\theta\right). \tag{4.81}$$

The entropy production is manifestly an analytical function of θ; in fact, for any β. It can be readily expanded in a power series. However, that is markedly false for $\Gamma_{\rm cl}$ and $\Gamma_{\rm qu}$. In this case, the functions are analytic only if β is small enough to make the series expansion of the second and last term in (4.80)-(4.81) convergent.

Moreover, in Fig. 4.5, I show the behaviors of these quantities as functions of $\beta\omega$ for several quench-sizes θ. As already argued, the process here is highly quantum, but, yet, $\Gamma_{\rm cl}$ inevitably delivers the dominant contribution at low temperatures. Further counter-

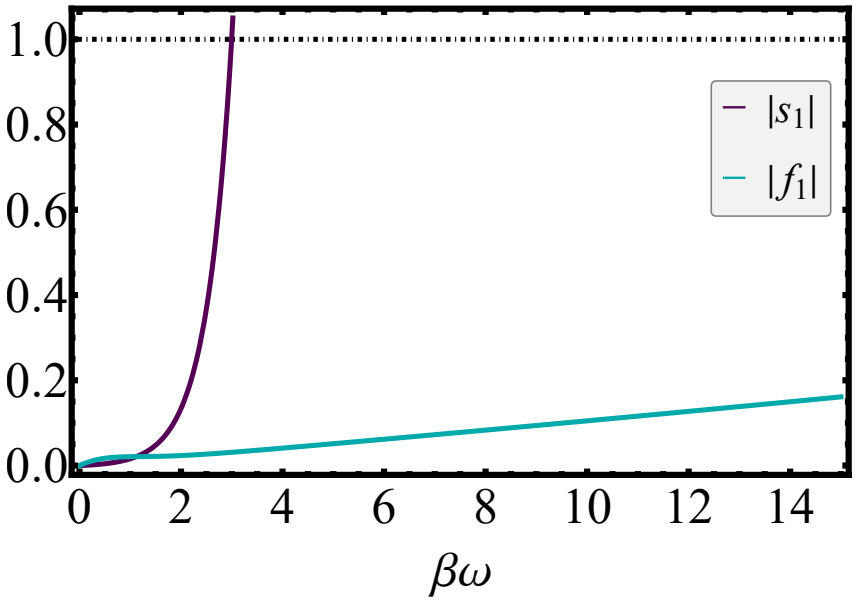

Figure 4.6: Comparison between Eqs. (4.82) and (4.83) as a function of $\beta\omega$ for $\theta = 0.1$. The condition for analyticity of $\gamma_{\rm cl}$ and $\gamma_{\rm qu}$ is quickly violated as the temperature decreases, while the one for σ holds over a much larger range of temperatures.

intuitively, the more the energy eigenbasis is rotated, the faster the coherence term becomes less important. Although I am focusing on quenches, I emphasize the dominance of $\Gamma_{\rm cl}$ also occurs in more general protocols. This is exemplified in [37], and should be clear also from the arguments presented in this section.

At the stochastic level, the problem of analyticity of the Γ-splitting comes from the term — see Eq. (4.73),

$$s_1 = \left(1 - e^{2\beta\omega}\right)\left(\frac{\sin\theta}{2}\right)^2. \tag{4.82}$$

The corresponding term associated with the analyticity of σ is given by

$$f_1 = 2(1+t)\tanh^{-1}(t)\sin^2(\theta/2)[1 + 2t\tanh^{-1}(t)\sin^2(\theta/2)] + \frac{1-t}{2}\tanh^{-1}(t)\sin\theta. \tag{4.83}$$

In Fig. 4.6 I compare the two as a function of $\beta\omega$. The condition $|s_1| < 1$ for analyticity of $\gamma_{\rm cl}$ and $\gamma_{\rm qu}$ is swiftly violated as the temperature is lowered. In contrast, the condition $|f_1| < 1$ and, hence, the analytical behavior of σ, holds over a much larger range of temperatures.

In addition, p_0, $p_1^\tau \propto e^{-\beta\omega}$ go exponentially to zero at low temperatures, while $q_1^\tau \to \sin^2(\theta/2)$. This ratify the discussion around Eq. (4.78). That is, the lower the temperature,

the less the thermal states ρ_0^{th} and ρ_τ^{th} are effectively full rank compared with the dephased state $\mathbb{D}_{H_\tau}(\rho_\tau)$. This leads to Γ_{cl} being considerably larger than Γ_{qu} at low temperatures.

This section demonstrates that regardless of its pleasant properties, the Γ-splitting does not provide a complete satisfactory characterization of the classical and quantum features of entropy production in nonequilibrium drives. This is specially true if we shift perspective and ask how much quantum or classical is the work protocol itself. This motivated us to introduce a new splitting for the entropy production particularly suitable to work protocols [37]. I present it in the subsequent chapter. Moreover, the new splitting will elucidate why the individual components of entropy production display a singularity at a quantum critical parameter even when the system is initially in arbitrarily high temperatures [40].

Chapter 5

Populations and Coherences: a New Splitting

The previous chapter demonstrates that splitting the entropy production in a nonequilibrium process into a classical and a quantum parts is not a trivial task. In fact, the customary mixing of populations and coherences makes an overall clear separation of classical and quantum contributions likely impossible.

On the other hand, the nonuniqueness of such a splitting offers the possibility of different insights. And, in the spirit of thermodynamics, we may hope for a particular division to enjoy an operational meaning in specific contexts.

All of these features are well illustrated in the Γ-splitting. For instance, if we consider anything coming from coherences as quantum, the association of its contribution related to populations with something classical is not strictly accurate. In a work protocol, its 'quantum' part Γ_{qu}, is related only to how much the energy eigenbasis is rotated and, therefore, with the creation of coherences. In contrast, Γ_{cl} depends not only on how much the energy eigenvalues are changed by the drive, but on the basis rotation too. In this sense, there is something quantum on Γ_{cl}.

Nonetheless, when we consider a thermalization process within the framework of a thermodynamic resource theory, this splitting appears handy and satisfactory.

As we argued in Section 4.2, though, besides analyticity issues, the Γ-splitting does not properly reveal how much coherent, meaning thereby quantum, is a work protocol.

Noticing that, in [37] we proposed a new splitting for the entropy production which

better captures the difference between coherent and commuting processes. Specifically, as aforesaid, the nonequilibrium driving g_t modifies the system Hamiltonian $H(g_t)$ by altering the energy eigenvalues and by rotating the energy eigenbasis. The former may be viewed as a (semi)classical transformation. The latter, however, leads to quantum coherences and is associated with the noncommutativeness of the Hamiltonian at different times: $[H(g_{t_1}), H(g_{t_2})] \neq 0$, for t_1 different from t_2. This corresponds, accordingly, to an inherent quantum feature distinguishing the protocol g_t from a classical (commuting) driving. The idea of our splitting is to more accurately evaluate the weight of these two types of processes in the entropy production.

Therefore, for convenience, we write the entropy production following a work protocol Eq. (3.9) in yet another form. First, I introduce the *nonequilibrium* free energy

$$F(\rho, H, T) = \mathrm{tr}\{\rho H\} - TS(\rho). \tag{5.1}$$

This is a function of the temperature T, the Hamiltonian H and the sate of the system ρ. In what follows, I will always consider the same temperature and the same Hamiltonian H_τ. This is the Hamiltonian of the system at the end of the work protocol and, T is the reference temperature in which the system is initially prepared. For this reason, I simplify notation and denote the nonequilibrium free energy simply as a function of the state, $F(\rho)$.

This allows us to write the entropy production as

$$\Sigma = \beta\Big(F(\rho_\tau) - F(\rho_\tau^{\mathrm{th}})\Big). \tag{5.2}$$

Again, $\beta = 1/T$ is the inverse temperature, and

$$F(\rho_\tau^{\mathrm{th}}) = \mathrm{tr}\big\{\rho_\tau^{\mathrm{th}} H_\tau\big\} - TS(\rho_\tau^{\mathrm{th}}) = -T \ln Z_\tau,$$

is just the equilibrium free energy associated with the thermal state ρ_τ^{th}.

The essential ingredient in the definition of the Γ-splitting was the introduction of an intermediate state $\mathbb{D}_{H_\tau}(\rho_\tau)$. This is nothing but the state of the system at the end of the driving, ρ_τ, dephased in the basis of the final Hamiltonian, H_τ.

Our splitting follows an analogous reasoning, but instead of dephasing ρ_τ in the basis

of H_τ, we do the inverse and dephase H_τ in the basis of ρ_τ. That is, we introduce the dephased Hamiltonian

$$\mathbb{D}_{\rho_\tau}(H_\tau) = \sum_i \tilde{\Pi}_i^\tau H_\tau \tilde{\Pi}_i^\tau. \tag{5.3}$$

Here, the eigenprojectors $\tilde{\Pi}_i^\tau$ of the state ρ_τ are related to the eigenprojectors of the initial thermal state ρ_0^{th} (and Hamiltonian H_0) through

$$\tilde{\Pi}_i^\tau = U_g(\tau,0)\Pi_i^0 U_g^\dagger(\tau,0).$$

In Chapter 4 I argued the eigenbasis of H_τ was a preferred basis in the thermalization of the system with this Hamiltonian fixed and a globally energy conserving evolution. In the context of work protocols, we may view the eigenbasis of the final state ρ_τ as a special basis imposed by the external agent performing the drive.

Next we define the intermediate state [37]

$$\tilde{\rho}_\tau^{\text{th}} = \frac{\exp\big(-\beta\mathbb{D}_{\rho_\tau}(H_\tau)\big)}{\text{tr}\big\{\exp\big(-\beta\mathbb{D}_{\rho_\tau}(H_\tau)\big)\big\}}. \tag{5.4}$$

This is a thermal state based solely on the incoherent part of the final Hamiltonian H_τ on the eigenbasis of ρ_τ. It further means, ρ_τ and $\tilde{\rho}_\tau^{\text{th}}$ commute ($[\rho_\tau, \tilde{\rho}_\tau^{\text{th}}] = 0$).

We are in the position now to define our new splitting [37],

$$\Sigma = \Lambda_{\text{cl}} + \Lambda_{\text{qu}}, \tag{5.5}$$

$$\Lambda_{\text{cl}} = \beta\Big(F(\rho_\tau) - F(\tilde{\rho}_\tau^{\text{th}})\Big), \tag{5.6}$$

$$\Lambda_{\text{qu}} = \beta\Big(F(\tilde{\rho}_\tau^{\text{th}}) - F(\rho_\tau^{\text{th}})\Big). \tag{5.7}$$

I will often refer to Eqs. (5.5)-(5.7) as the Λ-splitting of entropy production.

As in the Γ-splitting, both terms in Eq. (5.5) are nonnegative by construction. This is effortlessly shown to be the case for Λ_{cl} by noticing this can equally written as a relative entropy,

$$\Lambda_{\text{cl}} = S(\rho_\tau||\tilde{\rho}_\tau^{\text{th}}). \tag{5.8}$$

However, the same is not true for Λ_{qu}. Namely, in this case we have

$$\Lambda_{\text{qu}} = \text{tr}\big\{\rho_\tau(\ln\tilde{\rho}_\tau^{\text{th}} - \ln\rho_\tau^{\text{th}})\big\}. \tag{5.9}$$

Nonetheless, we can still prove Λ_{qu} is nonnegative and vanishes if and only if ρ_τ has no coherences in the final energy basis; i.e., if and only if $[\rho_\tau, H_\tau] = 0$. The proof goes as follows [37]. To begin, notice

$$F(\tilde{\rho}_\tau^{\text{th}}) = \text{tr}\big\{\tilde{\rho}_\tau^{\text{th}} H_\tau\big\} - TS(\tilde{\rho}_\tau^{\text{th}}) = \text{tr}\big\{\tilde{\rho}_\tau^{\text{th}}\mathbb{D}_{\rho_\tau}(H_\tau)\big\} - TS(\tilde{\rho}_\tau^{\text{th}}), \tag{5.10}$$

where the trace operation and the fact that $[\rho_\tau, \tilde{\rho}_\tau^{\text{th}}] = 0$ allows us to replace H_τ by $\mathbb{D}_{\rho_\tau}(H_\tau)$. But since the latter Hamiltonian is the same appearing in the definition of $\tilde{\rho}_\tau^{\text{th}}$, the free energy (5.10) is in fact the *equilibrium* free energy associated with this thermal state.

Next, note we can write $H_\tau = \mathbb{D}_{\rho_\tau}(H_\tau) + H_\tau^{\text{c}}$, where $H_\tau^{\text{c}} = H_\tau - \mathbb{D}_{\rho_\tau}(H_\tau)$. Then, from the Bogoliubov variational theorem [156] (also Klein's Inequality) we obtain

$$F(\rho_\tau^{\text{th}}) \leqslant F(\tilde{\rho}_\tau^{\text{th}}) + \text{tr}\big\{\tilde{\rho}_\tau^{\text{th}} H_\tau^{c}\big\}. \tag{5.11}$$

However, by construction, the *coherent* Hamiltonian H_τ^{c} possesses solely off-diagonal elements in the common eigenbasis of $\tilde{\rho}_\tau^{\text{th}}$ and ρ_τ. As a consequence, the second term in the above inequality vanishes, which leads directly to the nonnegativeness of Λ_{qu}:

$$\Lambda_{\text{qu}} = \beta\Big(F(\tilde{\rho}_\tau^{\text{th}}) - F(\rho_\tau^{\text{th}})\Big) \geqslant 0.$$

Secondly we prove $\Lambda_{\text{qu}} = 0$ if and only if ρ_τ is incoherent in the eigenbasis of H_τ, i.e. iff $[\rho_\tau, H_\tau] = 0$. For the *if* part, we notice when ρ_τ is incoherent, $\mathbb{D}_{\rho_\tau}(H_\tau) = \mathbb{D}_{H_\tau}(H_\tau) = H_\tau$ and, hence, $\tilde{\rho}_\tau^{\text{th}} = \rho_\tau^{\text{th}}$, which leads to $\Lambda_{\text{qu}} = 0$.

Conversely, assuming $\Lambda_{\text{qu}} = 0$, we must have $F(\tilde{\rho}_\tau^{\text{th}}) - F(\rho_\tau^{\text{th}}) = 0$, for $\beta > 0$. This implies

$$\sum_{\ell=0}^{+\infty} \frac{(-\beta)^\ell}{\ell!}\,\text{tr}\big\{(H_\tau)^\ell - [\mathbb{D}_{\rho_\tau}(H_\tau)]^\ell\big\} = 0,$$

which requires

$$\mathrm{tr}\big\{(H_\tau)^\ell - [\mathbb{D}_{\rho_\tau}(H_\tau)]^\ell\big\} = 0, \quad \forall \ell \in \mathbb{N}. \tag{5.12}$$

Now, for the case $\ell = 0$ the equality is trivial and for $\ell = 1$ the equality follows directly from the definition of $\mathbb{D}_{\rho_\tau}(H_\tau)$.

For $\ell = 2$, notice

$$\mathrm{tr}\big\{(H_\tau)^2\big\} = \mathrm{tr}\big\{[\mathbb{D}_{\rho_\tau}(H_\tau) + H_\tau^{\mathrm{c}}]^2\big\} = \mathrm{tr}\big\{[\mathbb{D}_{\rho_\tau}(H_\tau)]^2 + 2\mathbb{D}_{\rho_\tau}(H_\tau)H_\tau^{\mathrm{c}} + (H_\tau^{\mathrm{c}})^2\big\}.$$

Also from the definition of $\mathbb{D}_{\rho_\tau}(H_\tau)$, one easily verifies $\mathrm{tr}\{\mathbb{D}_{\rho_\tau}(H_\tau)H_\tau^{\mathrm{c}}\} = 0$, and we are left with

$$\mathrm{tr}\big\{(H_\tau)^2 - [\mathbb{D}_{\rho_\tau}(H_\tau)]^2\big\} = \mathrm{tr}\big\{(H_\tau^{\mathrm{c}})^2\big\} = 0.$$

But since $H_\tau^{\mathrm{c}} = H_\tau - \mathbb{D}_{\rho_\tau}(H_\tau)$ is also Hermitian, this second equality means $H_\tau - \mathbb{D}_{\rho_\tau}(H_\tau) = 0$. Straightaway, the condition $\mathbb{D}_{\rho_\tau}(H_\tau) = H_\tau$ implies (5.12) follows trivially and, more importantly, that $[\rho_\tau, H_\tau] = 0$. That is, ρ_τ must be incoherent in the final energy basis. This completes the proof that $\Lambda_{\mathrm{qu}} = 0$ iff $[\rho_\tau, H_\tau] = 0$.

After discussing the mathematical properties of Λ_{cl} and Λ_{qu} let us consider their meaning. The former, Λ_{cl}, computes the nonequilibrium free energy, or relative entropy, between the two commuting states ρ_τ and $\tilde{\rho}_\tau^{\mathrm{th}}$ and, therefore, is connected to their populations mismatch.

Conversely, Λ_{qu} compares the thermal states associated with the Hamiltonians H_τ and $\mathbb{D}_{\rho_\tau}(H_\tau)$. It, therefore, quantifies the difference in *equilibrium* free energy associated with quantum coherences due to the noncommutativeness between ρ_τ and H_τ. The Λ-splitting of entropy production is schematically represented in Fig. 5.1.

Throughout this chapter, as we work with this new splitting, I provide additional physical insight and justification for it. Notably, as shown in a subsequent section, the Λ-splitting corrects the shortcomings of the Γ-splitting and is remarkably suitable in the scenario of instantaneous quenches.

In [37] we likewise constructed a stochastic version of the Λ-splitting. This was again done within the framework of the two-point measurement scheme [107].

As discussed in Sec. 3.2, the stochastic formulation of the entropy production in a

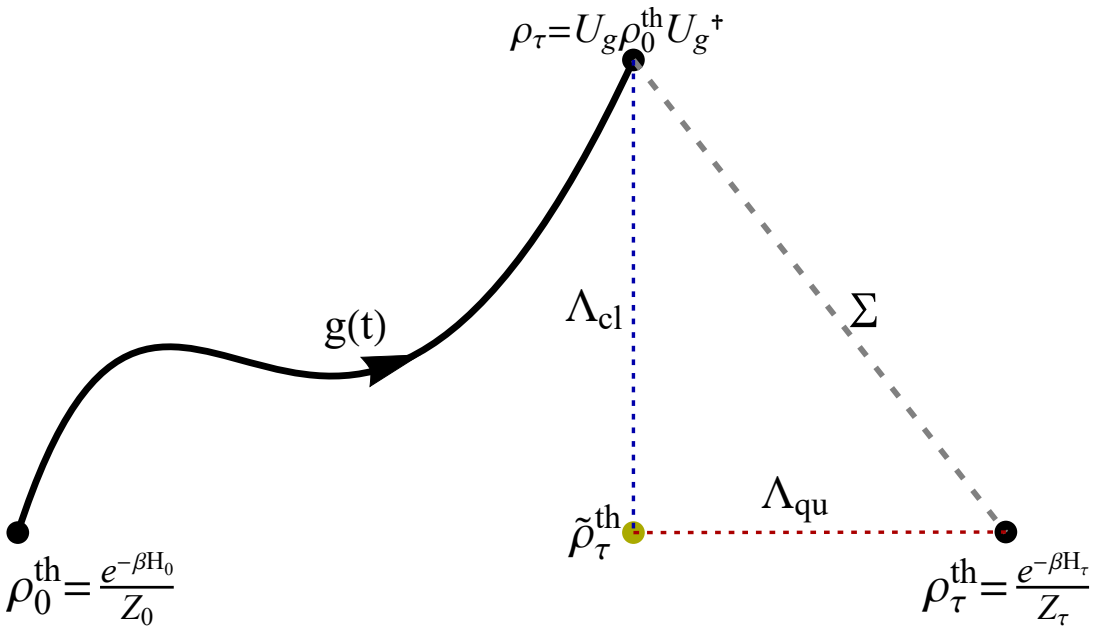

Figure 5.1: Λ-splitting of the entropy production in the work protocol described in Chapter 3. The entropy production Σ — represented by the gray dashed line — may be split into two contributions Λ_{cl} and Λ_{qu}. This is achieved by introducing the thermal state $\tilde{\rho}_\tau^{\text{th}}$ — yellow dot — related to the incoherent part of H_τ in the basis of ρ_τ (see text for details). Λ_{cl} is related to a mismatch in populations between the commuting states ρ_τ and $\tilde{\rho}_\tau^{\text{th}}$. Conversely, Λ_{qu} steam from the difference in equilibrium free energy associated with the coherent part of H_τ in the basis of ρ_τ and $\tilde{\rho}_\tau^{\text{th}}$.

work protocol is grounded on the outcomes of two energy measurements. One is made immediately before the driving and returns one of the eigenvalues ϵ_i^0 of the initial Hamiltonian H_0. The second is performed at the end of the driving and returns an eigenvalue ϵ_j^τ of the final Hamiltonian H_τ. The path probability associated with the forward trajectory $i \to j$ is given by

$$P_F[i,j] = p_i^0 \,\text{tr}\big\{\Pi_j^\tau U_g(\tau,0)\Pi_i^0 U_g^\dagger(\tau,0)\big\},$$

and the stochastic entropy production reads

$$\sigma[i,j] = \ln \frac{p_i^0}{p_j^\tau} = \beta(w[i,j] - \Delta F),$$

where $p_i^0 = e^{-\beta\epsilon_i^0}/Z_0$ and $p_j^\tau = e^{-\beta\epsilon_j^\tau}/Z_\tau$ are the populations of the thermal states associated with H_0 and H_τ while Π_i^0 and Π_j^τ are their respective eigenprojectors. Moreover, $w[i,j] = \epsilon_j^\tau - \epsilon_i^0$ is the stochastic work along the trajectory and $\Delta F = -T \ln Z_\tau/Z_0$ the

difference in equilibrium free energy between these states.

This variable is distributed according to

$$p_F(\sigma) = \sum_{i,j} \delta(\sigma - \sigma[i,j]) P_F[i,j].$$

As we saw, $\Sigma = \langle \sigma \rangle$ is simply its average. Moreover, σ satisfies the integral fluctuation theorem $\langle e^{-\sigma} \rangle = 1$.

To construct the stochastic versions of Λ_{cl} and Λ_{qu}, I notice the intermediate thermal state $\tilde{\rho}_\tau^{\text{th}}$ can be written as

$$\tilde{\rho}_\tau^{\text{th}} = \sum_i \tilde{p}_i^\tau \tilde{\Pi}_i^\tau, \tag{5.13}$$

where I recall $\tilde{\Pi}_i^\tau = U_g(\tau,0)\Pi_i^0 U_g^\dagger(\tau,0)$, and

$$\tilde{p}_i^\tau = \exp\{-\beta(\tilde{\epsilon}_i^\tau - F(\tilde{\rho}_\tau^{\text{th}}))\} = \frac{e^{-\beta\tilde{\epsilon}_i^\tau}}{\tilde{Z}_\tau}, \tag{5.14}$$

with $\tilde{\epsilon}_i^\tau = \text{tr}\left\{\tilde{\Pi}_i^\tau H_\tau\right\}$ the eigenvalues of the dephased Hamiltonian $\mathbb{D}_{\rho_\tau}(H_\tau)$ and $\tilde{Z}_\tau = e^{-\beta F(\tilde{\rho}_\tau^{\text{th}})}$ its partition function.

Next, we define [37]

$$\lambda_{\text{cl}}[i,j] = \ln p_i^0 / \tilde{p}_i^\tau, \tag{5.15}$$

$$\lambda_{\text{qu}}[i,j] = \ln \tilde{p}_i^\tau / p_j^\tau, \tag{5.16}$$

distributed according to

$$p_F(\lambda_{\text{cl}}) = \sum_{i,j} \delta(\lambda_{\text{cl}} - \lambda_{\text{cl}}[i,j]) P_F[i,j], \tag{5.17}$$

$$p_F(\lambda_{\text{qu}}) = \sum_{i,j} \delta(\lambda_{\text{qu}} - \lambda_{\text{qu}}[i,j]) P_F[i,j]. \tag{5.18}$$

Hence, we have $\sigma[i,j] = \lambda_{\text{cl}}[i,j] + \lambda_{\text{qu}}[i,j]$ and it is straightforward to show we obtain

the expected averages

$$\Lambda_{\text{cl}} = \langle \lambda_{\text{cl}} \rangle, \tag{5.19}$$

$$\Lambda_{\text{qu}} = \langle \lambda_{\text{qu}} \rangle. \tag{5.20}$$

Moreover, as is the case with σ, λ_{cl} satisfies an integral fluctuation theorem [37]

$$\langle e^{-\lambda_{\text{cl}}} \rangle = 1. \tag{5.21}$$

In contrast, this is not the case with λ_{qu}, and in general $\langle e^{-\lambda_{\text{qu}}} \rangle \neq 1$. However, I will show in what follows that this attribute is also claimed by λ_{qu} in the instantaneous and infinitesimal quench scenario.

Moving forward, I present the cumulant generating functions (CGFs) of these variables. Considering the joint probability distribution

$$p_F(\lambda_{\text{cl}}, \lambda_{\text{qu}}) = \sum_{i,j} \delta(\lambda_{\text{cl}} - \lambda_{\text{cl}}[i,j]) \delta(\lambda_{\text{qu}} - \lambda_{\text{qu}}[i,j]) P_F[i,j], \tag{5.22}$$

we obtain the joint CGF

$$\begin{aligned} K_{\lambda_{\text{cl}},\lambda_{\text{qu}}}(v,u) &= \ln \langle e^{-v\lambda_{\text{cl}} - u\lambda_{\text{qu}}} \rangle \\ &= \ln \operatorname{tr} \big\{ (\rho_\tau^{\text{th}})^u (\tilde{\rho}_\tau^{\text{th}})^{v-u} (\rho_\tau)^{1-v} \big\}. \end{aligned} \tag{5.23}$$

Likewise the Γ-splitting, the fact that this CGF cannot be written as a sum of CGFs of the two variables λ_{cl} and λ_{qu} means they are generally statistically dependent. Moreover, the reduced CGFs of these variables are obtained from the joint one by setting $u = 0$ and $v = 0$, respectively,

$$K_{\lambda_{\text{cl}}}(v) = \ln \operatorname{tr} \big\{ (\tilde{\rho}_\tau^{\text{th}})^v (\rho_\tau)^{1-v} \big\} = (v-1) S_v(\tilde{\rho}_\tau^{\text{th}} || \rho_\tau), \tag{5.24}$$

$$K_{\lambda_{\text{qu}}}(u) = \ln \operatorname{tr} \big\{ (\rho_\tau^{\text{th}})^u (\tilde{\rho}_\tau^{\text{th}})^{-u} \rho_\tau \big\}. \tag{5.25}$$

Again — see Eq. (4.28), the CGF of the full entropy production σ is obtained from

the joint CGF (5.23) by setting $u = v$,

$$K_\sigma(v) = K_{\lambda_{\text{cl}},\lambda_{\text{qu}}}(v, v) = (v-1)S_v(\rho_\tau^{\text{th}}||\rho_\tau).$$

This concludes the formulation of our new splitting of the entropy production following a work protocol. The Λ-splitting can be applied for general drivings g_t and associated unitaries U_g. In [37] we considered a spin of varying dimension evolving under a finite-time coherent pulse and computed the probability distributions and first four cumulants of σ and the Γ- and Λ-splittings. The results verified the behavior of the latter is much more intuitive and consistent with that of σ itself. In this thesis, though, I am largely concerned with the averages Λ_{cl} and Λ_{qu}, specially in sudden quench protocols. For this reason, I particularize to this scenario in the following section.

5.1 Instantaneous and infinitesimal quenches

Let us consider again the particular case of an instantaneous quench, where $U_{\text{quench}} = 1$. In this case, the state of the system at the end of the protocol is the same initial thermal state, $\rho_\tau = \rho_0^{\text{th}}$. Thus, dephasing in the eigenbasis of ρ_τ becomes equivalent to dephasing in the eigenbasis of ρ_0^{th} and, hence, of the initial Hamiltonian H_0. That is, the dephased Hamiltonian becomes

$$\mathbb{D}_{\rho_\tau}(H_\tau) = \mathbb{D}_{H_0}(H_\tau). \tag{5.26}$$

If we denote the perturbation by $\Delta H = H_\tau - H_0$, we have

$$\mathbb{D}_{H_0}(H_\tau) = H_0 + \Delta H^{\text{d}}, \tag{5.27}$$

where

$$\Delta H^{\text{d}} = \sum_i \Pi_i^0 \Delta H \Pi_i^0, \tag{5.28}$$

and $\{\Pi_i^0\}$ the eigenprojectors of H_0.

The *dephased* part of the perturbation ΔH^{d} following an instantaneous quench was

already introduced in Sec. 3.3 alongside the *coherent* complement

$$\Delta H^{\mathrm{c}} = \Delta H - \Delta H^{\mathrm{d}}. \tag{5.29}$$

The Λ-splitting is based on the intermediate thermal state (5.4). In this case, this state reads

$$\tilde{\rho}_{\tau}^{\mathrm{th}} = \frac{\exp\big[-\beta(H_0 + \Delta H^{\mathrm{d}})\big]}{\mathrm{tr}\big\{\exp\big[-\beta(H_0 + \Delta H^{\mathrm{d}})\big]\big\}}. \tag{5.30}$$

From now on, let us consider ΔH to be small. In Sec. 4.2 I showed the final reference thermal state $\rho_{\tau}^{\mathrm{th}} = e^{-\beta(H_0+\Delta H)}/Z_{\tau}$ could be Taylor expanded as [12, 154]

$$\rho_{\tau}^{\mathrm{th}} = \rho_0^{\mathrm{th}} - \beta\big(\mathbb{J}_{\rho_0^{\mathrm{th}}}[\Delta H] - \rho_0^{\mathrm{th}}\langle\Delta H\rangle_0\big) + \mathcal{O}(\beta^2\Delta H^2),$$

where $\langle\bullet\rangle_0 = \mathrm{tr}\big\{\bullet\,\rho_0^{\mathrm{th}}\big\}$ and

$$\mathbb{J}_{\rho}[X] = \int_0^1 \mathrm{d}x\, \rho^x X \rho^{1-x}.$$

This culminates in an entropy production to leading order on ΔH given by

$$\Sigma = \frac{1}{2}\beta^2\bigg(\mathrm{tr}\Big\{\Delta H\mathbb{J}_{\rho_0^{\mathrm{th}}}[\Delta H]\Big\} - \langle\Delta H\rangle_0^2\bigg). \tag{5.31}$$

Following the same logic, we obtain for the intermediate thermal state (5.30),

$$\tilde{\rho}_{\tau}^{\mathrm{th}} = \rho_0^{\mathrm{th}} - \beta\big(\mathbb{J}_{\rho_0^{\mathrm{th}}}[\Delta H^{\mathrm{d}}] - \rho_0^{\mathrm{th}}\langle\Delta H^{\mathrm{d}}\rangle_0\big) + \mathcal{O}(\beta^2(\Delta H^{\mathrm{d}})^2). \tag{5.32}$$

Note that $\langle\Delta H^{\mathrm{d}}\rangle_0 = \langle\Delta H\rangle_0$, or, equivalently, $\langle\Delta H^{\mathrm{c}}\rangle_0 = 0$. Then, it follows that,

$$\Sigma = \Lambda_{\mathrm{cl}} + \Lambda_{\mathrm{qu}}, \tag{5.33}$$

$$\Lambda_{\mathrm{cl}} = \frac{1}{2}\beta^2\bigg(\mathrm{tr}\Big\{\Delta H^{\mathrm{d}}\mathbb{J}_{\rho_0^{\mathrm{th}}}[\Delta H^{\mathrm{d}}]\Big\} - \langle\Delta H^{\mathrm{d}}\rangle_0^2\bigg), \tag{5.34}$$

$$\Lambda_{\mathrm{qu}} = \frac{1}{2}\beta^2\,\mathrm{tr}\Big\{\Delta H^{\mathrm{c}}\mathbb{J}_{\rho_0^{\mathrm{th}}}[\Delta H^{\mathrm{c}}]\Big\}. \tag{5.35}$$

Therefore, in the instantaneous and infinitesimal quench protocol, Λ_{cl} and Λ_{qu} are

related to Σ through a simple separation of the perturbation ΔH into a dephased and coherent parts. Additionally, in contrast with the Γ-splitting, the Λ-splitting is analytic in a similar range of parameters as Σ. This follows from the intermediate state in the latter splitting being also a thermal state, leading to completely analogous series expansions for Λ_{cl} and Λ_{qu} as the one for Σ. This is further noticeable from the similarity between Eqs. (5.31) and (5.34)-(5.35).

Moreover, as shown in a moment, Λ_{qu} is indeed the dominant contribution at low temperatures and highly coherent protocols. Thus, in summary, the shortcomings of the Γ-splitting discussed in Sec. 4.2 disappear in the Λ-splitting.

Next, I provide further physical insight to Λ_{cl} and Λ_{qu}. Since we are considering a small perturbation ΔH, we are in the regime of linear response theory. In a classical (commuting) process, $\mathbb{J}_{\rho_0^{\text{th}}}[\Delta H] = \Delta H \rho_0^{\text{th}}$, and Eq. (5.31) can be recast as [98]

$$\Sigma = \frac{1}{2}\beta^2 \,\text{Var}_0[\Delta H], \tag{5.36}$$

where the subscript 0 is a short notation for ρ_0^{th} and

$$\text{Var}_\rho[X] = \text{tr}\{X^2\rho\} - \text{tr}\{X\rho\}^2$$

is the variance of X in the state ρ.

Equation (5.36) establishes a connection between the equilibrium fluctuations of the perturbation ΔH with a response of the system given by Σ. In fact, $\beta^2\text{Var}_0[\Delta H]$ gives the fluctuations of entropy production itself [12, 13] — this is demonstrated below. Hence, this constitutes an example of a fluctuation-dissipation relation (FDR). In addition, in this case of commuting drives, the higher order cumulants of the entropy production vanish [12, 13], which makes its probability distribution Gaussian — see below. As a consequence, Eq. (5.36) further means, in this situation of classical (commuting) drives, the entropy production probability distribution is completely characterized by the average Σ.

However, for a general work protocol, the FDR (5.36) does not hold and instead we have [12, 13]

$$\Sigma = \frac{1}{2}\beta^2 \left(\text{Var}_0[\Delta H] - \mathcal{Q}\right), \tag{5.37}$$

where

$$\mathcal{Q} = \int_0^1 \mathrm{d}y I^y(\rho_0^{\mathrm{th}}, \Delta H) \geqslant 0. \tag{5.38}$$

The quantity in the integrand is the Wigner-Yanase-Dyson skew information [157, 158],

$$I^y(\rho, X) = -\frac{1}{2}\,\mathrm{tr}\big\{[\rho^y, X][\rho^{1-y}, X]\big\},$$

which is always nonnegative and vanishes if and only if $[\rho, X] = 0$. In the same way as the relative entropy of coherence, the skew information is a monotone in the resource theories of asymmetry and thermal operations [151, 159] — see also Appendix B.

Therefore, the term $\mathcal{Q}$ accounts for a purely quantum feature: it becomes nonzero as soon and as long as energetic coherences are created by drive.

As another consequence, the creation of coherences further implies a breaking in the Gaussianity of the entropy production probability distribution [12]. That is, the distribution ceases to be characterized by the average alone and its reconstruction requires knowledge of higher order cumulants.

Indeed, this follows directly from the integral fluctuation theorem $\langle e^{-\sigma}\rangle = 1$ [12]:

$$K_\sigma(1) = \ln\langle e^{-\sigma}\rangle = -\Sigma + \frac{1}{2}\langle(\sigma - \Sigma)^2\rangle + \sum_{n=3}^{+\infty} \frac{(-1)^n}{n!}\kappa_n^\sigma = 0, \tag{5.39}$$

where K_σ is the entropy production CGF and I denoted by κ_n^σ its cumulants. As stated before and shown at the end of the section, the variance, or second cumulant, of the entropy production is given by $\langle(\sigma - \Sigma)^2\rangle = \beta^2\,\mathrm{Var}_0[\Delta H]$. Hence, combining the above with Eq. (5.37), we obtain that $\mathcal{Q} \neq 0$ implies nonvanishing higher order cumulants [12, 13]

$$\mathcal{Q} = 2\beta^{-2} \sum_{n=3}^{+\infty} \frac{(-1)^{n+1}}{n!}\kappa_n^\sigma. \tag{5.40}$$

Similarly, employing exactly the same reasoning to Λ_{cl} and Λ_{qu}, we obtain [37]

$$\Lambda_{\mathrm{cl}} = \frac{1}{2}\beta^2\,\mathrm{Var}_0[\Delta H^{\mathrm{d}}], \tag{5.41}$$

$$\Lambda_{\mathrm{qu}} = \frac{1}{2}\beta^2\left(\mathrm{Var}_0[\Delta H^{\mathrm{c}}] - \mathcal{Q}\right). \tag{5.42}$$

Hence, the classical part of our splitting of entropy production obeys the standard fluctuation-dissipation relation, whereas in the quantum part this gets modified by the quantum term $\mathcal{Q}$. Moreover, this means the probability distribution of λ_{cl} is Gaussian, while that of λ_{qu}, and consequently of σ, deviates from this behavior.

Moving forward, the expressions (5.37) and (5.41)-(5.42) also facilitates the analysis of the high- ($\beta \to 0$) and low-temperature ($\beta \to \infty$) limits of Σ and the Λ-splitting. Beginning with the former ($\beta \to 0$), it is straightforward to show

$$\text{Var}_0[\Delta H^{(\text{d,c})}] = \text{Var}_{\mathbb{1}/d}[\Delta H^{(d,c)}] + \mathcal{O}(\beta),$$

$$\mathcal{Q} = \mathcal{O}(\beta),$$

where the latter follows from $\kappa_n^\sigma = \mathcal{O}(\beta^n)$ and $\mathbb{1}/d$ is the maximally mixed state for a system with dimension d. Thus, to leading order on $\beta \to 0$ [37],

$$\Lambda_{\text{cl}} = \frac{\beta^2}{2}\text{Var}_{\mathbb{1}/d}[\Delta H^{\text{d}}], \quad \Lambda_{\text{qu}} = \frac{\beta^2}{2}\text{Var}_{\mathbb{1}/d}[\Delta H^{\text{c}}], \quad \Sigma = \Lambda_{\text{cl}} + \Lambda_{\text{qu}}. \tag{5.43}$$

Without loss of generality we can assume the Hamiltonian of the system $H(g)$ is linear on the working parameter g. In this case, $\Delta H^{(\text{d,c})} \propto \delta g$, where δg is the quench amplitude. Hence, at sufficiently high temperatures all quantities scale with $\beta^2 \delta g^2$. Moreover, the relative contributions from Λ_{cl} and Λ_{qu} to the total entropy production will depend on the relative sizes of the variances of ΔH^{d} and ΔH^{c} on the maximally mixed state; that is, on the details of the process. Accordingly, a highly coherent protocol will mean a large contribution from Λ_{qu} even in this limit of temperatures.

Next, consider the opposite limit $\beta \to \infty$. To leading order on β we can replace the thermal state ρ_0^{th} by the projector onto the ground-state of the initial Hamiltonian, Π_i^0. In this case,

$$\text{Var}_0[\Delta H^{\text{d}}] \to \text{tr}\{(\Delta H^{\text{d}})^2 \Pi_i^0\} - \text{tr}\{\Delta H^{\text{d}} \Pi_i^0\}^2 = \Delta H_{ii}^2 - \Delta H_{ii}^2 = 0,$$

$$\text{Var}_0[\Delta H^{\text{c}}] - \mathcal{Q} \to \text{tr}\{\Pi_i^0 \Delta H^{\text{c}} \Pi_i^0 \Delta H^{\text{c}}\} \neq 0 \quad \text{(in general)},$$

where the first equation follows from (5.28). Hence, at low temperatures $\Lambda_{\text{cl}} \to 0$ while

that is generally not the case for Λ_{qu}. That is, the quantum part dominates the entropy production in this limit, as intuitively expected. Therefore, we can conclude the Λ-splitting corrects both the shortcoming of the previous Γ-splitting. Namely, the quantum Λ_{qu} is the dominant contribution at low temperatures and highly coherent processes and both contributions are analytic over a range of temperatures similar to Σ.

Although the above results are obtained for the instantaneous and infinitesimal quench protocol, we believe them to be more general. In fact, this is corroborated by results in [37] where we also used other types of protocols.

After discussing the properties of the Λ-splitting in the instantaneous and infinitesimal quench protocol at the level of averages, let us consider next its stochastic formulation.

For simplicity, let us consider the Hamiltonian of the system to be nondegenerate. As showed in Sec. 4.2, in this case, the forward path probability becomes

$$P_F[i,j] = p_i^0 |\langle j_\tau | i_0 \rangle|^2,$$

where $\{|i_0\rangle\}$ and $\{|j_\tau\rangle\}$ are the eigenstates of the initial and final Hamiltonians. Again, $p_i^0 = e^{-\beta\epsilon_i^0}/Z_0$ are the populations of the initial thermal state ρ_0^{th}.

Moreover, up to second order on ΔH, we have

$$|\langle j_\tau | i_0 \rangle|^2 = \begin{cases} \frac{|\Delta H_{ij}|^2}{(\epsilon_j^0 - \epsilon_i^0)^2}, & \text{if } j \neq i \\ 1 - \sum_{\ell \neq j} |\langle j_\tau | \ell_0 \rangle|^2, & \text{if } j = i, \end{cases}$$

and

$$\epsilon_j^\tau = \epsilon_j^0 + \Delta H_{jj} + E_j^{(2)},$$

with

$$E_j^{(2)} = \sum_{\ell \neq j} \frac{|\Delta H_{j\ell}|^2}{\epsilon_j^0 - \epsilon_\ell^0}.$$

where ϵ_j^τ are the eigenvalues of H_τ and $\Delta H_{ij} = \langle i_0 | \Delta H | j_0 \rangle$.

To discuss the issue of analyticity of the Λ-splitting at the stochastic level, we Taylor expand the populations $\{\tilde{p}_i^\tau\}$ and $\{p_j^\tau\}$ of the intermediate and final thermal states. They

read [37]

$$\tilde{p}_i^{\tau} = p_i^0(1-\tilde{f}_i), \tag{5.44}$$

$$p_j^{\tau} = p_j^0(1-f_j), \tag{5.45}$$

where

$$\tilde{f}_i = \beta(1-\beta\langle\Delta H^{\mathrm{d}}\rangle_0)(\Delta H_{ii}-\langle\Delta H^{\mathrm{d}}\rangle_0)+\frac{1}{2}\beta^2(\Delta H_{ii}^2-\langle(\Delta H^{\mathrm{d}})^2\rangle_0 \tag{5.46}$$

$$f_j = \tilde{f}_j+\beta\big(E_j^{(2)}-\langle E^{(2)}\rangle_0\big), \tag{5.47}$$

with $\langle E^{(2)}\rangle_0 = \sum_i p_i^0 E_i^{(2)}$. Equations (5.45) and (5.47) repeat Eqs. (4.71) and (4.72).

Similarly to what was done in Sec. 4.2 for the Γ-splitting, we insert Eqs. (5.44) and (5.45) on Eqs. (5.15)-(5.16) to obtain [37]

$$\sigma[i,j] = \ln p_i^0/p_j^0 - \ln(1-f_j), \tag{5.48}$$

$$\lambda_{\mathrm{cl}}[i,j] = -\ln\Big(1-\tilde{f}_i\Big) \tag{5.49}$$

$$\lambda_{\mathrm{qu}}[i,j] = \ln p_i^0/p_j^0 + \ln\Big(1-\tilde{f}_i\Big) - \ln(1-f_j). \tag{5.50}$$

As showed in the aforementioned section, in the Γ-splitting, a function s_j given in (4.73) performs an analogous role to that of $\tilde{f}_i$ and f_j on the above. This function s_j depends polynomially on the perturbation ΔH but increases exponentially with β. Hence, the bound $|s_j|<1$ required for analyticity of the Γ-quantities is swiftly saturated with decreasing temperatures.

In contrast, $\tilde{f}_i$ and f_j are polynomial functions of $\beta\Delta H$. Therefore, the conditions $|\tilde{f}_i|<1$ and $|f_j|<1$ for analyticity of σ and λ_{cl} and λ_{qu} are satisfied over a considerably broader and similar range of temperatures. This shows the Λ-quantities will be analytical in the same range of parameters as Σ [37].

Lastly, utilizing Eqs. (5.49) and (5.50) we may easily compute the joint CGF of the Λ-slitting (5.23) for an instantaneous and infinitesimal quench. To leading order on ΔH

it reads [37]

$$K_{\lambda_{\rm cl},\lambda_{\rm qu}}(v,u) = K_{\lambda_{\rm cl}}(v) + K_{\lambda_{\rm qu}}(u), \tag{5.51}$$

where

$$K_{\lambda_{\rm cl}}(v) = \frac{\beta^2}{2}(v^2 - v)\,\mathrm{Var}_0[\Delta H^{\rm d}], \tag{5.52}$$

$$K_{\lambda_{\rm qu}}(u) = \frac{\beta^2}{2}(u^2 - u)\,\mathrm{Var}_0[\Delta H^{\rm c}] + \frac{\beta^2}{2}\int_0^u \mathrm{d}x \int_x^{1-x} \mathrm{d}y I^y(\rho_0^{\rm th}, \Delta H^{\rm c}). \tag{5.53}$$

Moreover, since $K_\sigma(v) = K_{\lambda_{\rm cl},\lambda_{\rm qu}}(v,v)$ [12, 37],

$$K_\sigma(v) = K_{\lambda_{\rm cl}}(v) + K_{\lambda_{\rm qu}}(v). \tag{5.54}$$

We can make several important remarks about these results. To begin with, the separation of $K_{\lambda_{\rm cl},\lambda_{\rm qu}}$ onto the two CGFs in Eq. (5.51) means the variables $\lambda_{\rm cl}$ and $\lambda_{\rm qu}$ become *statistically independent* in the instantaneous and small quench limit. What is more, from (5.54), we note not only $\Sigma = \Lambda_{\rm cl} + \Lambda_{\rm qu}$ but all cumulants of σ get split in terms of cumulants of $\lambda_{\rm cl}$ and $\lambda_{\rm qu}$ [12, 37]:

$$\kappa_n(\sigma) = \kappa_n(\lambda_{\rm cl}) + \kappa_n(\lambda_{\rm qu}). \tag{5.55}$$

Also from (5.54), it follows that, in this limit, $\lambda_{\rm qu}$ satisfies an integral fluctuation theorem

$$\langle e^{-\lambda_{\rm qu}} \rangle = 1. \tag{5.56}$$

Next, for all practical purposes, the total decoupling of $\lambda_{\rm cl}$ and $\lambda_{\rm qu}$ signify these components of entropy production can be regarded as emerging from completely *independent processes* [12, 37]. The entropy production $\Lambda_{\rm cl}$ is associated with a quench from $H_0 \to \mathbb{D}_{H_0}(H_\tau)$, where only the energy eigenvalues are altered. Conversely, $\Lambda_{\rm qu}$ is the entropy production steaming from a second quench, from $\mathbb{D}_{H_0}(H_\tau) \to H_\tau$, where the energy eigenbasis is rotated [12].

The splitting of the CGF of entropy production in (5.54) was first noted in [12], where the authors were studying a quasi-isothermal process as a series of quantum quenches.

In fact, it was the incompatibility of Eqs. (5.37) and (5.54) with the Γ-splitting and its shortcomings what motivated us to construct the alternative Λ-splitting [37].

With Eqs. (5.52) and (5.53) at hand we can finally prove the variance of the entropy production $\kappa_2(\sigma) = \langle(\sigma - \Sigma)^2\rangle$ is equal to $\beta^2 \operatorname{Var}_0[\Delta H]$. From the former it is evident that

$$\kappa_2(\lambda_{\text{cl}}) = \frac{\mathrm{d}^2}{\mathrm{d}v^2} K_{\lambda_{\text{cl}}}(v)|_{v=0} = \langle(\lambda_{\text{cl}} - \Lambda_{\text{cl}})^2\rangle = \beta^2 \operatorname{Var}_0[\Delta H^{\text{d}}]. \tag{5.57}$$

Moreover,

$$\begin{aligned}\kappa_2(\lambda_{\text{qu}}) &= \langle(\lambda_{\text{qu}} - \Lambda_{\text{qu}})^2\rangle \\ &= \beta^2 \operatorname{Var}_0[\Delta H^{\text{c}}] - \frac{\beta^2}{2}\big(I^1(\rho_0^{\text{th}}, \Delta H^c) + I^0(\rho_0^{\text{th}}, \Delta H^c)\big) \\ &= \beta^2 \operatorname{Var}_0[\Delta H^{\text{c}}],\end{aligned} \tag{5.58}$$

since $I^0(\rho, X) = I^1(\rho, X) = 0$. Therefore,

$$\kappa_2(\sigma) = \langle(\sigma - \Sigma)^2\rangle = \beta^2 \operatorname{Var}_0[\Delta H]. \tag{5.59}$$

An interesting feature of the Γ- and Λ-splitting of entropy production is the fact that they coincide at sufficiently high temperatures for instantaneous and infinitesimal quenches. That is, if T (β) is large (small) enough so that we can treat the Γ-splitting perturbatively, then $\Gamma_{\text{cl}} = \Lambda_{\text{cl}}$ and $\Gamma_{\text{qu}} = \Lambda_{\text{qu}}$. This is shown as follows.

For an instantaneous quench, we have

$$\Gamma_{\text{cl}} = \langle\gamma_{\text{cl}}\rangle = \sum_{i,j} \ln \frac{q_j^\tau}{p_j^\tau} p_i^0 |\langle j_\tau | i_0\rangle|^2. \tag{5.60}$$

To order ΔH^2, we know $p_j^\tau = p_j^0(1 - f_j)$, f_j given by (5.47), and $q_j^\tau = p_j^0(1 - s_j)$, where s_j is given by Eq. (4.73),

$$s_j = \sum_{\ell \neq j} \frac{1 - p_\ell^0/p_j^0}{(\epsilon_j^0 - \epsilon_\ell^0)^2} |\Delta H_{\ell j}|^2.$$

Moreover,

$$|\langle j_\tau|i_0\rangle|^2 = \delta_{ij}\left(1 - \sum_{\ell\neq j}\frac{|\Delta H_{\ell j}|^2}{(\epsilon_j^0 - \epsilon_\ell^0)^2}\right) + (1-\delta_{ij})\frac{|\Delta H_{ij}|^2}{(\epsilon_i^0 - \epsilon_j^0)^2}. \tag{5.61}$$

Hence, if $|s_j| < 1$, to order ΔH^2,

$$\begin{aligned}
\Gamma_{\text{cl}} &= \sum_{i,j} \ln\left(\frac{1-s_j}{1-f_j}\right) p_i^0 |\langle j_\tau|i_0\rangle|^2 = \sum_{i,j}(f_j - s_j)p_i^0|\langle j_\tau|i_0\rangle|^2 \\
&= \sum_i (f_i - s_i)p_i^0 \\
&= \sum_i \frac{\beta^2}{2}(\Delta H_{ii}^2 - \langle(\Delta H^{\text{d}})^2\rangle_0)p_i^0 - \sum_{j\neq i}\frac{p_i^0 - p_j^0}{(\epsilon_i^0 - \epsilon_j^0)^2}|\Delta H_{ij}|^2 \\
&= \sum_i \frac{\beta^2}{2}(\Delta H_{ii}^2 - \langle(\Delta H^{\text{d}})^2\rangle_0)p_i^0 = \frac{\beta^2}{2}\text{Var}_0[\Delta H^{\text{d}}] = \Lambda_{\text{cl}},
\end{aligned} \tag{5.62}$$

where the last line follows from

$$\sum_{j\neq i}\frac{p_i^0 - p_j^0}{(\epsilon_i^0 - \epsilon_j^0)^2}|\Delta H_{ij}|^2 = \sum_{j\neq i}\frac{p_j^0 - p_i^0}{(\epsilon_j^0 - \epsilon_i^0)^2}|\Delta H_{ji}|^2 = -\sum_{j\neq i}\frac{p_i^0 - p_j^0}{(\epsilon_i^0 - \epsilon_j^0)^2}|\Delta H_{ij}|^2 = 0,$$

with the second equality obtained by a simple exchange of the indices i and j. As a consequence, also $\Gamma_{\text{qu}} = \Lambda_{\text{qu}}$.

5.2 Λ-splitting in the quantum Ising model

At last, we are in the position to study the behaviors of Λ_{cl} and Λ_{qu} in a quantum critical system. This is complementary to what I presented in Sec. 4.1 for the Γ-splitting and Sec. 3.3 for the total entropy production.

Let us begin, yet again, with our general Hamiltonian for the alternating transverse field Ising model,

$$H = -\sum_{j=1}^{N}\left[\sigma_j^x\sigma_{j+1}^x + (g - (-1)^j h)\sigma_j^z\right]. \tag{5.63}$$

In Sec. 2.1, we saw this Hamiltonian has critical points at $|g^2 - h^2| = 1$ and could

be exactly diagonalized. After the mapping to a fermionic system, this Hamiltonian splits into two parts, depending on if the system contains an even or odd number of particles; or spins pointing down. However, to more easily compute our quantities of interest, we can make an approximation and ignore this change in the Hamiltonian when we change parity (number of down spins). The approximation becomes exact in the thermodynamic limit $N \to \infty$.

Also, as before, at each realization of the work protocol, I consider the field h to be fixed. That is, I take g to be the working parameter.

With all of this, we saw we can write our Hamiltonian in diagonal form as

$$H(g) = \sum_{k \in K^+} \sum_{s=-,+} \epsilon_k^s(g)(2\eta_{k,s}^\dagger(g)\eta_{k,s}(g) - 1), \tag{5.64}$$

where $K^+ = \{k = \pm(2n+1)\pi/N;\ n = 0, 1, ..., N/4 - 1\}$,

$$\epsilon_k^\pm(g) = \sqrt{1 + g^2 + h^2 \pm 2\sqrt{g^2h^2 + g^2\cos^2 k + h^2 \sin^2 k}} \tag{5.65}$$

are the dispersion relations and $\{\eta_{k,s}\}$ are fermionic operators,

$$\{\eta_{k,s},\ \eta_{k',s'}^\dagger\} = \delta_{k,k'}\delta_{s,s'}, \quad \{\eta_{k,s},\ \eta_{k',s'}\} = 0. \tag{5.66}$$

At the start of the work protocol, the system is prepared in the thermal state

$$\rho_0^{\text{th}} = \frac{e^{-\beta H_0}}{Z_0} = \prod_{k \in K^+} \prod_{s=-,+} \frac{e^{\beta\epsilon_{k|0}^s}|0_{k,s}\rangle\langle 0_{k,s}| + e^{-\beta\epsilon_{k|0}^s}|1_{k,s}\rangle\langle 1_{k,s}|}{2\cosh\left(\beta\epsilon_{k|0}^s\right)}, \tag{5.67}$$

where g_0 is the initial field, $\beta = 1/T$ is the inverse temperature, $\epsilon_{k|0}^\pm = \epsilon_k^\pm(g_0)$ and $|0_{k,s}\rangle$ ($|1_{k,s}\rangle$) is the state annihilated (created) by $\eta_{k,s}(g_0)$ ($\eta_{k,s}^\dagger(g_0)$).

Next, with the system isolated, we perform an instantaneous quench that changes the working parameter g to a final value $g_\tau = g_0 + \delta g$. Accordingly, the reference equilibrium state of the system is updated to

$$\rho_\tau^{\text{th}} = \frac{e^{-\beta H_\tau}}{Z_\tau} = \prod_{k \in K^+} \prod_{s=-,+} \frac{e^{\beta\epsilon_{k|\tau}^s}|0_{k,s}^\tau\rangle\langle 0_{k,s}^\tau| + e^{-\beta\epsilon_{k|\tau}^s}|1_{k,s}^\tau\rangle\langle 1_{k,s}^\tau|}{2\cosh\left(\beta\epsilon_{k|\tau}^s\right)}, \tag{5.68}$$

where, following the same logic, $\epsilon^{\pm}_{k|\tau} = \epsilon^{\pm}_{k}(g_\tau)$, $\left|0^{\tau}_{k,s}\right\rangle = 0$ is the state annihilated by $\eta_{k,s}(g_\tau)$ and $\left|1^{\tau}_{k,s}\right\rangle = \eta^{\dagger}_{k,s}(g_\tau)\left|0^{\tau}_{k,s}\right\rangle$.

The Λ-splitting of entropy production following an instantaneous quench is based on the intermediate thermal state

$$\tilde{\rho}^{\text{th}}_{\tau} = \frac{\exp\left[-\beta(H_0 + \Delta H^{\text{d}})\right]}{\text{tr}\left\{\exp\left[-\beta(H_0 + \Delta H^{\text{d}})\right]\right\}},$$

where ΔH^{d} is the dephased part of the perturbation $\Delta H = H_\tau - H_0$ in the eigenbasis of the initial thermal state ρ^{th}_0; consequently, the eigenbasis of H_0.

In Sec. 3.3, I showed that since our Hamiltonian H is continuous and linear on g we must have

$$\begin{aligned}\Delta H &= \delta g\,(\partial_g H(g))|_{g_0}, \\ &= \delta g \sum_i (\partial_{g_0}\epsilon^0_i)\Pi^0_i + \delta g \sum_i \epsilon^0_i(\partial_{g_0}\Pi^0_i),\end{aligned} \tag{5.69}$$

where ϵ^0_i and $\{\Pi^0_i\}$ are the eigenvalues and eigenprojectors of H_0, which are given by linear combinations of $\epsilon^{\pm}_{k|0}$ and $|0_{k,s}\rangle\langle 0_{k,s}|$ and $|1_{k,s}\rangle\langle 1_{k,s}|$. Moreover, I denote by $\partial_{g_0}\epsilon^0_i = \partial_g \epsilon_i(g)|_{g_0}$ and similarly for $\partial_{g_0}\Pi^0_i$. Equation (5.69) holds as long as h is kept fixed during the protocol. Importantly, since the system presents only continuous transitions, these derivatives are continuous functions of g and, hence, well-defined even at a critical point.

From the previous relation we immediately verify that

$$\Delta H^{\text{d}} = \delta g \sum_i (\partial_{g_0}\epsilon^0_i)\Pi^0_i, \tag{5.70}$$

$$\Delta H^{\text{c}} = \delta g \sum_i \epsilon^0_i(\partial_{g_0}\Pi^0_i), \tag{5.71}$$

where $\Delta H^{\text{c}} = \Delta H - \Delta H^{\text{d}}$ is the coherent part of the perturbation in the eigenbasis of H_0. In words, these equations mean the dephased and coherent parts of the perturbation are directly connected to the derivatives of the system initial eigenenergies and eigenbasis, respectively.

Instead of Eqs. (5.70) and (5.71), however, it is more practical to consider the equiva-

lent forms,

$$\Delta H^{\mathrm{d}} = \delta g \sum_{k\in K^+} \sum_{s=-,+} (\partial_{g_0}\epsilon^s_{k|0})(2\eta^\dagger_{k,s}\eta_{k,s} - 1), \tag{5.72}$$

$$\Delta H^{\mathrm{c}} = \delta g \sum_{k\in K^+} \sum_{s=-,+} 2\epsilon^s_{k|0}(\partial_{g_0}\eta^\dagger_{k,s}\eta_{k,s}). \tag{5.73}$$

As a particular but significant case, for the homogeneous field Ising model ($h = 0$), these can be written as [37]

$$\Delta H^{\mathrm{d}} = 2\delta g \sum_{k\in K^+_{I>}} \cos\theta_k(\eta^\dagger_k\eta_k + \eta^\dagger_{-k}\eta_{-k} - 1), \tag{5.74}$$

$$\Delta H^{\mathrm{c}} = 2\delta g \sum_{k\in K^+_{I>}} \sin\theta_k(\eta^\dagger_{-k}\eta^\dagger_k - \eta_{-k}\eta_k), \tag{5.75}$$

where K^+_I, ϵ^0_k, $\{\eta_k\}$, $\cos\theta_k$ and $\sin\theta_k$ are defined in Eqs. (4.32)-(4.37) — see also below.

Finally, the intermediate thermal state $\tilde{\rho}^{\mathrm{th}}_\tau$ can be explicitly written as

$$\tilde{\rho}^{\mathrm{th}}_\tau = \prod_{k\in K^+}\prod_{s=-,+} \frac{e^{\beta\tilde{\epsilon}^s_{k|\tau}}|0_{k,s}\rangle\langle 0_{k,s}| + e^{-\beta\tilde{\epsilon}^s_{k|\tau}}|1_{k,s}\rangle\langle 1_{k,s}|}{2\cosh\left(\beta\tilde{\epsilon}^s_{k|\tau}\right)}, \tag{5.76}$$

where $\tilde{\epsilon}^\pm_{k|\tau} = \epsilon^\pm_{k|0} + \delta g(\partial_{g_0}\epsilon^\pm_{k|0})$ are the single-particle energies associated with the dephased Hamiltonian $H_0 + \Delta H^{\mathrm{d}}$.

It is now straightforward to compute the general expressions for Λ_{cl} and Λ_{qu} in the quenched alternating transverse field Ising model. Already taking the thermodynamic limit $N \to \infty$, they read

$$\Lambda_{\mathrm{cl}} = \frac{N}{2\pi}\sum_{s=-,+}\int_{-\frac{\pi}{2}}^{\frac{\pi}{2}} \mathrm{d}k \left\{ \ln\left[\frac{\cosh\left(\beta\tilde{\epsilon}^s_{k|\tau}\right)}{\cosh\left(\beta\epsilon^s_{k|0}\right)}\right] - \beta\delta g(\partial_{g_0}\epsilon^s_{k|0})\tanh\left(\beta\epsilon^s_{k|0}\right)\right\}, \tag{5.77}$$

and

$$\Lambda_{\mathrm{qu}} = \frac{N}{2\pi}\sum_{s=-,+}\int_{-\frac{\pi}{2}}^{\frac{\pi}{2}} \mathrm{d}k\, \ln\left[\frac{\cosh\left(\beta\epsilon^s_{k|\tau}\right)}{\cosh\left(\beta\tilde{\epsilon}^s_{k|\tau}\right)}\right]. \tag{5.78}$$

I emphasize these general formulae are valid for an instantaneous quench with fixed field h but any quench size δg. Thus far, I have not assumed the latter to be small.

Adding the two contributions, we recover the full entropy production given in (3.71),

$$\Sigma = \frac{N}{2\pi}\sum_{s=-,+}\int_{-\frac{\pi}{2}}^{\frac{\pi}{2}} \mathrm{d}k \left\{ \ln\left[\frac{\cosh\left(\beta\epsilon^s_{k|\tau}\right)}{\cosh\left(\beta\epsilon^s_{k|0}\right)}\right] - \beta\delta g(\partial_{g_0}\epsilon^s_{k|0})\tanh\left(\beta\epsilon^s_{k|0}\right)\right\}. \tag{5.79}$$

As was done in Sec. 3.3 for Σ, let us begin considering the particular case $h = 0$. That is, let us start our analysis with the homogeneous field Ising model. In this case, for easier comparison with the Γ-splitting, it is more convenient to rewrite our Λ-quantities as [37]

$$\Lambda_{\text{qu}} = N\int_0^{\pi}\frac{\mathrm{d}k}{2\pi}2\ln\left[\frac{\cosh(\beta\epsilon^{\tau}_k)}{\cosh(\beta\tilde{\epsilon}^{\tau}_k)}\right], \tag{5.80}$$

$$\Lambda_{\text{cl}} = N\int_0^{\pi}\frac{\mathrm{d}k}{2\pi}2\left\{\ln\left[\frac{\cosh(\beta\tilde{\epsilon}^{\tau}_k)}{\cosh(\beta\epsilon^{0}_k)}\right] - \beta\delta g\cos\theta_k\tanh\left(\beta\epsilon^0_k\right)\right\}, \tag{5.81}$$

$$\Sigma = N\int_0^{\pi}\frac{\mathrm{d}k}{2\pi}2\left\{\ln\left[\frac{\cosh(\beta\epsilon^{\tau}_k)}{\cosh(\beta\epsilon^{0}_k)}\right] - \beta\delta g\cos\theta_k\tanh\left(\beta\epsilon^0_k\right)\right\}, \tag{5.82}$$

where $\epsilon^t_k = \epsilon_k(g_t) = \sqrt{1+g_t^2-2g_t\cos k}$ and $\tilde{\epsilon}^{\tau}_k = \epsilon^0_k + \delta g\cos\theta_k$, with

$$\left(\cos\theta_k,\ \sin\theta_k\right) = \left(\frac{g_0-\cos k}{\epsilon^0_k},\ \frac{\sin k}{\epsilon^0_k}\right). \tag{5.83}$$

Equations (5.80) and (5.81) are easily obtained using (5.74) and (5.75) and should be contrasted with Γ_{qu} and Γ_{cl} in (4.45) and (4.46).

In Fig. 5.2 I compare the classical and quantum parts of the Γ- and Λ-splittings of entropy production as a function of β for the homogeneous transverse field Ising model. I considered an initial field $g_0 = 0.5$ here, and quenches of size $\delta g = 0.01$. As expected from the discussion in the previous section, at high temperatures, the two splittings coincide; that is, we have $\Gamma_{\text{cl}} = \Lambda_{\text{cl}}$ and $\Gamma_{\text{qu}} = \Lambda_{\text{qu}}$. However, as the initial temperature of the system is lowered, Γ_{cl} and Γ_{qu} begin to severely differ from Λ_{cl} and Λ_{qu}. The region of starting deviation agrees with the point where Γ_{cl} and Γ_{qu} cease to be analytic.

Notably, at high temperatures $T \to \infty$ ($\beta \to 0$) all quantities scale with β^2. On the other hand, as $T \to 0$, Γ_{cl} grows linearly with β while Λ_{cl} approaches zero. Contrastingly, for the quantum parts, Γ_{qu} saturates at low temperatures while Λ_{qu} grows linear with β.

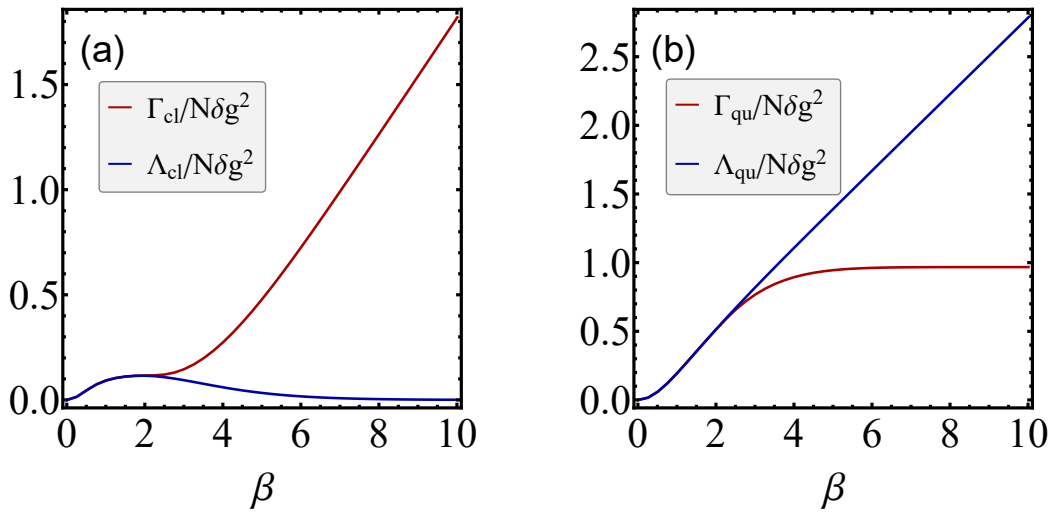

Figure 5.2: Comparison between the (a) classical and (b) quantum parts of the two splittings of entropy production as a function of β for $g_0 = 0.5$. At high temperatures the two coincide. However, they differ at low temperatures. In all points $\delta g = 0.01$.

These behaviors of $\Lambda_{\rm cl}$ and $\Lambda_{\rm qu}$ are further confirmed by their Taylor expansion on the perturbation δg. To leading order on it, we obtain

$$\Lambda_{\rm cl}/N = \beta^2 \delta g^2 \int_0^\pi \frac{{\rm d}k}{2\pi} \,{\rm sech}^2(\beta\epsilon_k^0) \cos^2\theta_k, \tag{5.84}$$

$$\Lambda_{\rm qu}/N = \beta^2 \delta g^2 \int_0^\pi \frac{{\rm d}k}{2\pi} \frac{\tanh(\beta\epsilon_k^0)}{\beta\epsilon_k^0} \sin^2\theta_k. \tag{5.85}$$

When $\beta \to 0$, ${\rm sech}^2(\beta\epsilon_k^0)$ and $\tanh(\beta\epsilon_k^0)/\beta\epsilon_k^0$ are close to 1, while the former approaches zero and the latter tends to $1/\beta\epsilon_k^0$ as $\beta \to \infty$.

Hence, at low temperatures, the quantum part $\Lambda_{\rm qu}$ gives the dominant contribution in the Λ-splitting. These results agree with the general analysis in Sec. 5.1.

Moving forward, let us consider the Λ-splitting in the vicinity of the Ising critical point at $(g = 1, h = 0)$. In Fig. 5.3 I show the behaviors of $\Lambda_{\rm cl}$ and $\Lambda_{\rm qu}$ per particle as a function of the initial field g_0 for several β and quench-sizes $\delta g = 0.01$.

At low temperatures, the quantum part $\Lambda_{\rm qu}$ presents a peak near the critical field $g_0 = 1$ which becomes sharper with decreasing temperatures. In the Λ-splitting, this is the contribution associated with the ensuing divergence of the total entropy production in the limit $T \to 0$ ($\beta \to \infty$). Contrarily, in this limit, $\Lambda_{\rm cl}$ is much smaller in general, and suddenly drops to zero at $g_0 = 1$.

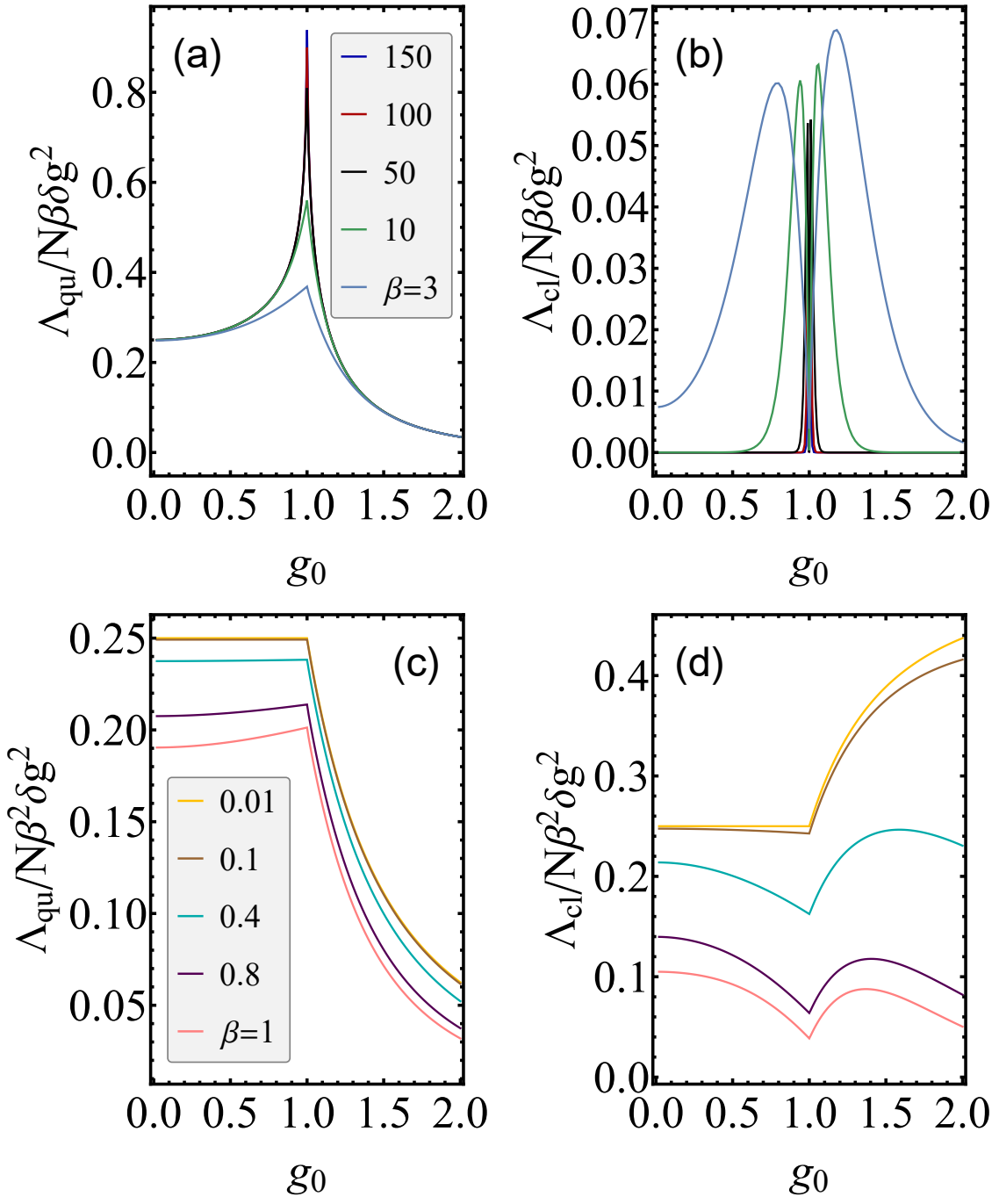

Figure 5.3: Λ_{qu} and Λ_{cl} per spin in the vicinity of the Ising critical point. Above, the behaviors at low temperatures (large β) of (a) Λ_{qu} and (b) Λ_{cl}. In this limit, Λ_{qu} display a cusp at $g_0 = 1$ which becomes a divergence in the limit $T = 0$. On the other hand, Λ_{cl} experiences a sudden drop at this point. The divergence in the entropy production, thus, comes from the quantum part Λ_{qu}. Below, the behaviors at high temperatures of (c) Λ_{qu} and Λ_{cl}. Here both contributions scale with β^2 at sufficiently high temperatures. Moreover, in this regime $\Lambda_{qu} = \Gamma_{qu}$ and $\Lambda_{cl} = \Gamma_{cl}$ for an instantaneous quench. Again, contrarily to the full entropy production, even in this limit the quantum critical point is indicated by a kink in Λ_{qu} and Λ_{cl}. In all points, $\delta g = 0.01$.

As noted before, the increase in entropy production near a critical point at low temperatures results from the creation of excitations in the modes $\pm k$, when the quench is performed [38]. This is particularly clear in Eq. (4.50),

$$\Sigma/N = \beta \int_0^{\pi} \frac{\mathrm{d}k}{2\pi} \epsilon_k^{\tau} p_k,$$

where $p_k = \sin^2(\Delta_k/2) \approx (1/4)\delta g^2 \sin^2\theta_k/(\epsilon_k^0)^2$ provides the probability of such transitions to occur.

In the Γ-splitting, this enters Γ_{cl} as a population mismatch between the pre- and postquench equilibrium states ρ_0^{th} and ρ_τ^{th} on the final energy basis. Consequently, this corresponds to the most substantial component of the entropy production.

Conversely, p_k can be equivalently regarded as a measure of the rotation in the energy eigenbasis resulting from the quench [37]. In the Λ-splitting, any contributions to the entropy production steaming from a basis change and, hence, from quantum coherences, enters Λ_{qu}. Hence, the increase in this quantity in the vicinity of the critical field.

The drop in Λ_{cl} at $g_0 = 1$ can also be understood as follows [37]. In our quenched Ising model, this component merely quantifies the contribution to the entropy production associated with a change in the energy levels given by $\tilde{\epsilon}_k^{\tau} - \epsilon_k^0 = \delta g \cos\theta_k$. At low temperatures, the ground and low lying excited states are the most relevant, and close to the critical point $g_0 = 1$, the latter corresponds to creating excitations with momenta $k \to 0$. But one can easily show that at $g_0 = 1$, $\cos\theta_k = |\sin(k/2)|$, which goes to zero when $k \to 0$ and, hence, the drop in Λ_{cl}.

Let us consider in the sequence the high-temperature limit. In this case, $\Gamma_{\text{cl}} = \Lambda_{\text{cl}}$ and $\Gamma_{\text{qu}} = \Lambda_{\text{qu}}$ and the plots in Fig. 5.3(c) and (d) are exactly the same as in Fig. 4.2(c) and (d).

Notably, Λ_{cl} and Λ_{qu} behave differently depending if the initial field g_0 is associated with a ferromagnetic or paramagnetic phase of the model at $T = 0$. Particularly, in the limit $T \to \infty$ ($\beta \to 0$), Λ_{qu} presents a plateau for field values identified with the ordered phase and decreases monotonically if the contrary. In contrast, Λ_{cl} increases monotonically for $g_0 > 1$ while exhibiting a flat depression in the region $g_0 < 1$.

Moreover, they both present kinks at the quantum critical field $g_0 = 1$, although that

is not the case for the total entropy production, as showed in Fig. 3.3(b).

As argued before, the Γ-splitting gives no intuition as to why theses kinks appear in the components of entropy production even in the high-temperature limit. In light of the Λ-splitting we are able to explain these behaviors. This goes as follows [40].

In Sec. 5.1 I showed that for sufficiently high temperatures and leading order on β and δg, we have — see (5.43)

$$\Lambda_{\text{cl}} = \frac{\beta^2}{2}\text{Var}_{\mathbb{1}/d}[\Delta H^{\text{d}}], \quad \Lambda_{\text{qu}} = \frac{\beta^2}{2}\text{Var}_{\mathbb{1}/d}[\Delta H^{\text{c}}], \tag{5.86}$$

where $\mathbb{1}/d$ is the maximally mixed state of a system with dimension d.

By construction, $\text{tr}\{\Delta H^{\text{c}}\} = 0$, but without loss of generality we can also assume this to be the case for ΔH^{d}; i.e., consider $\text{tr}\{\Delta H^{\text{d}}\} = 0$. Next, we utilize the dephased and coherent parts of the perturbation are related to the derivatives of the initial Hamiltonian eigenenergies and eigenbasis, Eqs. (5.70) and (5.71).

This allows us to write [40]

$$\Lambda_{\text{cl}} = \frac{1}{2}\beta^2\delta g^2 \sum_i \frac{d_i}{d}(\partial_{g_0}\epsilon_i^0)^2, \tag{5.87}$$

$$\Lambda_{\text{qu}} = \frac{1}{2}\beta^2\delta g^2 \sum_i \frac{||\epsilon_i^0(\partial_{g_0}\Pi_i^0)||^2}{d}, \tag{5.88}$$

where $||X|| = \sqrt{\text{tr}\{X^\dagger X\}}$ is the Hilbert-Schmidt norm of X and $d_i = \text{tr}\{\Pi_i^0\}$ is the dimension of projector Π_i^0.

Therefore — in this limit of infinitesimal quenches and extremely high temperatures — Λ_{cl} and Λ_{qu} are given by a weighted sum of the square of the first derivatives of the initial Hamiltonian eigenvalues and eigenprojectors, respectively.

Now, by definition, the ground-state and ground-state energy of a quantum critical system are singular in the vicinity of a critical point. Particularly, if it is a second-order critical point, their first derivatives will have a kink/cusp at such a point. Moreover, in fact, many low-lying energy levels present the ground state singular behavior in the asymptotic regime $N \to \infty$. These first derivatives singularities are precisely what is captured by Λ_{cl} and Λ_{qu} and it is why their plots in Figs. 5.3 present a kink at $g_0 = 1$ [40].

More generally, when ρ_0^{th} cannot be replaced by $\mathbb{1}/d$, the derivatives in Eqs. (5.87) and (5.88) appear multiplied by some continuous functions of β and the energy eigenvalues ϵ_i^0 — see Eqs. (5.84) and (5.85). These function-coefficients come, for instance, from the thermal averages of the eigenprojectors Π_i^0. As a consequence, the kinks on Λ_{cl} and Λ_{qu} — ultimately steaming from the kink singularities on the Hamiltonian spectrum at a critical point — persist at every finite temperature [40].

This argument can be easily checked. Starting with Λ_{cl}, we have

$$\begin{aligned}\Lambda_{\text{cl}} &= \frac{\beta^2}{2}\,\text{Var}_0[\Delta H^{\text{d}}] = \frac{\beta^2}{2}\left(\,\text{tr}\{(\Delta H^{\text{d}})^2\rho_0^{\text{th}}\} - \text{tr}\{\Delta H^{\text{d}}\rho_0^{\text{th}}\}^2\right)\\ &= \frac{\beta^2\delta g^2}{2}\left[\sum_i(\partial_{g_0}\epsilon_i^0)^2\,\text{tr}\{\Pi_i^0\rho_0^{\text{th}}\} - \left(\sum_i(\partial_{g_0}\epsilon_i^0)\,\text{tr}\{\Pi_i^0\rho_0^{\text{th}}\}\right)^2\right],\end{aligned} \tag{5.89}$$

It is evident in the above equation the presence of the ground state energy derivative $\partial_{g_0}\epsilon_0^0$ multiplied by a continuous function of β and ϵ_i^0. If this derivative has a kink/cusp, this gets inherited by Λ_{cl}.

For Λ_{qu}, we have

$$\begin{aligned}\Lambda_{\text{qu}} &= \frac{\beta^2}{2}\left(\text{Var}_0[\Delta H^{\text{c}}] - \mathcal{Q}\right) = \frac{\beta^2}{2}\int_0^1 \text{d}y\,\text{tr}\{(\rho_0^{\text{th}})^y\Delta H^{\text{c}}(\rho_0^{\text{th}})^{1-y}\Delta H^{\text{c}}\}\\ &= \frac{1}{2}\beta\sum_{j\neq i}\frac{p_i^0 - p_j^0}{(\epsilon_j^0 - \epsilon_i^0)}\,\text{tr}\{\Pi_i^0\Delta H^{\text{c}}\Pi_j^0\Delta H^{\text{c}}\}.\end{aligned} \tag{5.90}$$

In general, the function-coefficients $(p_i^0 - p_j^0)/(\epsilon_j^0 - \epsilon_i^0)$ are continuous and smooth, though a possibly exception would occur when $\epsilon_j^0 \to \epsilon_i^0$. Hence, close to a critical point, we need to be careful with the ground and first-excited levels. For this reason, let $\Delta \geqslant 0$ be their energy gap. Then,

$$\frac{p_0^0 - p_1^0}{\epsilon_1^0 - \epsilon_0^0} = p_0^0\frac{1 - e^{-\beta\Delta}}{\Delta}. \tag{5.91}$$

However, as long as β is finite ($T > 0$), $(1 - e^{-\beta\Delta})/\Delta$ is finite, since this approaches β as $\Delta \to 0$.

Finally, the kinks on Λ_{qu} arise from the fact that $\text{tr}\{\Pi_i\Delta H^{\text{c}}\Pi_j\Delta H^{\text{c}}\}$ contains the singular but continuous first derivatives of Hamiltonian eigenprojectors.

It is crucial to note this reasoning applies to a system presenting only continuous transitions. In this case, the free energy is itself a continuous function with continuous first-order derivatives and so is the thermal state ρ_0^{th}. Otherwise, in the case of a system presenting first-order transitions, singularities could appear because of a kink in the free energy itself.

Following these results, in [40] we proposed Λ_{cl} and Λ_{qu} as tools for detecting second-order quantum critical points. This adds to a plethora of already used information-theoretic quantities ranging from fidelities [57, 63, 64, 66]; passing through entanglement [67, 69] and quantum discord [70, 71, 160, 161]; to other coherence quantifiers [72–74, 162–165]; and, of course, the full entropy production itself [33].

Most of these quantities, however, possess singularities at $g = g_c$ only precisely at $T = 0$, and are capable of sharply estimating the position of the critical point only at extremely low temperatures. In fact, this is completely reasonable since a quantum critical point truly exists exactly at zero temperature. The advantage of Λ_{cl} and Λ_{qu}, therefore, is that they still present a singularity at $g = g_c$ even when the system is prepared in an arbitrarily high temperature.

The viability of these quantities as quantum critical point detectors, however, depends on ones ability to measure them. In [40] we further proposed a scheme to determine Λ_{cl} and Λ_{qu} experimentally. I will not enter into details here and defer this to a subsequent section.

This concludes the analysis on the behavior of Λ_{cl} and Λ_{qu} in the vicinity of the Ising critical point at $(g = 1, h = 0)$.

An extra advantage of the Λ-splitting in comparison with the Γ, is that the former is generally much more tractable mathematically.

This simplicity allows us to analyse the behaviors of Λ_{cl} and Λ_{qu} also circa the fourth-order critical point of the alternating transverse field Ising model located at $(g = 0, h = 1)$.

As shown in Chapter 2, this fourth-order critical point is surrounded by second-order Ising-type critical point. Particularly, there is one such point precisely in the same spot as the fourth-order type. Hence, we have to be careful with the path selected to approach this point so that we effectively capture the behavior we are interested in here.

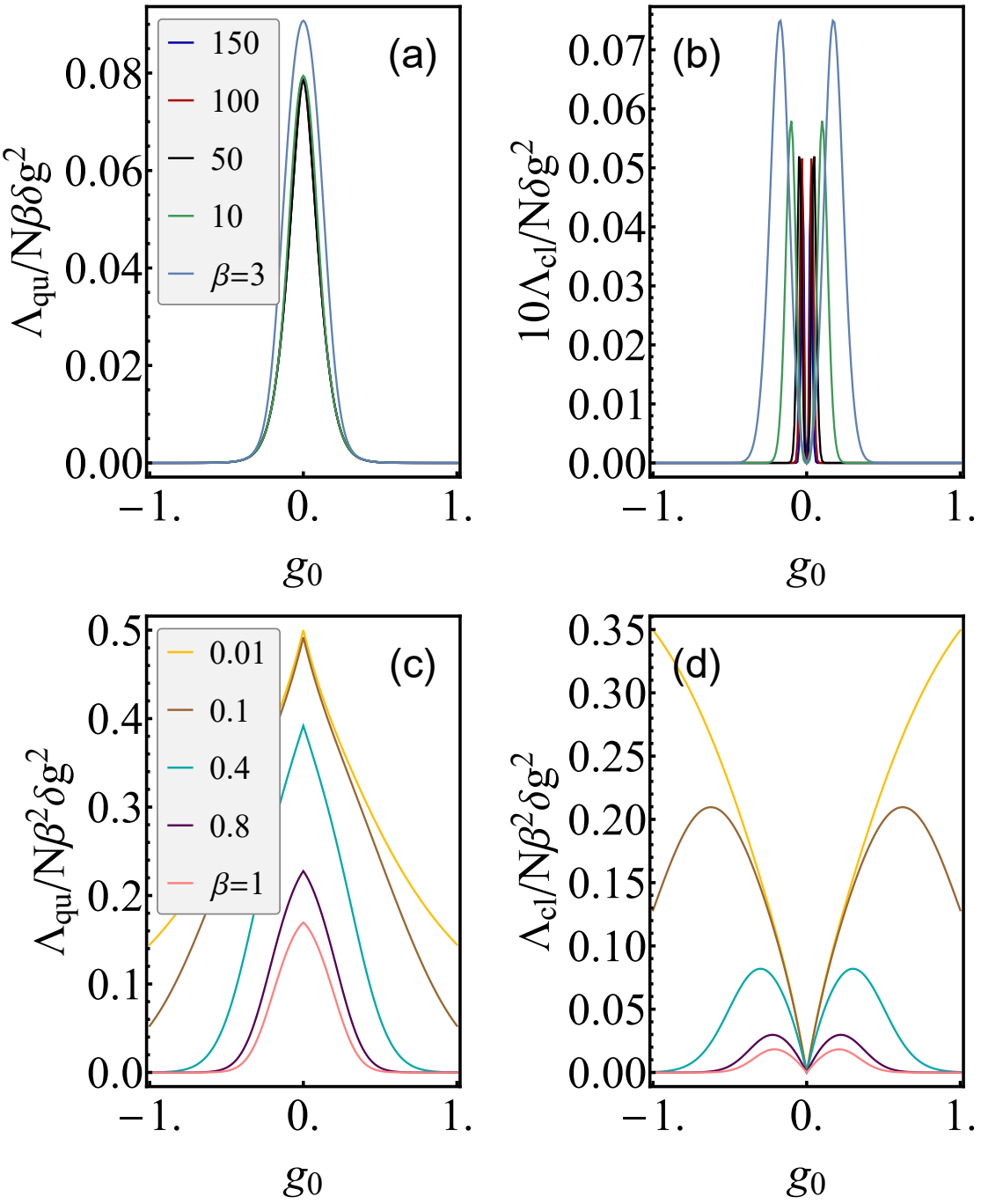

Figure 5.4: Λ_{qu} and Λ_{cl} per spin in the vicinity of the fourth-order critical point in the alternating transverse field Ising model. Above, the behaviors at low temperatures (large β) of (a) Λ_{qu} and (b) Λ_{cl}. Below, the behaviors at high temperatures of (c) Λ_{qu} and Λ_{cl}. The kink at $g_0 = 0$ on Λ_{cl} and Λ_{qu} on this limit does not come from the fourth-order CP but, in fact, from a singularity in the middle of the energy spectrum. In all points, $\delta g = 0.01$.

As was done with the full entropy production Σ in Sec.3.3, I choose to approach this point along the path $h = 1+10g^2$. That is, in each realization of the instantaneous quench protocol, h is kept fixed at the same initial value $h_0 = 1 + 10g_0^2$ while g is changed by an amount $\delta g = 0.01$. This way, Eqs. (5.77) and (5.78) always hold.

In Fig. 5.4 I show the behaviors of Λ_{cl} and Λ_{qu} per spin as a function of the initial field g_0 at several inverse temperatures β.

At low temperatures, Fig. 5.4(a), Λ_{qu} presents a smooth peak at the critical value $g_0 = 0$ and scale linearly with β for sufficiently low temperatures. A transient regime from a β^2 dependence to linear makes the curves for $\beta = 3$ and $\beta = 10$ lie above the others in this figure. Λ_{qu} is the dominant contribution to the entropy production. Conversely, the classical component Λ_{cl} display a sharp drop at the critical field $g_0 = 0$. This is similar to its behavior in the vicinity of the Ising critical point discussed before. Since we are probing now a fourth-order critical point, no singularities appear on Λ_{cl} and Λ_{qu} in this limit.

Increasing the system temperature causes a broadening of the peak/dip in $\Lambda_{\text{qu}}/\Lambda_{\text{cl}}$ near $g_0 = 0$ — Fig. 5.4(c) and (d). When $\beta \to 0$ both quantities scale with β^2. Curiously, in the high-temperature limit, Λ_{cl} and Λ_{qu} exhibit a kink at $g_0 = 0$. This singularity, however, is not a signature of the fourth-order critical point. Instead, they occur due to singularities in the middle of the Hamiltonian spectrum at $g_0 = 0$. For instance, the energy per spin of one such singular level is given in thermodynamic limit by

$$\frac{1}{N}\epsilon_{\text{mid}} = -\int_{-\frac{\pi}{2}}^{\frac{\pi}{2}} \frac{\mathrm{d}k}{2\pi}\,(\epsilon^{+}_{k|0} - \epsilon^{-}_{k|0}), \tag{5.92}$$

where $\epsilon^{\pm}_{k|0}$ are the single-particle energies associated with the η_+- and η_--fermions. This is the energy level obtained when all η_+ modes are grounded and all η_- modes are excited. In particular, the first derivative of ϵ_{mid}/N possesses a kink singularity at $g_0 = 0$ due a logarithmical divergence in its second derivative — this is the same behavior of the ground state energy of the homogeneous transverse field model at $g = 1$.

In fact, the ground state of each η-fermion species have such Ising-like singularities. These cancel each other out on the ground state of the whole system. However, exciting all modes of one species is equivalent to changing the sign of its ground state singularity. In

this case the singularities of each species add to each other in levels like (5.92). Therefore, it is these first derivatives kink singularities in the middle of the Hamiltonian spectrum which are being imprinted on Λ_{cl} and Λ_{qu} at high temperatures. Since these levels are unoccupied at low temperatures, the kinks disappear in this limit.

This shows the Λ-quantities provide a true glance at the spectrum of the system Hamiltonian at high temperatures.

This finishes the analysis of the Λ-splitting of entropy production in the vicinity of both types of critical point in the alternating transverse field Ising model.

5.3 Experimental evaluation of Λ_{cl} and Λ_{qu}

Let us return now to the discussion on how the classical and quantum contributions to the entropy production, Λ_{cl} and Λ_{qu}, could, in principle, be assessed experimentally. Our idea relies on the stochastic formulation of the Λ-splitting using the two-point measurement (TPM) scheme and the fact that they obey fluctuation theorems [40].

Let us assume for simplicity a nondegenerate Hamiltonian and recapitulate. Our protocol starts with the system prepared in the thermal state

$$\rho_0^{\text{th}} = \frac{e^{-\beta H_0}}{Z_0} = \frac{e^{-\beta \epsilon_i^0}}{Z_0} |i_0\rangle\langle i_0|$$

where β is the inverse temperature and $H_0 = \sum_i \epsilon_i^0 |i_0\rangle\langle i_0|$ is the initial Hamiltonian.

In the TPM scheme, we perform an energy measurement at $t = 0$. As a result, we obtain the eigenvalue ϵ_i^0 with probability $p_i^0 = e^{-\beta\epsilon_i^0}/Z_0$, while the state of the system is updated to $|i_0\rangle$ due to the measurement backaction.

Next, we apply our instantaneous quench protocol, changing the system Hamiltonian to $H_\tau = H_0 + \Delta H = \sum_j \epsilon_j^\tau |j_\tau\rangle\langle j_\tau|$, and, subsequently, perform the second energy measurement. The result will be the eigenvalue ϵ_j^τ with probability $p_{\text{quench}}(i \to j) = |\langle j_\tau | i_0\rangle|^2$.

Hence, the path probability associated with the stochastic trajectory $|i_0\rangle \to |j_\tau\rangle$ reads $P_F[i,j] = p_i^0 |\langle j_\tau | i_0\rangle|^2$. The stochastic entropy production is defined by [36]

$$\sigma[i,j] = \beta(\epsilon_j^\tau - \epsilon_i^0) - \beta\Delta F, \tag{5.93}$$

where $w[i,j] = \epsilon_j^\tau - \epsilon_i^0$ is the stochastic work done on the system, and $\Delta F = -T \ln Z_\tau / Z_0$ is the change in equilibrium free energy.

As we saw, $\langle \sigma \rangle = \sum_{i,j} \sigma[i,j] P_F[i,j] = \Sigma$ produces the correct average. Moreover, σ satisfies an integral fluctuation theorem [128, 129], $\langle e^{-\sigma} \rangle = 1$, from which it follows the Jarzynski relation $\langle e^{-\beta w[i,j]} \rangle = e^{-\beta \Delta F}$ [98].

Therefore, if in an experiment, one can determine the work $w[i,j]$ and the path probability $P_F[i,j]$, one readily obtains ΔF from the Jarzynski relation and, finally, the entropy production $\Sigma = \beta(\langle w \rangle - \Delta F)$. In Chapter 3 I presented several experimental proposals and implementations to determine these quantities, including one that is applicable, in principle, to a many-body system [140].

Having said that, note the stochastic versions of Λ_{cl} and Λ_{qu} in Eqs. (5.15)-(5.16) can be equivalently written as

$$\lambda_{\text{cl}}[i,j] = \ln p_i^0 / \tilde{p}_i^\tau = \beta(\tilde{\epsilon}_i^\tau - \epsilon_i^0) - \beta \Delta \tilde{F}_{\tau 0}, \tag{5.94}$$

$$\lambda_{\text{qu}}[i,j] = \ln \tilde{p}_i^\tau / p_j^\tau = \beta(\epsilon_j^\tau - \tilde{\epsilon}_i^\tau) - \beta \Delta \tilde{F}_{\tau\tau}, \tag{5.95}$$

where $\tilde{\epsilon}_i^\tau = \epsilon_i^0 + \Delta H_{ii} = \epsilon_i^0 + \delta g(\partial_g \epsilon_i^0)$, with $\Delta H_{ii} = \langle i_0 | \Delta H | i_0 \rangle$, are the eigenenergies associated with the dephased Hamiltonian $H_0 + \Delta H^{\text{d}}$. Moreover, we have $\Delta \tilde{F}_{\tau 0} = -T \ln \tilde{Z}_\tau / Z_0$ and $\Delta \tilde{F}_{\tau\tau} = -T \ln Z_\tau / \tilde{Z}_\tau$, with $\tilde{Z}_\tau = \text{tr}\left\{ e^{-\beta(H_0 + \Delta H^{\text{d}})} \right\}$. The former indicates the change in equilibrium free energy associated with incoherent part of the perturbation $\Delta H^{\text{d}} = \sum_i \Delta H_{ii} |i_0\rangle\langle i_0|$. Conversely, the latter yields the additional difference in free energy associated with the perturbation's coherent part $\Delta H^{\text{c}} = \Delta H - \Delta H^{\text{d}}$.

Once more, from these stochastic definitions we recover the averages $\Lambda_{\text{cl}} = \langle \lambda_{\text{cl}} \rangle = \sum_{i,j} \lambda_{\text{cl}}[i,j] P_F[i,j]$ and $\Lambda_{\text{qu}} = \langle \lambda_{\text{qu}} \rangle = \sum_{i,j} \lambda_{\text{qu}}[i,j] P_F[i,j]$. Additionally, λ_{cl} satisfies the integral fluctuation theorem, $\langle e^{-\lambda_{\text{cl}}} \rangle = 1$, and this is equally valid for λ_{qu} in the infinitesimal and instantaneous quench limit — see Sec. 5.1.

Now we observe that, up to second-order on the perturbation δg, the final energy

eigenvalues are given by

$$\begin{aligned}\epsilon_j^\tau &= \epsilon_j^0 + \delta g(\partial_g \epsilon_j^0) + \frac{1}{2}\delta g^2(\partial_g^2 \epsilon_j^0) \\ &= \epsilon_j^0 + \Delta H_{jj} + \frac{1}{2}\sum_{\ell\neq j}\frac{|\Delta H_{j\ell}|^2}{\epsilon_j^0 - \epsilon_\ell^0},\end{aligned} \tag{5.96}$$

where $\Delta H_{ij} = \langle i_0|\Delta H|j_0\rangle$.

Therefore, in this limit of instantaneous and infinitesimal quenches, the first term in Eq. (5.94), $w^{\rm d}[i,i] = \tilde{\epsilon}_i^\tau - \epsilon_i^0$, is approximated by $w^{\rm d}[i,i] \approx w[i,j]\delta_{ij}$ [40]. This approximation is certainly fine away from a critical point. In the latter case, the third term on the r.h.s. of Eq. (5.96) can become relevant, though. Nevertheless, the smaller δg is, the better the approximation and smaller the interval where it breaks down. In the limit $\delta g \to 0$, it fails only precisely at the critical point.

Consequently, we may obtain $w^{\rm d}$ from the measured stochastic work w by *post-selecting* the cases where after the second measurement the system is found in a state with the same $j = i$ [40]. With $w^{\rm d}$ at hand, we use again a Jarzynski relation, $\langle e^{-\beta w^{\rm d}}\rangle = e^{-\beta\Delta\tilde{F}_{\tau 0}}$, to get $\Delta\tilde{F}_{\tau 0}$ and, ultimately, $\Lambda_{\rm cl} = \beta(\langle w^{\rm d}\rangle - \Delta\tilde{F}_{\tau 0})$. From $\Lambda_{\rm cl}$ and Σ, we further obtain $\Lambda_{\rm qu} = \Sigma - \Lambda_{\rm cl}$ [40].

This approach, therefore, conveniently enables the determination of $\Lambda_{\rm cl}$ and $\Lambda_{\rm qu}$ trough a simple post-selection of the experimental data obtained from the two-point measurement protocol [40].

Since no experiment is performed on a infinite system, let us also analyse the behavior of an Ising model with a finite number of spins N. In this case, $\Lambda_{\rm cl}$ and $\Lambda_{\rm qu}$ become smooth functions of the initial field g_0. However, as shown bellow, the thermodynamic limit behavior is swiftly approached with increasing N [40]. This means our proposal could be tested in a system with a somewhat small number of spins.

For simplicity I take $h = 0$ in our general Hamiltonian (5.63) and work with the homogeneous transverse field Ising model. Moreover, I focus on the infinitesimally small quench and sufficiently high-temperature limit, which allows us to use Eqs. (5.43). That is, I assume the initial thermal $\rho_0^{\rm th}$ state can be treated as the maximally mixed state. Thus,

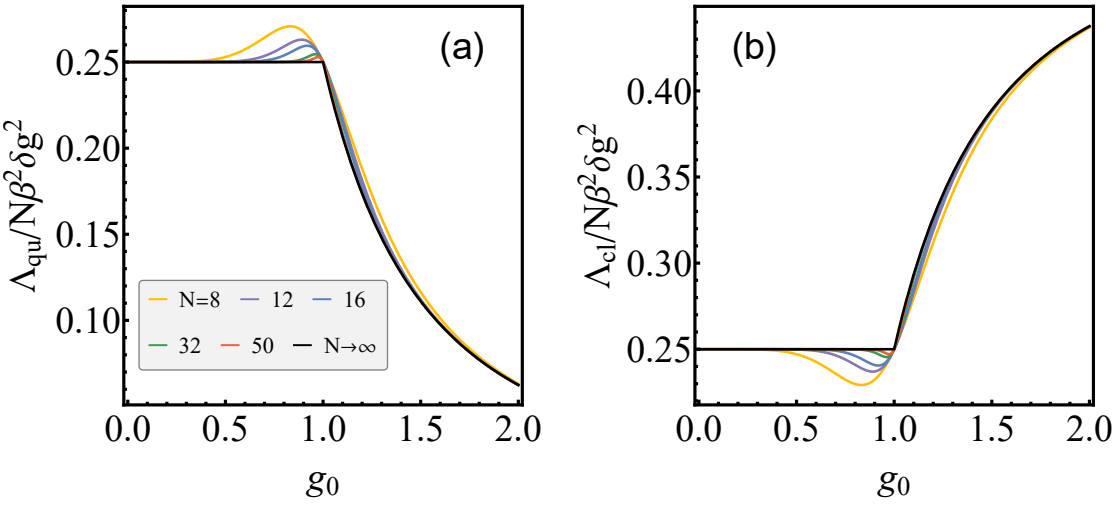

Figure 5.5: Plots of (a) $\Lambda_{\rm qu}$ and (b) $\Lambda_{\rm cl}$ per spin scaled by $\beta^2\delta g^2$ as functions of the initial field g_0, for several values of N. The figure shows the limit $N \to \infty$ is quickly approached with increasing N in the limit $T \to \infty$ ($\beta \to 0$). In fact, away from the critical value $g_0 = 1$, the error in approximating a finite N plot by the $N \to \infty$ is of order $1/N^2$.

in light of (5.74) and (5.75), we have [40]

$$\Lambda_{\rm cl} = \frac{\beta^2}{2}\,{\rm tr}\left\{\frac{\mathbb{1}}{2^N}(\Delta H^{\rm d})^2\right\} = \beta^2\delta g^2 \sum_{k>0}\cos^2\theta_k, \tag{5.97}$$

$$\Lambda_{\rm qu} = \frac{\beta^2}{2}\,{\rm tr}\left\{\frac{\mathbb{1}}{2^N}(\Delta H^{\rm c})^2\right\} = \beta^2\delta g^2 \sum_{k>0}\sin^2\theta_k, \tag{5.98}$$

where 2^N is the dimension of the Hilbert space of a system with N spins, $k = \pm(2n+1)\pi/N$, n ranging from 0 to $N/2-1$, and, again,

$$\left(\cos\theta_k,\,\sin\theta_k\right) = \left(\frac{g_0-\cos k}{\epsilon_k^0},\,\frac{\sin k}{\epsilon_k^0}\right),$$

with $\epsilon_k^0 = \sqrt{1+g_0^2-2g_0\cos k}$ and g_0 the initial transverse field.

In Fig. 5.5 I plot $\Lambda_{\rm cl}$ and $\Lambda_{\rm qu}$ per spin as functions of g_0 for several N. The plots show the thermodynamic limit behaviors — indicated by the black curves — are quickly approximated with increasing N.

These results may be further elucidated as follows [40]. Equations (5.97) and (5.98)

can be rewritten as

$$\frac{\Lambda_{\text{cl}}}{N\beta^2\delta g^2} = \sum_{k>0} \cos^2\theta_k \frac{\Delta k}{2\pi}, \tag{5.99}$$

$$\frac{\Lambda_{\text{qu}}}{N\beta^2\delta g^2} = \sum_{k>0} \sin^2\theta_k \frac{\Delta k}{2\pi}, \tag{5.100}$$

where $\Delta k = 2\pi/N$.

If we consider a partition

$$P = \left\{ \left[0, \frac{2\pi}{N}\right], \left[\frac{2\pi}{N}, \frac{4\pi}{N}\right], ..., \left[\pi - \frac{2\pi}{N}, \pi\right] \right\}$$

of the interval $[0, \pi]$, the r.h.s. of (5.99) and (5.100) are equivalent to midpoint Riemann sums of the functions $\cos^2\theta_k$ and $\sin^2\theta_k$ over $[0, \pi]$ with partition P.

The absolute difference between these sums and the respective thermodynamic limit integrals in (5.84) and (5.85), with the appropriate limit $\beta \to 0$, is bounded by

$$\left| \int_0^\pi \frac{\mathrm{d}k}{2\pi} f(k) - \sum_{k>0} f(k) \frac{\Delta k}{2\pi} \right| \leqslant \frac{M\pi^3}{6N^2}, \tag{5.101}$$

where $f(k)$ is either $\cos^2\theta_k$ or $\sin^2\theta_k$, and $M = \max_{k\in[0,\pi]} |\partial_k^2 f(k)|$ is the maximum absolute value of the second derivative of $f(k)$ in the interval $[0, \pi]$. Clearly, f is also a function of the initial field g_0, but I omit this to simplify the notation. This second derivative reads

$$|\partial_k^2 f(k)| = \frac{2}{(\epsilon_k^0)^4} |\sin^2\theta_k (g_0^2 - 1)^2 + \epsilon_k^0 \cos\theta_k (1 - g_0 \cos k) \cos k|. \tag{5.102}$$

It is straightforward to graphically verify the maximum of this function occurs at the boundary $k = 0$ for $g_0 \geqslant 0$. Precisely, we have

$$M = \frac{2}{(g_0 - 1)^2}, \quad \text{if } g_0 \geqslant 0. \tag{5.103}$$

That is, except at $g_0 = 1$, the functions Λ_{cl}/N and Λ_{qu}/N for a finite chain converge to the thermodynamic limit behavior with a swiftly decreasing error of order $1/N^2$. The

divergence of M at $g_0 = 1$ further clarifies the slower convergence in this region.

Conclusions

A summary of our results is propitious now. In this thesis I have shown how a quantum thermodynamic work protocol may be used to probe quantum critical systems. It was already known the entropy production at low temperatures exhibits a peak near a second-order quantum critical point, signaling its existence. In fact, this quantity is intimately related to the susceptibility of the control parameter of the phase transition, which diverges at zero temperature at the critical point. Naturally, as I showed in Chapter 3, in the case of higher-order quantum critical points it is a derivative of the entropy production which diverges in this limit.

Moving forward, I revealed further insight may be gained by considering a splitting of the entropy production into a classical and quantum parts or, yet, into populations imbalances and coherences. In Chapter 4 I analysed a previous known separation, where the quantum part is based on the relative entropy of coherence. It turned out, although of great significance in the broader field of quantum thermodynamics, this splitting presents some weaknesses in the scenario of Jarzynski-type work protocols. Notably, the dominance of the 'classical' part at low temperatures and highly coherent protocols and the failure in analyticity when no such issue arises in the total entropy production. Nonetheless, this partitioning demonstrated these individual components could signal the existence of a quantum critical point with protocols realized at any temperature, again in contrast with their sum. As an additional flaw, however, the splitting offered no intuition on as to why this happens.

In Chapter 5 I presented a new splitting, which corrects the shortcomings of the previous one and offers a more consistent and intuitive picture in the context of work protocols. This was shown to be remarkably accurate in the case of instantaneous quenches. In this scenario, the classical and quantum parts of the new splitting are intrinsically connected

with the diagonal and coherent parts of the perturbation Hamiltonian. For a system with a linear dependence on the control parameter, this is respectively equivalent to a connection with the first derivatives of the unperturbed energy eigenvalues and eigenbasis.

The quantum critical point signatures on these components of entropy production was then explained as arising from the kinks on the derivatives energy spectrum. The kinks on the classical and quantum parts of the splitting occur even in protocols performed at arbitrarily high temperatures and mean they can function as valuable quantum critical points detectors. I concluded the chapter with a proposal on how these quantities could be determined experimentally using their stochastic formulation within the two-point measurement framework.

As a general conclusion, this work reveals how it can be highly non-trivial to distinguish the quantum contribution to the entropy production in a nonequilibrium process. In this case, it seems different approaches suit better different contexts. In a way, this is similar to the splitting of energy in a quantum system into work and heat.

As a direct follow-up, we could investigate the behaviors of the higher-order cumulants of entropy production and its splittings in a critical system like the Ising model. Also, it would be interesting to consider more general time-dependent protocols in these types of many-body systems. Then, a connection could be established with some recent studies on quantum batteries using finite-time charging protocols [30, 166, 167].

Moreover, the new splitting of entropy production presented here could be tested on different scenarios. For instance, in the context of heat exchange or in general open systems, including open work protocols. For a system evolving in contact with a heat bath, one could investigate under what conditions, if any, the components of the new splitting constitute monotones in a resource theory.

Appendix A

Gap and Bounds in the ATFIM

In this Appendix I provide the steps necessary to obtain the gap expressions given in Section 2.1. We derived these in [39]. The arguments closely follows the ones first presented in [94].

A.1 Gap Expressions

Using the Fourier series (2.47)-(2.48) and the fact that $\epsilon^{\pm}_{-k} = \epsilon^{\pm}_{k}$, we obtain

$$\epsilon^{+} = -2\sum_{l=0}^{\infty}(u_l + v_l)\sum_{k\in K^{+}_{>}}\cos(2kl), \tag{A.1}$$

$$\epsilon^{-} = -2\sum_{l=0}^{\infty}(u_l + v_l)\sum_{k\in K^{-}_{>}}\cos(2kl) - 2\sqrt{1+g^2} - 2\sqrt{1+h^2}. \tag{A.2}$$

Next we make use of the relations

$$\sum_{n=0}^{m-1}\cos(x+ly) = \cos[x+(m-1)y/2]\sin(my/2)\csc(y/2),$$

$$\lim_{x\to nN/2}\frac{1}{2}\frac{\sin(\pi x)}{\sin(2\pi x/N)} = \frac{N}{4}(-1)^n, \qquad \text{for } n\in\mathbb{N},$$

to derive that

$$\begin{aligned}\sum_{k\in K_>^+}\cos(2kl) &= \frac{N}{4}(-1)^n\delta_{l,nN/2},\\ \sum_{k\in K_>^-}\cos(2kl) &= \frac{N}{4}\delta_{l,nN/2}-\delta_{l,2n},\end{aligned} \tag{A.3}$$

for $n\in\mathbb{N}$.

Then,

$$\epsilon^+ = -\frac{N}{2}\Big[\big(u_0+v_0\big)-\big(u_{N/2}+v_{N/2}\big)+\big(u_N+v_N\big)-\big(u_{3N/2}+v_{3N/2}\big)+\ldots\Big], \tag{A.4}$$

$$\begin{aligned}\epsilon^- = &-\frac{N}{2}\Big[\big(u_0+v_0\big)+\big(u_{N/2}+v_{N/2}\big)+\big(u_N+v_N\big)+\big(u_{3N/2}+v_{3N/2}\big)+\ldots\Big]\\ &+2\Big(u_0+u_2+u_4+\ldots-\sqrt{1+h^2}\Big)+2\Big(v_0+v_2+v_4+\ldots-\sqrt{1+g^2}\Big).\end{aligned} \tag{A.5}$$

For the latter, however, we note

$$\epsilon^+_{k=0} = \sum_{l=0}^{\infty}u_l\cos(0) = u_0+u_1+u_2+u_3+\ldots = \Big||g|+\sqrt{1+h^2}\Big|, \tag{A.6}$$

$$\epsilon^+_{k=\frac{\pi}{2}} = \sum_{l=0}^{\infty}u_l\cos(\pi l) = u_0-u_1+u_2-u_3+\ldots = \Big||h|+\sqrt{1+g^2}\Big|, \tag{A.7}$$

$$\epsilon^-_{k=0} = \sum_{l=0}^{\infty}v_l\cos(0) = v_0+v_1+v_2+v_3+\ldots = \Big||g|-\sqrt{1+h^2}\Big|, \tag{A.8}$$

$$\epsilon^+_{k=\frac{\pi}{2}} = \sum_{l=0}^{\infty}v_l\cos(\pi l) = v_0-v_1+v_2-v_3+\ldots = \Big||h|-\sqrt{1+g^2}\Big|. \tag{A.9}$$

Hence,

$$\begin{aligned}&u_0+u_2+u_4+\ldots-\sqrt{1+h^2}+v_0+v_2+v_4+\ldots-\sqrt{1+g^2}\\ &=\frac{1}{2}\Big(\Big||g|+\sqrt{1+h^2}\Big|+\Big||g|-\sqrt{1+h^2}\Big|\Big)-\sqrt{1+h^2}\\ &\quad+\frac{1}{2}\Big(\Big||h|+\sqrt{1+g^2}\Big|+\Big||h|-\sqrt{1+g^2}\Big|\Big)-\sqrt{1+g^2}\\ &=\Big(|g|-\sqrt{1+h^2}\Big)\Theta\Big(|g|-\sqrt{1+h^2}\Big)+\Big(|h|-\sqrt{1+g^2}\Big)\Theta\Big(|h|-\sqrt{1+g^2}\Big).\end{aligned} \tag{A.10}$$

where

$$\Theta(x) = \begin{cases} 1 & \text{if } x > 0, \\ 0 & \text{if } x < 0, \end{cases}$$

is the Heaviside step function.

Finally,

$$\begin{aligned}\epsilon^- = &2\Big(|g| - \sqrt{1+h^2}\Big)\Theta\Big(|g| - \sqrt{1+h^2}\Big) + 2\Big(|h| - \sqrt{1+g^2}\Big)\Theta\Big(|h| - \sqrt{1+g^2}\Big) \\ &- \frac{N}{2}\Big[\big(u_0 + v_0\big) + \big(u_{N/2} + v_{N/2}\big) + \big(u_N + v_N\big) + \big(u_{3N/2} + v_{3N/2}\big) + \dots\Big].\end{aligned} \tag{A.11}$$

Subtracting (A.4) from (A.11) we arrive at

$$\begin{aligned}\Delta = &2\Big(|g| - \sqrt{1+h^2}\Big)\Theta\Big(|g| - \sqrt{1+h^2}\Big) + 2\Big(|h| - \sqrt{1+g^2}\Big)\Theta\Big(|h| - \sqrt{1+g^2}\Big) \\ &- N\sum_{l=0}^{\infty}\Big(u_{(2l+1)N/2} + v_{(2l+1)N/2}\Big).\end{aligned} \tag{A.12}$$

It is worth noticing that the first line vanishes when $|g^2 - h^2| \leqslant 1$.

To compute the sum in the above expression we use that since $\epsilon_k^{\pm} \geqslant 0$, $(\epsilon_k^+ + \epsilon_k^-) = \sqrt{(\epsilon_k^+ + \epsilon_k^-)^2}$, and, thus,

$$\begin{aligned}u_l + v_l &= \frac{2}{\pi}\int_{-\frac{\pi}{2}}^{\frac{\pi}{2}} \mathrm{d}k \cos(2kl)(\epsilon_k^+ + \epsilon_k^-) \\ &= \frac{\sqrt{2}}{\pi}\int_{-\pi}^{\pi} \mathrm{d}k \cos(kl)\left[1 + g^2 + h^2 + \sqrt{\sin^2 k + \big[(g^2 - h^2) - \cos k\big]^2}\right]^{\frac{1}{2}}.\end{aligned} \tag{A.13}$$

Now we have to consider the cases $|g^2 - h^2| = 0$, $0 \neq |g^2 - h^2| \neq 1$ and $|g^2 - h^2| = 1$ separately.

Let us begin with $|g^2 - h^2| = 0$. Then,

$$u_l + v_l = \frac{\sqrt{2}}{\pi}\int_{-\pi}^{\pi} \mathrm{d}k \cos(kl)\sqrt{2 + g^2 + h^2} = 4\sqrt{1 + (g^2 + h^2)/2}\,\delta_{l,0}. \tag{A.14}$$

Hence,

$$\Delta = 0, \quad \text{if } g^2 - h^2 = 0. \tag{A.15}$$

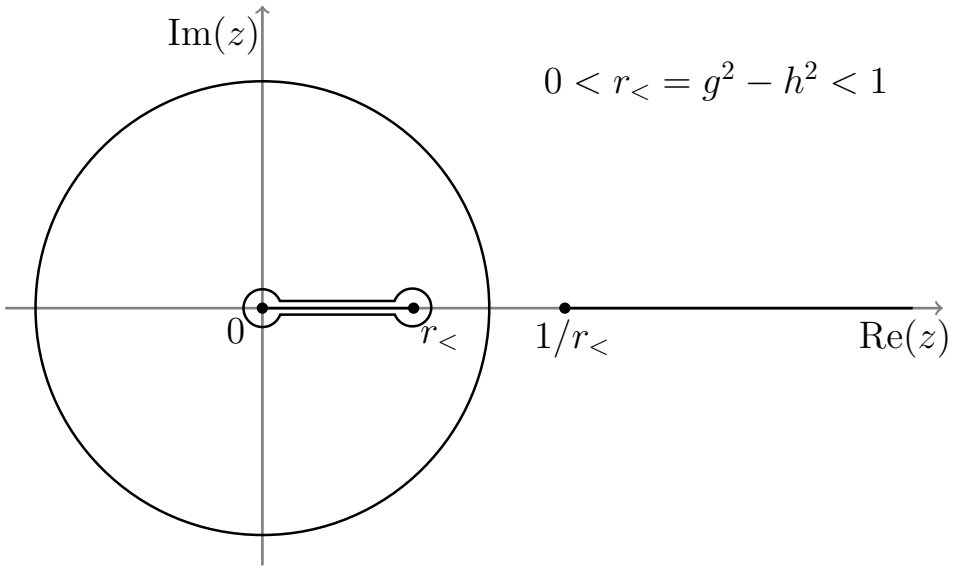

Figure A.1: Illustration of the branch cuts and integration path used to obtain Eq. (A.21).

Next, we take $0 \neq |g^2 - h^2| \neq 1$. Then we make the change of variables $z = e^{ik}$ to obtain,

$$u_l + v_l = -\frac{i\sqrt{2}}{\pi} \oint_{|z|=1} \mathrm{d}z\, z^{l-1} \left[1 + g^2 + h^2 + \sqrt{\frac{[z - (g^2 - h^2)][1 - (g^2 - h^2)z]}{z}} \right]^{\frac{1}{2}}. \tag{A.16}$$

Consider first $0 < g^2 - h^2 = r_< < 1$. To solve this integral we make branch cuts over the interval $(0, r_<) \cup (1/r_<, \infty)$ and deform the integration contour. The procedure is represented in Fig. A.1 This results in

$$u_l + v_l = i\frac{2\sqrt{2}}{\pi} r_<^l \int_0^1 \mathrm{d}t\, t^{2l-1} \left(\sqrt{Z(t)} - \sqrt{\overline{Z(t)}} \right), \tag{A.17}$$

where

$$Z(t) = R + i\sqrt{(1 - t^2)(1 - r_<^2 t^2)/t^2}, \tag{A.18}$$

$$R = 1 + g^2 + h^2, \tag{A.19}$$

and $\overline{Z(t)}$ is its complex conjugate.

Since $\mathrm{Re}(Z) > 0$ and $\mathrm{Im}(Z) > 0$, we have

$$\sqrt{Z(t)} - \sqrt{\overline{Z(t)}} = i\sqrt{2}\sqrt{|Z| - \mathrm{Re}(Z)}. \tag{A.20}$$

Therefore

$$u_l + v_l = -\frac{4}{\pi} r_<^l \int_0^1 \mathrm{d}t\, t^{2l-1} \left[\sqrt{\frac{(1-t^2)(1-r_<^2 t^2)}{t^2} + R^2} - R \right]^{\frac{1}{2}}, \tag{A.21}$$

for $0 < r_< = g^2 - h^2 < 1$.

For the other intervals for which $0 \neq |g^2 - h^2| \neq 1$, we follow basically these same steps, adjusting the branch cuts. In the end we obtain

$$u_l + v_l = -\frac{4}{\pi} |g^2 - h^2|^l \int_0^1 \mathrm{d}t \quad t^{2l-1} \left[\sqrt{\frac{(1-t^2)(1-|g^2-h^2|^2 t^2)}{t^2} + R^2} - R \right]^{\frac{1}{2}}, \tag{A.22}$$

$$u_l + v_l = -\frac{4}{\pi |g^2 - h^2|^l} \int_0^1 \mathrm{d}t\, t^{2l-1} \left[\sqrt{\frac{(1-t^2)(|g^2-h^2|^2 - t^2)}{t^2} + R^2} - R \right]^{\frac{1}{2}}, \tag{A.23}$$

for $|g^2 - h^2| < 1$ and $|g^2 - h^2| > 1$, respectively.

Replacing Eq. (A.22) in (A.12), and using that

$$\sum_{l=0}^{\infty} x^l = \frac{1}{1-x}, \quad |x| < 1,$$

we arrive at Eq. (2.50). Similarly, using (A.23) in (A.12) instead, we get (2.60).

Finally, for $|g^2 - h^2| = 1$ we take the limits $g^2 - h^2 \to \pm 1$ in Eqs. (A.22) and (A.23), or equivalently, in Eqs. (2.50) and (2.60), to obtain Eq. (2.57).

A.2 Bounds on the gap

We can derive bounds for the size of the gap using the above expressions.

Let us start with the gap for $|g^2 - h^2| = 1$. This is the condition for the lines of quantum critical points.

First we observe that Eq. (2.57) may be rewritten as

$$\Delta = \frac{4N}{\pi}\int_0^1 \mathrm{d}t\, \frac{t^{N-3/2}}{1-t^{2N}}\frac{1-t^2}{\sqrt{\sqrt{(1-t^2)^2+(2G^2t)^2}+2G^2t}}. \tag{A.24}$$

Now, the function $f(t) = \sqrt{\sqrt{(1-t^2)^2+(2G^2t)^2}+2G^2t}$ is monotonically increasing in the interval $t \in [0,1]$, for $G^2 \geqslant 1$. Hence,

$$\frac{1}{2\sqrt{G^2}}\frac{4N}{\pi}\int_0^1 \mathrm{d}t\, \frac{t^{N-3/2}(1-t^2)}{1-t^{2N}} \leqslant \Delta \leqslant \frac{8N}{\pi}\int_0^1 \mathrm{d}t\, \frac{t^{N-3/2}(1-t)}{1-t^{2N}}. \tag{A.25}$$

where I also used that $1-t^2 \leqslant 2(1-t)$ to obtain the right hand side.

Next, we have that

$$\frac{4N}{\pi}\int_0^1 \mathrm{d}t\, \frac{t^{N-3/2}(1-t)}{1-t^{2N}} = 2\tan\left(\frac{\pi}{4N}\right), \tag{A.26}$$

$$\begin{aligned}\frac{4N}{\pi}\int_0^1 \mathrm{d}t\, \frac{t^{N-1/2}(1-t)}{1-t^{2N}} &= \frac{4}{\pi}\left[\psi^{(0)}\left(\frac{1}{2}+\frac{3}{4N}\right)-\psi^{(0)}\left(\frac{1}{2}+\frac{1}{4N}\right)\right] \\ &= \frac{1}{\pi N}\sum_{n=0}^{\infty}\frac{1}{(n+\frac{1}{2}+\frac{3}{4N})(n+\frac{1}{2}+\frac{1}{4N})} \\ &> \frac{1}{\pi N}\sum_{n=0}^{\infty}\frac{1}{(n+1)^2} = \frac{\pi}{6N},\end{aligned} \tag{A.27}$$

where $\psi^{(0)}(z) = \frac{d}{dz}\ln\Gamma(z)$ is the Digamma function [168].

This leads directly to Eq. (2.58)

$$\frac{1}{2\sqrt{G^2}}\left[2\tanh\left(\frac{\pi}{4N}\right)+\frac{\pi}{6N}\right] \leqslant \Delta \leqslant 4\tanh\left(\frac{\pi}{4N}\right). \tag{A.28}$$

Now let us consider the case where $|g^2-h^2|<1$. This is the region of parameters associated with an ordered phase in the thermodynamic limit.

In this case we have, for the lower bound,

$$\begin{aligned}\Delta &= -N\sum_{l=0}^{\infty}\Big(u_{(2l+1)N/2}+v_{(2l+1)N/2}\Big)\\ &> -N(u_{N/2}+v_{N/2})\\ &= |g^2-h^2|^{\frac{N}{2}}\frac{4N}{\pi}\int_0^1 \mathrm{d}t\, t^{N-\frac{3}{2}}[\sqrt{(1-t^2)(1-|g^2-h^2|^2t^2)+R^2t^2}-Rt]^{\frac{1}{2}}\\ &= |g^2-h^2|^{\frac{N}{2}}\frac{4N}{\pi}\int_0^1 \mathrm{d}t\, t^{N-\frac{3}{2}}\frac{\sqrt{(1-t^2)(1-|g^2-h^2|t^2)}}{[\sqrt{(1-t^2)(1-|g^2-h^2|^2t^2)+R^2t^2}+Rt]^{\frac{1}{2}}}.\end{aligned} \tag{A.29}$$

The second line follows from the observation that $-(u_l+v_l)\geqslant 0$;

Now we use again that the function in the denominator of this integral is monotonically increasing in the interval $t\in[0,1]$. Hence,

$$\begin{aligned}\Delta &\geqslant \frac{1}{\sqrt{2R}}|g^2-h^2|^{\frac{N}{2}}\frac{4N}{\pi}\int_0^1 \mathrm{d}t\, t^{N-3/2}\sqrt{(1-t^2)(1-|g^2-h^2|^2t^2)}\\ &\geqslant \frac{1}{\sqrt{2R}}|g^2-h^2|^{\frac{N}{2}}\frac{4N}{\pi}\int_0^1 \mathrm{d}t\, t^{N-3/2}\sqrt{(1-t)(1-|g^2-h^2|t)}.\end{aligned} \tag{A.30}$$

To arrive at the second line I used $\sqrt{(1+t)(1+|g^2-h^2|t)}\geqslant 1$.

The next step is to notice that

$$\begin{aligned}\sqrt{(1-t)(1-|g^2-h^2|t)} &= \sqrt{(1-t)(1-|g^2-h^2|)+|g^2-h^2|(1-t)^2}\\ &\geqslant \max\{\sqrt{1-|g^2-h^2|}\sqrt{1-t},\sqrt{|g^2-h^2|}(1-t)\}\end{aligned} \tag{A.31}$$

and then integrate. Further using $16N/\pi(4N^2-1)\geqslant 4/\pi N$ and $\Gamma(N-1/2)/\Gamma(N)>1/\sqrt{N}$, it follows,

$$\Delta \geqslant \frac{|g^2-h^2|^{\frac{N}{2}}}{\sqrt{2R}}\max\left\{\frac{2}{\sqrt{\pi}}\frac{\sqrt{1-|g^2-h^2|}}{\sqrt{N}},\frac{4|g^2-h^2|^{\frac{1}{2}}}{\pi N}\right\}. \tag{A.32}$$

Now, for the upper bound,

$$\begin{aligned}\Delta &= -N\sum_{l=0}^{\infty}\left(u_{(2n+1)N/2}+v_{(2n+1)N/2}\right)\\ &= \sum_{l=0}^{\infty}\frac{4N}{\pi}\int_0^1 \mathrm{d}t\frac{t^{(2l+1)N-3/2}\,|g^2-h^2|^{\frac{(2l+1)N}{2}}\sqrt{(1-t^2)(1-|g^2-h^2|^2t^2)}}{\left[\sqrt{(1-t^2)(1-|g^2-h^2|^2t^2)}+R^2t^2+Rt\right]^{\frac{1}{2}}}\\ &\leqslant \sqrt{2(1+|g^2-h^2|)}\sum_{l=0}^{\infty}\int_0^1\frac{\mathrm{d}t\,4Nt^{(2l+1)N|g^2-h^2|^{\frac{(2l+1)N}{2}}}}{\pi t^{\frac{3}{2}}}\sqrt{(1-t)(1-|g^2-h^2|t)},\end{aligned} \tag{A.33}$$

where I used the monotonicity of the function in the denominator on the second line and that $\sqrt{(1+t)(1+|g^2-h^2|t)}\leqslant\sqrt{2(1+|g^2-h^2|)}$ to arrive at the last line.

Next we observe that

$$\begin{aligned}\sqrt{(1-t)(1-|g^2-h^2|t)} &= \sqrt{(1-t)(1-|g^2-h^2|)+|g^2-h^2|(1-t)^2}\\ &\leqslant \sqrt{1-|g^2-h^2|}\sqrt{1-t}+\sqrt{|g^2-h^2|}(1-t),\end{aligned} \tag{A.34}$$

and integrate to obtain

$$\begin{aligned}\Delta \leqslant 2N\sqrt{2(1+|g^2-h^2|)}|g^2-h^2|^{\frac{N}{2}}\Bigg(&|g^2-h^2|^{\frac{1}{2}}\frac{2}{\pi}\sum_{l=0}^{\infty}\frac{|g^2-h^2|^{lN}}{(2l+1)^2N^2-1/4}\\ &+\frac{\sqrt{1-|g^2-h^2|}}{\sqrt{\pi}}\sum_{l=0}^{\infty}\frac{\Gamma((2l+1)N-1/2)}{\Gamma((2l+1)N+1)}|g^2-h^2|^{lN}\Bigg),\end{aligned} \tag{A.35}$$

where $\Gamma(z)$ is the Gamma function.

Finally, we use [94]

$$\frac{1}{l^2-1/4}<\frac{1}{l^2}\frac{2N}{2N-1},\qquad \frac{\Gamma(l-1/2)}{\Gamma(l+1)}<\frac{1}{l^{\frac{3}{2}}}\sqrt{\frac{N}{N-1}}, \tag{A.36}$$

and perform the sums replacing $|g^2-h^2|^{lN}$ by 1.

Further using $(2\sqrt{2}-1)\zeta(3/2)/2\sqrt{2\pi}<1$, the final result is

$$\Delta\leqslant|g^2-h^2|^{\frac{N}{2}}\sqrt{2(1+|g^2-h^2|)}\left(\frac{\pi|g^2-h^2|^{\frac{1}{2}}}{2N-1}+2\frac{\sqrt{1-|g^2-h^2|}}{\sqrt{N-1}}\right). \tag{A.37}$$

Appendix B

Elements of Quantum Information

In this Appendix I review some of the concepts of quantum mechanics and quantum information theory applicable to this thesis.

A finite isolated driven system, described by a time-dependent Hamiltonian $H(t)$, with initial density operator $\rho(0)$, evolves according to

$$\rho(0) \to \rho(t) = U(t,0)\rho(0)U^{\dagger}(t,0), \tag{B.1}$$

where $U^{\dagger}(t,0) = U^{-1}(t,0)$ is the unitary time-evolution operator satisfying

$$U(t,0)U^{\dagger}(t,0) = U^{\dagger}(t,0)U(t,0) = \mathbb{1}, \tag{B.2}$$

$$U(t,0) = U(t,t')U(t',0). \tag{B.3}$$

Moreover, U obeys the Schrödinger equation

$$\frac{\partial}{dt}U(t,0) = -iH(t)U(t,0), \quad U(0,0) = \mathbb{1}, \tag{B.4}$$

where I made $\hbar = 1$ and $\mathbb{1}$ is the identity operator.

The formal solution to equation (B.4) is given by

$$\begin{aligned} U(t,0) &= \mathcal{T}\exp\left\{-i\int_0^t H(t')\,\mathrm{d}t'\right\} \\ &= \mathbb{1} + \sum_{n=1}^{\infty}\frac{(-i)^n}{n!}\int_0^t \mathrm{d}t_1\int_0^t \mathrm{d}t_2 ... \int_0^t \mathrm{d}t_n \mathcal{T}H(t_1)H(t_2)...H(t_n), \end{aligned} \tag{B.5}$$

where $\mathcal{T}$ establishes an increasing time-ordering from right to left. That is, $\mathcal{T}$ is such that

$$\mathcal{T}H(t_1)H(t_2) = \begin{cases} H(t_1)H(t_2) \text{ if } t_1 > t_2, \\ \pm H(t_2)H(t_1) \text{ if } t_1 < t_2, \end{cases} \tag{B.6}$$

where "$\pm$" depends on whether the operators $H(t)$ obey canonical commutation $(+)$ or anticommutation relations $(-)$.

Let $\mathcal{H}$ be the Hilbert space associated with the quantum system. For every state ρ representing the system we may compute its von Neumann entropy, given by

$$S(\rho) = -\operatorname{tr}\{\rho \ln \rho\}. \tag{B.7}$$

This is an always nonnegative quantity,

$$S(\rho) \geqslant 0,$$

that vanishes only for pure states. In addition, if $\mathcal{H}$ has dimension d, it's maximal value equals $\ln d$ and occurs for the maximally mixed state $\mathbb{1}/d$. Hence, the von Neumman entropy may be interpreted as measuring the mixedness of the state ρ.

Other notable properties of the von Neumann entropy are its invariance under unitary operations and subadditivity,

$$S(U\rho U^\dagger) = S(\rho), \tag{B.8}$$

$$S(\rho_{12}) \leqslant S(\rho_1) + S(\rho_2), \tag{B.9}$$

where U is a unitary, ρ_{12} is the state of a bipartite system with Hilbert space $\mathcal{H} = \mathcal{H}_1 \otimes$

$\mathcal{H}_2$, and $\rho_1 = \mathrm{tr}_2\{\rho_{12}\}$ and $\rho_2 = \mathrm{tr}_1\{\rho_{12}\}$ are the reduced states of systems 1 and 2, respectively.

In this thesis the von Neumann entropy is considered to be an appropriate thermodynamic entropy. Equation (B.8), therefore, may be seen as equivalent to the thermodynamic requirement that entropy remains constant for a reversible (unitary) transformation.

In (B.9), equality holds if only if $\rho_{12} = \rho_1 \otimes \rho_2$. The general increase in entropy in its right-hand side may be interpreted as a consequence of the loss of information when correlations between the two systems are discarded. This constitutes an important ingredient in the definition of entropy production in this thesis. Particularly, the mismatch between both sides of (B.9) defines the *quantum mutual information*,

$$I(\rho_{12}) = S(\rho_1) + S(\rho_2) - S(\rho_{12}) \geqslant 0. \tag{B.10}$$

The mutual information is a measure of the total amount of correlations shared by the systems 1 and 2 in the state ρ_{12}.

A related quantity is the quantum relative entropy. For two states ρ and σ it reads

$$S(\rho||\sigma) = \mathrm{tr}\{\rho(\ln\rho - \ln\sigma)\}. \tag{B.11}$$

This is also a nonnegative quantitiy [155],

$$S(\rho||\sigma) \geqslant 0, \tag{B.12}$$

with equality if and only $\rho = \sigma$. Hence, the relative entropy is regarded as a measure of the distinguishability between two quantum states. In terms of it, the quantum mutual information may be written as

$$I(\rho_{12}) = S(\rho_{12}||\rho_1 \otimes \rho_2), \tag{B.13}$$

making the previous interpretation of the mutual information clear.

In contrast with the von Neumann entropy, however, the quantum relative entropy is not bounded from above. In particular, when the support of ρ intersects the kernel of σ,

$S(\rho||\sigma)$ diverges:

$$S(\rho||\sigma) = +\infty, \quad \text{if } \mathrm{supp}(\rho) \cap \ker(\sigma) \neq 0. \tag{B.14}$$

Another significant property of the quantum relative entropy is its monotonicity under any completely positive and trace preserving (CPTP) map. If $\mathcal{E}$ is CPTP, then [155]

$$S(\mathcal{E}(\rho)||\mathcal{E}(\sigma)) \leqslant S(\rho||\sigma). \tag{B.15}$$

The relative entropy can be generalized by the Rényi divergences

$$S_\alpha(\rho||\sigma) = \frac{1}{\alpha - 1} \ln \mathrm{tr}\{\rho^\alpha \sigma^{1-\alpha}\}, \tag{B.16}$$

for $\alpha \in (0,1) \cup (1,\infty)$. The special cases $\alpha = 0,\ 1,\ \infty$ are obtained by appropriate limits. Noticeably,

$$\lim_{\alpha \to 1} S_\alpha(\rho||\sigma) = S(\rho||\sigma). \tag{B.17}$$

The Rényi entropies are also nonnegative,

$$S_\alpha(\rho||\sigma) \geqslant 0$$

with equality if and only $\rho = \sigma$.

In several parts of the main text, I refer to some resource theories and monotones within them.

A resource is some physical feature or property of a quantum system that can be consumed to perform a specific task. A resource theory is thus defined by a set of free states and a set of free operations. The former is composed by those states which do not contain the resource, and the latter by operations, i.e. quantum maps, which cannot create it.

There are several examples of resource theories. Perhaps, the most famous one is the resource theory of entanglement. In this case, entanglement is the resource, obviously; the set of free states is composed by all separable states — those which are not entangled; and the free operations are Local Operations and Classical Communications (LOCC) — these operations can only decrease the entanglement of a system.

Reference [1] formalized a resource theory of coherences — see also [2] for a review.

Since coherence is a basis depend property, the first step is to introduce a reference orthonormal basis of the system Hilbert space. Let us denote this reference basis by the set $\{|i\rangle\}$. The free states in this resource theory are all states which are incoherent (diagonal) in the reference basis. If $I_{|i\rangle}$ is the set of free states, $\rho \in \mathcal{I}_{|i\rangle}$, means

$$\rho = \sum_i p_i |i\rangle\langle i|. \tag{B.18}$$

The free operations in this case, called *incoherent operations*, are composed by quantum maps with Kraus decomposition $\mathcal{E}_{\text{IO}}(.) = \sum_m K_m(.)K_m^\dagger$, such that for any m and any incoherent state $\rho_f \in \mathcal{I}_{|i\rangle}$,

$$\frac{K_m \rho_f K_m^\dagger}{\text{tr}\left\{K_m \rho_f K_m^\dagger\right\}} \in \mathcal{I}_{|i\rangle}. \tag{B.19}$$

In this approach, coherence is defined as a resource under the set of incoherent operations $\mathcal{E}_{\text{IO}}$.

Given a resource theory, a *monotone* is any function satisfying

1. $f(\rho_f) = 0$ for any free state ρ_f.
2. $f(\mathcal{E}_{\text{free}}(\rho)) \leqslant f(\rho)$, for any free operation $\mathcal{E}_{\text{free}}$.

That is, a monotone is a nonnegative function from states to real numbers that vanishes for free states and is nonincreasing under the set of free operations.

As showed in [1], the *relative entropy of coherence*

$$C(\rho) = \min_{\sigma \in \mathcal{I}_{|i\rangle}} S(\rho||\sigma) = S(\rho||\mathbb{D}_{|i\rangle}(\rho)) = S(\mathbb{D}_{|i\rangle}(\rho)) - S(\rho), \tag{B.20}$$

where

$$\mathbb{D}_{|i\rangle}(\rho) = \sum_i |i\rangle\langle i|\rho|i\rangle\langle i|, \tag{B.21}$$

is a monotone in the resource theory of coherences defined by incoherent operations. Its monotonicity follows directly from (B.15).

An alternative to the aforementioned resource theory is the resource theory of coherence as asymmetry with respect to a translation group [151, 159].

In this case, given a fixed operator, which I will assume is a time-independent Hamiltonian H, the free states are all those states which are translationally invariant,

$$e^{-itH}\rho_f e^{itH} = \rho_f, \quad \forall t \in \mathbb{R}. \tag{B.22}$$

In fact, this is equivalent to the set of states that commute with the Hamiltonian. Consequently, the resourceful states are those containing energy coherences. Denoting by $\mathcal{I}_H$ the set of incoherent states, the three conditions are equivalent:

$$\rho \in \mathcal{I}_H \iff [\rho, H] = 0 \iff e^{-itH}\rho e^{itH} = \rho. \tag{B.23}$$

Similarly, the set of free operations is composed of the quantum maps that are translationally invariant (TIO); i.e., those for which

$$e^{-itH}\mathcal{E}_{\text{TIO}}(\rho)e^{itH} = \mathcal{E}_{\text{TIO}}(e^{-itH}\rho e^{itH}), \quad \forall t \in \mathbb{R}, \tag{B.24}$$

for any state ρ.

Such maps are implemented by applying a globally energy preserving unitary acting jointly on the system of interest and an environment prepared in an incoherent state [159].

One monotone of this resource theory is the Wigner-Yanase-Dyson skew information [151, 159]:

$$I^y(\rho, H) = -\frac{1}{2}\operatorname{tr}\big\{[\rho^y, H][\rho^{1-y}, H]\big\}. \tag{B.25}$$

This satisfies $I^y(\rho, H) \geqslant 0$, with equality if and only if $\rho \in \mathcal{I}_H$ [157, 158].

Moreover, since translationally invariant operations are a subset of incoherent operations [2, 159], the relative entropy of coherence is also a monotone in the resource theory of asymmetry [2, 159].

One also have resource theories of thermodynamics. In this case, the resources are anything that can be converted into work.

The resource theory of thermodynamics is commonly defined in terms of thermal operations [120, 121], and is closely related to the resource theory of asymmetry.

As in TIOs, thermal operations (TOs) are implemented by energy conserving unitaries acting on the system and an environment. The difference is that the initial incoherent state of the environment is required to be a thermal state. Thus, a TO can be written as

$$\mathcal{E}_{\text{th}}(\rho_S) = \text{tr}_E\{U_{SE}(\rho_S \otimes \rho_E^{\text{th}})U_{SE}^\dagger\}, \quad [U_{SE}, H_S + H_E] = 0, \tag{B.26}$$

where $H_{S/E}$ is the Hamiltonian of the system/environment and $\rho_E^{\text{th}} = e^{-\beta H_E}/\,\text{tr}\{e^{-\beta H_E}\}$ is a thermal state of the environment at inverse temperature $\beta = 1/T$.

Thermal operations satisfy [9, 10]:

$$e^{-itH_S}\mathcal{E}_{\text{th}}(\rho_S)e^{itH_S} = \mathcal{E}_{\text{th}}(e^{-itH_S}\rho_S e^{itH_S}), \tag{B.27}$$

$$\mathcal{E}_{\text{th}}(\rho_S^{\text{th}}) = \rho_S^{\text{th}} \tag{B.28}$$

where $\rho_S^{\text{th}} = e^{-\beta H_S}/\,\text{tr}\{e^{-\beta H_S}\}$.

The first equation means TOs are translationally invariant with respect to the system Hamiltonian H_S. The second, that the thermal state ρ_S^{th} is the free state of the resource theory — this means no work can be extracted from it, and that we cannot drive the system out of equilibrium without performing work.

Therefore, thermal operations constitute a subset of translationally invariant operations. As a consequence, both the Wigner-Yanase-Dyson skew information and the relative entropy of coherence are monotones in the resource theory of thermodynamics [9].

Two other important monotones in this case are

$$S(\mathcal{E}_{\text{th}}(\rho_S)||\rho_S^{\text{th}}) \leqslant S(\rho_S||\rho_S^{\text{th}}), \tag{B.29}$$

which is used to define entropy production, and

$$S(\mathcal{E}_{\text{th}}(\rho_S)||\mathbb{D}_H(\mathcal{E}_{\text{th}}(\rho_S))) \leqslant S(\rho_S||\mathbb{D}_H(\rho_S)), \tag{B.30}$$

where

$$\mathbb{D}_H(\rho) = \sum_i \Pi_i \rho \Pi_i, \tag{B.31}$$

with Π_i the eigenprojectors of H and $\mathbb{D}_H$ the dephasing map on the energy subspaces. Equation (B.30) is used to define the resource of athermality [121]. Note that $\mathbb{D}_H$ and $\mathcal{E}_{\text{th}}$ commute [9]. Equation (B.31) is a generalization of (B.21) for the cases where the spectrum of H is degenerate.

Appendix C

Time-Reversed Dynamics

Although its name suggests the change $t \to -t$, what the time-reversal operation really reverses is the "motion" of the system. Meaning, it reverses linear and angular momenta, as well as magnetic fields.

In quantum theory, the time-reversal operator Θ is the operator satisfying [130]

$$\begin{aligned} \Theta \mathbf{Q} \Theta^{-1} &= \mathbf{Q}, \qquad \Theta \mathbf{P} \Theta^{-1} = -\mathbf{P}, \\ \Theta \mathbf{J} \Theta^{-1} &= -\mathbf{J}, \qquad \Theta \mathbf{B} \Theta^{-1} = -\mathbf{B}, \end{aligned} \tag{C.1}$$

where $\mathbf{Q}$, $\mathbf{P}$ and $\mathbf{J}$ are, respectively, the position, linear and angular momentum operators; while $\mathbf{B}$ stands for a magnetic field. Therefore, Θ must be an antiunitary operator, meaning it fulfills

$$\Theta c = c^* \Theta, \text{ for any complex number c,} \tag{C.2}$$

$$\langle \Theta\psi | \Theta\phi \rangle = \langle \psi | \phi \rangle^*, \text{ for any two vectors } |\psi\rangle, |\phi\rangle \in \mathcal{H}, \tag{C.3}$$

$$\exists \Theta^{-1} \mid \Theta^{-1}\Theta = \mathbb{1}, \tag{C.4}$$

where "$*$" denotes complex conjugation and $\mathcal{H}$ is the system Hilbert space. Condition (C.2) states the antilinearity of Θ, while (C.3) and (C.4) show that the operation preserves probability and norm and is invertible.

Let us consider now a Hamiltonian $H(g(t); \mathbf{B})$, where g is a parameter that changes in time. We assume this Hamiltonian is invariant under time-reversal operation with the

change $\mathbf{B} \to -\mathbf{B}$,

$$\Theta H(g(t);\mathbf{B})\Theta^{-1} = H(g(t);-\mathbf{B}). \tag{C.5}$$

As in Chapter 3, let us consider that in the forward process the work parameter g changes during the time $0 \leqslant t \leqslant \tau$ according to a function g_t. We denote by $U_g(t,0;\mathbf{B})$ the unitary time-evolution operator generated by the protocol g_t. Conversely, in the backward process, g changes according to $\tilde{g}_t = g_{\tau-t}$. That is, the temporal sequence of values of g is reversed. We denote by $U_{\tilde{g}}(t,0;\mathbf{B})$ the backward time-evolution operator.

For a system with time-reversal symmetry (C.5), we may expect the following: Suppose we start in a state ρ_i and drive it in accordance with the protocol g_t up to some time t_f. At this point, we perform a time-reversal operation and subsequently apply $\tilde{g}_t$ for the same amount of time. In the end we time-reverse the system again. This should result in the same state ρ_i. Put differently, if a system is initially in a state ρ_i and evolves according to the unitary $U_g(t_f,0)$ to the state $\rho_f = U_g(t_f,0;\mathbf{B})\rho_i U_g^\dagger(t_f,0;\mathbf{B})$; then the time-reversed state $\Theta\rho_f\Theta^{-1}$ should evolve under the action of $U_{\tilde{g}}(t_f,0)$ to the state $\Theta\rho_i\Theta^{-1} = U_{\tilde{g}}(t_f,0;-\mathbf{B})\Theta\rho_f\Theta^{-1}U_{\tilde{g}}^\dagger(t_f,0;-\mathbf{B})$. A simple exercise gives

$$U_{\tilde{g}}(t,0;-\mathbf{B}) = \Theta U_g^\dagger(t,0;\mathbf{B})\Theta^{-1}. \tag{C.6}$$

The proof of Eq. (C.6) goes as follows [169]. The unitary U_g obeys the Schrödinger equation

$$\frac{\partial}{\partial t}U_g(t,0;\mathbf{B}) = -iH(g_t;\mathbf{B})U_g(t,0;\mathbf{B}), \quad U_g(0,0;\mathbf{B}) = \mathbb{1}, \tag{C.7}$$

while for $U_{\tilde{g}}$,

$$\frac{\partial}{\partial t}U_{\tilde{g}}(t,0;\mathbf{B}) = -iH(\tilde{g}_t;\mathbf{B})U_{\tilde{g}}(t,0;\mathbf{B}), \qquad U_{\tilde{g}}(0,0;\mathbf{B}) = \mathbb{1}. \tag{C.8}$$

Making the change of variable $t \to \tau - t$ in (C.7), we get

$$\frac{\partial}{\partial t}U_g(\tau-t,0;\mathbf{B}) = iH(g_{\tau-t};\mathbf{B})U_g(\tau-t,0;\mathbf{B}). \tag{C.9}$$

Applying Θ to the left, multiplying by $U_g^\dagger(\tau,0;\mathbf{B})\Theta^{-1}$ to the right and using that $g_{\tau-t} =$

$\tilde{g}_t$, this becomes

$$\frac{\partial}{\partial t}\Theta U_g(\tau - t, 0; \mathbf{B})U_g^\dagger(\tau, 0; \mathbf{B})\Theta^{-1} = -i\Theta H(\tilde{g}_t; \mathbf{B})U_g(\tau - t, 0; \mathbf{B})U_g^\dagger(\tau, 0; \mathbf{B})\Theta^{-1}. \tag{C.10}$$

Now, one should note that $U_g(\tau - t, 0; \mathbf{B})U_g^\dagger(\tau, 0; \mathbf{B}) = U_g^\dagger(t, 0; \mathbf{B})$ and $\Theta U_g^\dagger(0, 0; \mathbf{B})\Theta^{-1} = \mathbb{1}$. Finally, using that the Hamiltonian is time-reversal invariant, i.e., satisfies (C.5), we see that $\Theta U_g^\dagger(t, 0; \mathbf{B})\Theta^{-1}$ obeys the same linear differential equation with the same initial condition as $U_{\tilde{g}}(t, 0; -\mathbf{B})$. In other words,

$$\frac{\partial}{\partial t}\Theta U_g^\dagger(t, 0; \mathbf{B})\Theta^{-1} = -iH(\tilde{g}_t; -\mathbf{B})\Theta U_g^\dagger(t, 0; \mathbf{B})\Theta^{-1}, \qquad \Theta U_g^\dagger(0, 0; \mathbf{B})\Theta^{-1} = \mathbb{1}. \tag{C.11}$$

Hence, we must have $U_{\tilde{g}}(t, 0; -\mathbf{B}) = \Theta U_g^\dagger(t, 0; \mathbf{B})\Theta^{-1}$ for $0 \leqslant t \leqslant \tau$.

Appendix D

Full vs. Positive Parity Thermodynamics

In this Appendix I compare the entropy production after an instantaneous quench using the positive parity and the full Ising Hamiltonians.

For simplicity, lets us take $h = 0$ in (2.11), and work with the usual homogeneous transverse field Ising model. Moreover, we set $J = 1$.

In this case, the homogeneous transverse field Ising Hamiltoian,

$$H_{\rm I} = -\sum_{j=1}^{N} \left(\sigma_j^x \sigma_{j+1}^x + g\sigma_j^z\right), \tag{D.1}$$

may be written as [94]

$$H_{\rm I} = P^+ H_{\rm I}^+ P^+ + P^- H_{\rm I}^- P^-, \tag{D.2}$$

where $P^\pm$ are the projectors onto the positive and negative subspaces of the parity operator,

$$P^\pm = \frac{1}{2}(1 \pm P), \quad P = \prod_{j=1}^{N} \sigma_j^z. \tag{D.3}$$

As shown in Sec 4.1 for the positive parity Hamiltonian, but with completely similar results for the negative parity part, we may write them in diagonal form as

$$H_{\rm I}^\pm = \sum_{k \in K_{\rm I}^\pm} \epsilon_k (2\eta_k^\dagger \eta_k - 1). \tag{D.4}$$

Here, $\{\eta_k\}$ are fermionic operators,

$$K_{\rm I}^{+} = \Big\{k = \pm(2n+1)\frac{\pi}{N};\; n = 0, 1, ..., N/2-1\Big\}, \tag{D.5}$$

$$K_{\rm I}^{-} = \Big\{k = 0,\; k = \pm 2n\frac{\pi}{N},\; k = \pi;\; n = 1, ..., N/2-1\Big\}, \tag{D.6}$$

where I assumed N is an even number, and

$$\epsilon_k = \sqrt{(g-\cos k)^2 + \sin^2 k}, \tag{D.7}$$

$$\epsilon_{k=0} = g - 1, \tag{D.8}$$

$$\epsilon_{k=\pi} = g + 1, \tag{D.9}$$

are the dispersion relations.

Moreover, the following commutation relations hold

$$[H_{\rm I}, P] = [H_{\rm I}^{\pm}, P^{\pm}] = 0. \tag{D.10}$$

In Chapter 2 I argued the transformation that diagonalizes $H_{\rm I}^{\pm}$ does not preserve particle number, but it, nonetheless, preserves parity. So, let us assume we can write

$$P^{\pm} = \frac{1}{2} \pm \frac{1}{2}\exp\left(i\pi \sum_{k\in K_{\rm I}^{\pm}} \eta_k^{\dagger}\eta_k\right) \tag{D.11}$$

Let us compute the partition function,

$$\begin{aligned} Z_F &= \mathrm{tr}\Big\{e^{-\beta H}\Big\} = \mathrm{tr}\Big\{P^{+}e^{-\beta H^{+}} + P^{-}e^{-\beta H^{-}}\Big\} \\ &= \frac{1}{2}\Bigg(\mathrm{tr}\Big\{e^{-\beta H^{+}}\Big\} + \mathrm{tr}\left\{\exp\left(i\pi \sum_{k\in K_{\rm I}^{+}} \eta_k^{\dagger}\eta_k\right)e^{-\beta H^{+}}\right\} \\ &\qquad + \mathrm{tr}\Big\{e^{-\beta H^{-}}\Big\} - \mathrm{tr}\left\{\exp\left(i\pi \sum_{k\in K_{\rm I}^{-}} \eta_k^{\dagger}\eta_k\right)e^{-\beta H^{-}}\right\}\Bigg). \end{aligned} \tag{D.12}$$

We can evaluate each term individually,

$$Z_{c+} = \mathrm{tr}\Big\{e^{-\beta H^+}\Big\} = \prod_{k\in K_{\mathrm{I}}^+} \mathrm{tr}\Big\{e^{-\beta\epsilon_k(2\eta_k^\dagger\eta_k - 1)}\Big\} = \prod_{k\in K_{\mathrm{I}}^+} 2\cosh(\beta\epsilon_k), \tag{D.13}$$

$$Z_{s+} = \mathrm{tr}\left\{\exp\left(i\pi\sum_{k\in K_{\mathrm{I}}^+}\eta_k^\dagger\eta_k\right)e^{-\beta H^+}\right\} = \prod_{k\in K_{\mathrm{I}}^+}\mathrm{tr}\Big\{e^{(i\pi-2\beta\epsilon_k)\eta_k^\dagger\eta_k+\beta\epsilon_k}\Big\} \tag{D.14}$$

$$= \prod_{k\in K_{\mathrm{I}}^+} 2\sinh(\beta\epsilon_k),$$

$$Z_{c-} = \mathrm{tr}\Big\{e^{-\beta H^-}\Big\} = \prod_{k\in K_{\mathrm{I}}^-} \mathrm{tr}\Big\{e^{-\beta\epsilon_k(2\eta_k^\dagger\eta_k - 1)}\Big\} = \prod_{k\in K_{\mathrm{I}}^-} 2\cosh(\beta\epsilon_k), \tag{D.15}$$

$$Z_{s-} = \mathrm{tr}\left\{\exp\left(i\pi\sum_{k\in K_{\mathrm{I}}^-}\eta_k^\dagger\eta_k\right)e^{-\beta H^-}\right\} = \prod_{k\in K_{\mathrm{I}}^-}\mathrm{tr}\Big\{e^{(i\pi-2\beta\epsilon_k)\eta_k^\dagger\eta_k+\beta\epsilon_k}\Big\} \tag{D.16}$$

$$= \prod_{k\in K_{\mathrm{I}}^-} 2\sinh(\beta\epsilon_k),$$

The total partition function is, thus, given by

$$Z_F = \frac{1}{2}\big(Z_{c+} + Z_{s+} + Z_{c-} - Z_{s-}\big). \tag{D.17}$$

This result was also obtained in [55] following a similar reasoning and in [147] using a different method.

We may also compute the internal energy

$$E = \mathrm{tr}\left\{H\frac{e^{-\beta H}}{Z_F}\right\} = \mathrm{tr}\left\{\frac{1}{Z_F}\Big(P^+H^+e^{-\beta H^+} + P^-H^-e^{-\beta H^-}\Big)\right\}. \tag{D.18}$$

Following the same steps employed in the calculation of the partition function we

obtain,

$$E = -\frac{1}{2Z_F}\Bigg(Z_{c+}\sum_{k\in K^+}\epsilon_k\tanh(\beta\epsilon_k) + Z_{s+}\sum_{k\in K^+}\epsilon_k\coth(\beta\epsilon_k) \\ +Z_{c-}\sum_{k\in K^-}\epsilon_k\tanh(\beta\epsilon_k) - Z_{s-}\sum_{k\in K^-}\epsilon_k\coth(\beta\epsilon_k)\Bigg). \tag{D.19}$$

Similarly, in an infinitesimally and instantaneously quenched system, the work done is given by

$$W_F = \mathrm{tr}\{\Delta H\rho^{\mathrm{th}}\} = \mathrm{tr}\{\Delta H^{\mathrm{d}}\rho^{\mathrm{th}}\} \tag{D.20}$$

$$= -\frac{\delta g}{2Z_F}\Bigg(Z_{c+}\sum_{k\in K^+}\partial_g\epsilon_k\tanh(\beta\epsilon_k) + Z_{s+}\sum_{k\in K^+}\partial_g\epsilon_k\coth(\beta\epsilon_k) \tag{D.21}$$

$$+Z_{c-}\sum_{k\in K^-}\partial_g\epsilon_k\tanh(\beta\epsilon_k) - Z_{s-}\sum_{k\in K^-}\partial_g\epsilon_k\coth(\beta\epsilon_k)\Bigg), \tag{D.22}$$

where I used that the dephased part of the perturbation ΔH^{d} is given by

$$\Delta H^{\mathrm{d}} = P^+\sum_{k\in K^+}\delta g(\partial_g\epsilon_k)(2\eta_k^\dagger\eta_k - 1) + P^-\sum_{k\in K^-}\delta g(\partial_g\epsilon_k)(2\eta_k^\dagger\eta_k - 1). \tag{D.23}$$

Finally, the full Hamiltonian entropy production is given by

$$\Sigma_F = \beta(W_F - \Delta F) = \ln\frac{Z_{F|\tau}}{Z_{F|0}} + \beta W_F, \tag{D.24}$$

where $Z_{F|0/\tau}$ is the full partition function associated with the field value g_0/g_τ.

Let us compare now the full partition function (D.17) with the positive parity partition function Z_{c+}. The comparison is shown in Fig. D.1(a) and (b) for chains of a hundred and a thousand spins, respectively. At high temperatures and/or the paramagnetic region, $g > 1$, the approximation $Z_F \approx Z_{c+}$ is precise. However, at low temperatures and in the ferromagnetic region, $g < 1$, Z_{c+} corresponds to only half of the total partition function Z_F. The area covered by the error slightly decreases with increasing number of spins [147]. As explained in [147], this deviation at low temperatures occurs because of

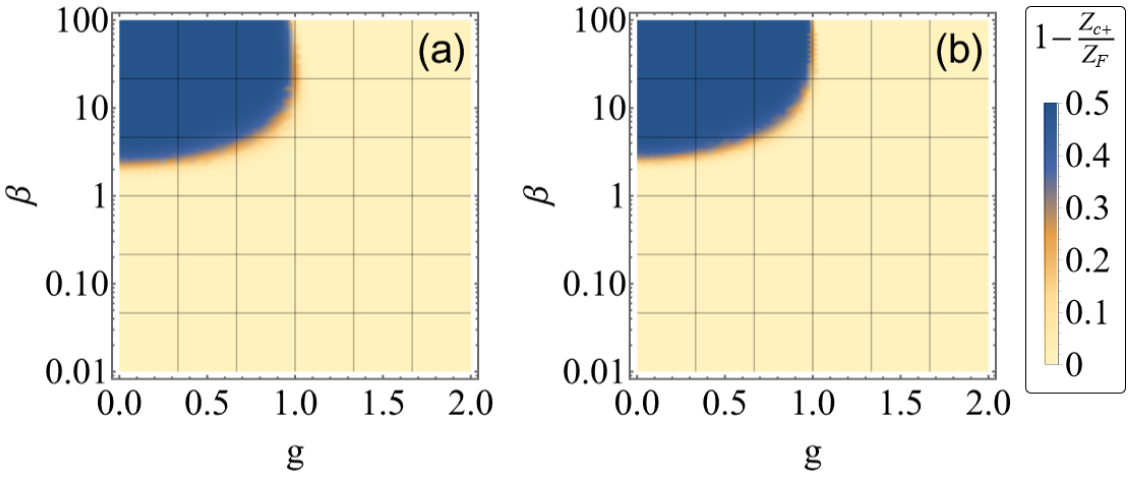

Figure D.1: Comparison between the partition functions of the full Ising Hamiltonian Z_F, and the positive parity Hamiltonian Z_{c+}. (a) For a chain of 100 spins. (b) For a chain of 1000 spins.

the exponentially vanishing energy gap between the positive and negative parity ground states (see Eq. (2.53)) in the ferromagnetic region.

We can make a similar comparison between the full entropy production (D.24) and the positive parity entropy production,

$$\Sigma_+ = \sum_{k\in K_{\rm I}^+} \left(\ln \frac{\cosh(\beta\epsilon_k^\tau)}{\cosh(\beta\epsilon_k^0)} - \beta(g_\tau - g_0)\cos\theta_k \tanh\big(\beta\epsilon_k^0\big) \right), \tag{D.25}$$

where $\epsilon_k^\alpha = \epsilon_k(g_\alpha)$ and $\partial_{g_0}\epsilon_k^0 = \cos\theta_k = (g_0 - \cos k)/\epsilon_k^0$.

The results are shown in Fig. D.2. Contrary to what happens for the partition function, the approximation $\Sigma_F \approx \Sigma_+$ is extremely suitable for almost all points in the $\beta - g$ plane, even for a fairly small chain of 50 spins — Fig. D.2(a). There is only a small deviation of around 10% in the vicinity of the critical field. As expected, when N increases, the region of discrepancy decreases — Fig. D.2(b) for a 100 spins and (c) for 200 spins.

In Fig. D.3 I further compare the shape of the curves of the full and positive parity entropy production as a function of the initial field g_0. The plots are for an inverse temperature $\beta = 100$, quench amplitude $\delta g = 0.01$ and chain sizes of (a) 100, (b) 1000 and (c) 10000 spins. The curves are quiet close to each other with a small discrepancy in the vicinity of the critical field $g_0 = 1$. Again, the difference decreases as the size of the chain increases.

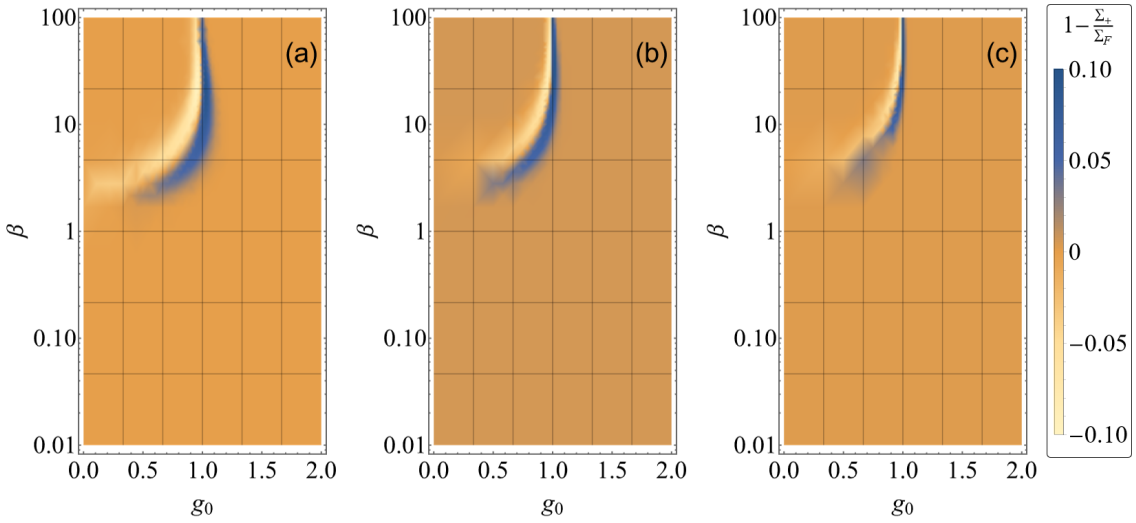

Figure D.2: Comparison between the entropy production of the full Ising Hamiltonian Σ_F, and the positive parity Hamiltonian Σ_{c+} for chains of (a) 50 (b) 100 and (c) 200 spins. In all points, the quench amplitude is $\delta g = 0.01$.

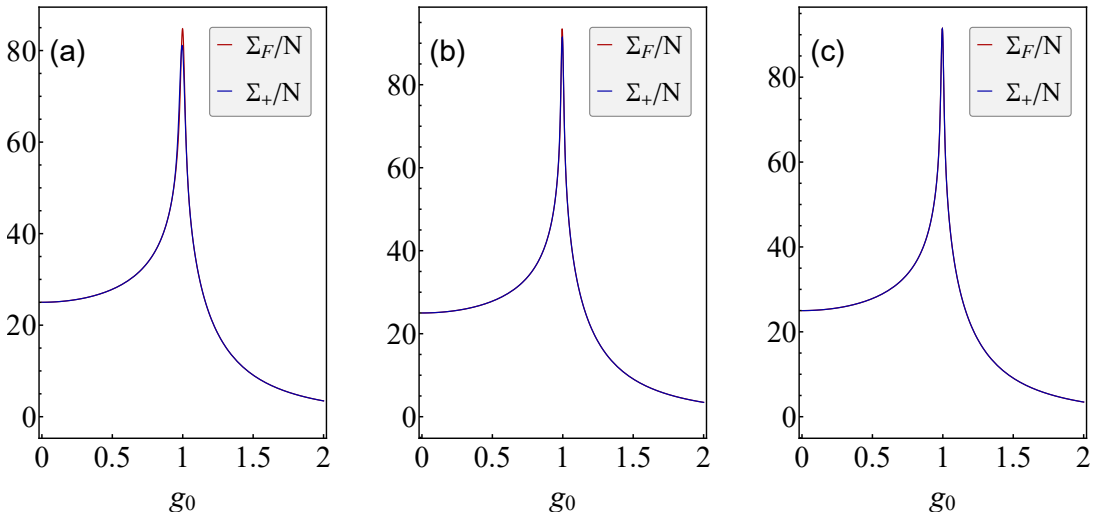

Figure D.3: Comparison between the entropy production per spin of the full Ising Hamiltonian Σ_F/N, and the positive parity Hamiltonian Σ_{c+}/N as a function of the initial field g_0 for chains of (a) 100 (b) 1000 and (c) 1000 spins. Other parameters values are $\beta = 100$ and quench amplitude $\delta g = 0.01$. The curves are also scaled by δg^2.

Bibliography

1. Baumgratz, T., Cramer, M. & Plenio, M. B. Quantifying coherence. *Physical Review Letters* **113,** 140401. ISSN: 10797114. arXiv: 1311.0275 (2014).
2. Streltsov, A., Adesso, G. & Plenio, M. B. Colloquium : Quantum coherence as a resource. *Reviews of Modern Physics* **89.** ISSN: 1539-0756. http://dx.doi.org/10.1103/RevModPhys.89.041003 (Oct. 2017).
3. Perarnau-Llobet, M., Bäumer, E., Hovhannisyan, K. V., Huber, M. & Acin, A. No-Go Theorem for the Characterization of Work Fluctuations in Coherent Quantum Systems. *Physical Review Letters* **118,** 070601. ISSN: 10797114. arXiv: 1606.08368 (2017).
4. Micadei, K., Landi, G. T. & Lutz, E. Quantum Fluctuation Theorems beyond Two-Point Measurements. *Phys. Rev. Lett.* **124,** 090602. https://link.aps.org/doi/10.1103/PhysRevLett.124.090602 (9 Mar. 2020).
5. Micadei, K., Landi, G. T. & Lutz, E. *Extracting Bayesian networks from multiple copies of a quantum system* 2021. arXiv: 2103.14570 [quant-ph].
6. Levy, A. & Lostaglio, M. Quasiprobability Distribution for Heat Fluctuations in the Quantum Regime. *PRX Quantum* **1,** 010309. https://link.aps.org/doi/10.1103/PRXQuantum.1.010309 (1 Sept. 2020).
7. Allahverdyan, A. E. Nonequilibrium quantum fluctuations of work. *Physical Review E* **90.** https://doi.org/10.1103/physreve.90.032137 (Sept. 2014).
8. Janzing, D. Quantum thermodynamics with missing reference frames: Decompositions of free energy into non-increasing components. *Journal of statistical physics* **125,** 761–776. https://doi.org/10.1007/s10955-006-9220-x (2006).
9. Lostaglio, M., Jennings, D. & Rudolph, T. Description of quantum coherence in thermodynamic processes requires constraints beyond free energy. *Nature communications* **6,** 6383. ISSN: 2041-1723. arXiv: 1405.2188. http://www.nature.com/ncomms/2015/150310/ncomms7383/full/ncomms7383.html (2015).
10. Lostaglio, M., Korzekwa, K., Jennings, D. & Rudolph, T. Quantum coherence, time-translation symmetry, and thermodynamics. *Physical Review X* **5,** 1–11. ISSN: 21603308. arXiv: 1410.4572 (2015).

11. Cwiklinski, P., Studzinski, M., Horodecki, M. & Oppenheim, J. Limitations on the evolution of quantum coherences: Towards fully quantum second laws of thermodynamics. *Physical Review Letters* **115,** 210403. ISSN: 10797114. arXiv: 1405.5029 (2015).
12. Scandi, M., Miller, H. J. D., Anders, J. & Perarnau-Llobet, M. Quantum work statistics close to equilibrium. *Physical Review Research* **2,** 023377. ISSN: 2643-1564. arXiv: 1911.04306. http://arxiv.org/abs/1911.04306%20https://link.aps.org/doi/10.1103/PhysRevResearch.2.023377 (June 2020).
13. Miller, H. J. D., Scandi, M., Anders, J. & Perarnau-Llobet, M. Work fluctuations in slow processes: quantum signatures and optimal control. *Physical Review Letters* **123,** 230603. arXiv: 1905.07328. http://arxiv.org/abs/1905.07328 (2019).
14. Micadei, K. *et al.* Reversing the direction of heat flow using quantum correlations. *Nature Communications* **10,** 2456. arXiv: 1711.03323. http://arxiv.org/abs/1711.03323%20https://doi.org/10.1038/s41467-019-10333-7 (2019).
15. Lloyd, S. Use of mutual information to decrease entropy: Implications for the second law of thermodynamics. *Physical Review A* **39,** 5378–5386. ISSN: 10502947 (1989).
16. Jennings, D. & Rudolph, T. Entanglement and the thermodynamic arrow of time. *Physical Review E - Statistical, Nonlinear, and Soft Matter Physics* **81,** 061130. ISSN: 15393755. arXiv: 1002.0314 (2010).
17. Jevtic, S. *et al.* Exchange fluctuation theorem for correlated quantum systems. *Physical Review E* **92,** 042113. ISSN: 15502376. arXiv: 1204.3571 (2015).
18. Åberg, J. Catalytic coherence. *Physical Review Letters* **113,** 150402. ISSN: 10797114. arXiv: 1304.1060 (2014).
19. Allahverdyan, A. E., Balian, R. & Nieuwenhuizen, T. M. Maximal work extraction from finite quantum systems. *Europhysics Letters (EPL)* **67,** 565–571. https://doi.org/10.1209/epl/i2004-10101-2 (Aug. 2004).
20. Scully, M. O., Zubairy, M. S., Agarwal, G. S. & Walther, H. Extracting Work from a Single Heat Bath via Vanishing Quantum Coherence. *Science* **299,** 862–865 (2007).
21. Korzekwa, K., Lostaglio, M., Oppenheim, J. & Jennings, D. The extraction of work from quantum coherence. *New Journal of Physics* **18,** 023045 (2016).
22. Manzano, G., Plastina, F. & Zambrini, R. Optimal Work Extraction and Thermodynamics of Quantum Measurements and Correlations. *Physical Review Letters* **121,** 120602. ISSN: 0031-9007. arXiv: 1805.08184. http://arxiv.org/abs/1805.08184%20https://link.aps.org/doi/10.1103/PhysRevLett.121.120602 (Sept. 2018).

23. Lörch, N., Bruder, C., Brunner, N. & Hofer, P. P. Optimal work extraction from quantum states by photo-assisted Cooper pair tunneling. *Quantum Science and Technology* **3,** 035014. https://doi.org/10.1088/2058-9565/aacbf3 (June 2018).

24. Rodrigues, F. L. S., De Chiara, G., Paternostro, M. & Landi, G. T. Thermodynamics of weakly coherent collisional models. *Physical Review Letters* **123,** 140601. arXiv: 1906.08203. http://arxiv.org/abs/1906.08203%20https://journals.aps.org/prl/abstract/10.1103/PhysRevLett.123.140601 (2019).

25. Francica, G. *et al.* Quantum Coherence and Ergotropy. *Physical Review Letters* **125,** 180603. ISSN: 0031-9007. arXiv: 2006.05424. http://arxiv.org/abs/2006.05424%20https://link.aps.org/doi/10.1103/PhysRevLett.125.180603 (Oct. 2020).

26. Correa, L. A., Palao, J. P., Alonso, D. & Adesso, G. Quantum-enhanced absorption refrigerators. *Scientific reports* **4,** 3949. ISSN: 2045-2322. arXiv: arXiv:1308.4174v1. http://www.nature.com/srep/2014/140204/srep03949/full/srep03949.html (2014).

27. Rossnagel, J., Abah, O., Schmidt-Kaler, F., Singer, K. & Lutz, E. Nanoscale heat engine beyond the carnot limit. *Physical Review Letters* **112,** 030602. ISSN: 00319007. arXiv: 1308.5935 (2014).

28. Uzdin, R., Levy, A. & Kosloff, R. Equivalence of Quantum Heat Machines, and Quantum-Thermodynamic Signatures. *Physical Review X* **5,** 031044. ISSN: 2160-3308. http://link.aps.org/doi/10.1103/PhysRevX.5.031044 (2015).

29. Hammam, K., Hassouni, Y., Fazio, R. & Manzano, G. Optimizing autonomous thermal machines powered by energetic coherence. *arXiv preprint arXiv:2101.11572* (2021).

30. Campaioli, F. *et al.* Enhancing the Charging Power of Quantum Batteries. *Physical Review Letters* **118,** 150601. ISSN: 0031-9007. arXiv: 1612.04991. http://link.aps.org/doi/10.1103/PhysRevLett.118.150601 (2017).

31. Julià-Farré, S., Salamon, T., Riera, A., Bera, M. N. & Lewenstein, M. Bounds on the capacity and power of quantum batteries. *Phys. Rev. Research* **2,** 023113. https://link.aps.org/doi/10.1103/PhysRevResearch.2.023113 (2 May 2020).

32. Mascarenhas, E. *et al.* Work and quantum phase transitions: Quantum latency. *Physical Review E* **89,** 062103. ISSN: 1539-3755. arXiv: arXiv:1307.5544v2. https://link.aps.org/doi/10.1103/PhysRevE.89.062103 (June 2014).

33. Dorner, R., Goold, J., Cormick, C., Paternostro, M. & Vedral, V. Emergent Thermodynamics in a Quenched Quantum Many-Body System. *Physical Review Letters* **109,** 160601. ISSN: 0031-9007. http://link.aps.org/doi/10.1103/PhysRevLett.109.160601 (Oct. 2012).

34. Goold, J., Plastina, F., Gambassi, A. & Silva, A. in *Thermodynamics in the Quantum Regime: Fundamental Aspects and New Directions* (eds Binder, F., Correa, L. A., Gogolin, C., Anders, J. & Adesso, G.) 317–336 (Springer International Publishing, Cham, 2018). ISBN: 978-3-319-99046-0. https://doi.org/10.1007/978-3-319-99046-0_13.

35. Santos, J. P., Céleri, L. C., Landi, G. T. & Paternostro, M. The role of quantum coherence in non-equilibrium entropy production. *npj Quantum Information* **5,** 23. arXiv: 1707.08946. http://arxiv.org/abs/1707.08946 (2019).

36. Francica, G., Goold, J. & Plastina, F. The role of coherence in the non-equilibrium thermodynamics of quantum systems. *Physical Review E* **99,** 042105. arXiv: 1707.06950 (2019).

37. Varizi, A. D., Cipolla, M. A., Perarnau-Llobet, M., Drumond, R. C. & Landi, G. T. Contributions from populations and coherences in non-equilibrium entropy production. *New Journal of Physics* **23,** 063027. https://doi.org/10.1088/1367-2630/abfe20 (June 2021).

38. Varizi, A. D., Vieira, A. P., Cormick, C., Drumond, R. C. & Landi, G. T. Quantum coherence and criticality in irreversible work. *Phys. Rev. Research* **2,** 033279. https://link.aps.org/doi/10.1103/PhysRevResearch.2.033279 (3 Aug. 2020).

39. Varizi, A. D. & Drumond, R. C. Quantum Ising model in a period-2 modulated transverse field. *Physical Review E* **100.** ISSN: 2470-0053. http://dx.doi.org/10.1103/PhysRevE.100.022104 (Aug. 2019).

40. Varizi, A. D., Drumond, R. C. & Landi, G. T. *Quantum quench thermodynamics at high temperatures* 2021. arXiv: 2109.03714 [quant-ph].

41. Salinas, S. *Introdução à Física Estatística* Segunda, 472 (EDUSP, 2013).

42. Yang, C. N. & Lee, T. D. Statistical Theory of Equations of State and Phase Transitions. I. Theory of Condensation. *Phys. Rev.* **87,** 404–409. https://link.aps.org/doi/10.1103/PhysRev.87.404 (3 Aug. 1952).

43. Goldenfeld, N. *Lectures On Phase Transitions And The Renormalization Group* ISBN: 9780429962042. https://books.google.com.br/books?id=pF0PEAAAQBAJ (CRC Press, 2018).

44. Ma, S. *Modern Theory Of Critical Phenomena* ISBN: 9780429967436. https://books.google.com.br/books?id=t8TADwAAQBAJ (Taylor & Francis, 2018).

45. Bhattacharjee, S. M. *Critical Phenomena: An Introduction from a modern perspective* 2000. arXiv: cond-mat/0011011 [cond-mat.stat-mech].

46. Kramers, H. A. & Wannier, G. H. Statistics of the Two-Dimensional Ferromagnet. Part I. *Phys. Rev.* **60,** 252–262. https://link.aps.org/doi/10.1103/PhysRev.60.252 (3 Aug. 1941).

47. Onsager, L. Crystal Statistics. I. A Two-Dimensional Model with an order-disorder transition. *Physical Review* **737,** 117. http://link.aps.org/doi/10.1103/PhysRev.65.117 (1944).

48. Yang, C. The spontaneous magnetization of a two-dimensional Ising model. *Physical Review* **1244.** http://prola.aps.org/abstract/PR/v85/i5/p808%7B%5C_%7D1 (1952).

49. Sachdev, S. *Quantum phase transitions* (Cambridge University Press, 2011).

50. Kadanoff, L. P. Scaling laws for ising models near T_c. *Physics Physique Fizika* **2,** 263–272. https://link.aps.org/doi/10.1103/PhysicsPhysiqueFizika.2.263 (6 June 1966).

51. Vojta, T. *Annalen der Physik* **9,** 403–440. ISSN: 1521-3889. http://dx.doi.org/10.1002/1521-3889(200006)9:6%3C403::AID-ANDP403%3E3.0.CO;2-R (June 2000).

52. Vojta, M. Quantum phase transitions. *Reports on Progress in Physics* **66,** 2069–2110. https://doi.org/10.1088/0034-4885/66/12/r01 (Nov. 2003).

53. Sondhi, S. L., Girvin, S. M., Carini, J. P. & Shahar, D. Continuous quantum phase transitions. *Rev. Mod. Phys.* **69,** 315–333. https://link.aps.org/doi/10.1103/RevModPhys.69.315 (1 Jan. 1997).

54. De Gennes, P. G. Collective motions of hydrogen bonds. *Solid State Communications* **1,** 132–137. ISSN: 00381098 (1963).

55. Katsura, S. Statistical Mechanics of the Anisotropic Linear Heisenberg Model. *Phys. Rev.* **127,** 1508–1518. https://link.aps.org/doi/10.1103/PhysRev.127.1508 (5 Sept. 1962).

56. Pfeuty, P. The one-dimensioal ising model with a transverse field. *Annals of Physics* **57,** 79–90 (1970).

57. Heyl, M., Polkovnikov, A. & Kehrein, S. Dynamical quantum phase transitions in the transverse-field ising model. *Physical Review Letters* **110,** 135704. ISSN: 00319007. arXiv: 1206.2505 (2013).

58. Verstraete, F., García-Ripoll, J. J. & Cirac, J. I. Matrix Product Density Operators: Simulation of Finite-Temperature and Dissipative Systems. *Physical Review Letters* **93,** 207204. ISSN: 0031-9007. http://link.aps.org/doi/10.1103/PhysRevLett.93.207204 (Nov. 2004).

59. Orús, R. A practical introduction to tensor networks: Matrix product states and projected entangled pair states. *Annals of Physics* **349,** 117–158. ISSN: 1096035X. arXiv: 1306.2164. http://dx.doi.org/10.1016/j.aop.2014.06.013 (2014).

60. Haikka, P., Goold, J., McEndoo, S., Plastina, F. & Maniscalco, S. Non-Markovianity, Loschmidt echo, and criticality: A unified picture. *Phys. Rev. A* **85,** 060101. https://link.aps.org/doi/10.1103/PhysRevA.85.060101 (6 June 2012).

61. Fusco, L. *et al.* Assessing the Nonequilibrium Thermodynamics in a Quenched Quantum Many-Body System via Single Projective Measurements. *Physical Review X* **4,** 031029. ISSN: 2160-3308. https://link.aps.org/doi/10.1103/PhysRevX.4.031029 (Aug. 2014).

62. Fei, Z. & Quan, H. T. Group-theoretical approach to the calculation of quantum work distribution. *Physical Review Research* **1,** 033175. ISSN: 2643-1564. https://link.aps.org/doi/10.1103/PhysRevResearch.1.033175 (Dec. 2019).

63. Zanardi, P. & Paunkovi ć, N. Ground state overlap and quantum phase transitions. *Phys. Rev. E* **74,** 031123. https://link.aps.org/doi/10.1103/PhysRevE.74.031123 (3 Sept. 2006).

64. Zanardi, P., Quan, H. T., Wang, X. & Sun, C. P. Mixed-state fidelity and quantum criticality at finite temperature. *Phys. Rev. A* **75,** 032109. https://link.aps.org/doi/10.1103/PhysRevA.75.032109 (3 Mar. 2007).

65. GU, S.-J. Fidelity approach to quantum phase transitions. *International Journal of Modern Physics B* **24,** 4371–4458. ISSN: 1793-6578. http://dx.doi.org/10.1142/S0217979210056335 (Sept. 2010).

66. Quan, H. T., Song, Z., Liu, X. F., Zanardi, P. & Sun, C. P. Decay of Loschmidt Echo Enhanced by Quantum Criticality. *Phys. Rev. Lett.* **96,** 140604. https://link.aps.org/doi/10.1103/PhysRevLett.96.140604 (14 Apr. 2006).

67. Osterloh, A., Amico, L., Falci, G. & Fazio, R. Scaling of entanglement close to a quantum phase transition. *Nature* **416,** 608–610. ISSN: 1476-4687. https://doi.org/10.1038/416608a (Apr. 2002).

68. Osborne, T. J. & Nielsen, M. A. Entanglement in a simple quantum phase transition. *Phys. Rev. A* **66,** 032110. https://link.aps.org/doi/10.1103/PhysRevA.66.032110 (3 Sept. 2002).

69. Wu, L.-A., Sarandy, M. S. & Lidar, D. A. Quantum Phase Transitions and Bipartite Entanglement. *Phys. Rev. Lett.* **93,** 250404. https://link.aps.org/doi/10.1103/PhysRevLett.93.250404 (25 Dec. 2004).

70. Dillenschneider, R. Quantum discord and quantum phase transition in spin chains. *Phys. Rev. B* **78,** 224413. https://link.aps.org/doi/10.1103/PhysRevB.78.224413 (22 Dec. 2008).

71. Werlang, T., Ribeiro, G. A. P. & Rigolin, G. Spotlighting quantum critical points via quantum correlations at finite temperatures. *Phys. Rev. A* **83,** 062334. https://link.aps.org/doi/10.1103/PhysRevA.83.062334 (6 June 2011).

72. Karpat, G., Çakmak, B. & Fanchini, F. F. Quantum coherence and uncertainty in the anisotropic XY chain. *Phys. Rev. B* **90,** 104431. https://link.aps.org/doi/10.1103/PhysRevB.90.104431 (10 Sept. 2014).

73. Malvezzi, A. L. *et al.* Quantum correlations and coherence in spin-1 Heisenberg chains. *Phys. Rev. B* **93,** 184428. https://link.aps.org/doi/10.1103/PhysRevB.93.184428 (18 May 2016).

74. Chen, J.-J., Cui, J., Zhang, Y.-R. & Fan, H. Coherence susceptibility as a probe of quantum phase transitions. *Phys. Rev. A* **94,** 022112. https://link.aps.org/doi/10.1103/PhysRevA.94.022112 (2 Aug. 2016).

75. Coldea, R. *et al.* Quantum Criticality in an Ising Chain: Experimental Evidence for Emergent E8 Symmetry. *Science* **327,** 177–180. ISSN: 0036-8075. http://science.sciencemag.org/content/327/5962/177 (2010).

76. Simon, J. *et al.* Quantum simulation of antiferromagnetic spin chains in an optical lattice. *Nature* **472,** 307–312. ISSN: 00280836. arXiv: 1103.1372. http://dx.doi.org/10.1038/nature09994 (2011).

77. Perk, J., Capel, H., Zuilhof, M. & Siskens, T. On a soluble model of an antiferromagnetic chain with alternating interactions and magnetic moments. *Physica A: Statistical Mechanics and its Applications* **81,** 319–348. ISSN: 0378-4371 (1975).

78. Okamoto, K. & Yasumura, K. Competition between the Bond Alternation and the Anisotropy in a Spin-1/2 XY Chain. *Journal of the Physical Society of Japan* **59,** 993–1001. https://doi.org/10.1143/JPSJ.59.993 (1990).

79. Deng, S., Ortiz, G. & Viola, L. Dynamical non-ergodic scaling in continuous finite-order quantum phase transitions. *EPL (Europhysics Letters)* **84,** 67008 (2008).

80. Dutta, A. *et al. Quantum phase transitions in transverse field spin models: from statistical physics to quantum information* 2015. arXiv: 1012.0653.

81. Souza, F., Lyra, M. L., Strečka, J. & Pereira, M. S. Magnetization processes and quantum entanglement in a spin-1/2 Ising-Heisenberg chain model of a heterotrimetallic Fe-Mn-Cu coordination polymer. *Journal of Magnetism and Magnetic Materials* **471,** 423–431. ISSN: 0304-8853. https://www.sciencedirect.com/science/article/pii/S0304885318321607 (2019).

82. Niazi, A., Paulose, P. L. & Sampathkumaran, E. V. Inhomogeneous Magnetism in Single Crystalline $Sr_3CuIrO_{6+\delta}$: Implications to Phase-Separation Concepts. *Phys. Rev. Lett.* **88,** 107202. https://link.aps.org/doi/10.1103/PhysRevLett.88.107202 (10 Feb. 2002).

83. Yin, W.-G. *et al.* Ferromagnetic Exchange Anisotropy from Antiferromagnetic Superexchange in the Mixed $3d-5d$ Transition-Metal Compound Sr_3CuIrO_6. *Phys. Rev. Lett.* **111,** 057202. https://link.aps.org/doi/10.1103/PhysRevLett.111.057202 (5 Aug. 2013).

84. Visinescu, D. *et al.* First Heterotrimetallic 3d-4d-4f Single Chain Magnet, Constructed from Anisotropic High-Spin Heterometallic Nodes and Paramagnetic Spacers. *Chemistry – A European Journal* **15,** 11808–11814 (2009).

85. Bhatt, P., Thakur, N., Mukadam, M. D., Meena, S. S. & Yusuf, S. M. One-Dimensional Single-Chain Molecular Magnet with a Cross-Linked π-π Coordination Network [{CoII(Δ)CoII(Λ)}(ox)2(phen)2]n. *The Journal of Physical Chemistry C* **118,** 1864–1872. eprint: https://doi.org/10.1021/jp411302d. https://doi.org/10.1021/jp411302d (2014).

86. Coronado, E. *et al.* Structural and magnetic study of tetraaqua(EDTA)dinickel dihydrate [Ni2(EDTA)(H2O)4.cntdot.2H2O]. Alternating Lande factors in a two-sublattice 1D system. *Journal of the American Chemical Society* **108,** 900–905. eprint: https://doi.org/10.1021/ja00265a009. https://doi.org/10.1021/ja00265a009 (1986).

87. Kenzelmann, M. *et al.* $S = \frac{1}{2}$ chain in a staggered field: High-energy bound-spinon state and the effects of a discrete lattice. *Phys. Rev. B* **71,** 094411. https://link.aps.org/doi/10.1103/PhysRevB.71.094411 (9 Mar. 2005).

88. Krokhmalskii, T., Verkholyak, T., Baran, O., Ohanyan, V. & Derzhko, O. Spin-$\frac{1}{2}$ XX chain in a transverse field with regularly alternating g factors: Static and dynamic properties. *Phys. Rev. B* **102,** 144403. https://link.aps.org/doi/10.1103/PhysRevB.102.144403 (14 Oct. 2020).

89. Jordan, P. & Wigner, E. Über das Paulische Äquivalenzverbot. *Zeitschrift für Physik* **47,** 631–651. ISSN: 0044-3328. https://doi.org/10.1007/BF01331938 (Sept. 1928).

90. Lieb, E. H., Schultz, T. & Mattis, D. Two soluble models of an antiferromagnetic chain. *Annals of Physics* **16,** 407–466. http://www.sciencedirect.com/science/article/pii/0003491661901154 (1961).

91. DENG, S., VIOLA, L. & ORTIZ, G. Generalized entanglement in static and dynamic quantum phase transitions. *Recent Progress in Many-Body Theories.* http://dx.doi.org/10.1142/9789812779885_0050 (June 2008).

92. Pfeuty, P. An exact result for the 1D random Ising model in a transverse field. *Physics Letters A* **72,** 245–246. ISSN: 0375-9601. https://www.sciencedirect.com/science/article/pii/0375960179900173 (1979).

93. Derzhko, O., Richter, J., Krokhmalskii, T. & Zaburannyi, O. Regularly alternating spin-$\frac{1}{2}$ anisotropic XY chains: The ground-state and thermodynamic properties. *Phys. Rev. E* **69,** 066112. https://link.aps.org/doi/10.1103/PhysRevE.69.066112 (6 June 2004).

94. Damski, B. & Rams, M. M. Exact results for fidelity susceptibility of the quantum Ising model: the interplay between parity, system size, and magnetic field. *Journal of Physics A: Mathematical and Theoretical* **47,** 025303 (2014).

95. Derzhko, O. & Krokhmalskii, T. Quantum Phase Transitions in $s = \frac{1}{2}$ Ising Chain in a Regularly Alternating Transverse Field. *Czechoslovak J. of Physics* **55,** 605. https://doi.org/10.1007/s10582-005-0065-3 (May 2005).

96. McCoy, B. M. Spin Correlation Functions of the $X - Y$ Model. *Phys. Rev.* **173,** 531–541. https://link.aps.org/doi/10.1103/PhysRev.173.531 (2 Sept. 1968).

97. Barouch, E. & McCoy, B. M. Statistical Mechanics of the XY Model. II. Spin-Correlation Functions. *Phys. Rev. A* **3,** 786–804. https://link.aps.org/doi/10.1103/PhysRevA.3.786 (2 Feb. 1971).

98. Jarzynski, C. Nonequilibrium Equality for Free Energy Differences. *Physical Review Letters* **78,** 2690–2693. ISSN: 0031-9007. http://link.aps.org/doi/10.1103/PhysRevLett.78.2690 (Apr. 1997).

99. Seifert, U. Stochastic thermodynamics, fluctuation theorems and molecular machines. *Reports on progress in physics. Physical Society (Great Britain)* **75,** 126001. ISSN: 1361-6633. arXiv: 1205.4176v1. http://www.ncbi.nlm.nih.gov/pubmed/23168354 (2012).

100. Alicki, R. The quantum open system as a model of the heat engine. *Journal of Physics A: Mathematical and General* **12,** L103 (1979).

101. Bera, M. N., Riera, A., Lewenstein, M. & Winter, A. Generalized laws of thermodynamics in the presence of correlations. *Nature Communications* **8,** 8–13. ISSN: 20411723. arXiv: 1612.04779. http://dx.doi.org/10.1038/s41467-017-02370-x (2017).

102. Horodecki, M. & Oppenheim, J. Fundamental limitations for quantum and nanoscale thermodynamics. *Nature communications* **4,** 2059. ISSN: 2041-1723. arXiv: arXiv:1111.3834v1. http://www.ncbi.nlm.nih.gov/pubmed/23800725 (2013).

103. Skrzypczyk, P., Short, A. J. & Popescu, S. Work extraction and thermodynamics for individual quantum systems. *Nature communications* **5,** 4185. ISSN: 2041-1723. arXiv: 1307.1558. http://www.ncbi.nlm.nih.gov/pubmed/24969511 (2014).

104. Yukawa, S. A Quantum Analogue of the Jarzynski Equality. *Journal of the Physical Society of Japan* **69,** 2367–2370. ISSN: 1347-4073. http://dx.doi.org/10.1143/JPSJ.69.2367 (Aug. 2000).

105. Kurchan, J. A Quantum Fluctuation Theorem. arXiv: 0007360 [cond-mat]. http://arxiv.org/abs/cond-mat/0007360 (2000).

106. Tasaki, H. Jarzynski Relations for Quantum Systems and Some Applications. arXiv: 0009244 [cond-mat]. http://arxiv.org/abs/cond-mat/0009244 (2000).

107. Talkner, P., Lutz, E. & Hänggi, P. Fluctuation theorems: Work is not an observable. *Physical Review E* **75,** 050102. ISSN: 1539-3755. http://link.aps.org/doi/10.1103/PhysRevE.75.050102 (May 2007).

108. Elouard, C. & Mohammady, M. H. in *Thermodynamics in the Quantum Regime: Fundamental Aspects and New Directions* (eds Binder, F., Correa, L. A., Gogolin, C., Anders, J. & Adesso, G.) 363–393 (Springer International Publishing, Cham, 2018). ISBN: 978-3-319-99046-0. https://doi.org/10.1007/978-3-319-99046-0_15.

109. Alipour, S., Rezakhani, A. T., Chenu, A., del Campo, A. & Ala-Nissila, T. *Unambiguous Formulation for Heat and Work in Arbitrary Quantum Evolution* 2019. arXiv: 1912.01939 [quant-ph].

110. Ahmadi, B., Salimi, S. & Khorashad, A. S. *Refined Definitions of Heat and Work in Quantum Thermodynamics* 2020. arXiv: 1912.01983 [quant-ph].

111. Vallejo, A., Romanelli, A. & Donangelo, R. Qubit thermodynamics far from equilibrium: Two perspectives about the nature of heat and work in the quantum regime. *Physical Review E* **103.** ISSN: 2470-0053. http://dx.doi.org/10.1103/PhysRevE.103.042105 (Apr. 2021).

112. Céleri, L. C. & Rudnicki, Ł. *Gauge invariant quantum thermodynamics: consequences for the first law* 2021. arXiv: 2104.10153 [quant-ph].

113. Esposito, M., Lindenberg, K. & Van den Broeck, C. Entropy production as correlation between system and reservoir. *New Journal of Physics* **12,** 013013. ISSN: 1367-2630. arXiv: 0908.1125. https://iopscience.iop.org/article/10.1088/1367-2630/12/1/013013 (Jan. 2010).

114. Santos, J., Landi, G. & Paternostro, M. Wigner Entropy Production Rate. *Physical Review Letters* **118.** ISSN: 10797114 (2017).

115. Goes, B. O., Fiore, C. E. & Landi, G. T. Quantum features of entropy production in driven-dissipative transitions. *Physical Review Research* **2,** 013136. arXiv: 1910.14133. http://arxiv.org/abs/1910.14133 (2020).

116. Goes, B. O. & Landi, G. T. Entropy production dynamics in quench protocols of a driven-dissipative critical system. *Physical Review A* **102,** 52202. ISSN: 0031-899X. arXiv: 2007.14445. http://arxiv.org/abs/2007.14445 (2020).

117. Landi, G. T. & Paternostro, M. *Irreversible entropy production, from quantum to classical* 2020. arXiv: 2009.07668 [quant-ph].

118. Strasberg, P. & Winter, A. *First and Second Law of Quantum Thermodynamics: A Consistent Derivation Based on a Microscopic Definition of Entropy* 2021. arXiv: 2002.08817 [quant-ph].

119. Deffner, S. & Lutz, E. Generalized clausius inequality for nonequilibrium quantum processes. *Physical Review Letters* **105,** 170402. ISSN: 00319007. arXiv: 1005.4495 (2010).

120. Janzing, D., Wocjan, P., Zeier, R., Geiss, R. & Beth, T. Thermodynamic cost of reliability and low temperatures: Tightening Landauer's principle and the second law. *International Journal of Theoretical Physics* **39,** 2717–2753. ISSN: 00207748. arXiv: 0002048 [quant-ph] (2000).

121. Brandão, F. G. S. L., Horodecki, M., Oppenheim, J., Renes, J. M. & Spekkens, R. W. Resource theory of quantum states out of thermal equilibrium. *Physical Review Letters* **111,** 250404. ISSN: 00319007. arXiv: 1111.3882 (2013).

122. Brandão, F. G. S. L., Horodecki, M., Ng, N. H. Y., Oppenheim, J. & Wehner, S. The second laws of quantum thermodynamics. *Proceedings of the National Academy of Sciences* **112,** 3275–3279. ISSN: 0027-8424. arXiv: 1305.5278. http://arxiv.org/abs/1305.5278 (2015).

123. Kondepudi, D. & Prigogine, I. *Modern Thermodynamics: From Heat Engines to Dissipative Structures* ISBN: 9781118698709. https://books.google.com.br/books?id=SPU8BQAAQBAJ (Wiley, 2014).

124. Belenchia, A., Mancino, L., Landi, G. T. & Paternostro, M. Entropy production in continuously measured Gaussian quantum systems. *npj Quantum Information* **6.** ISSN: 2056-6387. http://dx.doi.org/10.1038/s41534-020-00334-6 (Dec. 2020).

125. Landi, G. T., Paternostro, M. & Belenchia, A. *Informational steady-states and conditional entropy production in continuously monitored systems* 2021. arXiv: 2103.06247 [quant-ph].

126. Jarzynski, C. Equalities and Inequalities: Irreversibility and the Second Law of Thermodynamics at the Nanoscale. *Annual Review of Condensed Matter Physics* **2,** 329–351. ISSN: 1947-5454. http://www.annualreviews.org/doi/abs/10.1146/annurev-conmatphys-062910-140506 (Mar. 2011).

127. Van den Broeck, C. Stochastic thermodynamics: A brief introduction. *Proc. Of the International School of Physics 'Enrico Fermi'* **184** (Sept. 2014).

128. Esposito, M., Harbola, U. & Mukamel, S. Nonequilibrium fluctuations, fluctuation theorems, and counting statistics in quantum systems. *Reviews of Modern Physics* **81,** 1665–1702. ISSN: 0034-6861. http://link.aps.org/doi/10.1103/RevModPhys.81.1665 (Dec. 2009).

129. Campisi, M., Hänggi, P. & Talkner, P. Colloquium: Quantum fluctuation relations: Foundations and applications. *Reviews of Modern Physics* **83,** 771–791. ISSN: 0034-6861. http://link.aps.org/doi/10.1103/RevModPhys.83.771 (July 2011).

130. Ballentine, L. *Quantum Mechanics: A Modern Development (2nd Edition)* ISBN: 9789814578608. https://books.google.com.br/books?id=Yi48DQAAQBAJ (World Scientific Publishing Company, 2014).

131. Crooks, G. E. Nonequilibrium Measurements of Free Energy Differences for Microscopically Reversible Markovian Systems. *Journal of Statistical Physics* **90,** 1481–1487. http://link.springer.com/article/10.1023/A:1023208217925 (1998).

132. Bochkov, G. N. & Kuzovlev, Y. E. General theory of fluctuations in nonlinear systems. *Journal of Experimental and Theoretical Physics* **45.** http://jetp.ac.ru/cgi-bin/dn/e_045_01_0125 (Jan. 1977).

133. Dorner, R. *et al.* Extracting Quantum Work Statistics and Fluctuation Theorems by Single-Qubit Interferometry. *Physical Review Letters* **110,** 230601. ISSN: 0031-9007. http://link.aps.org/doi/10.1103/PhysRevLett.110.230601 (June 2013).

134. Mazzola, L., De Chiara, G. & Paternostro, M. Measuring the characteristic function of the work distribution. *Physical Review Letters* **110,** 230602. ISSN: 00319007. arXiv: 1301.7030 (2013).

135. Batalhão, T. B. *et al.* Experimental Reconstruction of Work Distribution and Study of Fluctuation Relations in a Closed Quantum System. *Physical Review Letters* **113,** 140601. ISSN: 0031-9007. http://link.aps.org/doi/10.1103/PhysRevLett.113.140601 (Oct. 2014).

136. Batalhão, T. B. *et al.* Irreversibility and the arrow of time in a quenched quantum system. *Physical Review Letters* **115,** 190601. ISSN: 0031-9007. arXiv: 1502.06704v1 (2015).

137. Roncaglia, A. J., Cerisola, F. & Paz, J. P. Work Measurement as a Generalized Quantum Measurement. *Physical Review Letters* **113,** 250601. ISSN: 0031-9007. http://link.aps.org/doi/10.1103/PhysRevLett.113.250601 (Dec. 2014).

138. Cerisola, F. *et al.* Using a quantum work meter to test non-equilibrium fluctuation theorems. *Nature Communications* **8,** 1–9. ISSN: 20411723. arXiv: 1706.07866 (2017).

139. An, S. *et al.* Experimental test of the quantum Jarzynski equality with a trapped-ion system. *Nature Physics* **11,** 193–199. ISSN: 1745-2473. arXiv: 1409.4485. http://dx.doi.org/10.1038/nphys3197 (2014).

140. Herrera, M., Peterson, J. P. S., Serra, R. M. & D'Amico, I. Easy Access to Energy Fluctuations in Nonequilibrium Quantum Many-Body Systems. *Phys. Rev. Lett.* **127,** 030602. https://link.aps.org/doi/10.1103/PhysRevLett.127.030602 (3 July 2021).

141. Bayocboc, F. A. & Paraan, P. N. C. Exact work statistics of quantum quenches in the anisotropic XY model. *Physical Review E* **92,** 032142. ISSN: 1539-3755. http://link.aps.org/doi/10.1103/PhysRevE.92.032142 (2015).

142. Sharma, S. & Dutta, A. One- and two-dimensional quantum models: Quenches and the scaling of irreversible entropy. *Phys. Rev. E* **92,** 022108. https://link.aps.org/doi/10.1103/PhysRevE.92.022108 (2 Aug. 2015).

143. Cosco, F., Borrelli, M., Silvi, P., Maniscalco, S. & De Chiara, G. Nonequilibrium quantum thermodynamics in Coulomb crystals. *Phys. Rev. A* **95,** 063615. https://link.aps.org/doi/10.1103/PhysRevA.95.063615 (6 June 2017).

144. Paganelli, S. & Apollaro, T. J. G. Irreversible Work versus Fidelity Susceptibility for infinitesimal quenches. *ArXiv,* 1–10. arXiv: 1610.02666. http://arxiv.org/abs/1610.02666 (2016).

145. Wang, Q., Cao, D. & Quan, H. T. Effects of the Dzyaloshinsky-Moriya interaction on nonequilibrium thermodynamics in the XY chain in a transverse field. *Phys. Rev. E* **98,** 022107. https://link.aps.org/doi/10.1103/PhysRevE.98.022107 (2 Aug. 2018).

146. Bayat, A. *et al.* Nonequilibrium critical scaling in quantum thermodynamics. *Phys. Rev. B* **93,** 201106. https://link.aps.org/doi/10.1103/PhysRevB.93.201106 (20 May 2016).

147. Białończyk, M., Gómez-Ruiz, F. & del Campo, A. Exact thermal properties of free-fermionic spin chains. *SciPost Physics* **11.** ISSN: 2542-4653. http://dx.doi.org/10.21468/SciPostPhys.11.1.013 (July 2021).

148. Gambassi, A. & Silva, A. *Statistics of the Work in Quantum Quenches, Universality and the Critical Casimir Effect* 2011. arXiv: 1106.2671 [cond-mat.stat-mech].

149. Zurek, W. H. Pointer basis of the quantum apparatus, Into what mixture does the wave packet collapse? *Physical Review D* **24,** 1516 (1981).

150. Zurek, W. H. Decoherence, einselection, and the quantum origins of the classical. *Reviews of Modern Physics* **75,** 715–775. ISSN: 00346861. arXiv: 0105127 [quant-ph] (2003).

151. Marvian, I. & Spekkens, R. W. Extending Noether's theorem by quantifying the asymmetry of quantum states. *Nature Communications* **5,** 1–8. ISSN: 20411723. arXiv: 1404.3236. http://dx.doi.org/10.1038/ncomms4821 (2014).

152. Elouard, C., Herrera-Martí, D., Esposito, M. & Auffèves, A. Thermodynamics of optical Bloch equations. *New Journal of Physics* **22,** 103039. ISSN: 1367-2630. arXiv: 2001.08033. https://iopscience.iop.org/article/10.1088/1367-2630/abbd6e (Oct. 2020).

153. Hiai, F. & Petz, D. *Introduction to Matrix Analysis and Applications* ISBN: 9783319041490. https://books.google.com.br/books?id=jz5HyAEACAAJ (Springer International Publishing, 2014).

154. Scandi, M. *Quantifying Dissipation via Thermodynamic Length* https://www.theorie.physik.uni-muenchen.de/TMP/theses/thesisscandi.pdf (Master thesis, 2018).

155. Nielsen, M. A. & Chuang, I. L. *Quantum Computation and Quantum Information* (Cambridge University Press, 2000).

156. Callen, H. B. *Thermodynamics and an introduction to Thermostatistics* 2nd, 493 (Wiley, 1985).

157. Wigner, E. P. & Yanase, M. M. INFORMATION CONTENTS OF DISTRIBUTIONS. *Proceedings of the National Academy of Sciences* **49,** 910–918. ISSN: 0027-8424. eprint: https://www.pnas.org/content/49/6/910.full.pdf. https://www.pnas.org/content/49/6/910 (1963).

158. Wehrl, A. General properties of entropy. *Reviews of Modern Physics* **50,** 221–260. ISSN: 00346861 (1978).

159. Marvian, I., Spekkens, R. W. & Zanardi, P. Quantum speed limits, coherence, and asymmetry. *Phys. Rev. A* **93,** 052331. https://link.aps.org/doi/10.1103/PhysRevA.93.052331 (5 May 2016).

160. Sarandy, M. S. Classical correlation and quantum discord in critical systems. *Phys. Rev. A* **80,** 022108. https://link.aps.org/doi/10.1103/PhysRevA.80.022108 (2 Aug. 2009).

161. Werlang, T., Trippe, C., Ribeiro, G. A. P. & Rigolin, G. Quantum Correlations in Spin Chains at Finite Temperatures and Quantum Phase Transitions. *Phys. Rev. Lett.* **105,** 095702. https://link.aps.org/doi/10.1103/PhysRevLett.105.095702 (9 Aug. 2010).

162. Li, Y.-C. & Lin, H.-Q. Quantum coherence and quantum phase transitions. *Scientific Reports* **6,** 26365. ISSN: 2045-2322. https://doi.org/10.1038/srep26365 (May 2016).

163. Lei, S. & Tong, P. Wigner–Yanase skew information and quantum phase transition in one-dimensional quantum spin-1/2 chains. *Quantum Information Processing* **15,** 1811–1825. ISSN: 1573-1332. https://doi.org/10.1007/s11128-016-1244-9 (Apr. 2016).

164. Yi, T.-C., You, W.-L., Wu, N. & Ole ś, A. M. Criticality and factorization in the Heisenberg chain with Dzyaloshinskii-Moriya interaction. *Phys. Rev. B* **100,** 024423. https://link.aps.org/doi/10.1103/PhysRevB.100.024423 (2 July 2019).

165. Hu, M.-L., Fang, F. & Fan, H. *Finite-size scaling of coherence and steered coherence in the Lipkin-Meshkov-Glick model* 2021. arXiv: 2107.13916 [quant-ph].

166. Binder, F. C., Vinjanampathy, S., Modi, K. & Goold, J. Quantacell: powerful charging of quantum batteries. *New Journal of Physics* **17,** 075015. https://doi.org/10.1088/1367-2630/17/7/075015 (July 2015).

167. Ferraro, D., Campisi, M., Andolina, G. M., Pellegrini, V. & Polini, M. High-Power Collective Charging of a Solid-State Quantum Battery. *Phys. Rev. Lett.* **120,** 117702. https://link.aps.org/doi/10.1103/PhysRevLett.120.117702 (11 Mar. 2018).

168. Abramowitz, M. & Stegun, I. *Handbook of Mathematical Functions* (Dover, New York, 1964).

169. Andrieux, D. & Gaspard, P. Quantum Work Relations and Response Theory. *Physical Review Letters* **100.** ISSN: 1079-7114. http://dx.doi.org/10.1103/PhysRevLett.100.230404 (June 2008).